Adaptive seascapes: disentangling the roles of genetic, symbiotic, and environmental drivers on coral heat tolerance

Thesis submitted by: Magena Rayne Marzonie MSc

Date: 7 June 2024

For the degree of Doctor of Philosophy in Natural and Physical Sciences

Colleges of Science and Engineering, James Cook University

Acknowledgements

While a PhD candidature feels largely independent at times, I stand by the saying that 'it takes a village to raise a PhD student'. I would like to acknowledge the community that has supported my candidature journey over the past four years.

I would like to acknowledge the First Nations people as the first ecologists on the land and sea country where this thesis was conducted. This includes the Meriam people of Torres Strait (Coral Sea), and the Wulgurukaba and Bindal people of Australia, whose continual connection to the land and sea country where we work motivates and informs the science we conduct in Australia and the surrounding sea country. This science would not happen without the two-way knowledge transfer and consent to use sea country. Thank you for your knowledge which has been passed down through generations and guides us in our scientific endeavours.

The synthesis of this research and my overall experience would not have been possible without the exceptional supervision of Line Bay and David Bourne. Line, you are a powerhouse and your strong network and ability to foster international collaborations, in parallel with your knowledge of coral adaptation, have created opportunities that would not have been possible without your excellent mentorship. You have been an excellent role model, supervisor, and have always been in my corner. You always know when I need extra help and hyping up, and for that I greatly appreciate you and your mentorship. David, your overall understanding of corals, microbiology, scientific writing, and academia have proven critical at many points throughout this PhD journey. Your quick feedback and diplomatic nature have also been extremely helpful throughout my candidature. I know you had way too many students and projects when I asked you onboard my supervisory panel, but you agreed anyway. You have consistently made time for feedback, meetings, and general support, and this does not go unnoticed. Thank you both for everything.

Hugo Harrison, this work would certainly not be possible without your ideas around adaptive seascapes, from which the foundation for my entire PhD thesis stems. Your cross-disciplinary thinking and big questions are a contagious way to think, and I know I have grown into a better scientist with you as a mentor. I went from never having opened R to being able to write code in real time with significant help and patience from you. Thank you.

My external collaborators have been essential into getting through the difficult molecular analyses. Matt Nitschke, you have provided excellent mentorship throughout my candidature and a willingness to share valuable insights and data analyses. Your knowledge of symbionts has fundamentally shaped multiple chapters of this thesis, and I thank you for selflessly dedicating many days to help me with coding, writing, ideas, and supervision, despite not being recognised as an official supervisor on my panel. I feel like a much brighter and well-rounded scientist with the help and mentorship you have provided. Thank you.

A huge thanks also to Oliver Selmoni, for collaborating across the world from Switzerland. Your knowledge of seascape genomics has greatly improved the quality of the genetic chapters of my PhD, and I am grateful for you to come onboard as an external collaborator during the second half of my PhD and lend your expertise. You have been another excellent mentor in terms of how to analyse data, have helped me troubleshoot code and brainstorm ideas, and I thank you for lending your knowledge and time as a collaborator for the last two chapters of my PhD.

A PhD requires a community of like-minded thinkers, and I am very grateful to my lab groups, the Bay Lab and Bourne Lab, and AIMS@JCU student community. In particular, Josephine Nielsen has been a great support for field experimental methods, kindly donating samples from the GBR to broaden the scope of my third data chapter, brainstorming ideas over the past four years, and keeping me sane in general. Also, Debs Burn has been extremely helpful with the statistical aspects of my PhD and her depth of knowledge on the Coral Sea. To my entire lab group, thank you for exchanging ideas, giving valuable feedback on presentations and written work, help with coding when the world felt like it was caving in one line of script at a time, and the occasional glass of sauv blanc to tolerate the long road to becoming a doctor.

My laboratory journey also began during Covid in 2020, so I would like to acknowledge Veronique Mocellin, Lesa Peplow, Sara Bell, Heidi Luter, Carlos Alvarez Roa, and Florita Flores for your molecular advice when my supervisors were not able to be on site during the pandemic. Thank you for your time and knowledge and making the PC2 lab seem a little less intimidating during this time. My confidence and ability in molecular labs have significantly improved based on the knowledge and support from these researchers, thank you.

I would like to acknowledge the academic and financial support from James Cook University, the ARC Centre of Excellence for Coral Reef Studies, the Australian Institute of Marine Science, AIMS@JCU, and Parks Australia. In particular, Andrew Hoey, Morgan Pratchett, Hugo Harrison, and Martin Russell for funding the Coral Sea expedition of 2020, which forms the basis of my PhD chapters. I would also like to thank the administration staff of the ARC Centre of Excellence, including Janet Swanson, Vivian Doherty, Alana Grech, and Olga Bazaka, who each made the financial and administration aspect ten-times smoother than it would have been on my own. I would also like to thank Parks Australia, in particular Martin Russell, the American Australian Association, AIMS@JCU, Australian Coral Reef Society, and JCU CodeR Club for academic funding and grants provided throughout my candidature.

Thank you to the extremely hard-working and knowledgeable team of the National Sea Simulator, especially Steve Green, Justin Hochen, and Andrea Severati for the design and build of the portable aquarium that was the crux of completing my field experiments. Also, thank you to Captain Rob Benn and the amazing crew of the Iron Joy for assistance with the 2020 Coral Sea expedition.

Of course, my friends and family have been critical throughout this journey, providing continuous encouragement throughout these long (and yet somehow short) four years. From helping me pick colour palettes for graphs, to showing up at odd hours across the world for Zoom presentations, I have felt a palpable support network near and far, and it has helped me celebrate the good, and persevere through the challenging moments with continual encouragement. This includes my grandparents, Robin and Barry, who first introduced me to the underwater world at the age of 13 and have continuously encouraged my pursuit of knowledge, research, and scuba. Additionally, my family, Noelle, Todd, Ian, Becci, Adriane, Marissa, Bella, Tom, and Maelle, have all been instrumental in my emotional and mental health during this journey. I would especially like to thank my ultimate cheerleaders, Taylor and June, for being my right-hand girls throughout the entire journey.

And lastly, to my mom, who wrote me a letter in my youth that said, ‘I hope you marry a doctor one day’. It looks like I don’t need to.

Statement on the contribution of others

Table 1.1. Statement of contribution to thesis chapters. MRM is Magena R. Marzonie, LKB is Line K. Bay, HBH is Hugo B. Harrison, DGB is David G. Bourne, MRN is Matthew R. Nitschke, JJVN is Josephine J.V. Nielsen, OS is Oliver Selmoni, SM is Samuel Matthews, AH is Andrew Hoey.

Chapter	Statement of contribution
Chapter 1: General introduction	MRM wrote the chapter with feedback from LKB and DGB.
Chapter 2: The effects of marine heatwaves on acute heat tolerance in corals	MRM, HBH, LKB, and JJVN conceived the research. MRM and HBH performed the field work. MRM, HBH, and SM analysed the data. MRM wrote the manuscript with feedback from HBH, LKB, JJVN, SM, AH, and DGB.
Chapter 3: Symbiodiniaceae diversity varies by host and environment across thermally distinct reefs	MRM, HBH, and LKB conceived the research. MRM and HBH performed the field work. MRM performed the laboratory analyses. MRM and MRN analysed the data. MRM wrote the manuscript with feedback from MRN, LKB, DGB, and HBH.
Chapter 4: Seascape genomics reveal contrasting patterns of population structure across a large thermal gradient	MRM, HBH, and LKB conceived the research. MRM, HBH, and JJVN performed the field work. MRM analysed the data with input from OS and MRN. MRM wrote the manuscript with feedback from OS, LKB, JJVN, HBH, MRN, and DGB.
Chapter 5: Natural and experimental detection of heat tolerance adapted loci in a common coral species	MRM, HBH, and LKB conceived the research. MRM and HBH performed the field work. MRM performed the laboratory analyses. MRM analysed the data. MRM wrote the manuscript with feedback from OS, LKB, HBH, MRN, and DGB.
Chapter 6: General discussion	MRM wrote the chapter with feedback from LKB and DGB.

Table 1.2. Authorship declaration for published chapters.

Chapter	Reference	Contributions of each author	Author consent to republish content in thesis
The effects of marine heatwaves on acute heat tolerance in corals	Marzonie, M. R., Bay, L. K., Bourne, D. G., Hoey, A. S., Matthews, S., V Nielsen, J. J., Harrison, H. B. (2023). The effects of marine heatwaves on acute heat tolerance in corals. Global Change Biology, 00, 1–13. https://doi.org/10.1111/gcb.16473	MRM, HBH, LKB, and JJVN conceived the research. MRM and HBH performed the field work. MRM, HBH, and SM analysed the data. MRM wrote the manuscript with feedback from HBH, LKB, JJVN, SM, AH, and DGB.	Line K. Bay David G. Bourne Andrew S Hoey Samuel Matthews Josephine J.V. Nielsen Hugo B. Harrison
Symbiodiniaceae diversity varies by host and environment across thermally distinct reefs	Marzonie, M.R., Nitschke, M.R., Bay, L.K., Bourne, D.G., Harrison, H.B. (2024). Symbiodiniaceae diversity varies by host and environment across thermally distinct reefs. *Molecular Ecology,* https://doi.org/10.1111/mec.17342	MRM, HBH, and LKB conceived the research. MRM and HBH performed the field work. MRM performed the laboratory analyses. MRM and MRN analysed the data. MRM wrote the manuscript with feedback from MRN, LKB, DGB, and HBH.	Matthew R. Nitschke Line K. Bay David G. Bourne Hugo B. Harrison

Abstract

The adaptive potential of heat tolerance in corals and their symbionts is a critical topic amidst a rapidly changing climate and heightened marine heatwaves. Bleaching events have increasingly affected reefs globally, both in frequency and magnitude. Therefore, separating the effects of environmental acclimatisation, and host and symbiont genetic adaptation are critical to determining the mechanisms which best predict tolerance of corals. These processes enable a better consensus on how to manage and protect reefs into the future. The overarching aim of this thesis investigates the environmental, symbiotic, and genetic mechanisms which underpin coral heat tolerance. To achieve this, I: i) quantify the spatial heterogeneity of heat tolerance across reefs and coral taxa (Chapter 2); ii) describe the population structure of coral taxa and the environmental predictors of genetic diversity and connectivity (Chapter 3); iii) understand the host and genetic drivers of Symbiodiniaceae and the role of symbionts in coral heat tolerance, and iv) detect genetic signals of heat tolerance adaptation in the coral host (Chapter 4). Each of the chapters use experimental and genetic data collected from Australia's Coral Sea Marine Park, with information derived from one or more coral species, including *Acropora* cf *humilis, Pocillopora meandrina,* and *Pocillopora verrucosa.*

In **Chapter 2**, I estimated empirical thresholds of coral heat tolerance as a quantitative metric for bleaching. Using acute heat stress experiments, I quantified a 50% decline in photosynthetic efficiency (ED50) to detect differences in heat tolerance across three coral species and spatially heterogenous reefs. Heat tolerance was highly variable among the three species and across spatially distinct reefs. Additionally, increased heat tolerance was highest at reefs that had experienced mild marine heatwaves over the past 35 years. Conversely, heat tolerance was lowest at reefs which had experienced severe marine heatwaves in the past five years; indicating that corals can adapt, but only at a certain pace.

The remaining three chapters focus on expanding the understanding of heat tolerance mechanisms across coral taxa and reefs. In **Chapter 3**, I examined the environmental and genetic drivers of Symbiodiniaceae to uncover the interactions that shape Symbiodiniaceae distribution, and whether thermal disturbances affect symbiont diversity and distribution among reefs. Symbiont community structure was highly dependent on host species, host population structure, and environmental gradients. However, the most important host and

environmental predictors were strongly linked to the mode of symbiont transmission. Horizontally acquired symbionts in *Acropora* were strongly driven by thermal history and latitude, reflecting the symbiont community shifts in response to thermal disturbances. In vertically transmitted *Pocillopora* symbionts, host population structure was a stronger predictor of symbiont distributions. However, *P. meandrina* had 13 times stronger effect of host genetic structure compared to *P. verrucosa,* highlighting interspecific variability in both host and symbiont community structure.

In **Chapter 4**, I investigated how thermal and environmental gradients shape population structure and local adaptation across multiple host taxa. Specifically, I analysed interspecific trends of population structure in *Pocillopora verrucosa* and *Pocillopora meandrina* across the Coral Sea and Great Barrier Reef to quantify differences in their connectivity and genetic diversity. *Pocillopora meandrina* had stronger population structure than *P. verrucosa* across both the GBR and Coral Sea. I found species-specific differences in gene flow and genetic diversity, where *P. meandrina* had higher population structure across both regions compared to *P. verrucosa*. Genetic isolation was strongest in high latitude, offshore reefs for both species, indicating higher vulnerability to climate change based on less connectivity to source reefs. However, there was evidence of gene flow between the Great Barrier Reef and Coral Sea Marine Park for both *Pocillopora* spp., indicating connectivity among these regions.

In **Chapter 5**, I examined the relationship between genotype, phenotype, and environment and their relative contributions to determining heat tolerance adaptation in corals. Using a seascape genomics approach, I detected loci under selection in *Acropora* cf. *humilis* and identified the environmental drivers associated with adaptation, which included only long term thermal history metrics. I then modelled bleaching phenotype (ED50) against host genetics, symbiont community structure, and environmental parameters and found that both thermal history and Symbiodiniaceae were the best predictors of bleaching tolerance in corals. These contrasts indicate that recent, severe heatwaves impact the structure of host phenotype and the underlying symbiont community structure, but not that of host adaptive loci. Overall, my thesis indicates strong evidence of host and symbiont adaptation in response to long-term thermal history across a large environmental gradient. However, the lack of adaptive signal of the coral host in response to recent, severe heatwaves indicates that adaptation is unlikely to occur at the rate needed to sustain the diversity and function of reefs as we see them today. Overall, these findings have highlighted populations harbouring high and low heat tolerant corals will be

critical knowledge for management, restoration, and reef projections under various climate change scenarios in the near future.

Table of Contents

List of tables

Table 5.1. Environmental, symbiont, and host genetic predictors and conditional effects incorporated into the partial redundancy analyses.

Table 5.2. Library statistics for *Acropora* cf. *humilis*, including the number of samples (N), observed heterozygosity (H_O), expected heterozygosity (H_E), and population-level F_{IS}.

List of figures

of marine heatwaves between 1986 and 2020 where DHW was above or equal to 4 was the best predictor of heat tolerance (ED50) of reefs in the CSMP. (d-e). The return time between heatwaves where DHW was above or equal to 6 between 1986 and 2020 also explained sufficient variation in heat tolerance of reefs in the CSMP. (f-g). The average maximum DHW between 2016 and 2020 was the third environmental predictor to explain variance in heat tolerance. Each of the three predictors vary spatially across the seascape (c, e, g), including at the nine reefs where heat tolerance was quantified experimentally and depicted as white points.

Figure 3.1. Analysis of SymPortal post-MED ITS2 sequence data in *Pocillopora* (a) and *Acropora* (b). Each vertical bar represents the symbiont structure of one coral sample. The top third of each plot shows the UPGMA tree of the between-sample Generalised UniFrac distances. The middle third represents ITS2 sequence composition, with the proportion of individual sequences represented by different colours. The bottom third of each plot is coloured according to an assigned SymPortal ITS2 type profile, with grey representing the proportion of non-profile sequences found in each sample. For *Pocillopora* species (A), samples for *P. verrucosa, P. meandrina* and haplotype 8a are represented by tree leaf colours (green, orange, and blue, respectively) derived from the RFLP and mtORF molecular assays. Arrow 1 = *C. pacificum*/*C. latusorum* branch, 2 = *C. latusorum* 'north' and 'south' branch, and 3 = C3k 'max' and 'min' branch.

Figure 3.2. Tanglegram of ITS2 and psbA^{ncr} sequences. ITS2 sequences vs. psbA^{ncr} sequence UPGMA trees for *Pocillopora* spp. (A) and *Acropora* cf *humilis* (B). ITS2 sequence UPGMA trees are according to k-mer = 7 + GUniFrac (0.5) distances and psbA^{ncr} sequence UPGMA trees use k-mer = 7 distances. Blue and red arrows correspond to the phylogenetic split in each species tree shown in Figure 1a and b, respectively. Arrow 1 = *C. pacificum*/*C. latusorum* branch, 2 = *C. latusorum* 'north' and 'south' branch, and 3 = C3k 'max' and 'min' branch.

Figure 3.3. Procrustean rotation analysis of host and symbiont genetic diversity. *Pocillopora verrucosa* (a), *Pocillopora meandrina* (b) and *Acropora* cf *humilis* (c). Each point represents a sample, with host samples (circle) and symbiont samples (triangle) from the same individual linked by a line segment. Each point is coloured by the reef.

Figure 3.4. Schematic diagram depicting biogeographic patterns and relative proportion of host population structure and symbiont lineages detected throughout the Coral Sea Marine Park

at 13 reefs. (a) Pie charts represent host genetic clustering (admixture proportion) for *P. meandrina* (top) and symbiont lineage clustering (bottom) include *C. latusorum* 'north' and *C. latusorum* 'south'. (b) Host genetic clustering for *P. verrucosa* (top) and one symbiont lineage of *C. pacificum* (bottom). (c) Pie charts show relative abundance of three host genetic clusters of *A.* cf *humilis* (top) and symbiont lineage clustering (bottom) include C3k 'max' and C3k 'min'.

Figure 3.5. Distance-based redundancy analysis (dbRDA) ordinations of GUniFrac (0.5) ITS2 sequence composition. *Pocillopora meandrina* (a), *Pocillopora verrucosa* (b) and *Acropora* cf *humilis* (c). Each circle is coloured by latitude. Blue arrows represent significant environmental vectors derived from a backward stepwise model.

Figure 4.1. Population structure for *Pocillopora meandrina* and *P. verrucosa* across the GBR and Coral Sea. (a) Map of sectors partitioned in Australia's Great Barrier Reef (GBR) and Coral Sea Marine Park (CSMP). Sectors considered in the analysis of population structure include: Cape Grenville (CGR), Princess Charlotte Bay (PCB), Cairns (CNS), Townsville (TSV), Swains (SWN), Capricorn Bunkers (CPB), Coral Sea Sector 1-6 (CS1-6). (b) Pairwise comparisons of genetic diversity (F_{ST}) between sectors for *Pocillopora meandrina* and (c) for *Pocillopora verrucosa*.

Figure 4.2. Genetic membership probability and clustering of *Pocillopora meandrina* and *P. verrucosa.* Admixture analyses indicated two genetic clusters (K=2) for both species including (a) *P. meandrina* (PMCL1 and PMCL2) and (b) *P. verrucosa* (PVCL1 and PVCL2). Each vertical bar depicts one individual and the estimated ancestry coefficient to each cluster. Admixture coefficients in relation to biogeographic patterns of structure for (c) *P. meandrina* and (d) *P. verrucosa.*

Figure 4.3. Distance-based redundancy analysis (dbRDA) for the environmental drivers of genetic structure among individuals in (a) *P. meandrina* and (b) *P. verrucosa*. Plots are coloured by sectors within the Great Barrier Reef (GBR) and Coral Sea. Vectors indicate environmental predictors which are significant in the dbRDA models. Env PC1 refers to the first PC axis of multiple non-thermal environmental variables constrained in a PCA. Mean DHW refers to average monthly DHW experienced between 1985-2020. MMM refers to

Maximum Monthly Mean climatology of each reef. Biogeographic patterns of thermal history (c) and Environmental PC1 (d) vary across reefs in the GBR and Coral Sea.

Figure 5.1. Neutral population structure and cryptic speciation of *Acropora* cf *humilis.* (A) Three morphotypes of *Acropora* cf *humilis*, which correspond to the three genetic clusters detected in the SNP genetic dataset. (B) Map of the Coral Sea Marine Park indicates admixture proportion per reef as pie charts, with colours representing the three genetic lineages of *A.* cf *humilis.* (C) PCoA of allele frequencies indicates three distinct clusters which may indicate cryptic species. (D) Admixture proportions using the optimal number of K ancestral lineages (K=3) are coloured according to the three genetic clusters (AHCL1, AHCL2, and AHCL3).

Figure 5.2. ED50 density plots structured by individuals within reefs, host cluster, and symbiont community composition. (a). Density distribution of phenotypic performance in *Acropora* cf *humilis* across the eight populations where experiments were conducted. ED50 represents the temperature above Maximum Monthly Mean where a 50% bleaching threshold was reached per individual. (b). Density distribution of phenotypic ED50s relative to the three host genetic lineages (AHCL1, AHCL2, and AHCL3) and (c) relative to the multiple symbiont community clusters.

Figure 5.3. Candidate adaptive loci associated with *Acropora* cf *humilis*. Each point represents a SNP (locus) which are coloured by the strongest thermal predictor of the relative locus, including the number of DHW > 4 experienced between 1985-2020 (DHW4) and the return time between DHW > 6 events (return DHW6) (a). Polygenic scores (PGS) were then calculated based on the strongest environmental driver (return DHW6) using all candidate adaptive SNPs (b).

Figure 5.4. A bleaching predictor model for phenotypic heat tolerance. ED50 estimates against host adaptive genetic axes and the number of mild heatwaves (DHW4) for individuals experienced less than 7 events where DHW >4 between 1986-2020 (a), and those experiencing more than 7 events where DHW >4 between 1986-2020 (b).

Figure 6.1. The multifaceted nature of heat tolerance. (a) Heat tolerance variation occurs across several biological scales including host species, populations, and individual levels. (b) The thesis findings indicate increased heat tolerance in *Pocillopora* compared to *Acropora,* but

greater symbiont flexibility in Acroporids. Extrinsic processes including thermal history also mediate heat tolerance, where long-term, mild heatwaves provide increased heat tolerance, and more recent, severe heatwaves result in less heat tolerant populations and individuals. (c) Heat tolerance thresholds and the underlying factors influencing variation. Quantifying heat tolerance thresholds among populations and understanding the associated predictors can allow for the management and protection of both tolerant (red) and vulnerable reefs (blue).

Figure 6.2. Ecological bright spots show higher thermal tolerance in high latitude reefs (a) was associated with thermal history (b), distinct symbiont communities (c), and strongly separated host population structure (d).

Chapter 1. General introduction

1.1 The vulnerability of coral reefs in the Anthropocene

Coral reefs are facing a rapid decline in response to anthropogenic climate change and subsequent ocean warming (Hughes et al., 2017; Lough et al., 2018). Marine heatwaves are now the leading selective pressure on reef-building corals, resulting in more severe and frequent mass coral bleaching events (Oliver et al., 2018; Smale et al., 2019). The threat to coral functionality, diversity, and cover is already apparent, demonstrated by five mass bleaching events over the past 8 years (i.e., 2016, 2017, 2020, 2022, and 2024) across the Great Barrier Reef and Coral Sea (Hughes, et al., 2018; Harrison et al. 2019; Pratchett and Heron, 2021) and globally (van Woesik et al., 2022). A current global mass bleaching event is unfolding in the 2023/2024 summer, potentially representing the most devasting to date. Severe bleaching events are expected to occur annually on Australia's Great Barrier Reef by 2080 under high shared socioeconomic pathways (SSP) climate change emissions (McWhorter et al., 2022). Both current and near future bleaching scenarios highlight the need to identify the drivers and mechanisms of heat tolerance in corals, concomitant with the impacts of climate change. One area in question is whether corals and their symbionts harbour the natural adaptive capacity to keep pace with current rates of ocean warming. If they do, which populations, species, and individuals maintain high adaptive capacity? And what mechanisms underpin this functional variation in heat tolerance?

1.2 Evidence of heat tolerance adaptation in corals

Despite mass mortality attributed to recent bleaching events, some corals harbour a capacity to withstand rapid or sustained increases in sea-surface temperatures. At a global scale, coral heat tolerance has increased by 0.5 °C over the past decade (Sully et al., 2019), highlighting the

potential for acclimatisation and/or adaptation to thermal disturbances against a backdrop of rapid climate change. Yet, it is unclear whether this evidence of increased heat tolerance is a result of community-level shifts to more heat tolerant species (Guest et al., 2012), natural selection eliminating heat-susceptible individuals from populations (Humanes et al., 2022), or a combination of the two factors. The ecological memory (Hughes et al., 2019) and population recovery time (Dietzel et al., 2021) can additionally influence the capacity for corals to withstand marine heatwaves, but whether this is an adaptive or acclimatory response remains unclear. Lachs et al. (2023) found population-level bleaching tolerance has historically increased by 0.1°C per decade using reefs in Palau as a model system, indicating that adaptation in these populations will occur under both low and middle climate change scenarios (SSP 2 – 5), but not under predicted high climate change scenarios (SSP 5 – 8.5). To link empirical thermal tolerance of one population to broader scale findings, field or experimental studies encompassing multiple populations would improve the understanding of the rate and mechanisms of coral thermal adaptation, as well as future predictions of reef trajectories (McManus et al., 2020). The integration of field-based data, molecular data, and spatial predictive models will clarify some discrepancies found between *in situ* and satellite-based approaches to determine heat tolerant and more susceptible reefs (van Woesik et al., 2022).

1.3 The pillars of local adaptation

The three facets of adaptation: (1) genotype, (2) phenotype, and (3) environment, can be used to collectively detect signatures and patterns of heat tolerance adaptation in corals (Rellstab et al., 2015). Gene-environment associations assess the effects of variable environmental factors in relation to both neutral and adaptive genetic variation. These techniques were originally developed for terrestrial organisms, and more recently have extended to marine organisms, where greater gene flow requires a shifted framework given the higher connectivity between

populations (hereafter referred to as seascape genomics) (Riginos et al., 2016; Selmoni, Bay, et al., 2024). Applying seascape genomics is a critical approach to detect adaptive loci in corals in response to environmental fluctuations (Riginos et al., 2016; Riginos & Liggins, 2013; Selmoni, Bay, et al., 2024; Selmoni et al., 2020, 2021) allowing for a less intrusive method to understand how adaptation varies along environmental gradients. Complementary to this approach, genotype-phenotype studies can aid our understanding of the genetic architecture of corals using approaches such as genome-wide association studies (GWAS) or quantitative genetics (e.g., QTL mapping) (Quigley, 2023; Sardi & Gasch, 2017). Genotype-phenotype studies in corals, using selective breeding or common garden experiments in sympatry with examining the genetic architecture, have indicated that heat tolerance traits are both partially heritable (Dixon et al., 2015) and/or locally adapted to their environment (Howells et al., 2013; Quigley, Randall, et al., 2020).

To complete the G-P-E triangle, the relationships between environment and phenotype can be explored through *in-situ* reciprocal transplant or experimentally controlled aquarium experiments, where the adaptive capacity of corals is measured across individuals, species, and populations (Evensen et al., 2022; Evensen et al., 2023; Grottoli et al., 2021; Voolstra et al., 2020). To measure heat tolerance variation as a trait, a coral subjected to natural and experimental heat stress can be studied with GWAS and GEA applied to identify and cross-reference genes under selection. Similarly, phenotypic traits of interest can be cross-referenced using common garden experiments in parallel with natural observations of bleaching *in situ*.

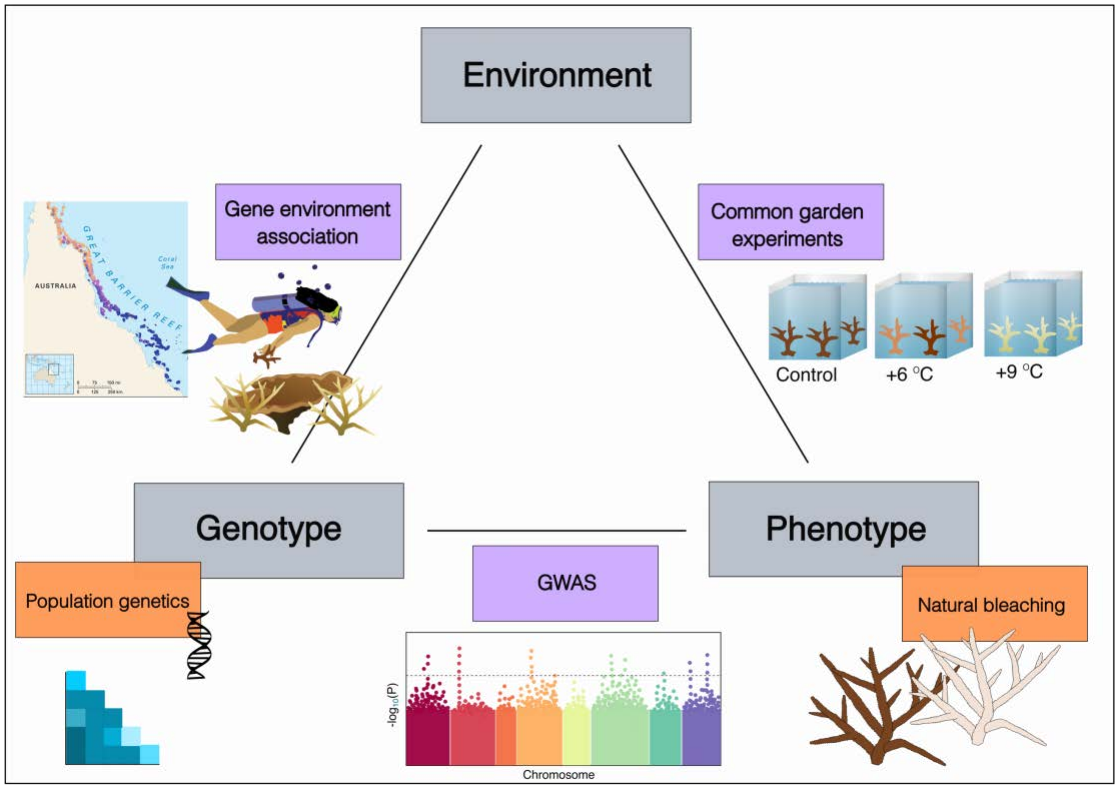

Figure 1.1. Modified schematic from Rellstab et al. (2015) illustrating the interactions between genotype, phenotype, and environment (G-P-E triangle) of coral heat tolerance. Specific themes and analyses required to understand links between some or all traits which underpin coral heat tolerance adaptation are displayed. Map modified from ARC Centre of Excellence for Coral Reef Studies. Coral and diver graphics sourced from Maryland Image Bank.

1.4 The genetic architecture of heat tolerance

Heat tolerance in corals has been determined as a complex and polygenic trait, indicating that multiple loci of small effect contribute to the heat tolerance trait, and that specific combinations of these loci can increase heat tolerance potential (Fuller et al., 2020; Parkinson et al., 2019; Selmoni, Bay, et al., 2024). The advantage of a polygenic trait is the ability to reach a more heat tolerant physiological outcome through multiple mechanisms, increasing the likelihood to adapt to rapidly changing environmental conditions. However, polygenic traits create higher

complexities in determining the mechanisms and genetic architecture of heat tolerance requiring large sample sizes to draw meaningful conclusions (Fuller et al., 2020) compared to other traits such as disease resistance (Vollmer et al., 2023.). As a trait, coral heat tolerance is at least partly heritable (Dixon et al., 2015; Elder et al., 2022; Kenkel et al., 2013; Bairos-Novak et al. 2022) and varies by coral taxa and environmental conditions (Drury & Lirman, 2021; Selmoni et al., 2021). The number of candidate loci attributed to heat tolerance can vary across species; for example, putatively heat-tolerant loci explained over two-thirds of variability in heat tolerance for *Platygyra daedalea* in the Persian Gulf (Kirk et al., 2018) compared to only 27% in *Acropora cervicornis* from Florida reefs (Drury & Lirman, 2021), indicating taxa- and region-specific trends in the mechanisms underlying phenotypic heat tolerance (reviewed in Selmoni et al., 2024). Heat tolerance variation within species can also be attributed to cryptic speciation or individual genotypes, which influence both thermal tolerance (Rose et al., 2021) and the subsequent environmental-genotype associations (Meziere et al., 2024; Starko et al., 2024). As genomic techniques (*e.g.,* whole genome sequencing, genotype-by-sequencing) become quintessential tools to identify the subtle trends associated with heat tolerance adaptation in corals, so too does the need to examine patterns across multiple taxa and environments.

1.5 The role of symbionts in heat tolerance

The role of symbionts mediates coral heat tolerance and is superimposed on the effects of host adaptation and acclimatisation to environmental conditions (van Oppen & Medina, 2020). Bleaching is the disassociation of symbionts from the coral host, which concomitantly results in less photosynthetic derived nutrition to the coral (Morris et al., 2019; Weis, 2008; Weis et al., 2008). Symbiodiniaceae are taxonomically diverse, and different genera and species can contribute to the variable heat tolerance of symbionts and consequently their host (LaJeunesse

et al., 2018). The genetic and physiological differences in coral symbiont communities can mediate the extent to which corals withstand bleaching events, thus, it is important to incorporate analyses of Symbiodiniaceae in bleaching studies to elucidate the mechanisms of thermal tolerance in corals. There is evidence that symbiont community composition harbours a strong role in coral persistence against the effects of marine heatwaves (Manzello et al., 2019) and the thermal tolerance ranges of coral taxa and individuals across biogeographic scales (Turnham et al., 2023). For example, symbionts belonging to the genus *Durusdinium* often possess greater heat tolerance than symbionts belonging to *Cladocopium* (Berkelmans & van Oppen, 2006).

The diversity of symbiont assemblages within a coral host varies according to host taxa and is mainly influenced by the mode of symbiont transmission. Vertically transmitted symbionts maintain a higher host-fidelity, often resulting in lower levels of symbiont diversity within a coral individual (Johnston et al., 2022; Turnham et al., 2021), while horizontally transmitted symbionts represent a greater flexibility in symbionts and subsequently higher symbiont diversity (Baird et al., 2007). However, the more recently described mixed-mode transmission of symbionts has introduced a greater complexity of these interactions (Quigley et al., 2017; Starko et al., 2024), warranting a need to test greater numbers of coral taxa with similar life-history demographics to clarify patterns in the host-symbiont relationship. In addition, understanding these patterns along strongly contrasting environments will better reveal how symbionts interact with host taxa and population structure in defining coral heat tolerance.

1.6 Isolated reefs and adaptive seascapes

Oceanic islands provide a lens to understand the ecological, evolutionary, and symbiotic relationships underpinning speciation, adaptation, and distribution (Borregaard et al., 2017;

Santos et al., 2016). Patterns of adaptation can be better understood when populations are in isolation, as opposed to highly connected reef systems which convolute the drivers of adaptation. The Coral Sea Marine Park is a unique seascape, where the remote and isolated nature of atoll reefs enable these reefs to act as 'natural laboratories' to elucidate the processes which drive adaptation (MacArthur & Wilson, 1967). This reef system spans 13º in latitude, 11º degree in longitude, and ranges in 2º C range in Maximum Monthly Mean temperatures. The Coral Sea is a physical bridge connecting the Great Barrier Reef (GBR), Coral Triangle, and other western Pacific provinces, and therefore represents significant ecological importance in connecting the flora and fauna between biodiversity hotspots (Bridge et al., 2019; Ceccarelli et al., 2013). Despite covering 1 million km^2, there is a paucity of data in the Coral Sea Marine Park relating to connectivity, biodiversity, and function of coral reefs. To date, only a single study has examined aspects of genetic structure or connectivity of corals in this region, with van Oppen et al. (2008) reporting the connectivity of *Seriatopora hystrix* from a single reef in the Coral Sea (Osprey reef) in relation to multiple reefs in the Great Barrier Reef. It is therefore important to gain new insights on interactions between reefs in the Coral Sea Marine Park to uncover patterns of adaptation and connectivity within the reef system, as well as with respect to other regions (i.e., GBR and western Pacific provinces).

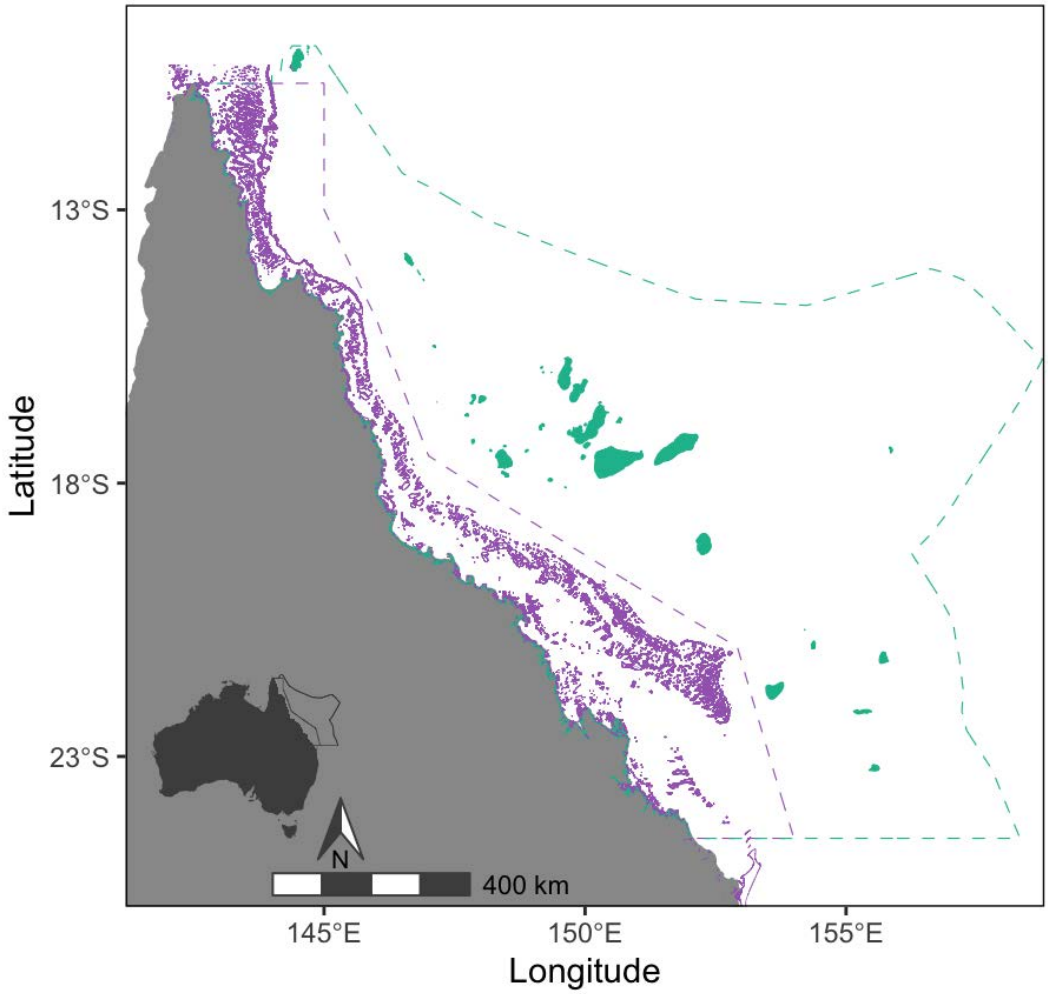

Figure 1.2. The Coral Sea Marine Park spans nearly 1 million km^2 and provides an avenue for connectivity of flora and fauna between western Pacific provinces and the Great Barrier Reef. The Coral Sea Marine Park is shown in green, and the Great Barrier Reef Marine Park is shown in purple.

1.7 Variable bleaching in the Coral Sea Marine Park

The Coral Sea Marine Park experienced severe, yet variable, bleaching during the mass bleaching events of 2016, 2017 (Harrison et al., 2019) and 2020 (Burn et al., 2023). The events in 2016 and 2017 revealed bleaching strongly correlated to the Degree Heating Weeks (DHW) experienced at each reef. The bleaching event in 2016 resulted in more localised heat stress to the central Queensland Plateau, compared to more geographically widespread, but less severe

bleaching in 2017 (Harrison et al., 2019). The experimental and genetic sampling collections for this thesis occurred during the peak of the 2020 bleaching event, allowing for the collection of samples of variable bleaching phenotypes, in tandem with ecological bleaching surveys. Of the 16 reefs monitored in 2020, bleaching responses were variable, where two sites had only 10-30% bleaching, four sites exhibited 30-60% bleaching, eight sites showed 60-80% bleaching, and two sites had over 80% bleaching overall (Burn et al., 2023). The bleaching severity in the 2020 event did not follow a latitudinal or longitudinal gradient, indicating other endogenous and/or exogenous factors attributed to shaping population-level bleaching responses. In my thesis, I aim to examine these factors, both attributed to extrinsic factors including past and current (2020) environmental and thermal conditions, as well as intrinsic factors including the adaptive and symbiotic components facilitating greater bleaching tolerance.

1.8 Thesis outline and aims

The overarching aim of this thesis is to disentangle the processes of coral heat tolerance adaptation at the level of individuals, populations, and species. Throughout all chapters, I use environmental gradients, symbiont community structure, experimental bleaching phenotypes, and host genetic structure to describe the patterns and understand the processes of coral heat tolerance. Chapter 2, published in the journal *Global Change Biology*, empirically investigates how heat tolerance varies among coral species and spatially among reefs spanning a heterogeneous environmental gradient. This chapter describes the patterns of species and population level differences in heat tolerance and identifies the contemporary (5 years) and historical thermal drivers (35 years) which underpin variability in tolerance. Chapter 3, published in the journal *Molecular Ecology*, investigates the relationship between coral symbiont (Symbiodiniaceae) diversity, the environment, coral host taxa, and host population

structure. Defining the host-environmental patterns of algal symbionts is critical to resolving the interactions and mechanisms which predominantly affect whether a coral will adapt or respond to changing thermal conditions. Chapter 4 assesses population demographics of genetic diversity and connectivity of two *Pocillopora* species to detect patterns in gene-environment associations. This chapter explicitly addresses the link between host genotype and environment, and whether patterns of selection occur in response to an environmental continuum. Finally, Chapter 5 investigates putative adaptive loci associated with heat tolerance in the coral host and the strongest predictors of phenotypic heat tolerance. Specifically, adaptive loci are identified in relation to environmental parameters to identify signals of selection on heat tolerance. To integrate all chapters, I also include a bleaching predictor model, where phenotypic heat tolerance from Chapter 2 (ED50) is modelled against symbiont communities, adaptive loci (polygenic score), neutral population structure, and environmental parameters. This final data chapter (Chapter 5) brings all these components together (phenotype, genotype, environment, symbionts) and provides strong link between phenotype, adaptive loci, and the influence of mild heatwaves.

Chapter 2: The effects of marine heatwaves on acute heat tolerance in corals

This chapter has been published as a peer-reviewed manuscript and the only text alterations are with respect to thesis formatting requirements, but otherwise appears as in the published version.

Marzonie, M. R., Bay, L. K., Bourne, D. G., Hoey, A. S., Matthews, S., V Nielsen, J. J., Harrison, H. B. (2023). The effects of marine heatwaves on acute heat tolerance in corals. *Global Change Biology*, *00*, 1–13. https://doi.org/10.1111/gcb.16473

2.1 Introduction

Marine heatwaves have emerged as the principal threat to coral reef ecosystems (Oliver et al., 2018; Smale et al., 2019), driving mass coral bleaching events and resulting in extensive coral mortality throughout tropical oceans (Hughes et al., 2018; Lough et al., 2018). Recent bleaching events have demonstrated a clear link between heat accumulation and coral bleaching (Hughes et al., 2017), whereby photosynthetic symbionts (Symbiodiniaceae) disassociate from the coral host during heat stress (either prolonged or acute), threatening the health and survival of corals (Baker, 2003; Glynn, 1984). The increasing persistence of marine heatwaves exposes corals to temperatures near, or above, their upper thermal limits (Heron et al., 2016) and will continue to threaten coral reefs globally (van Hooidonk et al., 2016). Despite the growing concerns of coral bleaching, there remains limited understanding of how different species and individuals respond to heat stress or the ability for corals to adapt or acclimate to changing environmental conditions. Therefore, investigating the phenotypic and genotypic diversity that underpins heat tolerance in coral populations is critical to predict the capacity for corals to acclimate and/or adapt to marine heatwaves.

Variation in bleaching susceptibility among coral species indicates there is considerable phenotypic variation in heat tolerance, primarily driven by phenotypic traits and physiological

trade-offs in metabolic costs (Grottoli et al., 2014; Loya et al., 2001; van Woesik et al., 2011). However, even within species, individual genotypes can exhibit variation in heat tolerance within the same environmental conditions (Barshis et al., 2013; Bay & Palumbi, 2014; Morikawa & Palumbi, 2019; Schoepf et al., 2015). Differences among genotypes are attributed to phenotypic plasticity (Oliver & Palumbi, 2011), underlying standing genetic variation of the coral host (Dixon et al., 2015; Drury, 2020; Fuller et al., 2020; Torda et al., 2017), and/or intraspecific variation in the symbiont community composition associated with individual colonies (Berkelmans & van Oppen, 2006; LaJeunesse et al., 2009). However, there is a paucity of data concerning the mechanisms or drivers of phenotypic variation in heat tolerance derived from standardised experimental approaches (Grottoli et al., 2021; McLachlan et al., 2020), in particular, those examining spatial variation in heat tolerance (Evensen et al., 2022).

Marine heatwaves on coral reefs are not evenly distributed in time and space and are key drivers of local- and regional-scale differences in coral community composition (Dietzel et al., 2021; Hughes et al., 2018; Oliver et al., 2018; Smale et al., 2019). Coral mortality associated with these events can result in strong selection for individuals with greater tolerance to heat stress (Palumbi et al., 2014; Sully et al., 2019). Therefore, heat tolerance in corals is expected to vary in relation to thermal exposure, influencing phenotypic diversity at the level of individual genotypes (Lundgren et al., 2013), fine-scale microhabitats (Cornwell et al., 2021; Hoogenboom et al., 2017; Schoepf et al., 2015) and populations (Berkelmans & Willis, 1999; Coles et al., 1976; Dixon et al., 2015; Guest et al., 2012; Howells et al., 2016). Meanwhile, temporal variability in thermal gradients, such as annual temperature ranges, the rate of summer warming, the frequency of warming events, and prior exposure to heat stress mediate the thermal optimum and thermal range of corals across days, seasons and years (Ainsworth et al., 2016; Jurriaans & Hoogenboom, 2020; Middlebrook et al., 2008). Overall, a complex

interplay of spatial and temporal variation in environmental conditions is an important determinant of the upper thermal limit in corals, which can lead to spatial variation in heat tolerance.

Early studies of heat tolerance in corals used long-term experiments (weeks to months) to simulate the accumulation of heat stress during natural bleaching events, establishing the conditions that trigger bleaching and identifying the thermal maxima (Coles et al., 1976; Jokiel & Coles, 1990). More recently, acute heat stress assays have demonstrated the capacity to effectively establish relative thermal tolerance of corals over much shorter periods (Barshis et al., 2013; Palumbi et al., 2014). While acute heat stress assays do not mimic natural bleaching events, proof-of-principle experiments have identified short-term acute heat stress assays (7 hours) as comparable to longer-term (21-day) heat stress assays in bleaching responses using dark-adapted maximum quantum yield (F_v/F_m) as a physiological metric, but not chlorophyll *a* or Symbiodiniaceae densities (Evensen et al., 2021; Voolstra et al., 2020). Additional ground-truthing has shown that estimates of absolute heat tolerance vary according to season and should be considered when comparing across studies (Cunning et al., 2021). However, relative estimates of heat tolerance rankings among coral genotypes remain consistent regardless of seasonality (Cunning et al., 2021). Hence, short-term acute heat stress assays provide a flexible and rapid approach to estimate heat tolerance for many individuals, populations and species, over much greater temporal and spatial scale than previously possible.

To understand the drivers of heat tolerance and improve forecasting for how coral assemblages will respond to future marine heatwaves, I quantified the spatial patterns of heat tolerance in three scleractinian coral species (*Acropora* cf *humilis, Pocillopora verrucosa* and *Pocillopora meandrina*) across nine widely separated populations in the Coral Sea Marine Park (CSMP),

Australia. Coral populations spanned 7.7 degrees in latitude (860 km) along a 1.6 ºC gradient in maximum monthly mean sea surface temperatures, providing a range of environmental conditions to investigate the possible drivers of heat tolerance. The isolated nature of reefs in the CSMP makes it an ideal system to investigate the possibility of local adaptation in heat tolerance, where the distance between reefs is likely to limit gene-flow between populations and where reefs are removed from other anthropogenic stressors (e.g., poor water quality). To investigate the possible drivers of phenotypic variation in heat tolerance, I compared spatial patterns of heat tolerance against trends in sea surface temperatures and the occurrence of marine heatwaves, consistent with local adaptation mediated by changing environmental conditions.

2.2. Methods

2.2.1 Coral species and sampling locations

The Coral Sea Marine Park (CSMP) is a critically important and significant ecosystem owing to its unique marine biodiversity and habitats (Ceccarelli et al., 2013). This seascape is characterised by isolated reef atolls with fauna distinct from that of the Great Barrier Reef (GBR). The geographic isolation of this reef system contributes to the genetic separation from Australia's GBR and other western Pacific biogeographic provinces (van Oppen et al., 2008), as well as isolation from local anthropogenic stressors. Colony fragments from three species of scleractinian corals were collected from nine reefs in the CSMP between February 16th and March 12th 2020 (Figure 2.1a). *Acropora* cf *humilis* (Dana, 1846; Figure 2.1b) is a digitate coral species, susceptible to heat stress and commonly found on exposed upper reef slopes (Hoogenboom et al., 2017). This species is denoted with 'cf' as coral samples most closely resemble *Acropora humilis*, but acknowledge that the complexities and rapidly changing taxonomy within the family Acroporidae may indicate multiple cryptic species are present in

the collection (Cowman et al., 2020). *Pocillopora meandrina* (Dana 1846; Figure 2.1c) and *Pocillopora verrucosa* (Ellis & Solander, 1786; Figure 2.1d) are both branching corals, distinguished by restriction fragment length polymorphism assays (Johnston et al., 2018), both characterised with a moderate heat sensitivity and commonly found in shallow waters in exposed and sheltered environments (Al-Sofyani & Floos, 2013). All three species are abundant in shallow habitats on reefs in the CSMP.

A high incidence of coral bleaching was observed over the course of sampling, owing to a severe marine heatwave in the CSMP in 2020. Sampled corals had therefore experienced 5.7 – 10.0 degree heating weeks (DHW) and exhibited different levels of bleaching prior to collection (Table 2.1). To account for the accumulated heat stress at each sampling location, the maximum DHW on the day each experiment took place was recorded (NOAA Coral Reef Watch 5km product, Table 2.1) to account for the effects of the experiments coinciding with a marine heatwave in all statistical analyses.

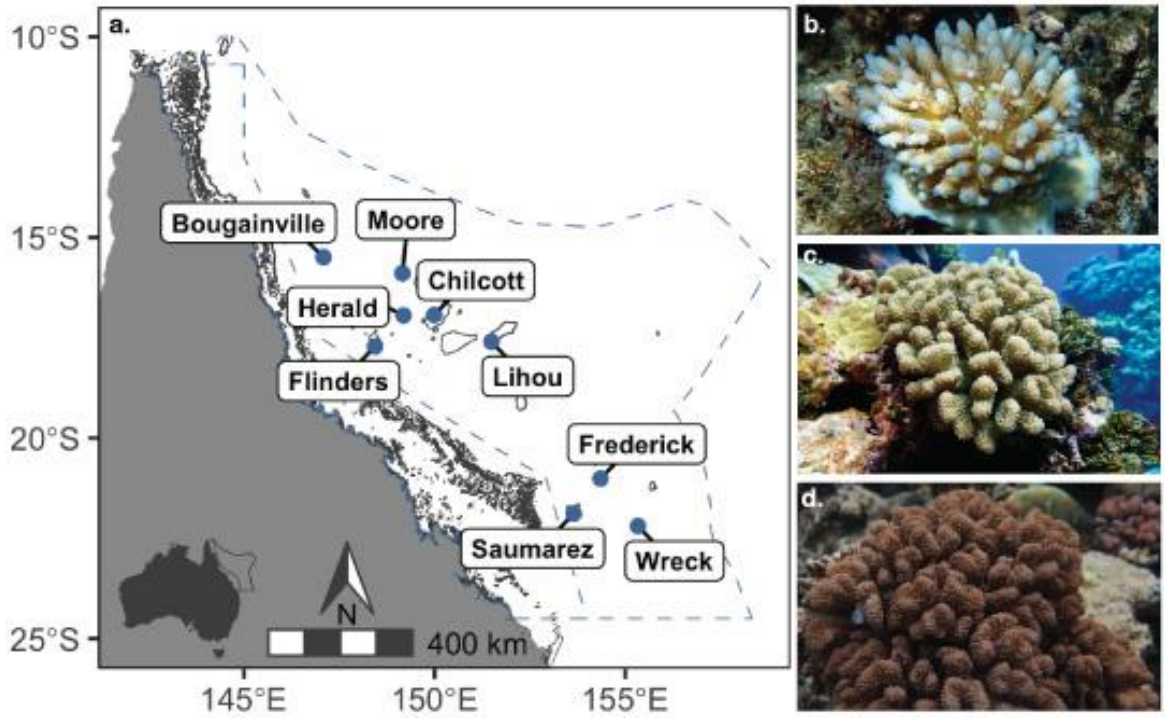

Figure 2.1. Map showing the location of the nine sampled reefs within the Coral Sea Marine Park (a). Coral fragments of each of the three coral species were collected from nine reefs between February and March 2020. The dashed line indicates the boundary of the CSMP. The three sampled coral species, *Acropora* cf *humilis* (b), *Pocillopora meandrina* (c) and *Pocillopora verrucosa* (d) are common on reefs throughout the CSMP.

2.2.2. Sample collection and processing

All samples were collected on SCUBA at an average depth of 8.0 ± 2.7 m, ranging between 1.9 – 16.4 m. Due to the ongoing bleaching event, colonies of all bleaching categories were sampled to avoid biasing collections towards bleached or unbleached coral colonies (SOM, Fig S1). During collection, each colony was assessed visually for bleaching from most bleached '1' to least bleached '6' using a Coral Watch Health Chart. Each coral colony was then photographed at three scales in the field, recording: (1) the unique bag identification number, (2) the whole colony and surrounding habitat with coral health chart and, (3) a detailed close-up of the colony. Coral fragments were collected from coral colonies > 5m apart to minimise the likelihood of collecting identical genotypes. Five fragments from each colony were collected; four were used in the heat stress experiment and the fifth was preserved in 100% ethanol for genetic analyses.

2.2.3 Experimental aquaria design and setup

The portable experimental aquaria system (National Sea Simulator, Australian Institute of Marine Science) consists of independent heating, lighting, sump and flow control elements. The system has four independent treatments with three 14L custom-made acrylic tanks per treatment, with space for 24 coral fragments in each tank (72 per treatment). Each treatment has independent custom lighting panels (600x340 mm, 300W white/blue LED) situated at a height of 650 mm above the tanks, heating elements (Omega 2kW titatium) in the sump, and

submersible pumps (Reefe RP2400LV 24v) to circulate water between the sump and insulating jackets (SOM, Fig S2a). Ambient seawater is directed through a titanium heating coil (Wateco 56" titanium heat exchanger) to the corresponding tanks in each treatment. Water flow to each tank was kept constant throughout each experimental heat stress assay (0.2 L min^{-1}). Tanks were equipped with a powerhead to increase water circulation within each tank. Lights were adjusted to maintain 600 PAR (µmol photons.$m^{-2}s^{-1}$) per tank as per average, mid-day summer light levels at 10 m at Lizard Island Research Station between 2012 – 2018 (Australian Institute of Marine Science, 2020).

Each tank, sump and jacket are equipped with independent water temperature sensors and two PAR sensors situated randomly within tanks to monitor and control temperature and lighting throughout the experiment. The temperature control system consists of three main elements: 1) a Programmable Logic Controller (PLC) system (Siemens S7 1511-1 PN PLC, 6ES7 511-1AK02-0AB0), 2) a Weidmuller UR20 Remote IO Signal Inputs & Outputs and 3) a Human Machine Interface (Siemens Simatic Human Machine Interface (HMI) KTP700 (6AV2123-2GB03-0AX0)). The PLC unit controls the lighting, pumps and heaters, interfacing with user parameters of the HMI to program parameter inputs, and to monitor and log temperatures in each tank.

2.2.4 Experimental design of acute heat stress assays

I conducted individual experimental acute heat stress assays for each of nine reefs where corals were collected. The planned experimental assay consisted of four temperature treatments: a control temperature treatment at the local maximum monthly mean (MMM), and three temperature treatments at +3 ºC, +6 ºC and +9 ºC above the local MMM. The local MMMs were calculated using sea surface temperature data obtained from the NOAA Coral Reef Watch Operational Daily Near-Real-Time Global 5-km Satellite Coral Bleaching Monitoring Product

Version 3.1 for each site within reef between 1986 to 2010. However, ambient temperatures were 1.0 – 2.2 ºC above local MMMs at the time of the experiments owing to a marine heatwave in the CSMP (Table 2.1), so the control treatments were done at ambient temperatures. A fragment of each sampled coral colony was placed randomly into each of the four temperature treatments following each collection dive. All genotypes across all species were present in each of the four treatments, and randomly placed in one of the three replicate tanks per treatment to minimise the effect of tank. Each coral fragment was identified by a unique clip and rack number corresponding to the original coral colony. Coral samples were held at local ambient temperatures until the start of each experiment, which started between 8 am and 10 am.

Each treatment followed a standardised temperature profile previously established by (Barshis et al. (2013), Palumbi et al. (2014), and Voolstra et al. (2020), to measure heat tolerance in corals. It consisted of a 3-hour ramp up to the desired treatment temperature, a 3-hour hold period at the treatment temperature and a 1-hour ramp down to ambient temperature (SOM, Fig S2b). The treatment temperature of each sump was randomised between experiments to control for any variability in ambient light among tanks. At the end of the temperature profiles, corals were maintained at ambient temperature for 11 hours prior to physiological measurements.

2.2.5 Measuring photochemical yield

Pulse amplitude modulated (PAM) fluorometry was used to measure photochemical yield (hereafter F_v/F_m), a non-obtrusive metric of chlorophyll-*a* fluorescence of the symbiotic algae (Schreiber, 2004) widely used as a proxy to rapidly measure heat tolerance in corals (Evensen et al., 2021; Nitschke et al., 2018; Suggett & Smith, 2011). Following the completion of the temperature profiles, experimental tanks were covered with a tarp to block all light for a

minimum of 5-hours. All measurements took place under indirect red light between 2am and 5am using a Diving-PAM fluorometer (Heinz Walz GmbH, Effeltrich, Germany). A clear piece of tubing was used to maintain a constant distance (2mm) between the fibre-optic probe (6mm Ø) and the coral tissue. PAM settings were adjusted between experiments to account for the latitudinal gradient in light and temperature and maintain baseline F_0 values between 130 – 500 units following standard procedures (Ralph et al., 2015). Detailed PAM settings for each experiment are outlined in SOM Table S1.

The photochemical yield of all coral fragments in all temperature treatments was measured three times to obtain average and median measures of F_v/F_m. False readings, where no fluorescence was measured, were discarded prior to averaging.

2.2.6. Species identification in Pocilloporidae

Species of *Pocillopora* can be difficult to distinguish *in situ* and from photographs, therefore all *Pocillopora* samples were identified to species level using a restriction fragment length polymorphism (RFLP) assay modified from (Johnston et al., 2018). Firstly, the mitochondrial open reading frame (mtORF) region was amplified with FatP6.1 primer (5'-TTTGGGSATTCGTTTAGCAG-3') and RORF primer (5'-SCCAATATGTTAAACASCATGTCA-3') (Flot et al. 2008). The PCR mix included 0.4 µl MyTaq Polymerase (5 u μl^{-1}, Meridian Bioscience), 4 µl Buffer (5x), 0.3 µl Purified BSA (100x, New England Biolabs), 0.25 µl of each primer (10mM), 13.8 µl of PCR-grade water and 1 µl of template DNA (5 ng μl^{-1}). PCR conditions were carried out with an initial denaturation step for 60 seconds at 94 °C, followed by 30 cycles of 94 °C for 30 seconds, 53 °C for 30 seconds, and 72 °C for 75 seconds, followed by a final elongation step at 72 °C for 5 minutes. Secondly, PCR products were digested using one of two enzymes to confirm the species identity of each sample. The *Aci*I restriction enzyme was first used to distinguish *P.*

verrucosa from all other species, and *Sac*I to distinguish *P. meandrina* from other Pocilloporidae. A volume of 8.9 µl of the PCR product was transferred to a new 96-well plate and 1.1 µl of *Aci*I restriction enzyme and buffer (New England Biolabs) was added to each sample. Samples were then incubated at 37 ºC for 60 minutes and transferred to 65 ºC for 20 minutes. The digest was run on a 2% agarose gel for 75 minutes at 70 volts. Samples with three bands at 209, 338 and 431 base pairs were identified as *P. verrucosa*, with other species having only two bands at 430 and 548 base pairs. Any remaining samples that were not identified as *P. verrucosa* were then digested using *Sac*I to distinguish *P. meandrina* from other Pocilloporidae. A volume of 8.95 µl of PCR product was transferred to a new 96-well plate and 1.05 µl of *Sac*I restriction enzyme and buffer (New England Biolabs) were added to each sample. Digestions followed the same protocol as above. Samples with two bands at 298 and 680 base pairs were identified as *P. meandrina* and samples with only one band at 978 base pairs were identified as *Pocillopora* spp. From the 243 total collected *Pocillopora*, 49 samples were identified as neither *P. verrucosa* nor *P. meandrina* and thus excluded from downstream analyses.

2.2.7 Modelling ED50 parameters for species and reefs

All analyses were performed in R v. 4.1.1 (R Core Team 2021) and are fully reproducible online (Appendix 1; https://github.com/HugoBH/CoralSea-ED50-GCB). To determine how heat tolerance varied among species or sampled reefs, a dose response curve was fit to the median yield of F_v/F_m across temperature treatment and compared the effective temperature to induce a 50% loss in median yield of F_v/F_m (hereafter ED50). It is comparable to the ED50 metric presented in (Evensen et al., 2021) and applied to other rapid heat stress experiments (Cunning et al., 2021; Evensen et al., 2022; Voolstra et al., 2021). First, measurements were removed where F_v/F_m values > 0.75 or where F_0 was < 110 to eliminate any false detections of the Diving PAM. For all ED50 estimate models, median yield was modelled against

temperature relative to local MMM (ºC) using a three-parameter dose response curve. Relative temperature was treated as a continuous variable and measured as the difference between the average temperature during the 3-hour hold period, and the local MMM (SOM, Table S2). All ED50 models were first constructed using the *drm* package to obtain reasonable starting coefficients (Ritz et al., 2015), which were then used to fit models in the *nlme* package v3.1-152 to account for random effects (Pinheiro et al., 2021). Model selection was informed by comparing AICc scores in the *MuMIn* package version 1.43.17 (Barton, 2022) and *post hoc* comparisons among fixed factors were performed using the *emmeans* package version 1.6.3 (Lenth, 2021).

To derive estimates of ED50 among the three coral species, I explored the importance of including parameter estimates for the slope, upper asymptote, and inflection point, as well as the influence of sampling depth, tank effects, and the severity of *in situ* bleaching of each coral colony. Lower asymptotes were fixed at zero. Model selection indicated all three parameters varied among species, with a small but non-negligible influence from the bleaching condition, but not depth or tank (SOM, Table S3). The best model included the interaction between 'Bleaching Category' and 'Species' for each parameter estimate of the dose response curve (SOM, Fig S3) and the random effect of 'Reef' to capture variability in responses that could be attributed to spatial variation. Plots of model residuals were visually inspected to check for patterns with respect to fitted values and predictor variables. *Post hoc* comparisons among fixed factors ('Species', 'Bleaching Category') were conducted to compare whether ED50s were significantly different among species (SOM, Table S4 and S5).

Separate models were constructed to derive estimates of ED50 among reefs since all species were not sampled at every reef. Model selection again included estimates for the slope, upper asymptote, and inflection point. Models were informed from the *A.* cf *humilis* data, which were the most comprehensive, and model parameters were then kept consistent for all species

(SOM, Table S6). The best fit model included the fixed factor of 'Reef' for the ED50 term and random effect of 'Bleaching Category' on the upper asymptote and 'Coral ID' on the ED50 parameter. To check the effect of unbalanced sample design, I tested the 'separate' reef models against a 'combined' model that incorporated all species but only with reefs in common between all three species. Estimates of reef ED50 values were comparable between models (SOM, Fig S4). *Post hoc* comparisons among fixed factors ('Reef') were conducted to compare whether ED50s were significantly different among reefs (SOM, Table S7, S8, and S9). ED50 values were also calculated for 'Absolute Temperatures' for each reef and species combination (SOM, Table S11) as an extension of the 'Relative Temperature' ED50 model values presented in the results (SOM, Table S10). To obtain 'Absolute Temperatures' thresholds, I added the local MMM of each reef to the Relative ED50 of each reef.

2.2.8 Environmental predictors of heat tolerance

To identify environmental drivers associated with coral heat tolerance, ED50 values derived from the Reef and Species models were related to a range of environmental predictors in the CSMP. These 24 environmental parameters represent recent (2016-2020) and historical (1986-2020) trends in the frequency and severity of marine heatwaves and sea surface temperatures in the CSMP (SOM, Table S12). The sea surface temperature and maximum degree heating weeks (DHW) values were generated from the NOAA Coral Reef Watch Operational Daily Near-Real-Time Global 5-km Satellite Coral Bleaching Monitoring Product Version 3.1 for each site within reefs from 1986-2020. These were used to calculate metrics that represent the temperature regimes and history of reefs in the CSMP. These included the historical (1986-2020) and recent (2016-2020) maximum and average DHW, the number of events where DHW exceeded 2, 3, 4, 6, 8 and 9 DHW (1986-2020), the average return time in years between these events, the DHW during the experiment, along with latitude and longitude (SOM, Fig S5). Each environmental predictor was individually fitted against ED50 values measured for each

reef within species to assess the strength of their correlation. All predictors with a correlation coefficient below 0.40 were removed from further candidate model selection (SOM, Fig S6). This left ten remaining variables of interest, which were each tested for collinearity. Any variables with a correlation > 0.80 were excluded from further analysis, including 'minSST', 'meanSST', 'DHW2020', 'MMM', 'Latitude' and 'rangeSST' (SOM Table S12, SOM Fig S10). After removing highly collinear variables, this left four variables to represent the different climatic regimes between reefs: the number of events were DHW exceeded 4 ('DHW4'), the average maximum DHW between 2016 and 2020 ('recent.maxDHW'), the return time in years between events were DHW exceeded 6 DHW ('returnDHW6'), and the variance in SST ('varSST') (SOM, FigS7). These response variables were tested in candidate model selection using the 'dredge' function in the package *MuMIn* (Barton 2022) and the model with the lowest AICc score was chosen. The final model included an interaction between Species and 'DHW4', and additional fixed effects of 'returnDHW6' and 'recent.maxDHW' (SOM, table S13). Results from the 'dredge' model were cross validated with a generalised boosted model (GBM) approach (Greenwell et al. 2020). While the GBM approach did not reach a parsimonious solution due to limited sample size, the results corroborated the importance of the number of mild bleaching events ('DHW4') as the strongest driver of increased ED50 values.

2.3 Results

2.3.1 Photochemical performance under natural heat stress

Our experiments were conducted during a severe marine heatwave in the CSMP that led to widespread coral bleaching throughout the region. Accumulated heat stress ranged from 5.7 DHW (Wreck Reef) to 10.0 DHW (Bougainville Reef), with ambient water temperatures between 1 to 2.2 ^{o}C above local MMM at the time of sampling (Table 2.1). The marine

heatwave was ongoing and analysis of SST and DHW over the subsequent months suggests the experiments were conducted at the peak of this event. I collected 182 *A.* cf *humilis* and 194 *Pocillopora*, identified as 101 *P. verrucosa* and 93 *P. meandrina* across all categories of bleaching (SOM, Fig S8) from nine reefs in the CSMP. Fluorescence analysis using PAM fluorometry of coral fragments kept at ambient temperature indicate a minor loss in photochemical yield at higher levels of bleaching (Contrast Category 1 - 2 vs 3 - 6), consistent with natural levels of heat stress (SOM, Fig S9). The minor effects of natural bleaching were accounted for by including the Bleaching Category as an interaction for estimates in ED50 values for both species and reef predictions (see *Methods* Section 2.7).

Table 2.1. Location and environmental conditions where corals were collected for acute heat stress experiments in the CSMP. Ambient sea surface temperature (SST, ºC) and degree heating weeks (DHW) were measured at the time of each experiment. Maximum monthly mean temperature (MMM, ºC) is defined for each reef as the average SST of the hottest month in each year between 1986 and 2010. Number of DHW4 events is measured as the number of events where DHW ≥ 4 (1986 – 2020), averaged among sites within a reef. The number of corals of *Acropora* cf *humilis*, *Pocillopora verrucosa* and *Pocillopora meandrina* collected from each reef that were included in the logistic regression model.

Experiment location	**Lat (DD.dddd)**	**Long (DD.dddd)**	**Ambient SST (ºC)**	**MMM (ºC)**	**DHW**	***A.* cf *humilis* (n = 182)**	***P. meandrina* (n = 101)**	***P. verrucosa* (n = 93)**
Bougainville	-15.4927	147.0863	29.99	28.96	10.00	23	10	17
Moore	-15.8921	149.1535	30.45	28.83	9.06	20	17	10
Chilcott	-16.9315	149.9898	29.93	28.59	6.65	18	10	3
Herald	-16.9434	149.1856	29.93	28.59	7.96	18	5	11
Lihou	-17.5970	151.4895	30.48	28.44	7.72	32	6	18
Flinders	-17.7135	148.4371	30.67	28.64	6.58	30	5	26
Frederick	-21.0113	154.3504	29.98	27.77	7.01	17	13	2
Saumarez	-21.8861	153.6476	29.63	27.90	5.50	-	22	-
Wreck	-22.1926	155.3340	29.55	27.41	5.71	24	13	6

2.3.2 Photochemical performance under acute heat stress

The F_v/F_m of coral fragments was measured across different temperature regimes to determine the tolerance of species and reefs to acute heat stress. Temperature treatments were maintained at ambient temperatures (29.55 – 30.67 ºC), and +3 ºC, +6 ºC and +9 ºC from local MMM (27.41 – 28.96 ºC). Temperatures exhibited some variability within and between experiments, though closely matched target temperatures (SOM, Table S2).

A greater inhibition of photochemical yield at the higher temperature treatments was observed as anticipated, reflecting the decline in F_v/F_m in response to increased temperature. A median F_v/F_m yield of 0.61 (± 0.06) was observed for fragments maintained at ambient temperatures. Relative to controls, a 1.3% increase in F_v/F_m was detected in the +3 ºC treatment (median yield: 0.62 ± 0.05). At +6 ºC, F_v/F_m decreased by 11.8% relative to controls (median yield: 0.55 ± 0.11) with high levels of variation among coral colonies. At +9 ºC, F_v/F_m decreased by 86.0% relative to controls (median yield: 0.09 ± 0.09).

2.3.3 Heat tolerances (ED50) among species and reefs

The effective temperature to induce a 50% loss in F_v/F_m (ED50) was used to compare heat tolerance among three species of corals and among reefs within species. Overall, I measured a 0.69 ºC range or 9% difference in ED50 between the most and least tolerant species (Fig 2a). For *Acropora* cf *humilis*, a 50% reduction in F_v/F_m (ED50) was observed at 7.05 ºC above MMM (95%CI: 6.75 – 7.35) compared to 7.42 ºC above MMM in *P. meandrina* (95%CI: 7.11 – 7.74), and 7.74 ºC above MMM in *P. verrucosa* (95%CI: 7.43 – 8.06). Non-overlapping 95% confidence intervals in the estimated marginal mean for *A.* cf *humilis* and *P. verrucosa* indicates the differences in ED50 are very likely to indicate a true difference in heat tolerance between species (SOM, Table S4). Within *Pocillopora*, ED50 was 0.32 ºC greater in *P. verrucosa* than in *P. meandrina* with Tukey's pairwise comparison indicating the difference was significant (t = 3.733, df = 1148, p = 0.006) (SOM Table S5).

Heat tolerance also varied amongst reefs within species whereby the range of ED50 values was greater between the most and least tolerant reefs than it was between species (Fig 2b). In *A.* cf *humilis*, I measured a 1.89 ºC range in ED50 between the lowest value measured at Herald Reef (ED50 = 6.37, 95%CI: 6.14 – 6.59) and highest value at Wreck Reef (ED50 = 8.26, 95% CI: 8.08 – 8.43). In *P. meandrina*, there was a 1.15 ºC range in ED50 between the lowest value

measured at Lihou Reef (ED50 = 6.96, 95%CI: 6.61 – 7.31) and highest value at Flinders Reef (ED50 = 8.11, 95% CI: 7.81 – 8.42). In *P. verrucosa*, I measured a 0.85 ºC range in ED50 between the lowest value measured at Herald Reef (ED50 = 7.26, 95%CI: 7.01 – 7.51) and Flinders Reef (ED50 = 8.11, 95% CI: 7.93 – 8.28). Though spatial patterns were not consistent between species, some reefs showed significantly higher (e.g., Wreck Reef) or lower (e.g., Herald Reef) heat tolerance that could not be explained by variation between individual colonies alone (Tukey's pairwise comparisons: Tables S7, S8 and S9).

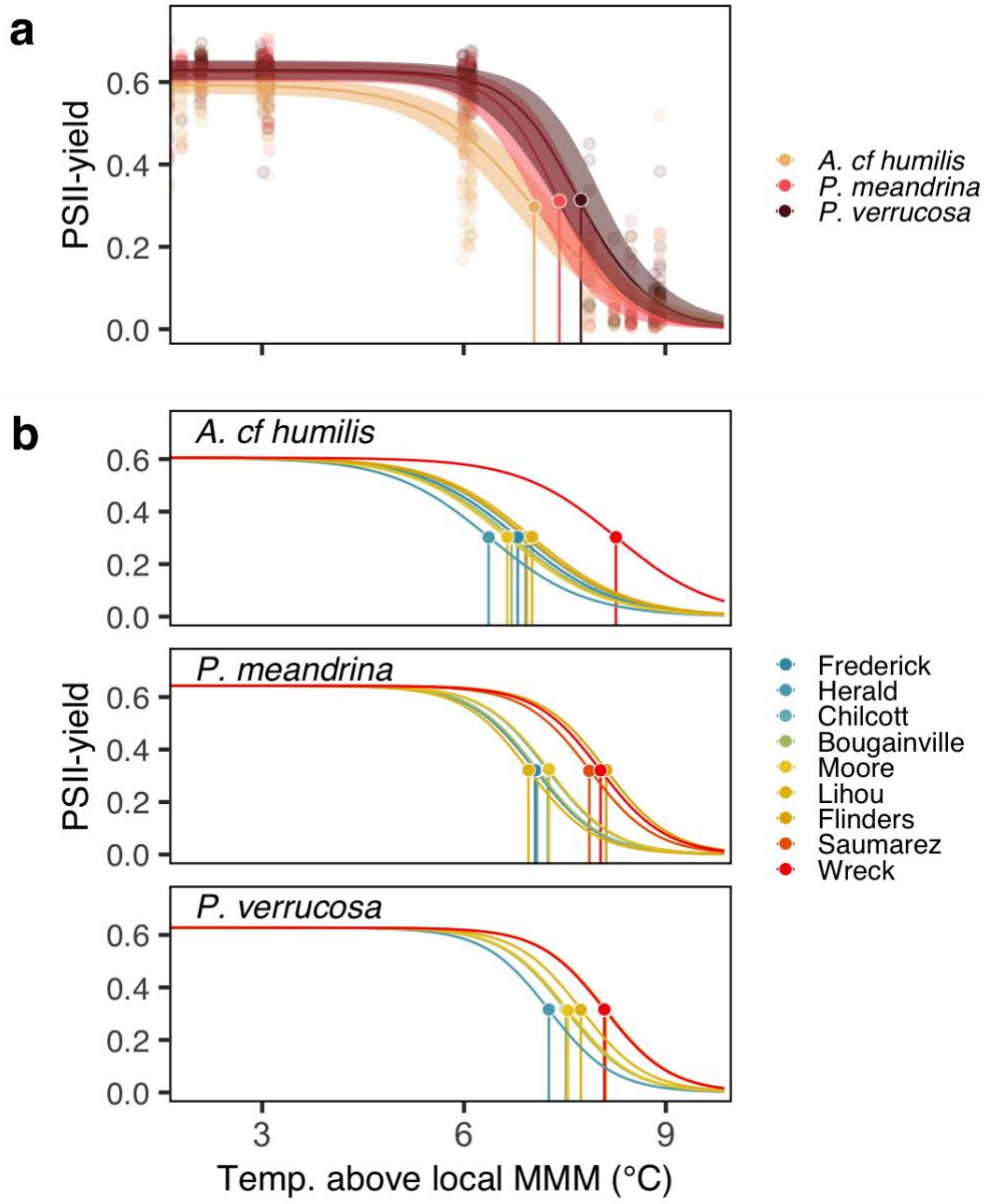

Figure 2.2. Temperature above local maximum monthly mean (MMM, ºC) at which 50% loss in F_v/F_m occurs (ED50) for three coral species. (a). Phenotypic variation in heat tolerance among species measured throughout the CSMP. Points indicate measures of F_v/F_m for individual coral genets in each treatment. Confidence bands indicate 95% confidence intervals (b). Phenotypic variation in heat tolerance among reefs for each species. Colour represents samples collected from distinct reefs in the CSMP. Reefs are sorted by colour from lowest ED50 values (blue) to highest (red) averaged across species. Vertical lines indicate the temperature above MMM to induce 50% loss in F_v/F_m (ED50)**.**

2.3.4 Predictors of heat tolerance

Spatial variation in ED50 values (Fig 3a) was explored against environmental variables that reflect the temperature regimes and exposure to temperature anomalies of reefs in the CSMP. A linear model that included three long-term and short-term thermal history metrics resulted in the best prediction of ED50 (SOM, Table S13). These environmental predictors included 1) the number of mild heatwaves where DHW was above or equal to 4 from 1986-2020 at each sampled reef (nDHW4), 2) the average maximum DHW experienced from 2016-2020 (recent maxDHW), and 3) the return time in years between heatwaves where DHW was above or equal to 6 (return DHW6). The model's total explanatory power was substantial ($R^2 = 0.81$). Species, the number of mild heatwaves (nDHW4) and their interaction explained 62.0% of model variance, while recent maximum DHW explained 21% of variation (recent maxDHW), and the return time between more severe heatwaves (return DHW6) accounted for 17% of variation. Other interactions among predictors were explored and none improved the model. Other variables, including reef complexity, longitude, reef area and a range of thermal history metrics (SOM, Fig S5) were either poorly correlated or insufficient to explain the spatial variation in heat tolerance.

The heat tolerance of all three species was most strongly driven by the number of mild heatwaves, the strength of which varied among species (Fig 3b) and for which spatial patterns were highly heterogeneous throughout the CSMP (Fig 3c). The strongest effect was observed for *A.* cf *humilis*, for which each mild heatwave increased ED50 by 0.25ºC (Slope = 0.255, t = 4.2, $p < 0.001$). The effect was weaker and not significantly different from 0 for both *P. meandrina* (Slope = 0.048, t = 0.83, p = 0.42) and *P. verrucosa* (Slope = 0.042, t = 0.61, p = 0.55) (SOM, Table S13), though these were different to *A.* cf *humilis* (t = 2.6, p = 0.05). Overall, greater exposure to mild heatwaves resulted in higher estimates of heat tolerance as measured by ED50 only in *A.* cf *humilis*. Meanwhile, greater exposure to higher DHW values between 2016 and 2020 has an effect of decreasing ED50 values (Fig 3d-e; Slope = -0.176, t = -2.3, p = 0.04), and greater intervals between more severe heatwaves (DHW $\geq$ 6) had the effect of increasing ED50 values (Fig 3f-g; Slope = 0.053, t = 2.4, p = 0.03). These patterns were strongly influenced by Wreck Reef with the greatest exposure to mild heatwaves between 1986 and 2020 (n = 10) and the high ED50 for all three species (SOM, Table S10). In contrast, Flinders reef appeared as an outlier with high ED50 for both Pocilloporidae despite low exposure to mild heatwaves (n = 5) (SOM, Table S10).

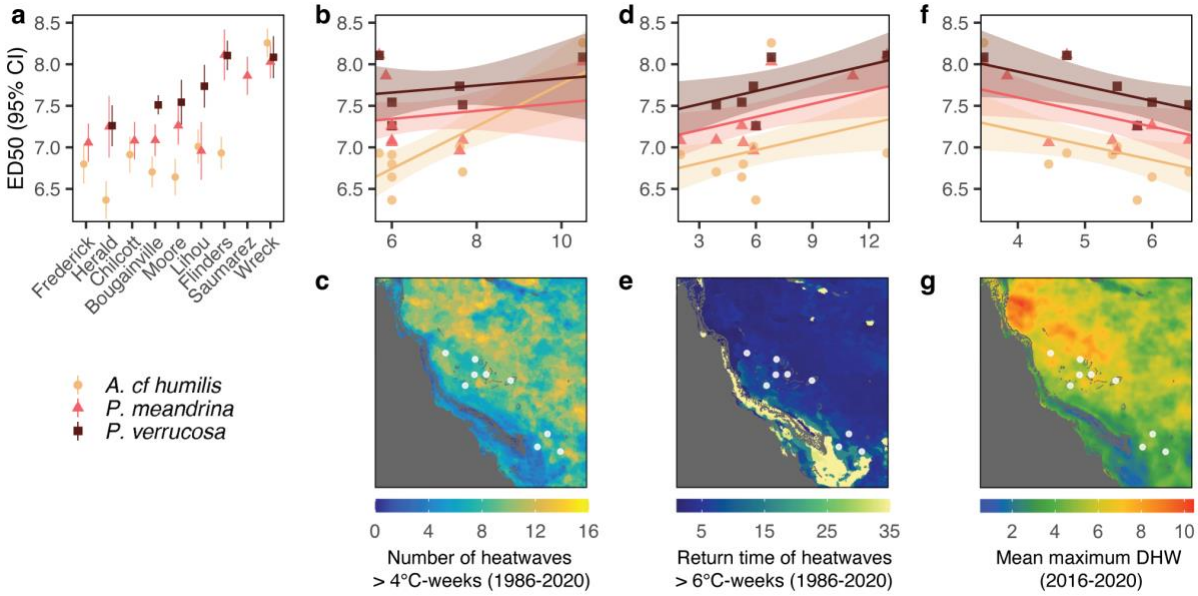

Figure 2.3. Spatial heterogeneity in heat tolerance (ED50) among reefs in the CSMP is strongly associated with their exposure to the number of mild marine heatwaves. (a). Heat tolerance as measured by the temperature above local MMM to induce a 50% loss in F_v/F_m (ED50) varies between species and between isolated reefs in the CSMP. Reefs are sorted by lowest ED50 values (left) to highest (right) averaged across species. Estimated marginal means of three environmental predictors (b, d, f) while other parameters are held constant. (b-c). The number of marine heatwaves between 1986 and 2020 where DHW was above or equal to 4 was the best predictor of heat tolerance (ED50) of reefs in the CSMP. (d-e). The return time between heatwaves where DHW was above or equal to 6 between 1986 and 2020 also explained sufficient variation in heat tolerance of reefs in the CSMP. (f-g). The average maximum DHW between 2016 and 2020 was the third environmental predictor to explain variance in heat tolerance. Each of the three predictors vary spatially across the seascape (c, e, g), including at the nine reefs where heat tolerance was quantified experimentally and depicted as white points.

2.4 Discussion

Acute heat stress experiments identify phenotypic variation for heat tolerance

Identifying spatial mosaics of heat tolerance across climatic and disturbance gradients is key to understanding the adaptative potential of corals to the increasing frequency of marine heatwaves. To date, smaller reciprocal transplant experiments have identified genetic mechanisms of the coral host (Kenkel et al., 2013) and symbiont community structure (Marhoefer et al., 2021) that influence thermotolerance and signify local adaptation to thermal regimes, but also indicate limits for corals to respond to temperatures outside of their local conditions (Howells et al., 2013). Building on these principles, standardised acute heat stress experiments have qualified as high throughput scans for phenotypic variation, successfully demonstrating that heat tolerance variation exists across coral nursery gardens in the Florida Keys (Cunning et al., 2021), thermally variable patch reefs across the Palau archipelago (Cornwell et al., 2021) and among microhabitats (Voolstra et al. 2020), and contrasting reef populations in the Red Sea (Evensen et al., 2022; Voolstra et al., 2021). The portability of the field-based, acute heat stress experimental aquaria system (designed and built at National Sea Simulator, AIMS) allowed us to quantify heat tolerance across a large spatial scale comprised of variable thermal history *in situ*. These findings provide further evidence that inter-reef differences in thermal tolerance broadly correspond with localised differences in thermal exposure. Thus, providing evidence that coral populations may be locally adapted to the increasing frequency of sub-lethal marine heatwaves they have been exposed to.

Phenotypic variation in heat tolerance among species within reefs

While knowledge of the mechanisms that confer heat tolerance in reef-building corals remains limited, experimental studies demonstrate the capacity for short-term acclimation (DeCarlo et al., 2019; Howells et al., 2013) and long-term adaptation in response to heat stress (Bay &

Palumbi, 2014; Dixon et al., 2015; Drury, 2020; Drury et al., 2017; Kenkel & Matz, 2017). Such variability between species, particularly within the same environment, is typically associated with gene-based adaptation (Fuller et al., 2020; Morikawa & Palumbi, 2019) and/or variation in symbiont community structure (Oliver & Palumbi, 2011). In my experiments, three coral species were exposed to the same local environmental and experimental conditions yet, exhibited variable ED50 thresholds ranging up to 0.7 ^{o}C. In the case of two closely related *Pocillopora* species (Johnston et al., 2017), the differences in heat tolerance may be attributed to variation in heat tolerance among symbionts, as *P. verrucosa* and *P. meandrina* are highly specific in symbiont community selection (Turnham et al., 2021), attributed to vertical transmission of symbionts to offspring (Hirose et al., 2000). Heat tolerance differences in these symbiont species can influence the ability of the host to respond to heat stress changes (Manzello et al., 2019), depending on the heat tolerance potential of the symbiont itself. Phenotypic variation within *A.* cf *humilis* may also be attributed to variation in symbiont species, though I could not exclude cryptic host speciation in the CSMP, as these samples have not been genetically confirmed as one species. The question of species identification may also lend itself to the broad range of ED50 values for *A.* cf *humilis* compared to the relatively narrow range for both species of *Pocillopora*, for which species identification has been confirmed. These questions require additional genetic studies to fully disentangle species level patterns of heat tolerance for *Acropora*.

Spatial variation in heat tolerance

Oceanic islands have served as model systems to evaluate the drivers of species richness, assembly rules of ecological communities and adaptive speciation, and provide insights into ecological and evolutionary processes (Borregaard et al., 2017; Santos et al., 2016). The geographic separation of reefs in the CSMP and distinct thermal histories may promote

phenotypic variation within species and adaptation to local thermal regimes, where limited gene flow can reinforce processes of genetic drift and natural selection in spatially heterogeneous environments (Kawecki & Ebert, 2004; Savolainen et al., 2013). Of the 24 environmental variables measured, three thermal history metrics were identified as possible drivers of heat tolerance of reefs, driving responses more than latitude, sea surface temperature, depth and the 2020 marine heatwave. Notably, the frequency of mild heatwaves in a local environment was a key driver of increased heat tolerance in *A.* cf *humilis*. Populations harbouring the most heat tolerant corals (e.g., Wreck Reef) experienced historically higher frequency of mild heatwaves over the past 35 years. Conversely, reefs which have evaded a high frequency of mild heatwaves (e.g., Herald Reef) tended to harbour assemblages of less tolerant individuals. For corals, a critical tipping point for bleaching-induced mortality occurs when accumulated heat reaches 3 - 4 DHW, indicating that DHW above this threshold can influence heat tolerance population-dynamics (Hughes et al., 2018). *Acropora* cf *humilis* in particular displayed a strong exposure relationship to mild heatwaves, which may be linked to this species' higher sensitivity to heat stress. In addition to mild heatwaves, a longer return time between severe heatwaves above or equal to 6 DHW aided acute heat tolerance, likely allowing sufficient time for populations to recover from lasting effects of severe heatwaves.

The beneficial selection of mild heatwaves, as well as a longer return time between heating events, may be hampered by recent severe heatwaves over the past five years, as indicated by the strong effect of recent maximum DHW on acute heat tolerance (i.e., average maximum DHW between 2016-2020). The effect of recent severe marine heatwaves over this period is an indication that corals may not be able to keep up with the pace of rapidly reoccurring marine heatwaves. Rapid environmental change, such as three mass bleaching events in five years, does not support rates of phenotypic plasticity for most individuals and species (Lindsey et al.

2013). Further, the lack of correlation between severe heatwaves (i.e., number of DHW events exceeding 6 or 9) and higher heat tolerance, suggests significant limits to adaptation potential in corals above a threshold where bleaching-induced mortality occurs (Ainsworth et al., 2016). The lack of improved prediction may be due to severe heatwaves causing increased coral mortality of all genotypes, rather than acting as a selective pressure. A similar phenomenon was observed during the back-to-back bleaching events of 2016 and 2017 on the GBR and Coral Sea, where a reduction in the incidence of bleaching in 2017 was attributed to extensive bleaching-induced mortality of corals in 2016, leaving few corals left to bleach in severely affected reefs (Harrison et al., 2019; Hughes et al., 2018). Thus, mild heatwaves provide environmental pressure that is strong enough to select for heat tolerance but not too strong to decimate entire populations.

Global comparisons of ED50 thresholds

There are several applications for colony-specific coral acute heat stress data. A few examples include the ability to rank heat tolerance among individuals, to investigate genotype – phenotype associations to identify molecular signatures of heat tolerance, and to explore cross-study comparisons of heat tolerance thresholds of corals. The ED50 estimates calculated here relate to ecologically meaningful temperatures, and the ranking of both relative and absolute ED50s allows for direct comparisons within and between studies, overcoming a major challenge in comparing heat stress experiments (Grottoli et al., 2021; McLachlan et al., 2020). Coral populations experiencing historically higher temperature regimes are generally less susceptible to bleaching than conspecifics in other regions (Howells et al., 2016). However, the absolute ED50 thresholds for *P. verrucosa* in the CSMP were very similar to conspecifics in the Red Sea (Absolute ED50/ED50: CSMP = 36.1 ^{o}C; Red Sea = 36.0 ^{o}C) (Evensen et al., 2022), despite the hotter conditions in the Red Sea, 1.3 ^{o}C above those in the CSMP.

Interestingly, *P. verrucosa* in the CSMP maintained overall higher relative ED50s (i.e., ºC above local MMM temperatures) than *P. verrucosa* in the Red Sea by 1.2 ºC (Relative ED50/ED50: CSMP = 7.7 ºC; Red Sea = 6.3 ºC) when comparing averages across each reef to characterise a region. The relative tolerance of corals in the CSMP compared to corals in other regions may indicate that corals in the CSMP are not living as close to their thermal limits as predicted. Potentially, the high disturbance history of the past three decades, layered with episodic heatwaves experienced in the last five years in the CSMP (Harrison et al., 2019) has selected for more heat tolerant individuals. Across a latitudinal gradient, *P. verrucosa* in both this study and Evensen et al. (2022) maintained higher relative thermal thresholds in high latitude reefs compared to low latitude reefs, supporting previous evidence that high latitude reefs may harbour higher heat tolerance and therefore serve as spatial refugia from bleaching events (Osman et al., 2018). These comparisons provide valuable insight to identify reefs and regions of high or low tolerance, albeit the comparisons across variable aquaria systems (e.g., lights, flow) may confound these interpretations and should also be considered.

Conclusions

Coral populations in this study demonstrated extensive phenotypic variation in heat tolerance across large spatial gradients, predominantly driven by the frequency of mild heatwaves. I identified that thermal regimes are a clear driving force in heat tolerance, explaining spatial variation in heat tolerance among coral reef populations. The strong link between acute heat tolerance and the frequency of mild heatwaves is evidence that coral populations are likely adapting or acclimatizing to both recent and long-term thermal history in their local environment. However, decreased coral heat tolerance in response to recent severe heatwaves warrants concern for the potential adaptation and acclimation limits of coral populations to marine heatwaves within ecologically relevant timeframes.

Chapter 3. Symbiodiniaceae diversity varies by host and environment across thermally distinct reefs

This chapter has been published as a peer-reviewed manuscript and the only text alterations are with respect to thesis formatting requirements, but otherwise appears as in the published version.

Marzonie, M.R., Nitschke, M.R., Bay, L.K., Bourne, D.G., Harrison, H.B. Symbiodiniaceae diversity varies by host and environment across thermally distinct reefs (2024). *Molecular Ecology*. https://doi.org/10.1111/mec.17342

3.1. Introduction

Tropical coral reefs rely on endosymbiotic algae, Symbiodiniaceae (LaJeunesse et al., 2018), that provide nutrition to support the function and survival of reef-building corals (Baker, 2003; Muscatine, 1990). Even a slight increase of 1-2 ºC above current sea surface temperatures (SST) can disrupt the delicate balance between corals and their symbionts (Weis, 2008; Weis et al., 2008), resulting in cascading negative effects on reef ecosystems (Baker et al., 2008; Graham et al., 2007). Symbiodiniaceae play a critical role in mediating coral susceptibility to thermal stress through adaptive and acclimatory mechanisms (Manzello et al., 2019; Marhoefer et al., 2021; Morikawa & Palumbi, 2019) that vary according to coral taxa (Quigley et al., 2022) and divergent symbiont lineages (Abrego et al., 2008; Butler et al., 2023). The increased frequency and duration of marine heatwaves have already impacted coral reefs globally (Hughes et al., 2017; Oliver et al., 2018). Thus, understanding the evolutionary relationships between corals and their symbionts can transform our understanding of adaptive traits in response to rapid environmental change.

The stability and flexibility of the coral symbiosis relies on the mode of symbiont transmission to coral offspring (Baker, 2003). Corals which vertically transmit symbionts directly to eggs often mediate strong co-diversification over long evolutionary periods (Turnham et al., 2021),

resulting in stronger host effects on symbionts and adaptive responses of corals to their environment (Seah et al., 2017). In contrast, horizontally transmitting coral species produce aposymbiotic larvae which acquire symbionts from the surrounding environment, promoting greater flexibility in symbiont selection and enabling the rapid acquisition or exchange of symbionts better suited for their environment (Baird et al., 2007; Cumbo et al., 2013). In the face of a disturbance, horizontally transmitting corals harbour a greater ability to shuffle or switch dominant and background symbiont species (Elder et al., 2023; Jones & Berkelmans, 2010), though can be disadvantageous during periods of stress if the symbionts are not well-adapted to variable or extreme conditions due to a lesser ability for host-symbiont co-diversification (LaJeunesse et al., 2010). There is also mounting evidence that some vertical transmitting corals have a mixed-mode of symbiont transmission, complicating the symbiont-host relationship over the lifespan of a coral (Quigley et al., 2017, 2018; Starko et al., 2024). Therefore, resolving the effect of host species on symbiont community structure requires parallel investigation of multiple species with similar demographics.

The transmission strategy of the coral host influences the extent to which the environment structures symbiont communities (van Oppen & Medina, 2020). Vertically transmitting species often maintain a stronger host genotypic effect as the primary driver of symbiont community structure in comparison to strong environmental gradients (Hume et al., 2020; Voolstra et al., 2021). In horizontally transmitting species, Symbiodiniaceae community changes are generally structured by their environment, including variable thermal fluctuations or chronic thermal disturbances (e.g., mass bleaching events) (Howells et al., 2020; Kennedy et al., 2016; Quigley et al., 2022). In addition to strong environmental effects, there is evidence of secondary host effects on symbiont community structure in horizontally transmitting corals such as *Acropora* spp. (Cooke et al., 2020; Matias et al., 2023), alluding to both host and environment influences

on symbiont community structure. Thus, it is likely that while vertical and horizontal transmission of the host is the dominant structuring predictor in symbiont communities, there are underlying influences of the environment which interact with host genotype. Analysing both host and symbiont genetic diversity in parallel with contrasting environmental gradients can provide insight into how host species, genotypes, and environment co-regulate the impacts on Symbiodiniaceae community structuring.

To address this knowledge gap, I investigate the influence of coral host genetics and environment on symbiont macroscale community structure. Here, symbiont macroscale community structure is defined as the diversity of Symbiodiniaceae among conspecific hosts living along an environmental continuum (hereafter defined as 'symbiont communities') (Davies et al., 2023; LaJeunesse et al., 2010). The diversity and distribution of Symbiodiniaceae in relation to host population structure and the environment, in particular, current and historical thermal stress, enables the identification of key genetic and environmental drivers that affect the capacity for corals and their symbionts to cope with climatic extremes into the future. To achieve this, I used ITS2 metabarcoding and a supporting genetic marker ($psbA^{ncr}$) to analyse patterns of symbiont community composition, in parallel with host genotype-by-sequencing, to describe trends of host population structure and host-symbiont co-phylogeny. My approach targeted three coral species, two with vertical symbiont transmission, *Pocillopora verrucosa* and *P. meandrina*, and one with horizontal transmission, *Acropora* cf *humilis*. All coral species were sampled across a 1,300 km gradient in Australia's Coral Sea Marine Park. Specifically, I tested the effects of biogeographic variables (latitude), historical thermal disturbances (maximum Degree Heating Weeks [maxDHW]), light attenuation in seawater (kd490), and individual-specific variables (depth and host genetic cluster). Samples were collected during the height of the mass bleaching event in 2020,

therefore, I also accounted for accumulated heat of each reef (DHW at collection) and the bleaching condition of each coral colony in relation to symbiont community structure.

3.2. Materials and Methods

3.2.1 Sampling location and study species

Coral samples were collected on SCUBA from 13 reefs within the Coral Sea Marine Park (CSMP) between February 16th and March 12th, 2020 (SOM, Table S3.1). Reefs in the CSMP have historically been exposed to a range of disturbances including regular and severe marine heatwaves (Harrison et al., 2019). There are currently no records for Symbiodiniaceae genetic diversity in the CSMP, despite this region covering nearly 1 million km^2 and connecting fauna of the Great Barrier Reef to other western Pacific reefs (Payet et al., 2022; van Oppen et al., 2008). For this study, a total of 609 coral samples were collected from two genera, including 346 *Pocillopora* samples and 262 *Acropora* samples. Samples were collected at an average depth of 7.8 m (± 2.7), ranging between 2-16 m and sampled during the 2020 bleaching event where reefs had been exposed to between 5.7 and 10.0 DHW at the time of collection. Corals were sampled during or immediately after the peak of the marine heatwave (SOM Figure S3.1). Within each reef, a range of bleaching phenotypes for each coral species was collected. The visual bleaching score of each coral colony was first scored against a six-point Coral Watch health chart (Siebeck et al., 2006) and collection depth was recorded in situ. Corals were photographed using an Olympus TG5 at the whole colony level and at a macro-scale to assist in species identification. Coral fragments were then collected using a hammer and chisel and each individual coral fragment was placed into a resealable, numbered Ziploc bag. After each dive, coral fragments were preserved in 100% ethanol and exchanged twice.

3.2.2 DNA extractions and genetic markers for Symbiodiniaceae identification

DNA was extracted from coral samples of *Pocillopora* and *Acropora* using a modified version of Wayne's method (Wilson et al., 2002). Following extractions and after a minimum of 24 hours, DNA concentrations were quantified using a Qubit dsDNA High Sensitivity Assay Kit (Invitrogen) with a Qubit 3 Fluorometer. Samples were then standardised to 10 ng μL^{-1} using an automated pipettor (QIAgility, QIAGEN). Normalised DNA was used to amplify two marker regions for Symbiodiniaceae species confirmation, the ITS2 and psbAncr regions.

3.2.3 ITS2 and psbA marker sequencing and Symbiodiniaceae identification

The Internal Transcribed Spacer 2 (ITS2) region was the primary marker used to distinguish Symbiodiniaceae. Amplicon sequencing of the ITS2 region was performed on an Illumina MiSeq platform at 2 x 300 bp paired-end V3 chemistry (Ramaciotti Centre for Genomics, UNSW). One MiSeq run was conducted for *Acropora* cf *humilis* and a separate run was done for *Pocillopora* spp., with each run conducted on one flow cell. Within each run, samples from each reef were randomly distributed across each plate. The raw sequence data are available under NCBI BioProject PRJNA1001407. Demultiplexed forward and reverse Fastq files were submitted to SymPortal.org for analysis of 'Defining Intragenomic Variants' (DIVs) and ITS2 type profiles (Hume et al., 2019). The SymPortal analytical pipeline assesses patterns of intragenomic variation for the ITS2 marker as there can be multiple copies of each gene present within Symbiodiniaceae genomes. These sequences are then partitioned as 'defining intragenomic variants' (DIVS), from which 'ITS2 type profiles' are derived as discrete biological entities. Using SymPortal outputs, three samples with < 1,500 reads were removed from the data set prior to community analyses. Filtered datasets for DIVs and type profiles were used in downstream statistical analyses.

Coupled with the ITS2 marker, the non-coding region of the plastid, mini-circle psbA gene (psbAncr) often contains hyper-variable nucleotide sequences well suited to

Symbiodiniaceae species confirmation, which can be used in tandem with the ITS2 marker (LaJeunesse & Thornhill, 2011; Moore et al., 2003) to validate ITS2 type profiles (Smith et al., 2017). Amplicons were sequenced in the forward and reverse direction using Sanger chemistry (Macrogen Inc.) and sequences were manually trimmed and aligned using DECIPHER (Wright, 2016).

3.2.4 Construction of phylogenetic trees, UniFrac distances, and ITS2-psbAncr tanglegrams

All statistical analyses were conducted in the R statistical environment (R Core Team, 2022) and code is available online as a live GitHub repository (https://github.com/magenamarzonie/CoralSeaSymbiont) and as a static release (Zenodo Link). I used post-MED (Minimum Entropy Decomposition) sequences from SymPortal outputs to incorporate rare variants into the analyses (Hume et al., 2019). A k-mer based approach was opted for to produce pairwise sequence comparisons of SymPortal post-MED sequences (Fujise et al., 2021), given the challenges of multiple sequence alignment of Symbiodiniaceae ITS2 sequences. A k-size of 7 was used with default settings using 'kdistance' in the kmer package (Wilkinson, 2018). I then produced a UPGMA phylogenetic tree of ITS2 sequences from the pairwise k-mer distances with 'UPGMA' in Phangorn (Schliep et al., 2011). This tree, along with post-MED sequence counts, was further analysed using Generalised UniFrac (GUniFrac, $\alpha = 0.5$) inter-sample distances, a method considered to apply fair weighting to both rare and abundant sequences (Chen et al., 2012). The GuniFrac distance approach was selected as it partitioned samples into clusters congruent with SymPortal ITS2 type profiles, while allowing for the non-DIV/non-profile sequences to contribute to inter-sample distances. psbAncr trees were then generated using the k-mer based approach as above and untangled using the step2side method in dendextend (Galili, 2015) to investigate psbAncr-ITS2 congruence.

3.2.5 Identification of coral host species of Pocillopora

Given the cryptic nature of Pocilloporids and their morphological plasticity in variable environments (Johnston et al., 2022), specimens were genetically resolved to species-level after collection. To confirm species identification, the mitochondrial open reading frame (mtORF region) of the coral host was amplified, and I applied a Restriction Fragment Length Polymorphism (RFLP) assay modified from Johnston et al. (2018) and detailed in Chapter 2. Of the 346 *Pocillopora* samples, 152 were identified as *P. verrucosa*, 134 as *P. meandrina*, and 61 ambiguous samples, which are referred to as 'unknown' *Pocillopora* spp. These remaining unknown samples of *Pocillopora* that were not identified as *P. meandrina* or *P. verrucosa* in the RFLP assay were then sequenced in both directions using Sanger Sequencing. Using the amplified mtORF region, samples underwent bi-directional Sanger Sequencing (Macrogen, South Korea). I manually applied sequence trimming parameters based on sequence quality and generated consensus sequences using DECIPHER (Wright, 2016). These sequences were aligned with the mtORF reference sequences collated from Forsman et al. (2013), Gélin et al., (2017), and Pinzón et al. (2013) using the 'AlignSeqs' function (DECIPHER). Hamming distances were computed using the 'dist.hamming' function from Phangorn to identify any unknown *Pocillopora* samples to previously described haplotypes or species (SOM Figure S3.2). Of the 61 unknown *Pocillopora* samples, 39 were identified as *Pocillopora* haplotype 8a, which is proposed to comprise a single species according to nuclear DNA (Johnston et al., 2022). An additional 22 samples were either unable to be mapped to previously described *Pocillopora* species, haplotypes, or were removed due to their low representation (e.g., two samples of *Pocillopora damicornis* cf *acuta*). These 22 samples were removed from downstream analyses.

3.2.6 Coral host genotype-by-sequencing

To assess the effects of host genotype and population structure on symbiont communities, host coral tissue was sequenced using a genotype-by-sequencing approach (DarT-sequencing; Kilian et al., 2012) at Diversity Arrays Technology (Canberra, Australia). For Pocillopora, all 61 unknown samples from the RFLP analysis were removed from the genotype-by-sequencing analysis, including host samples of haplotype 8a. A separate run was conducted for each host species *(A.* cf *humilis, P. verrucosa,* and *P. meandrina*). To reduce technical bias, samples from each reef were randomly distributed across 96-well plates. Libraries were constructed using the PstI and HpaII compatible adaptors with two restriction enzyme overhangs (Sansaloni et al., 2011) and sequencing was performed on Illumina HiSeq2500 across two lanes. For *Acropora* cf *humilis*, samples were mapped to the *Acropora tenuis* (Liew et al., 2016) and *A. millepora* (Fuller et al., 2020) genomes. For *Pocillopora verrucosa* and *P. meandrina*, samples were mapped to the *P. verrucosa* reference genome (Buitrago-López et al., 2020).

Quality filtering of SNPs was conducted for each host species separately in R software using the dartR package (Gruber et al., 2018). Filtering parameters are detailed in Appendix 1. Genetic pairwise comparisons (F_{ST}) of *Pocillopora* were assessed using a DarT-seq co-analysis to ensure the absence of cryptic species. F_{ST} values between species were greater than between host clusters within a species. The pairwise comparisons between *P. verrucosa* and *P. meandrina* resulted in an $F_{ST} = 0.501$, while the two clusters of *P. meandrina* had an FST range between 0.00 – 0.06 (SOM Figure S3.3). Host population structure was visually checked using unconstrained ordination (PcoA, vegan), then ADMIXTURE analyses were performed to assess group membership probability of each individual sample using LEA (Frichot & François, 2015). The optimal K was determined by running cross-entropy models using the 'snmf' function in LEA where K = 1:10 were tested. The K with the lowest cross-entropy value was selected for each host species. The host PC1 and PC2 from each host species PCA were

extracted and used as covariates to represent a host genetic predictor in downstream multivariate analyses of symbiont communities (dbRDA). In addition, a Neighbour-Joining tree was run on host individual pairwise genetic differences using the same genetic distances as admixture and PCAs to identify variation among clusters using the *ape* package (Paradis & Schliep, 2019). Clusters from the Neighbour-Joining trees were consistent with both PCAs and admixture group membership probability (SOM Figure S3.4, S3.5, and S3.6).

3.2.7 Host-symbiont cophylogenetic analysis

To measure the degree of co-phylogeny between coral host and symbiont phylogenetic structure, a Procrustean rotation analysis was implemented. This approach allows a quantitative measurement of the degree of alignment between two distance matrices, where two ordinations are overlaid and rotated to obtain the smallest distance between two points representing different community structure. Specifically, Generalised Procrustean Analysis allows for the rotation and transformation between two datasets with variable dimensions (i.e., host and symbiont genetic distances) to measure the distance between two observations of the same sample (Dray et al., 2003; Hutchinson et al., 2017). As dimensions of the host and symbiont distance matrices must match in a Procrustes analysis, new phylogenetic trees were constructed for symbionts using the same parameters and packages as per Methods Section 3.2.6, with a subset of samples corresponding to the host DArT-seq genetic samples.

For each host genetic data set, a distance matrix of the filtered SNP data was constructed in parallel using the 'euclidean' distance method (dartR). A Generalised Procrustes rotation analysis was implemented to align the UniFrac distances of the symbiont with the SNP-based Euclidean distances of the host ('procrustes', vegan). Residuals were checked and the distance between each host and symbiont was plotted using RDA. Significance was tested using 'protest' with 999 permutations per analysis (vegan).

3.2.8 Statistical analysis of environmental and host genetic predictors

A principal coordinates analysis was performed (PcoA; 'cmdscale' function, vegan [Oksanen et al., 2019]) on the symbiont ITS2 GuniFrac distances separately for each host species. Variation in symbiont communities were visualised by reef (SOM Figure S3.7) and by host bleaching category (SOM Figure S8) as the first signals of underlying environmental drivers relating to symbiont distribution. I then proceeded to test a suite of environmental variables predicted to influence symbiont communities given signals of reef-level structuring among PcoAs. To test additional environmental and host genetic covariates, ITS2 GuniFrac distances of the symbionts were incorporated into a constrained, distance-based Redundancy Analysis ('dbRDA', vegan). Thermal environmental variables were obtained for each reef from NOAA Coral Reef Watch Operational Daily Near-Real-Time Global 5-km Satellite Coral Bleaching Monitoring Product Version 3.1 from 1986-2020. As samples were collected during a bleaching event, a range of metrics were included to represent both climatic and environmental trends. The thermal metrics of the 'Environment' dbRDA model included accumulated Degree Heating Weeks (DHW) at the time of field collection (DHW2020), maximum historical DHW at each reef from 1986-2020 (maxDHW), and the bleaching condition of each coral individual at the time of collection (bleaching category). Other non-thermal variables were obtained from eReefs (Australian Institute of Marine Science) including kd490 (a measure of light attenuation to represent water turbidity), chlorophyll *a*, and secchi depth. Finally, spatial metrics collected during the expedition were incorporated, including collection depth, latitude, and longitude (SOM, Table S3.2).

To run the distance-based RDA models, I ran two separate conditional models for each species: an 'Environment' and a 'Host Genetic' model. Each model contained a subset of individuals from the full Symbiodiniaceae dataset with matching host genetic data. For the 'Environment' models, host genetic PC1 and PC2 (from host genetic PCAs) were defined as

conditional effects to account for the confounding influence of host genetics on the environment. The model parameters were reversed for the 'Host genetic' models, where significant environmental predictors were included as conditional effects. For both the 'Environment' and 'Host Genetic' models, correlation plots were inspected using 'corrplot' (Wei & Simko, 2021) and variance inflation factors (vegan). First, I removed one of two collinear variables where r > |0.8|. Model parameters were adjusted to keep the most significant factors, while concurrently removing any variables with high correlation (VIF score > 5) to reduce the effects of variable collinearity in the models (SOM, Figure S3.9, S3.10, and S3.11). A backward stepwise model was then run to further reduce parameters using the 'ordistep' function with 999 permutations until stopping criteria were met for each dbRDA model (vegan). The marginal effects of each predictor were tested in the ordination to control for the order of the included covariates. Significance was assessed by running a permutational analysis of variance (PERMANOVA) on the 'ordistep' output (vegan). Scores and vector information for each dbRDA were extracted and plotted in ggplot2 (Wickham, 2016).

3.3. Results

3.3.1 Characteristics of symbiont DIVs and type profiles among coral genera

Sequencing of the ITS2 locus yielded 15,336,586 total sequences of Symbiodiniaceae across all host species and environments. The average per-sample depth of post-MED sequences was 52,523 reads (*Acropora* cf *humilis:* 50,979 reads; *Pocillopora* spp.: 53,761 reads). Over 99.98% of sequences were from the genus *Cladocopium* (15,335,016 sequences), with only 1,552 sequences in the genus *Symbiodinium* and only 13 sequences from the genus *Durusdinium* (Table 3.1). Detailed SymPortal profiles for each coral host species can be found in the SOM (Tables S3.3 – S3.6).

Most coral samples had one ITS2 type profile associated with an individual. For *Pocillopora,* 324 samples contained a single ITS2 type profile, compared to four samples containing two ITS2 type profiles within a single host sample. Similarly, for *Acropora,* 250 samples contained a single ITS2 type profile, while 10 samples hosted two ITS2 type profiles. *Pocillopora* sequences had a lower proportion of non-profile sequences within each sample, on average making up 16.1% of each sample (Figure 3.1a) compared to 24.6% for *Acropora* samples. Within *Pocillopora, P. verrucosa* had a lower proportion of non-profile sequences (13.9%), while *P. meandrina* and haplotype 8a had a higher composition of non-profile sequences at 17.9% and 17.6%, respectively.

Table 3.1. Library statistics for Symbiodiniaceae for samples grouped by each coral host species.

Library Statistic	***Acropora* cf *humilis***	***Pocillopora verrucosa***	***Pocillopora meandrina***	***Pocillopora* haplotype 8a**
Total number of coral host samples	260	152	133	39
Total number of sequences	6,627,245	4,171,390	3,512,508	1,025,443
Average sequencing depth per sample (# reads)	50979	54887	52820	52587
Proportion profile sequences	0.7545413	0.8606516	0.8207196	0.8236049
Proportion non-profile sequences	0.2454587	0.1393484	0.1792804	0.1763951
Total number of ITS2 type profiles	23	16	12	7
Majority sequence(s)	C3k/C3	C1d	C1/C42.2	C1/C42.2

3.3.2 Pocillopora *symbiont communities*

SymPortal analysis of ITS2 sequences from *Pocillopora* yielded a total of 23 ITS2 profiles collectively and varied by host species (Table 3.1). The most common ITS2 type profile for *P. verrucosa* was C1d/C1/C42.2/C3-C1b-C3cg-C115k-C45c-C1au-C41p. For *P. meandrina* and haplotype 8a, the most common ITS2 type profile was C1/C42.2/C42g/C42a-C1b-C1au-C1az-C42h-C3. Among *Pocillopora* samples, the greatest split in symbiont genetic diversity was partitioned according to host species, where *P. verrucosa* samples formed a distinct lineage compared to *P. meandrina* and haplotype 8a (Figure 3.1a). The majority sequence in 84.2% of

P. verrucosa samples was 'C1d', whereas the majority sequence found in 89.0% of *P. meandrina* and haplotype 8a samples was 'C1/C42.2'.

Across all *Pocillopora* species, the majority sequences, 'C1', 'C42.2' and 'C1b', were present in most samples, though the mean relative abundance varied by host species. Some detected sequences were highly specific to a coral host species. For example, 'C1d' was exclusive to *P. verrucosa,* found in 92.7% of samples, and averaged 37.2% relative abundance of reads per sample. There was a major split in the right side of the UPGMA tree associated with two distinct symbiont lineages in *P. meandrina*. Of the two lineages, 'C42u' was a diagnostic sequence for the left branch associated with *P. meandrina*, found in 34.3% of samples, but was present in high relative abundance, averaging 24% of reads per sample (Figure 3.1a). In contrast, the right branch for *P. meandrina* was driven more by the presence of 'C42g', found in 64.0% of samples but in a lower mean proportion of 15.7% of reads per sample (Figure 1a). Hereafter, the symbiont lineage associated with *P. verrucosa* will be referred to as *C. pacificum* (Turnham et al., 2021), while the two symbiont lineages associated with *P. meandrina* will be referred to as *C. latusorum* (Turnham et al., 2021) 'north' and 'south' to reflect the biogeographic pattern in their distribution (Figure 3.1a and read below).

3.3.3 Acropora *symbiont communities*

Sequencing of *A.* cf *humilis* symbiont communities yielded 23 ITS2 type profiles across all samples, the most common being C3k/C3-C50a-C29-C21ab-C3b. The co-dominant majority sequences 'C3k/C3' were present in 99.2% of all *Acropora* samples, representing on average 74.8% of reads in these samples. There was a major split in the UPGMA tree for *Acropora* samples (Figure 3.1b). The two branches within the *Acropora* UPGMA tree were generally congruent with the proportion of non-profile sequences. The left branch had a relative abundance of 20.7% non-profile sequences averaged across samples (Figure 3.1b, n = 122),

significantly lower than 29.0% in the right branch (Figure 3.1b, n = 123) (t-test: $p < 0.001$, df = 231, t = -16.5). Hereafter, these lineages will be referred to as C3k 'max' and C3k 'min'. There were eight outlier samples that did not conform to the two main groups of symbionts, characterised by a high relative abundance of 'C1' and 'C1c' and found only in northern reefs, Osprey and Moore (Figure 3.1b).

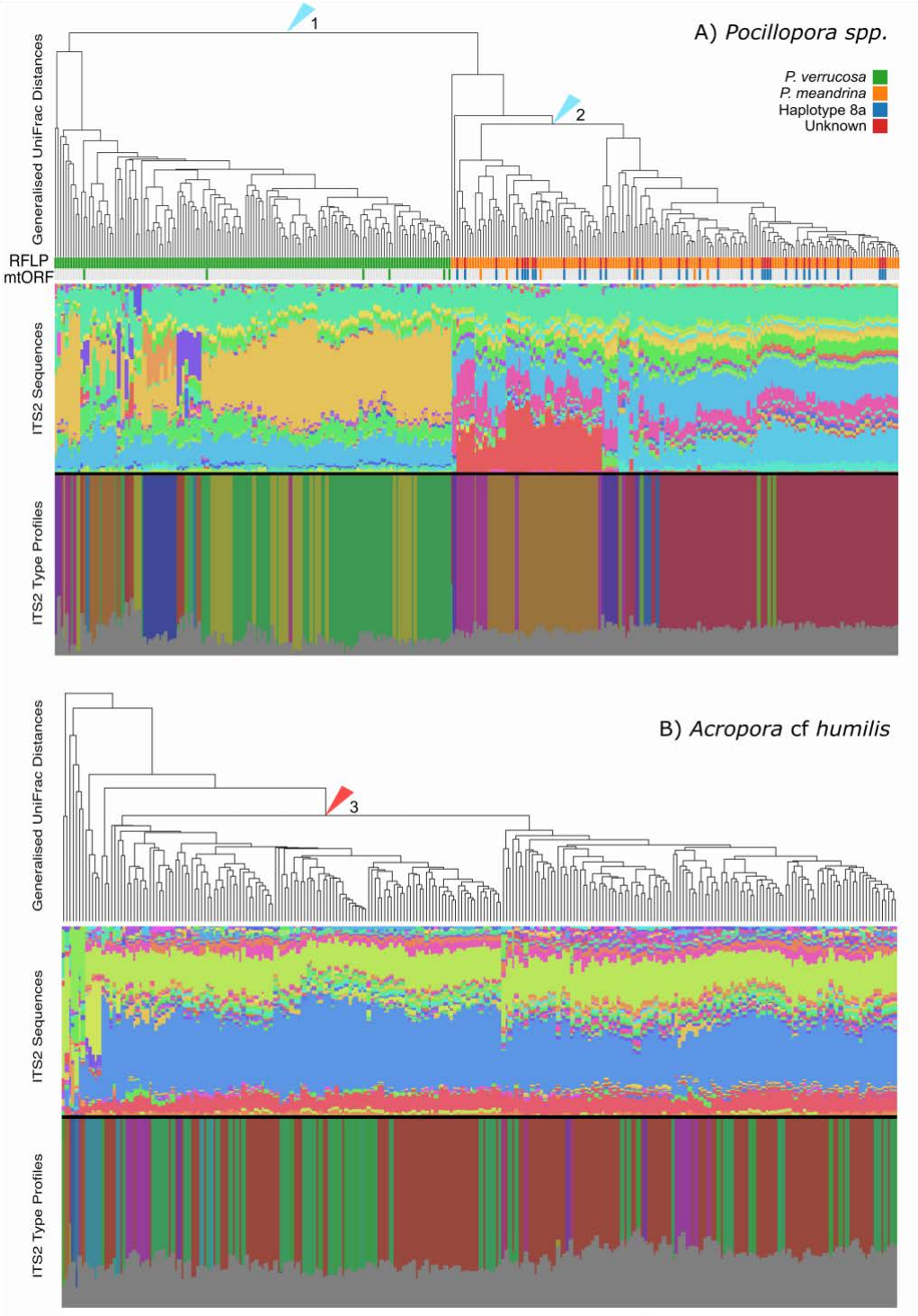

Figure 3.1. Analysis of SymPortal post-MED ITS2 sequence data in *Pocillopora* (a) and *Acropora* (b). Each vertical bar represents the symbiont structure of one coral sample. The top third of each plot shows the UPGMA tree of the between-sample Generalised UniFrac distances. The middle third represents ITS2 sequence composition, with the proportion of individual sequences represented by different colours. The bottom third of each plot is coloured according to an assigned SymPortal ITS2 type profile, with grey representing the proportion of non-profile sequences found in each sample. For *Pocillopora* species (A), samples for *P. verrucosa, P. meandrina* and haplotype 8a are represented by tree leaf colours (green, orange, and blue, respectively) derived from the RFLP and mtORF molecular assays. Arrow 1 = *C. pacificum*/*C. latusorum* branch, 2 = *C. latusorum* 'north' and 'south' branch, and 3 = C3k 'max' and 'min' branch.

3.3.4 psbA and ITS2 marker alignment indicates presence/absence of novel symbiont species

Sequencing of the psbA^{ncr} region allowed validation of ITS2 profiles as putative species (Smith et al., 2017). Here, a low entanglement score (0.012) highlighted the congruency between the ITS2 and psbA^{ncr} gene regions for *C. latusorum* in *P. meandrina*/haplotype 8a and *C. pacificum* in *P. verrucosa* as previously reported (Turnham et al., 2021) (Figure 3.2a). The two lineages belonging to *C. latusorum* in the ITS2-based UPGMA tree of GuniFrac distances (Figure 3.2a; *C. latusorum* 'north' and *C. latusorum* 'south') were completely congruent with the psbA^{ncr} marker. *P. meandrina* and haplotype 8a samples (according to mtORF identification) were distributed across the *C. latusorum* north and south lineages, therefore, these samples were grouped for further analysis (hereafter: '*P. meandrina*' *sensu* (Johnston et al., 2022). In contrast, there was a higher entanglement score between the ITS2 and psbA^{ncr} markers of C3k hosted by *A.* cf *humilis* (entanglement score = 0.199), and the psbA^{ncr} marker did not resolve differences between the two phylogenetic clusters of *A.* cf *humilis* for the ITS2 marker (Figure 3.2b).

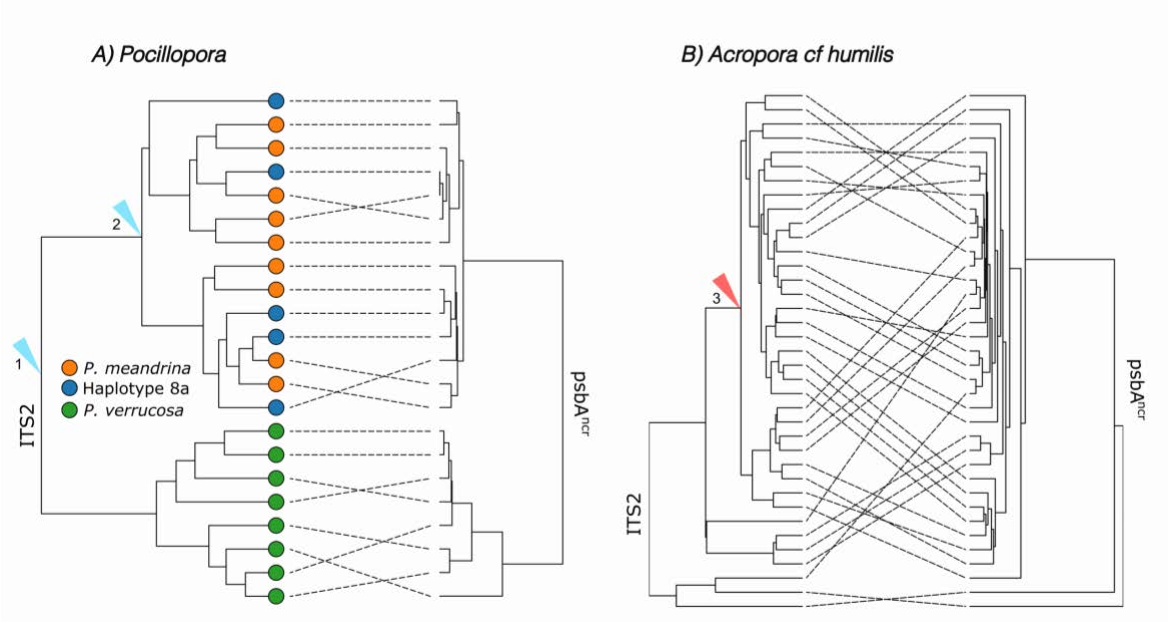

Figure 3.2. Tanglegram of ITS2 and psbA^{ncr} sequences. ITS2 sequences vs. psbA^{ncr} sequence UPGMA trees for *Pocillopora* spp. (A) and *Acropora* cf *humilis* (B). ITS2 sequence UPGMA trees are according to k-mer = 7 + GUniFrac (0.5) distances and psbA^{ncr} sequence UPGMA trees use k-mer = 7 distances. Blue and red arrows correspond to the phylogenetic split in each species tree shown in Figure 1a and b, respectively. Arrow 1 = *C. pacificum*/*C. latusorum* branch, 2 = *C. latusorum* 'north' and 'south' branch, and 3 = C3k 'max' and 'min' branch.

3.3.5 Cophylogeny of host and symbiont communities

Admixture, PcoAs, and neighbour-joining trees revealed two host genetic clusters for *P. meandrina,* two clusters for *P. verrucosa*, and three clusters for *A.* cf *humilis*. A Procrustean Rotation Analysis examined the relationship between the population structure of each coral host species and their respective symbiont communities, revealing a significant degree of cophylogeny for each host-symbiont partnership, the strength of which varied among host taxa. *P. meandrina* demonstrated the highest degree of cophylogeny, indicated by a strong, positive procrustean correlation (n = 66, Sum of Squares = 0.724, r = 0.52, $p < 0.001$) forming two

distinct clusters of host plus symbiont (indicated by short distances between two given points of the same sample, Figure 3.3a). In contrast, the degree of cophylogeny was weaker, yet significant, for *P. verrucosa* (n = 130, Sum of Squares = 0.882, r = 0.34, p = 0.02), characterised by one primary cluster and less partitioning within the ordination (Figure 3.3b).

Patterns of cophylogeny in *A.* cf *humilis* were significant when all three host genetic clusters were included (n = 257, Sum of Squares = 0.954, r = 0.21, p = 0.01) (Figure 3.3c). Symbionts were less organised than their respective host and formed one central cluster (SOM, Figure S3.12). A reduced Procrustes Rotation Analysis with only the numerically dominant host genetic cluster (AHCL1) did not yield a significant result (n = 201, Sum of Squares = 0.948, r = 0.22, p = 0.14) indicating a link between host genetic and symbiont cophylogeny (SOM, Figure S3.13).

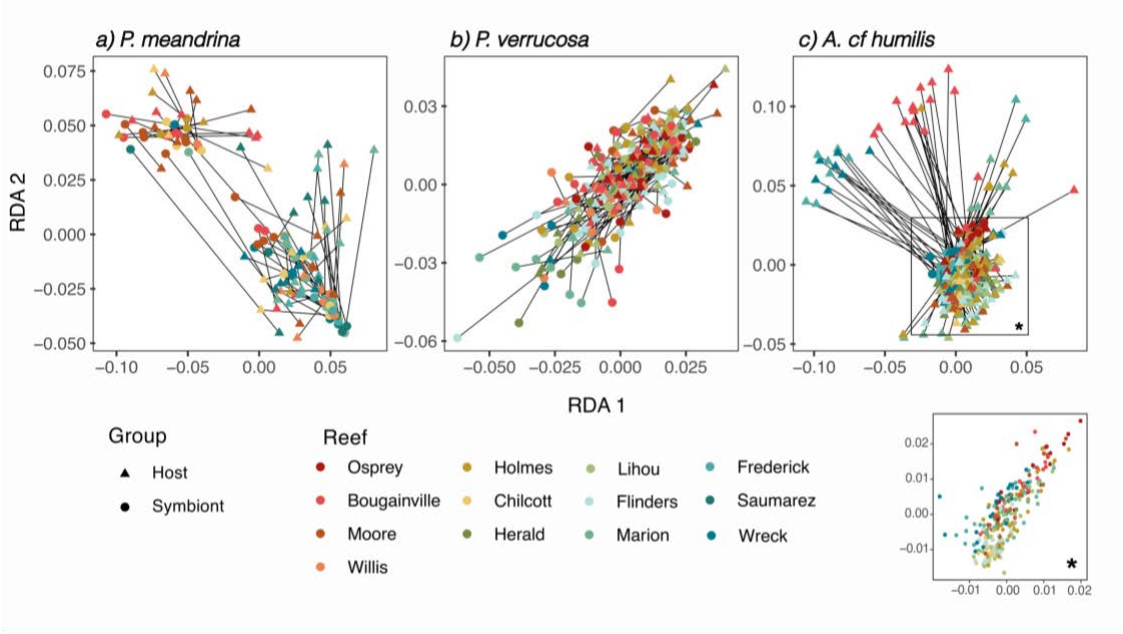

Figure 3.3. Procrustean rotation analysis of host and symbiont genetic diversity. *Pocillopora verrucosa* (a), *Pocillopora meandrina* (b) and *Acropora* cf *humilis* (c). Each point represents a sample, with host samples (circle) and symbiont samples (triangle) from the same individual linked by a line segment. Each point is coloured by reef. Inset shows symbiont points without host points overlaid to indicate symbiont distribution by reef.

3.3.6 Biogeographical distribution of Pocillopora *hosts and their symbionts*

The degree of host specificity lends itself to contrasting biogeographic patterns of host and symbiont structuring among the three coral taxa. *Pocillopora meandrina* was more abundantly sampled in high latitude reefs of the Coral Sea, while *P. verrucosa* was sampled abundantly in lower latitude reefs, likely reflecting biogeographic patterns in species distribution. *Pocillopora meandrina* comprised 77-100% of samples collected in the three highest latitude reefs positioned at 21-22° and was sampled in high abundance within low latitude, farthest offshore reefs, making up 72 and 81% of samples collected from Moore and Chilcott reefs, respectively. In contrast, *P. verrucosa* made up 74% of samples collected from the lowest latitude reef, Osprey, as well as 67-77% of samples collected from mid-latitude reefs in closest proximity to Australia's coast (Holmes and Flinders).

Intraspecific trends in host population structure were detected, with two sympatric genetic clusters per species of *Pocillopora*. For *P. meandrina,* the two genetic clusters confirmed by admixture analysis (PMCL1 and PMCL2) were divergent across a latitudinal gradient (Figure 3.4a), with PMCL2 accounting for 55% (range: 35 – 71%) of population structure in low latitude populations, compared to PMCL1, comprising 89% (range: 76 – 96%) of individuals in high latitude reefs. The two symbiont lineages, *C. latusorum* 'north' and 'south' mirrored trends of host genetic structure, where *C. latusorum* 'north' was detected on reefs where the host cluster PMCL2 was found. In three of the highest latitude reefs, corals hosted 100% *C. latusorum* 'south', as well as 85% relative abundance at Saumarez reef (Figure 4a). In contrast, *C. latusorum* 'north' was found in higher relative abundance (88 – 100%) in low latitude reefs closest to Australia's coast (Bougainville, Osprey) but not reefs further offshore (Moore: 33%).

Of the two genetic clusters detected within *P. verrucosa* with admixture analysis, (PVCL1 and PVCL2), PVCL1 was dominant across all reefs except Wreck, making up between 57 – 96% of individuals per reef population. PVCL2 was detected in highest abundance from Wreck and Marion reefs, found in 61% and 31% of individuals, respectively. I did not detect multiple lineages of the symbiont *C. pacificum*, which was ubiquitously found across the ten reef populations where *P. verrucosa* was sampled (Figure 3.4b), in contrast to patterns observed for symbionts hosted by *P. meandrina.*

3.3.7 Biogeographical distribution of Acropora *hosts and their symbionts*

The three genetic clusters of *A.* cf *humilis* (referred to as AHCL1, AHCL2, and AHCL3) were confirmed by admixture analysis. While the dominant cluster AHCL1 was detected across each of the 11 sampled reefs, the range in relative abundance varied between 20-92% of sampled individuals per population. The two less common clusters were more centralised to specific reefs, where AHCL2 accounted for 30% of population structure within Marion reef. AHCL3 was specific to Bougainville, Frederick, and Wreck reefs, making up 70, 42, and 33% of population structure, respectively (Figure 3.4c).

The two symbiont lineages detected in *A.* cf *humilis,* C3k 'max' and 'min' were both found in all 11 reefs where *Acropora* was collected and did not appear to be associated with latitude or shelf position (Figure 3.4c). C3k 'max' was detected in the highest relative proportion of samples (78 – 85%) in both low latitude reefs (Osprey, Bougainville, and Moore) and the highest latitude reefs (Wreck: 67% abundance). In contrast, C3k 'min' was found in highest proportion in central latitude reefs including Chilcott and Flinders reefs, detected in 93-94% of samples (Figure 3.4c).

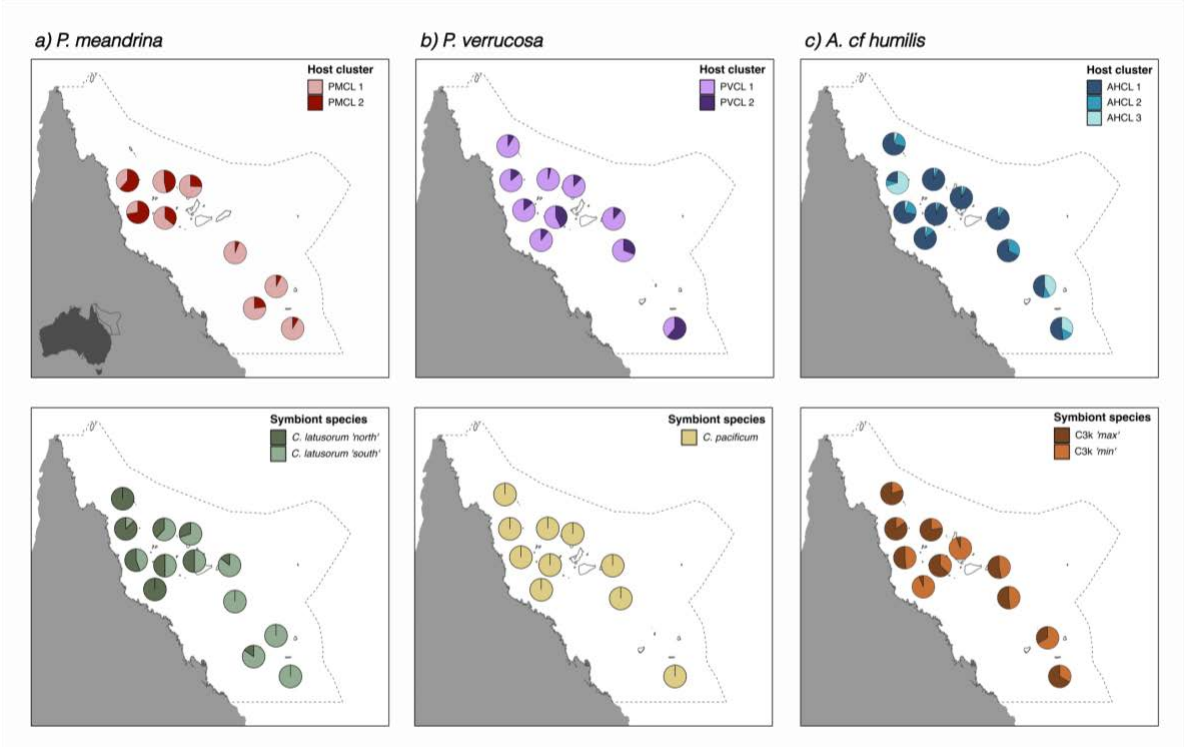

Figure 3.4. Schematic diagram depicting biogeographic patterns and relative proportion of host population structure and symbiont lineages detected throughout the Coral Sea Marine Park at 13 reefs. (a) Pie charts represent host genetic clustering (admixture proportion) for *P. meandrina* (top) and symbiont lineage clustering (bottom) include *C. latusorum* 'north' and *C. latusorum* 'south'. (b) Host genetic clustering for *P. verrucosa* (top) and one symbiont lineage of *C. pacificum* (bottom). (c) Pie charts show relative abundance of three host genetic clusters of *A.* cf *humilis* (top) and symbiont lineage clustering (bottom) include C3k 'max' and C3k 'min'.

3.3.8 Environmental and host genetic drivers of Pocillopora symbiont communities

A distance-based RDA evaluated symbiont community structure for each host species, in relation to environmental conditions and host genetic structure (Table 3.2; Figure 3.5a,b). Both *Pocillopora* species had significant symbiont structuring attributed to host genetics, while accounting for the conditional effects of environmental variables. Overall, the strongest predictors of *P. meandrina* symbionts were driven by host genetic structure, explaining 14.9%

of total model variance, compared to environment which explained 6.0% of total model variance (Figure 3.5a). In contrast, *Pocillopora verrucosa* symbionts had a lesser, but significant influence of host genetic structure, accounting for 3.4% of total variance, while all environmental factors accounted for 1.3% of explained variance (Table 3.2; Figure 3.5b).

The predictors of community structure in *C. latusorum* hosted by *P. meandrina* included host genetic cluster (df = 1, F = 16.985, p = 0.001), latitude (df = 1, F = 2.771, p = 0.021), bleaching condition (df = 1, F = 3.014, p = 0.001), and light attenuation (kd490; df = 1, F = 2.371, p = 0.04) (Table 3.2). ITS2 sequence dissimilarities of *C. pacificum* in *P. verrucosa* were significantly associated with host genetic clustering (df = 1, F = 5.055, p = 0.001). Of all environmental and thermal metrics, depth was the only significant covariate of *P. verrucosa* symbiont community structure (df = 1, F = 2.142, p = 0.043), when accounting for host genetics as a conditional effect in the model (Table 3.2).

Table 3.2. Distance-based redundancy analysis (dbRDA) model outputs. The Environmental model incorporates all symbiont samples, while the Environment + Host Genetic model incorporates a reduced number of symbiont samples with matching DArT-sequencing host data. The type of environmental predictor and their relative strength are comparable between the two model types.

	Environmental model					**Host Genetic model**				
Species	Fixed effect	DF	F	Pr(>F)	Adj R2	Fixed effect	DF	F	Pr(>F)	Adj R2
P. meandrina	Latitude	1	2.771	0.021	0.06	Host PC1	1	16.985	0.001	0.149
	Bleach Condition	1	3.0138	0.009		Residual	61			
	kd490	1	2.3708	0.04						
	Residual	60								
P. verrucosa	Depth	1	2.1429	0.04	0.013	Host PC1	1	5.0553	0.001	0.034
	Residual	124				Residual	124			
A.* cf *humilis	Max DHW	1	15.1981	0.001		Host PC1	1	1.7812	0.09	0.002
	DHW 2020	1	6.0457	0.001		Residual	249			
	kd490	1	6.829	0.001	0.149					
	Latitude	1	5.0415	0.001						
	Depth	1	3.0089	0.015						
	Bleach Condition	1	2.3774	0.048						
	Residual	248								

3.3.9 Environmental and host genetic drivers of Acropora symbiont communities

Communities of C3k symbionts hosted by *A.* cf *humilis* were structured predominantly by a suite of environmental factors, accounting for 15% of total model variance, compared to only 0.2% of total model variance explained by the host genetic model. For *Acropora* symbionts, the significant environmental predictors included historical thermal stress (maxDHW; df = 1, F = 15.198, p = 0.001), Degree Heating Weeks at the time of collection (DHW2020; df = 1, F = 6.046, p = 0.001), light attenuation (kd490; df = 1, F = 6.829, p = 0.001), latitude (df = 1, F = 5.042, p = 0.001), depth (df = 1, F = 3.009, p = 0.015), and host bleaching condition (df = 1, F = 2.377, p = 0.048) (Figure 5c). Additionally, a separate model was run using only the

dominant host genetic cluster of *A.* cf *humilis* (Host cluster: AHCL1, n = 198). Comparable to the full *Acropora* model, AHCL1 symbionts were consistently driven by the same four environmental predictors, except for bleaching category of the host, which was only significant in the full model but not the AHCL1 model (p = 0.116), indicating an interaction between host genotype and bleaching condition.

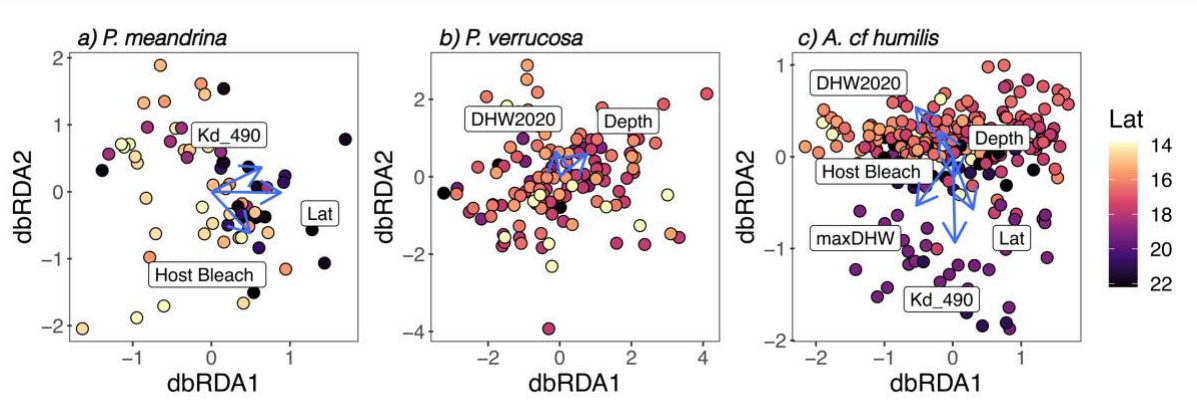

Figure 3.5. Distance-based redundancy analysis (dbRDA) ordinations of GUniFrac (0.5) ITS2 sequence composition. *Pocillopora meandrina* (a), *Pocillopora verrucosa* (b) and *Acropora* cf *humilis* (c). Each circle is coloured by latitude. Blue arrows represent significant environmental vectors derived from a backward stepwise model.

3.4 Discussion

Host specific trends of symbiont community structure among Pocillopora *and* Acropora Symbiodiniaceae community structure can be driven by a suite of host and environmental factors and varies by the host-symbiont partnership. Here, symbiont specificity was most strongly driven by host genera and their mode of symbiont transmission (i.e., *Acropora* and *Pocillopora*), with concomitant impacts of the environmental factors shaping their distribution. Both *Pocillopora* species maintained symbionts congruent with host genetic structure, 2.5-fold higher than structuring by their environment. The host genetic structure of *P. meandrina* was

considerably stronger in partitioning symbiont communities than *P. verrucosa*, demonstrated by 4-fold higher environment and host genetic influence, as well as high alignment between the two host genetic clusters and two symbiont clusters. In contrast, symbiont communities in *A.* cf *humilis* maintained an inverse trend, structured 75-times more by environmental predictors than by host genetics. Specifically, symbionts were partitioned by thermal history experienced at each reef. Both DHW experienced at the time of coral collection (DHW2020), and historical thermal stress patterns over 35 years (maxDHW) were influential, indicating the importance of historical and contemporary thermal stress in structuring symbiont communities in *Acropora*. Similarly, the light attenuation coefficient (kd490) was a stronger factor in driving *Acropora* symbionts, compared to either *Pocillopora* spp., further alluding to the higher symbiont structuring in *Acropora* in response to both thermal and environmental conditions.

Our data are consistent with the hypothesis that corals with horizontal transmission of symbionts have a greater capacity for adaptation via environmental sorting of symbionts adapted to the environment, compared to corals with vertical transmission driven by co-phylogeny (Chakravarti et al., 2017; van Oppen & Medina, 2020). The ability to validate such differences in Symbiodiniaceae and their respective environmental drivers can be attributed to the co-analysis of two genetic markers tested in this study. The congruence between the psbA^{ncr} and ITS2 markers for *Pocillopora* symbionts, but not *Acropora,* supports the evolutionary stability of the symbiotic partnership in vertically transmitting coral species but not horizontally transmitting corals.

Host genetic structure and cophylogeny as key traits for symbiont communities in Pocillopora

In Turnham et al. (2021), regionally distinct lineages of *C. latusorum* were presented across the Indo-Pacific. Here, I show that *C. latusorum* lineages in *P. meandrina* arise at much smaller spatial scales (< 2000 km), and with multi-gene congruence, these regionally differentiated

lineages may warrant descriptions as mutually exclusive species. Further, the stronger co-phylogeny in *P. meandrina* and symbionts indicates that host population structure attributes to the species-specific differences in symbiont community structure and the degree of host influence. *Pocillopora* host boundaries have previously been shown to vary among species, with *P. verrucosa* localised to low latitude reefs and *P. meandrina* to high latitude reefs (Johnston et al., 2018), similar to the species distribution ranges of *Pocillopora* in this study. A myriad of biological factors can shape species ranges, including depth distribution and the rate of larval development. In addition, abiotic factors including habitat heterogeneity or geological features mediate a species' ability to occupy space over a geographic break (Keith et al., 2013), possibly explaining the two distinct host and symbiont groups in high and low latitude populations observed in *P. meandrina*. The two host genetic clusters and two lineages of *C. latusorum* correspond to the strong bifurcation in the South Equatorial Current at 16°S (Ceccarelli et al., 2013). There is evidence that this oceanographic current acts as a defining barrier to gene flow for organisms with larval dispersal (Payet et al., 2022), providing an ecological context to study rates of cophylogenetic speciation rates in organisms with host-symbiont diversification.

Acropora *symbiont communities are primarily structured by thermal history*

The symbionts detected in *A.* cf *humilis* were nearly exclusive to the C3k radiation of *Cladocopium*, distinct from other C3-like species commonly found in *Acropora* within Australia's Great Barrier Reef and other Pacific islands (Butler et al., 2023). While symbionts were overall partitioned by thermal history, the effect of historical thermal stress (DHW between 1985-2020) explained twice as much variation as the concurrent bleaching event in 2020, suggesting that symbiont communities predominantly shift after, not during, a bleaching event (Silverstein et al., 2015). The two main lineages of *Acropora* symbionts (C3k 'max' and

'min') associated with reefs specifically experiencing high and low historical heat stress, respectively. Thus, C3k 'max' may foster higher thermal tolerance given its detection on reefs which have experienced historically higher DHW and highlight a potential source of increased resilience of *A*. cf *humilis* in response to rapid environmental change.

The predominant effect of environment and minimal effect of host genetic structure has been observed in *A. tenuis* symbiont partitioning on the GBR, where communities were structured primarily by reef shelf position (Matias et al., 2023) and their proximity to freshwater plumes (Cooke et al., 2020), with a lesser effect of host genetic structure. Further, the conspicuous absence of *Durusdinium,* a common genus found in horizontally transmitting species such as *Acropora* in the GBR, highlights the niche requirements of *Durusdinium* to live in marginal, in-shore environments or to be outcompeted in off-shore environments (Hoadley et al., 2019; LaJeunesse et al., 2014), leaving *Cladocopium* to dominate oligotrophic, offshore reefs such as those in the Coral Sea, explaining their detection in over 99.98% of samples quantified in this study.

Effects of bleaching on immediate symbiont community restructuring varies by host taxa

The concurrent bleaching event during the collection period exposed corals to between 5.7 – 10.0 DHW, dependent on the sampling location. Correlations between the extent of bleaching and the symbiont communities varied across the three host taxa and with respect to the accumulated heat stress in the environment. *Acropora* was the most thermally sensitive species, and it is thus consistent with *Acropora* symbiont community structure being predominantly influenced by all thermal and irradiance parameters in the model, including DHW at the time of collection, historical thermal stress (maximum DHW between 1986-2020), and light attenuation. Host bleaching condition strongly dictated symbiont structure in *A.* cf *humilis* when accounting for the three host genetic clusters but not for the main host genetic cluster

alone (AHCL1), indicating an interaction between host genetic lineages and bleaching condition on symbiont community structure. In Quigley et al. (2022), repeat mass bleaching events resulted in variable levels of symbiont restructuring among three species of *Acropora* in the Great Barrier Reef, highlighting a host taxa-specific effect of bleaching on symbionts. I found similar patterns of symbiont structuring at the host population level, applying not only to species-specific, but possibly to the level of host populations or individual genotypes (Rose et al., 2021).

In the case of *Pocillopora, P. meandrina* symbiont communities were in alignment with host bleaching condition, but the communities harboured by *P. verrucosa* were not. Variable physiological limits of the host may explain the disparities in symbiont responses to the concurrent bleaching event. *P. meandrina* has demonstrated a 0.3 °C lower thermal threshold in heat stress experiments compared to *P. verrucosa* across nine of the reefs measured here, as presented in Chapter 2. Further, *Acropora* exhibited the greatest sensitivity to heat stress evidenced by a 0.4 – 0.7 °C lower thermal threshold compared to both *Pocillopora* spp., corroborating the strong influence of multiple thermal disturbance and irradiance metrics (i.e., maxDHW, DHW2020, kd490, bleaching condition) for symbiont structure in *Acropora* observed here. The degree of thermal and light sensitivity of the host may influence the biogeography of symbiont communities, where lower tolerance to heat stress incurs higher bleaching and consequently a more pronounced symbiont community restructuring in response to recurrent thermal disturbances. However, due to the high collinearity between light attenuation and other environmental variables (e.g., PAR), I acknowledge there may be other environmental variables that contribute to shaping symbiont community structure in both *Acropora* and *Pocillopora*, but maintain unaccounted for.

Conclusion

This study provides evidence that the diversity of coral-symbiont assemblages is influenced by a range of host-specific and environmental factors. The ability for the coral-symbiont partnership to adjust to fluctuating environmental conditions may rely on a suite of both host factors (i.e., host co-phylogeny, symbiont mode of transmission, population structure) and the environment (i.e., thermal history, climatology, and irradiance). Contextualising both host and symbiont genetic structure in response to environmental drivers is critical in the search for the mechanisms of coral adaptation. As climate change continues to impact coral reefs in the coming decades, there will undoubtedly be shifts in symbiont community structure. Tracking these changes is essential to quantifying coral species and populations with both high and low adaptive potential against a backdrop of rapid ocean warming and should be done with a combination of molecular and environmental data for both hosts and their symbionts.

Chapter 4. Seascape genomics reveal contrasting patterns of population structure across a large thermal gradient

4.1 Introduction

Increasing sea surface temperatures and marine heatwaves are challenging corals to undergo profound thermal adaptation beyond their current limits (McManus et al., 2021). In response to increasing thermal pressures, phenotypic variation in bleaching responses (i.e., the dissociation of the coral-Symbiodiniaceae relationship (Weis et al., 2008) can result from either physiological acclimation within a generation (McRae et al., 2021; Yu et al., 2020), evolutionary adaptation of the host across multiple generations (Kenkel et al., 2013), or shifts in the coral's community of algal symbionts (Symbiodiniaceae) (Berkelmans & van Oppen, 2006). In the case of host evolutionary adaptation, populations may benefit when the historical climate better matches the predicted future conditions (Kawecki & Ebert, 2004;Torda et al., 2017). As coral reef communities exist along an environmental continuum, adaptation can occur to a range of local abiotic and biotic factors (Savolainen et al., 2013). This is evidenced by variability in bleaching responses across a range of spatial scales, including within and among populations (Dixon et al., 2015; Howells et al., 2016; Humanes et al., 2022), and among species (Álvarez-Noriega et al., 2023), and habitats (Marhoefer et al., 2021). Phenotypic variation occurs spatially across populations spanning vast latitudinal ranges (Ayre & Hughes, 2000; Thomas et al., 2017), or highly variable temperature environments (Barshis et al., 2013; Bay & Palumbi, 2014; Palumbi et al., 2014; Safaie et al., 2018). This variation in heat tolerance across spatial gradients highlights the potential for corals to adapt to changing environmental conditions, although how taxa- and environment-specific interactions affects the adaptive potential in corals remains unclear.

The capacity for organisms to adapt to rapid environmental changes relies on specific demographic traits (e.g., thermal optimum, thermal breadth) that facilitate their evolutionary potential to environmental disturbances (Hoffmann & Sgró, 2011). However, underlying processes that mediate population genetic structure across environmental gradients can also contribute to the adaptive potential of coral populations. Genetic drift and migration can alter the neutral and adaptive genetic structure among populations, while selection to extrinsic factors can drive divergence between populations, therefore reinforcing the genetic differentiation among populations (Riginos & Liggins, 2013). Disentangling the environmental processes shaping population structure is complicated, particularly in broadcast spawning marine organisms with prolonged larval dispersal (Lowe & Allendorf, 2010). To better understand gene-environment associations, it is necessary to investigate corals across large spatial gradients with contrasting environmental conditions or disturbance history. Doing so can elucidate the environmental patterns that shape the neutral population structure and genetic diversity of corals (Holderegger et al., 2006), and subsequently the potential for populations to withstand or recover from the impacts of recurrent disturbances.

The levels of gene flow among coral reefs also shape population resilience and replenishment following disturbances (Bernhardt & Leslie, 2013). Abiotic factors that influence connectivity include the spatial distance between reefs, hydrodynamic water flow, and physical geographic barriers (Keith et al., 2013; Wood et al., 2014). Biotic factors can also shape connectivity, the development and behaviour of larvae, the duration of larval phases, and post-settlement survivorship of new recruits (Graham et al., 2008; Miller & Mundy, 2003). Subsequently, reefs and species with higher connectivity promote the redistribution of standing genetic variation among populations and present an avenue for alleles comprising signatures of thermal selection to enter a population (Matz et al., 2018). Such abiotic and biotic factors can result in

biogeographically isolated reefs with high population structure due to larger geographical distances and a paucity of source reefs for recruitment and population replenishment (Thomas et al., 2017). Isolated reefs therefore benefit from stronger local adaptation to present environmental conditions in the absence of extensive dispersal (Borregaard et al., 2017; Santos et al., 2016). At the same time, such geographically isolated reefs face heightened vulnerability to environmental change, owing to lower connectivity and therefore lower larval replenishment potential following disturbances.

Biotic factors including the reproductive mode of the host and subsequent migration potential influence both taxa-specific genetic diversity and connectivity in corals. Species of brooding corals release larvae, often settling closer to, or within their natal reef, resulting in higher rates of genetic subdivision (Underwood et al., 2009; van der Ven et al., 2021). In contrast, broadcast spawning corals with pelagic fertilisation have a longer larval duration period and dispersal range, resulting in higher genetic connectivity and weaker population structure among reefs (Buitrago-López et al., 2023; Underwood et al., 2020). More subtle processes also play a role in shaping taxa-specific patterns of genetic diversity and connectivity, including the extent to which species boundaries (Keith et al., 2013) and cryptic species lineages (Sheets et al., 2018) impact population demographics. Previously, most seascape genomic studies of corals have targeted one species to identify the specific extrinsic factors which shape neutral genetic structure (Selmoni et al., 2024). Differentiating the amount of genetic variation due to connectivity compared to the environment presents a challenge when using one or multiple study species. However, integrating multiple species sharing similar life history traits (e.g., mode of reproduction, morphology) can convey a more comprehensive view of the specific environmental processes which drive genetic variation.

Seascape genomics are a field where genetic variation in marine organisms are analysed in relation to environmental gradients, providing an understanding of the demographic and evolutionary processes that shape population structure and adaptation (Manel et al 2003; Saenz-Agudelo et al. 2015; Riginos et al., 2016; Grummer et al. 2019; Selmoni et al., 2020). Using a seascape genomics approach, I assessed population structure and connectivity for two coral species, *Pocillopora verrucosa* and *Pocillopora meandrina*, across environmentally heterogenous seascapes. I additionally investigated the predominant extrinsic factors that influence genetic variation, including the effects of (1) thermal and (2) non-thermal environmental predictors while controlling for spatial autocorrelation. The study systems included thermally and spatially contrasting seascapes: Australia's Coral Sea Marine Park, which consists of geographically isolated atoll reefs forming distinct habitat patches, and the adjacent Great Barrier Reef, which maintains greater spatial connectivity among reefs based on a greater density of reefs per km^2 (Ceccarelli et al., 2013; Hoey et al., 2022). To my knowledge, only a single study has quantified gene flow between the Coral Sea and GBR. This work focused on a brooding coral species displaying minimal connectivity between Osprey Reef and several reefs in the GBR (van Oppen et al., 2008), highlighting the paucity of empirical data to determine the existing connectivity between these regions. Both seascapes have been exposed to five recent mass bleaching events in 2016, 2017, 2020, 2022, and 2024 (Harrison et al., 2019; Hughes et al., 2018; Pratchett and Heron, 2021), where thermal stress varied markedly across reefs and taxa (Burn et al., 2023). The detection of neutral population structure in contrasting seascapes and species can provide a baseline to identify reefs which harbour higher genetic resilience or vulnerability amidst rapidly changing environmental conditions.

4.2 Methods

4.2.1 Coral collection and sampling

Two common Pocilloporid coral species, *Pocillopora meandrina* and *Pocillopora verrucosa,* were collected, both of which are mixed-mode (spawning/brooding) corals (Schmidt-Roach et al., 2012) with vertical transmission of algal-symbionts (Hirose et al., 2000). Corals were collected from Australia's Great Barrier Reef (hereafter, GBR) and Coral Sea Marine Park (hereafter, Coral Sea) (Figure 4.1a). Corals were collected from 16 sites among the GBR and 13 sites among the Coral Sea. In total, I collected tissue fragments from 188 *P. meandrina* and 255 *P. verrucosa* coral colonies across both regions that were used for downstream molecular analyses. Tissue fragments were collected on SCUBA from the GBR between January 2019 and April 2021 on four separate expeditions, and samples from the Coral Sea were collected on one expedition between February and March 2020. Reef coordinates and details for all 29 sampling locations are specified in SOM Table S4.1. Samples were collected from distinct coral colonies > 5 m apart to minimise the likelihood of collecting duplicate genotypes, of which none were detected. For each coral individual, photographs were taken at the colony and macro-scale using an Olympus TG-5, and bleaching scores were recorded *in situ* using a Coral Health Chart (Siebeck et al., 2006). A branch of each coral individual was collected using a hammer and chisel. Each individual fragment was placed into a separate, numbered Ziploc bag and stored in 100% ethanol within one hour of collection.

4.2.2 Species identification and sample selection

Corals were genetically identified to species-level by amplification of the mitochondrial open reading frame (mtORF) marker using two complementary approaches. First, I conducted a Restriction Fragment Length Polymorphism (RFLP) assay modified from Johnston et al. (2018) and detailed in Chapter 2. I then used Sanger sequencing of the mtORF region to resolve

any unidentified samples and to confirm species-level identification from the RFLP assay. Samples that were confirmed as either *P. verrucosa* (n = 255) or *P. meandrina* (n = 188) were selected for a genotype-by-sequencing approach.

4.2.3 Genotype-by-sequencing approach

Coral tissue samples of *P. verrucosa* and *P. meandrina* were sent to Diversity Arrays Technology (Canberra, Australia), where DNA extractions, library preparation, and sequencing were performed. Briefly, DNA was extracted from *Pocillopora* samples using a NucleoMag kit (Machery-Nagel). Libraries were constructed following a proprietary method of reduced-representation sequencing (DArT-seq; Kilian et al., 2012) following a double digestion with *Pst*I and *Hpa*II to maximise the complementarity of reads between samples (Sansaloni et al., 2011). The two *Pocillopora* species were subject to separate sequencing runs on an Illumina NovaSeq 6000, each across two lanes. Sequencing reads from both *Pocillopora* species were mapped to the *P. verrucosa* reference genome (Buitrago-López et al., 2020) and a DArT species database was developed for each of the two species. Data were initially filtered using proprietary DArT-sequencing pipelines (DArTsoft14). Filtering was then performed on raw sequences using a minimum Phred pass score of 30 for the barcode region, and a minimum Phred score of 10 for the entire read. Of the 255 samples of *P. verrucosa*, 206 (80.8%) passed initial quality control. Of the 188 samples of *P. meandrina* submitted, 115 (61.2%) passed initial quality control and were used in downstream analyses.

4.2.4 QC filtering of SNPS

All statistical analyses were conducted in R (R Core Team 2015) and code can be found at the live Github repository (https://github.com/magenamarzonie/Pocillopora_DartSeq). The initial filtering was conducted using the 'dartR' package (Gruber et al., 2018) and filtering steps were carried out separately for the two *Pocillopora* species with identical filtering parameters. SNPs

were filtered for linkage disequilibrium to retain a single SNP within a fragment when more than one SNP tag was detected. Loci were then filtered for reproducibility (< 0.98) to remove clones or duplicate samples before being further filtered by call rate (< 0.80) to exclude loci and/or individuals with more than 20% missing data. Further, loci with a read depth < 5x were also removed from the analysis. SNPs with minor allele frequencies (MAF) below 0.05 were filtered out to minimise the effects of rare variants. Monomorphic loci were excluded from downstream analyses and missing data were imputed using the 'nearest neighbour' function (*dartR*). The number of loci retained after each filtering step can be found in SOM Table S4.2. Multiple call rate filtering scenarios were tested for downstream estimates of pairwise genetic comparisons (F_{ST}) and multidimension analyses to ensure that population estimates of F_{ST} were stable irrespective of filtering.

4.2.5 Neutral population structure analyses

Reefs were grouped into 'sectors' which were determined based on reefs with the closest spatial proximity (Figure 4.1a) for pairwise comparisons of genetic structure to balance sample sizes after molecular confirmation of *P. verrucosa* and *P. meandrina*. The partitioning into sectors and additional collection metadata can be found in SOM Table S4.1. Heterozygosity (H_e and H_o) and inbreeding (F_{IS}) statistics for each sector were calculated using the package *hierfstat* (Goudet & Jombart, 2022). Pairwise F_{ST} values using the 'WC84' method (*hierfstat*) were computed following Weir & Cockerham (1984). Additionally, samples were randomly selected and subsampled (n=5) from each sector and F_{ST} values were computed, where no strong effect of unbalanced sample sizes among sectors was detected (SOM, Figures S4.1 and S4.2). An Analysis of Molecular Variance (AMOVA) was run with 999 permutations in *poppr* (Kamvar et al., 2015) to assess the proportion of genetic variance explained within samples, between samples, and between sectors (SOM Tables S4.3 and S4.4). The relationship between the linearised genetic distance and the log of geographic distance was then measured to explore

patterns of isolation-by-distance (IBD) between reefs. Significance of IBD was assessed using a Mantel test in *vegan* (Oksanen et al., 2022) (SOM Figure S4.3).

A principal component analysis (PCA) was performed to visualise genetic variation among samples without predictor constraints on population structure (SOM Figure S4.4). Group membership probabilities were then computed with admixture analysis using the 'snmf' function in *LEA* to define the number of *K*-clusters for each species and *q*-value proportions per individual (Frichot & François, 2015). I selected the optimal number of *K* ancestral populations between 1 and 10 and chose the model with the lowest cross-entropy value (SOM Figure S4.5). Once the optimal *K* was selected, ten repetitions were performed, and the repetition with the lowest cross entropy was selected. I then extracted *Q*-coefficients for each individual sample under the optimal number of *K*-clusters and plotted admixture coefficients in *ggplot2* (Wickham, 2016).

4.2.6 Environmental drivers of genetic structure

A redundancy analysis (RDA) was used to assess environmental covariates associated with host population structure using genetic distances of each individual as the response variable in the *vegan* package (Oksanen et al., 2022). The analysis was performed separately for each species and using 'reefs' as populations instead of 'sectors' to account for finer spatial variation in environmental predictors. I included several predictors related to 1) climatic (thermal related), 2) environmental (non-thermal related), and 3) geographic distance between reefs. Climatic predictors included the mean of monthly maxima Degree Heating Weeks (mean DHW) from 1985-2020, average Sea Surface Temperature (SST) (1985-2020), and Maximum Monthly Mean (MMM) climatology (1986-2012). The average number of maximum DHW summarise heat stress trends per reef and correlates significantly both with heat wave frequency and maximal intensity of heat waves (Selmoni, et al., 2024). Environmental predictors were acquired from RECIFS; (Selmoni et al., 2023) and from eReefs (Australian

Institute of Marine Science). The selected variables included light irradiance (kd490) and sea current velocity (SCV) of each reef (Table 4.1), which likely influence patterns of thermal and environmental variation among populations. To account for the geographic and spatial proximity between reefs, I incorporated distance-based Moran's Eigenvector Maps (db-MEMs) to estimate spatial distribution across sites at multiple spatial scales. Db-MEMs were extracted from each reef site using the 'dbMEM' function in *adespatial* (Dray et al., 2023) and used as predictor variables to account for geographic structure in the dbRDA models (SOM Fig S4.6 and S4.7).

After model construction, I checked for correlation among all climate, environment, and geographic predictors to minimise the effects of collinearity and removed one of two variables when $r > |0.8|$ using 'corrplot' (Wei & Simko, 2021) (SOM Fig S4.8). Variance inflation factor (VIF) scores of selected variables were < 5 and did not exhibit strong collinearity. A backward stepwise model was run with the selected variables using the 'ordistep' function (*vegan*) which iteratively runs all factors and reduces the model until the highest adjusted R^2 value is reached. The significant factors from the ordistep model were selected as the final predictors in each distance-based RDA model (Table 4.1).

Table 4.1. Climatic, environmental, and geographic metrics used in redundancy analyses to determine the significant predictors of genetic variance in *Pocillopora verrucosa* and *P. meandrina.*

Type of predictor	Variable	Definition
Climatic	Mean DHW	The mean of monthly maxima Degree Heating Weeks from 1985-2020.
	Mean SST	The average sea surface temperature experienced from 1985-2020.
	MMM	Maximum Monthly Mean climatology (1986-2012)
Environmental	Kd490	Light irradiance
	SCV	Mean sea current velocity
Geographic	MEM1	Moran eigenvector map (1)
	MEM2	Moran eigenvector map (2)
	MEM3	Moran eigenvector map (3)

4. 3. Results

4.3.1 Library statistics

Dart-sequencing analysis resulted in the detection of 43,980 single-nucleotide polymorphisms (SNPs) across 108 individuals for *P. meandrina*, and 44,310 SNPs across 200 individuals for *P. verrucosa.* After quality filtering, a total of 2,075 SNPs for *P. meandrina* and 3,722 SNPs for *P. verrucosa* were retained. There were no instances of duplicate samples or clones observed for either species, indicating the absence of clones or duplicate samples. The observed heterozygosity estimates were 1.3 times higher for *P. verrucosa* compared to *P. meandrina* across all samples (t-test; $p < 0.001$, $F = 28.63$, $Df = 1$).

Table 4.2. Library statistics for *P. verrucosa* and *P. meandrina* across sectors in the Great Barrier Reef and Coral Sea Marine Parks. The number of samples sequenced per species within each sector (N) and the corresponding number of samples passing quality control (N_{QC}). Population statistics calculated include observed heterozygosity (H_O), expected heterozygosity (H_E), and population-level F_{IS} statistics per coral species within each sector.

		P. verrucosa					***P. meandrina***				
Region	Sector	N	N_{QC}	H_o	H_e	F_{is}	N	N_{QC}	H_o	H_e	F_{is}
GBR	Cape Grenville	30	24	0.10	0.13	0.221	-	-	-	-	-
	Princess Charlotte Bay	30	23	0.10	0.13	0.223	19	13	0.08	0.11	0.229
	Cairns	8	5	0.09	0.13	0.192	-	-	-	-	-
	Townsville	30	15	0.09	0.13	0.235	7	4	0.08	0.11	0.229
	Swains	-	-	-	-	-	24	8	0.07	0.12	0.325
	Capricorn Bunkers	6	-	-	-	-	24	14	0.08	0.12	0.26
Coral Sea	CS1	29	29	0.10	0.13	0.239	14	8	0.07	0.12	0.285
	CS2	46	38	0.10	0.13	0.229	12	4	0.08	0.12	0.227
	CS3	24	20	0.10	0.13	0.214	28	18	0.07	0.12	0.283
	CS4	14	10	0.13	0.14	0.082	15	8	0.07	0.12	0.276
	CS5	31	31	0.10	0.13	0.225	17	8	0.08	0.12	0.223
	CS6	8	5	0.09	0.14	0.229	48	23	0.08	0.11	0.257

4.3.2 Genetic structure among regions and sectors

Pairwise comparisons of global F_{ST} values revealed that *P. meandrina* exhibited stronger overall population structure among reef sectors (F_{ST} range: 0 – 0.146; mean F_{ST} = 0.030 ± 0.035), which were generally higher than pairwise comparisons among sectors for *P. verrucosa* (F_{ST} range: 0 – 0.024; mean F_{ST} = 0.004 ± 0.007). The analysis of molecular variance (AMOVA) indicated genetic differences between sectors were small but significant and stronger for *P. meandrina* (*P. meandrina* = 0.7%, p = 0.04; *P. verrucosa* = 0.1%; p = 0.02). For both species, higher genetic variation was attributed to variation between colonies sampled within a sector (*P. meandrina* = 36.6%; *P. verrucosa* = 25.9%; p < 0.001), and most genetic

variation occurred for both species within individual colonies (*P. meandrina* = 62.7%; *P. verrucosa* = 74.0%, $p < 0.001$).

The species *P. verrucosa* demonstrated overall reduced population structure compared to *P. meandrina*. Except for CS6, all sectors and regions displayed extremely low population structure for *P. verrucosa* (F_{ST} range: 0 – 0.009) (Figure 4.1c). The strongest genetic differences were detected within reefs of the Coral Sea, between the highest latitude sector (CS6) and the two lowest latitude sectors, CS1 and CS2 (F_{ST} range: 0.021 – 0.024). Similar levels of genetic differences were also observed between the lowest latitude sectors in the GBR, Cape Grenville and PCB (F_{ST} range: 0.021 – 0.022), suggesting comparably low rates of genetic structure within and between regions for this species. Stronger sector-level genetic differences for *P. meandrina* occurred between spatial extremes in the sampling, namely a low latitude sector of the GBR (Princess Charlotte Bay) and the two highest latitude sectors of the Coral Sea (CS5, CS6). The highest latitude Coral Sea sectors (CS5, CS6) and the GBR were genetically similar in population structure (Capricorn Bunkers; F_{ST} range: 0.007 – 0.018). Interestingly, there were greater genetic differences between CS5 and CS6 and the geographically closer, offshore Swain reefs (F_{ST} range: 0.084 – 0.105) (Figure 4.1b), indicating that geographic distance was not the predominant influence on population structure.

Isolation-by-distance (IBD) models revealed a significant relationship between geographic and genetic distances for *P. verrucosa* ($R^2 = 0.325$; $p = 0.038$) that was predominantly driven by high latitude reef sectors in the Coral Sea (CS5 and CS6) and a weaker trend in IBD resulted when removing these reefs from the analysis for *P. verrucosa*. There was a weak, non-significant trend in IBD for *P. meandrina* ($R^2 = 0.058$; $p = 0.058$) (Figure S4.3).

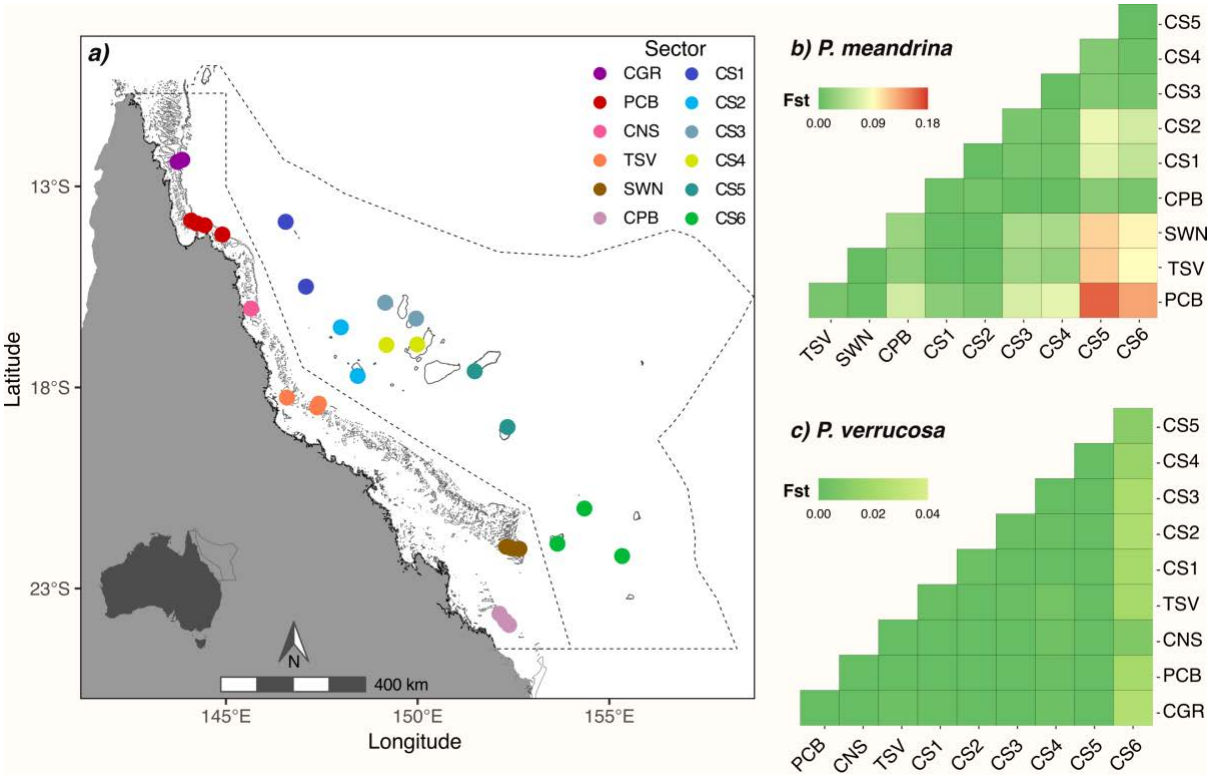

Figure 4.1. Population structure for *Pocillopora meandrina* and *P. verrucosa* across the GBR and Coral Sea. (a) Map of sectors partitioned in Australia's Great Barrier Reef (GBR) and Coral Sea Marine Park (CSMP). Sectors considered in the analysis of population structure include: Cape Grenville (CGR), Princess Charlotte Bay (PCB), Cairns (CNS), Townsville (TSV), Swains (SWN), Capricorn Bunkers (CPB), Coral Sea Sector 1-6 (CS1-6). (b) Pairwise comparisons of genetic diversity (F_{ST}) between sectors for *Pocillopora meandrina* and (c) for *Pocillopora verrucosa*.

4.3.3 Model-based estimation of ancestry

Admixture analyses indicated the presence of two distinct genetic clusters for *P. meandrina*, PMCL1 and PMCL2, which were detected across all sectors within the GBR and Coral Sea (Figure 4.2a,c). Although both genetic lineages were evenly present in the study area (frequency of PMCL1 = 47.0%; PMCL2 = 52.9%), their relative abundance varied markedly by region. The two lineages were unevenly distributed throughout the two regions, where

PMCL1 was found in higher prevalence across the GBR (72.6%) compared to the Coral Sea (32.6%). Conversely, PMCL2 was found more commonly in the Coral Sea (67.3%) compared to the GBR (27.3%) (Figure 4.2a,c). Strong contrasts also occurred among sectors within regions (Figure 4.2a,c). The strongest differences occurred between the high latitude sectors of the Coral Sea (CS5 and CS6) and the low latitude sectors of the GBR (Princess Charlotte Bay and Townsville). The genetic cluster PMCL1 comprised 69.9% of sampled colonies in Princess Charlotte Bay and Townsville, compared to only 12.3% of sampled colonies in CS5 and CS6. The detection of PMCL1 increased in the Coral Sea in lower latitude reefs, comprising 70.0% of group membership in CS1 and CS2. The Swains sector of the GBR represented surprisingly high group membership to PMCL1 (87.1%), compared to the Capricorn Bunker region (62.9%), despite the Swains sector in geographical proximity to the CS5 and CS6 sectors where high PMCL2 group membership occurred (87.7%) (Figure 4.2a,c).

Two distinct genetic clusters for *P. verrucosa* (PVCL1 and PVCL2) were detected through admixture analysis across the GBR and Coral Sea (Figure 4.2b,d). There was less defined spatial structuring in *P. verrucosa* compared to *P. meandrina* across both regions. The minimal spatial structuring in *P. verrucosa* was attributed to a dominance of the lineage PVCL1 which accounted for an average membership coefficient of 86.3% per individual across both regions. In contrast, PVCL2 represented 13.6% of membership across all sectors. There were not marked differences in the proportion of PVCL1 and PVCL2 between the GBR and Coral Sea, where PCVL1 made up 92.1% of group membership in samples across the GBR region and 83.5% of samples in the Coral Sea. The proportion of group membership to PVCL2 ranged markedly from 6.2% in the lowest latitude GBR sector (Cape Grenville) to 72.5% in the highest latitude Coral Sea sector (CS6) (Figure 4.2b,d).

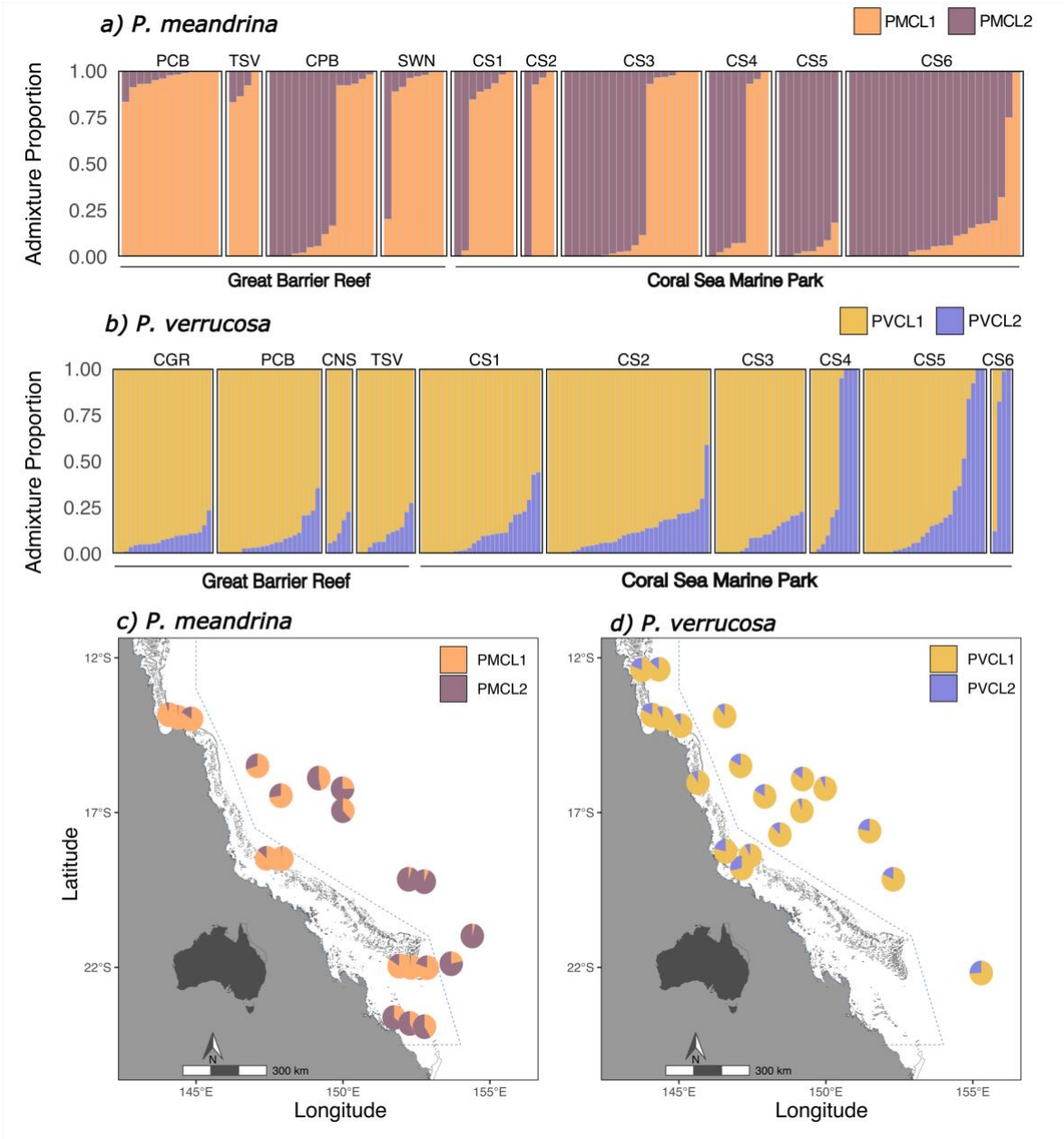

Figure 4.2. Genetic membership probability and clustering of *Pocillopora meandrina* and *P. verrucosa*. Admixture analyses indicated two genetic clusters (*K*=2) for both species including (a) *P. meandrina* (PMCL1 and PMCL2) and (b) *P. verrucosa* (PVCL1 and PVCL2). Each vertical bar depicts one individual and the estimated ancestry coefficient to each cluster. Admixture coefficients in relation to biogeographic patterns of structure for (c) *P. meandrina* and (d) *P. verrucosa.*

4.3.4 Environmental correlations with individual genetic structure

A distance-based partial redundancy analysis (pRDA) revealed that genetic differences amongst individuals were partially attributed to a combination of climatic and environmental gradients throughout the two reef systems, while accounting for the conditional effects of geographic structure using dbMEMs. The two main axes of variation explained 4.3% of genetic variation in *P. meandrina*, compared to 0.2% of *P. verrucosa*. For *P. meandrina,* the first axis alone explained 4.2% of genetic variation among samples and was significantly associated with both thermal history (mean Degree Heating Weeks [DHW]) and sea current velocity (SCV). The second axis had negligible influence from both significant predictors, explaining 1.0% of variation (Figure 4.3a). The significant predictors in the RDA model included mean SCV ($F = 2.77$, $Df = 1$, $p < 0.001$) and mean DHW ($F = 1.98$, $Df = 1$, $p = 0.003$) (Table 4.3). Individual genetic differences between *P. verrucosa* were associated only with thermal metrics compared to non-thermal predictors. However, the first axis explained only 0.1% of variation and associated with mean Sea Surface Temperature (SST), while the second axis explained an additional 0.1% of variation and associated with thermal disturbance history (mean DHW) (Figure 3b). For *P. verrucosa,* genetic variation was significantly explained by mean SST ($F = 1.71$, $Df = 1$, $p < 0.001$) and mean DHW ($F = 1.15$, $Df = 1$, $p < 0.001$) (Table 4.3).

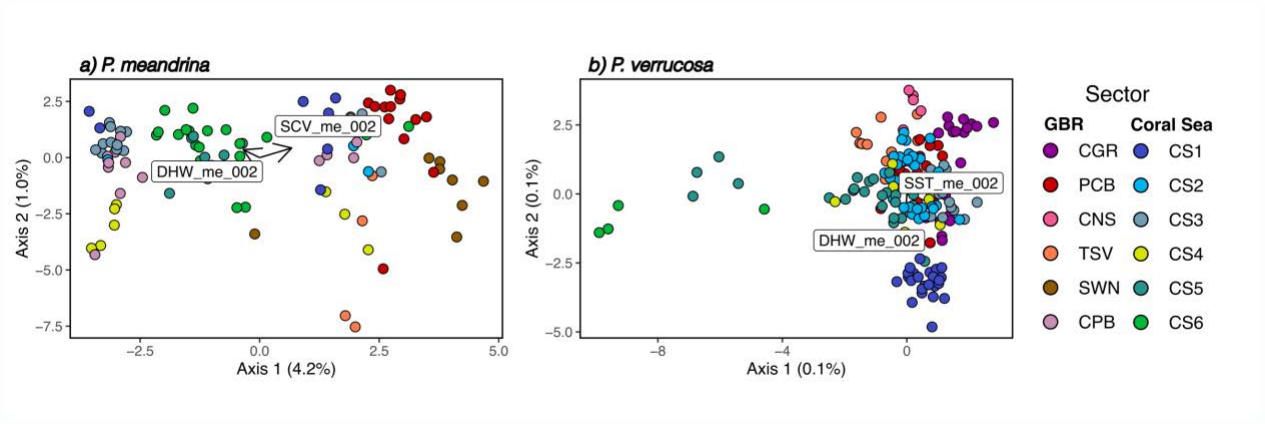

Figure 4.3. Distance-based partial redundancy analysis (pRDA) for the environmental drivers of genetic structure among individuals in (a) *P. meandrina* and (b) *P. verrucosa*. Plots are coloured by sectors within the Great Barrier Reef (GBR) and Coral Sea Marine Parks. Vectors indicate environmental predictors which are significant in the partial RDA models.

Table 4.3. Backward stepwise partial redundancy analysis outputs for the environmental predictors of individual genetic structure for *P. meandrina* and *P. verrucosa.*

Species	Variable	Df	Variance	F	Pr (>F)
P. meandrina	mean DHW	1	11.15	1.9843	0.003
	Mean SCV	1	15.59	2.7738	0.001
	Residual	103	579.01		
P. verrucosa	Mean DHW	1	7.96	1.1463	0.001
	Mean SST	1	11.86	1.7088	0.001
	Residual	175	1214.50		

4.3.5 Spatial distribution of environmental predictors across the Coral Sea and GBR

Strong climate history (mean DHW and mean SST; Figure 4.4a-b) and environmental history (SCV; Figure 4.4c) were the strongest predictors of genetic structure across the two regions for both *P. meandrina* and *P. verrucosa* when accounting for the conditional effects of geographic distance. Notably, the high latitude reefs of the Coral Sea had contrasting patterns of thermal and environmental variation compared to other adjacent reefs in the GBR (Fig 4.4a-c). The

maximum mean DHW ranged between 0.30-0.69 DHW in the GBR, and 0.54-0.88 DHW in the Coral Sea and varied significantly by region (t-test; $p < 0.001$, $F = 37.15$, $Df = 1$). In contrast, the average SST ranged between 24.39- 26.85 °C in the GBR, and 25.16- 27.11 °C in the Coral Sea and were not significantly variable by region (t-test; $p = 0.09$, $F = 3.00$, $Df = 1$). Between the two sectors, the strength of sea current velocity was not significantly variable between the GBR (0.06- 0.23 m/s) compared to the Coral Sea (0.07- 0.26 m/s) (t-test; $p = 0.74$, $F = 0.11$, $Df = 1$).

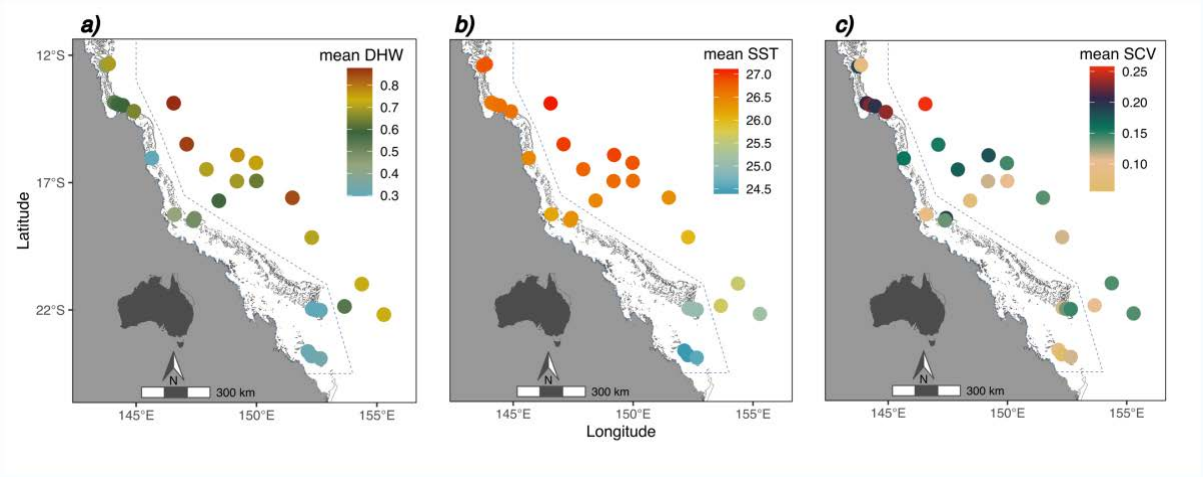

Figure 4.4. Spatial distribution of significant model predictors for *P. meandrina* and *P. verrucosa* across the Great Barrier Reef and Coral Sea Marine Parks. (a) Mean DHW refers to mean monthly maximum DHW experienced at each reef. (b) Mean SST refers to the average sea surface temperature at each location. (c) Mean SCV refers to the strength of sea current velocity at each reef. All variables are averaged between 1985-2020 using 5km resolution.

4.4. Discussion

Few studies have assessed the population structure and connectivity of corals between the Coral Sea and GBR, which are key metrics to quantify the genetic diversity and connectivity

of these ecologically important seascapes. My analyses revealed the genetic structure of Pocilloporids across reefs and regions in the Coral Sea and GBR spanning 12° in both latitude and longitude. The presence of gene flow across large seascapes indicates the capacity for the GBR and Coral Sea to act as reciprocal population replenishment sources, with important implications for co-management of marine estates in both the GBR and Coral Sea Marine Parks (Roberts et al., 2021). These taxa-specific patterns of population structure occurred for two closely related Pocilloporids, where *Pocillopora meandrina* maintained higher population structure compared to *P. verrucosa*. These taxa-specific contrasts in genetic structure emphasise the importance of quantifying gene-environment trends in taxa with similar demographic traits. The genetic structure of both species of Pocilloporids correlated with a gradient in thermal history across the GBR and Coral Sea, as well as sea surface temperature for *P. verrucosa* and sea current velocity for *P. meandrina*.

High latitude reefs are genetically distinct

High latitude, offshore reef populations maintained the strongest genetic isolation for both *Pocillopora* species in this study. Specifically, high latitude reefs in the Coral Sea were most genetically distinct from low latitude reefs in the GBR. This genetic structuring indicates potential edge effects of species existing close to their environmental or thermal range limits with cascading effects on their genetic structure (Ries et al., 2004). The geographic isolation of high latitude reefs may promote greater local adaptation, but also vulnerability, following disturbances (Hughes, et al., 2018). Empirical evidence from Chapter 2 shows that high latitude reefs in the Coral Sea and GBR have experienced higher recent thermal history (recent maximum DHW between 2016-2020) compared to lower latitude reefs in the Coral Sea and GBR, leading to selection for more heat tolerant species and individuals. The observed genetic differentiation of high latitude reefs may therefore reflect selection for traits associated with

heat tolerance. Similar patterns of genetic differentiation have been demonstrated in high latitude reef populations in Western Australia, where strong population structure has been quantified compared to lower latitude and spatially proximate reefs (Thomas et al., 2017). This study corroborates this evidence in Eastern Australian coral populations, highlighting local adaptation, and isolation of high latitude reefs.

Despite reduced gene flow to the high latitude reefs of the Coral Sea, all populations maintained comparable levels of genetic diversity. This suggests that even geographically isolated reefs still comprise sufficient genetic diversity against a backdrop of climatic or environmental disturbances. My results support that corals with mixed-mode reproduction have the capacity to travel farther distances and maintain connectivity among reefs and regions in the Coral Sea and GBR. This empirical evidence in two common coral species confirms the genetic exchange among reefs in the GBR and Coral Sea, highlighting the importance of the Coral Sea and GBR as reciprocal sources of population replenishment across spatially separated regions.

Taxa specific trends in population structure

Comparisons across Pocilloporids with similar traits (e.g., mixed-mode reproduction with vertical symbiont transmission) revealed the importance of quantifying population structure and connectivity not only in distinct taxa, but also between similar taxa. There are several biological and environmental factors that may attribute to the contrasts observed in closely related species. First, *P. verrucosa* has a higher thermal tolerance than *P. meandrina*, which has been empirically quantified through controlled heat stress experiments in Chapter 2, and is evidenced by variable distribution across warmer and cooler reefs in both the Coral Sea and GBR in this study, as well as across Hawaiian reefs in Johnston et al. (2018). The thermal limits of these species may in part, explain the contrasting genetic patterns observed in this study.

The strong population structure in *P. meandrina* may also be attributed to cryptic speciation within this species complex compared to *P. verrucosa*, which has been reflected in the strong division among two symbiont groups residing in the tissue of *P. meandrina* (*Cladocopium latusorum* 'north' and 'south') compared to a more homogenous symbiont community in *P. verrucosa* (*Cladocopium pacificum*) across the Coral Sea, as shown in Chapter 3. The lack of empirical evidence for the reproductive mode in both *P. meandrina* and *P. verrucosa* may also indicate that *P. meandrina* relies more on brooding as a reproductive mechanism, contributing to higher population structure, compared to *P. verrucosa* which may rely more on broadcast spawning (Hirose et al., 2000; Schmidt-Roach et al., 2012). Minimal spatial structuring and panmictic populations have been observed in *P. verrucosa* across the Western Indian Ocean (Oury et al., 2021), Eastern African coast (Gélin et al., 2017), and Red Sea (Buitrago-López et al., 2023), though less evidence exists specifically for the population structure of *P. meandrina*. Species-specific population structure has also been observed in two brooding *Pocillopora* species in New Caledonia, where *P. damicornis* comprised higher population structure than *P. acuta* (Selmoni et al., 2021), reflecting the taxa-specific trends observed here.

Climatic, environmental, and geographic drivers of genetic structure

Considering variable species-specific structure, climate maintained the strongest influence on the population structure for both species. Maximum Degree Heating Weeks was a strong predictor compared to non-thermal geographic predictors for both Pocilloporids. These findings indicate the significant influence of marine heatwaves on population structure across distinct regions and species over a short ecological timeframe (1985-2020). Additionally, the co-dominant clusters of *P. meandrina* were influenced by sea current velocity, indicating that non-thermal factors also play a role in shaping the higher partitioning of population structure

observed. Mean current speed has been shown as a predictor of the brooding coral species, *Stylophora pistallata,* across the GBR (Meziere et al., 2024), corroborating evidence of oceanographic processes in driving population structure. The Southern Equatorial Current bifurcates north and south in the Coral Sea and GBR at between 15 and 17° latitude dependent on depth (Ceccarelli et al., 2013), and may explain the geographic partitioning in the two genetic lineages of *P. meandrina* (PMCL1 and PMCL2) and the greater influence of non-thermal predictors. However, *P. verrucosa* was distinctively influenced only by thermal predictors including SST and DHW, where several genetically distinct individuals in the high latitude, Coral Sea reefs strongly pulled this trend. This pattern indicates strong patterns of local adaptation to variable environment in these reefs which have experienced stronger thermal history (Burn et al., 2023; Harrison et al., 2019). Given samples were genetically confirmed as *P. verrucosa* and *P. meandrina* with multiple genetic markers (mtORF marker, SNPs), this trend is likely not an artefact of sampling or sequencing, but indeed a biological signal of adaptation and/or this species reaching the end of their thermal range limits in high latitude reefs.

An important caveat to note with gene-environment associations (i.e., partial RDAs) is that many of the tested variables are likely correlated and signals of one predictor may also be explained by the influence of other untested predictors that were removed due to high collinearity (Capblancq & Forester, 2021). While significant efforts were made to reduce the effects of strongly related variables while still accounting for as much variation explained as possible, there is a challenge in pinpointing a specific non-thermal environmental predictor without acknowledging that other factors may be contributing drivers to population structure. Thus, there may be confounding effects with climate or environment that are masked through this analysis and should be acknowledged as possible drivers of population structure.

Conclusion

This study presented an opportunity to measure the population structure of two common Pocilloporid coral species in the GBR and Coral Sea and demonstrates pervasive genetic connectivity throughout the Coral Sea and GBR with implications for population replenishment between reefs following disturbances. *Pocillopora meandrina* and *P. verrucosa* were both strongly partitioned by thermal history, suggesting that neutral population structure in *Pocillopora* spp. may have been influenced by the strong severity of disturbance history experienced at reefs, as well as the variation in the frequency and magnitude of these disturbances among reefs and regions. While not explicitly addressing the occurrence of loci associated with heat tolerance across spatially distinct reefs, this study provides a strong foundation for identifying the environmental predictors in alignment with genetic structure across large marine seascapes. Detecting the environmental trends that shape the genetic structure of coral populations and species can improve our understanding of how reefs are naturally equipped to adapt or respond to the effects of thermal and environmental disturbances.

Chapter 5. Adaptive loci under selection correlate to thermal history and symbiont community structure in a common *Acropora* coral species

5.1. Introduction

Coral reefs are highly vulnerable to anthropogenic climate change pressures and increasingly subjected to severe marine heatwaves (Hughes et al., 2018). Widespread coral bleaching has already resulted in devasting impacts to coral reef ecosystems globally, driving mass-mortality events (Oliver et al., 2018; Smale et al., 2019). Severe and annual coral bleaching events are expected to occur globally under high carbon emission scenarios in the next decades (McWhorter et al., 2022), reducing reef species diversity and compromising ecosystem function. High temperatures result in dysbiosis in the relationship of corals and their endosymbiotic algae, Symbiodiniaceae, driving the process of coral bleaching (Morris et al., 2019; Weis et al., 2008). However, phenotypic bleaching responses do not always correlate directly to the severity of marine heatwaves across large seascapes (Burn et al., 2023; Guest et al., 2012; Harrison et al., 2019), indicating that other intrinsic and extrinsic factors mediate heat tolerance. To understand the trajectories of reef health in the present and future, it is essential to identify the intrinsic (host and symbiont adaptation) and extrinsic (climate and environment) factors of adaptation underlying the variable patterns of heat tolerance among corals.

The adaptive potential of reef corals and their symbionts are key biological mechanisms which can elevate the heat tolerance of corals against selective pressures (Matz et al., 2018). The ability for evolutionary adaptation at the rate of environmental change will depend on (1) how rapidly ocean warming occurs and (2) the rate of adaptation compared to genetic fixation in coral heat tolerance (Lachs et al., 2023). Specifically, low carbon emission scenarios combined

with high adaptation rates will enable coral persistence, while high emission scenarios and fixed rates of heat tolerance will result in the most concerning outlook on coral mortality (Lachs et al., 2023). For corals to adapt, mechanisms must occur at the level of individuals, populations, and species, yet modelling approaches are unable to discern whether increased heat tolerance is due to population-level adaptation versus community level shifts in heat tolerant species (Sully et al., 2019). To clarify adaptation in corals, this requires efforts across several regions and coral species to confirm how climate change and coral heat tolerance adaptation will interact.

Heat tolerance in corals can be shaped by acclimatisation over an individual's lifespan or through adaptation over generations (DeCarlo et al., 2019; Torda et al., 2017). The genetic architecture of corals partially mediates coral heat stress, where some detected single nucleotide polymorphisms (SNPs) in corals are correlated with heat stress gradients (Selmoni et al., 2021) and natural bleaching resistance (Fuller et al., 2020). Cryptic speciation of the coral host can also regulate thermal tolerance thresholds, where morphologically indistinguishable species have shown differential bleaching responses to heat stress (Rose et al., 2021; Starko et al., 2024). For example, the environmental drivers (i.e., temperature, irradiance, currents) linked to cryptic speciation can vary in their relative role of shaping species distribution (Meziere et al., 2024), highlighting the importance of distinguishing cryptic species to better detect both environmental and genetic mechanisms of phenotypic variance in heat tolerance. Unveiling cryptic speciation across multiple reef systems is valuable where differential genetic lineages potentially mask other more subtle predictors (i.e., environmental, symbiont communities, host adaptive loci).

Heat tolerance across coral species is a polygenic trait influenced by many genes with small effect sizes (Fuller et al., 2020; Quigley et al., 2020; Rose et al., 2018). The polygenic nature

of heat tolerance has been confirmed in corals through sampling during natural bleaching events (Fuller et al., 2020), across temperature mosaics within thermally variable reef habitats (Palumbi et al., 2014), and through exposure to controlled heat stress (e.g., common garden experiments) (Thomas et al., 2022). Effectively pinpointing the genetic architecture of heat tolerance in corals requires large sample sizes and/or higher gene coverage (i.e., whole genome sequencing) to determine genes under selection compared to other traits such as disease resistance (Vollmer et al., 2023). As such, there remains a challenge to effectively translate the genetic mechanisms underpinning phenotypic heat tolerance. The additional adaptive capacity of the symbionts residing in the coral host adds an additional layer to their heat tolerance potential and needs to be examined in combination with the coral host genetics and environmental gradients (Starko et al., 2024).

Seascape genomics is an approach increasingly used to understand coral adaptation, by defining the patterns of population genetic structure along contrasting environment gradients (gene-environment association; GEA) (Riginos et al., 2016; Selmoni, Bay, et al., 2024). Examining genetic structure along an environmental gradient enables the detection of neutral and adaptive population structure of corals to different thermal clines (e.g., climatic gradients along latitude or populations with variable marine heatwave exposure) (Rellstab et al., 2015). A seascapes genomics approach benefits from sampling high numbers of individuals across a contrasting environmental gradient to detect loci associated with their environment. In tandem, controlled experiments offer a complementary approach where experimentally derived heat tolerance thresholds and genetic analyses (genotype-phenotype interactions) can ground-truth the putatively adaptive loci derived from seascape genomics. However, experimental systems are limited to reduced sample sizes, and it is still unclear whether experimental heat tolerance accurately reflects natural heat tolerance. Therefore, a combination of seascape genomics and controlled experimental studies can provide a complementary and more comprehensive

understanding of the genetic basis of heat tolerance and better means to distinguish the mechanisms that underpin thermal adaptation in corals.

Here, I investigated the adaptive (genetic and symbiont) and environmental drivers of coral heat tolerance in a common *Acropora* species (*Acropora* cf. *humilis*) across an environmental gradient. I used acute heat stress experiments to determine heat tolerance phenotype on 168 *Acropora* cf. *humilis* corals and sequenced the host and symbiont genetics of 260 *A.* cf *humilis* individuals throughout the isolated atolls of the Coral Sea Marine Park. In this region, limited gene flow between reefs is expected, allowing a greater resolution of adaptive and evolutionary processes shaping heat tolerance (Thomas et al. 2017). First, a seascape genomics approach was used to identify the environmental, thermal, and geographic predictors of putatively adaptive loci. In parallel, I investigated how empirical heat tolerance (ED50) was predicted and the relative contributions of symbionts, host genetics, environment. Identifying the strongest predictors of heat tolerance among individuals and populations is a critical step to understanding adaptive and acclimatory mechanisms in response to a rapidly changing climate.

5.2. Materials and Methods

5.2.1 Coral experimental approach and field genetic sampling

Corals were collected on SCUBA across 11 reefs in the Coral Sea Marine Park (CSMP) spanning 1,300 kilometres and a 1.8°C range in Maximum Monthly Mean (MMM) temperatures. Acute heat stress experiments were conducted for 8 of the 11 reefs using a portable, flow-through seawater aquarium system to quantify thermal stress across individuals, species, and reefs. Corals were exposed to an ambient temperature (control), as well as a +3, +6, and +9 °C treatment above the local MMM of each reef. For each individual sampled (n = 5 branches per individual colony), one branch was placed in each of the four temperature

treatments, with the remaining branch stored in 100% ethanol for genetic sequencing. Photosynthetic efficiency of each coral branch across all treatments (F_v/F_m) was quantified using dark-adapted PAM fluorometry as a proxy for bleaching. Using the F_v/F_m response for the same individual across four treatments, a 50% bleaching threshold (ED50) was quantified as a dose response curve. The 50% threshold was used as a heat tolerance metric for each individual and population, and detailed statistical methods can be found in Chapter 2. Briefly, individual-level dose response curves were calculated with a three-parameter log-logistic model in the package *medrc* (Ritz et al., 2015). The median yield of F_v/F_m for each individual was modelled against the ambient temperature relative to local MMM (^oC). Each individual colony was included as an additional random effect, as a branch of each colony was included in each of the four experimental treatments.

Samples were collected during the February-March 2020 mass bleaching event in the Coral Sea. The number of accumulated Degree Heating Weeks (DHW) ranged from 5.7-10.0 across reefs during the month of collection. Genetic samples of coral individuals were collected from three reefs in addition to the eight reefs where experiments were conducted for molecular identification of the coral host and associated endosymbiotic algae (Symbiodiniaceae). Bleaching phenotype scores (Coral Watch Health Chart) and collection depth (m) were recorded *in situ* for each individual colony prior to the collection of samples.

5.2.2 Host molecular sequencing methods

For host genetic sequencing, coral tissue from each coral individual was transferred to 70% ethanol and sent to Diversity Arrays Technology (Canberra, Australia) for DNA extractions, library preparation, and sequencing. A genotype-by-sequencing approach was used to obtain single-nucleotide polymorphisms (SNPs). Coral samples were sequenced using DArT-sequencing (Kilian et al., 2012), a proprietary form of restriction-site-associated sequencing. Libraries were constructed using the *Pst*I and *Hpa*II restriction enzymes (Sansaloni et al., 2011)

and sequencing was performed on the Illumina HiSeq2500 platform. Samples from each reef and region were randomly distributed across each 96-well plate to minimise the effect of plate position. Sequences were mapped against the *Acropora tenuis* (Liew et al., 2016) and *A. millepora* (Fuller et al., 2020) genomes. Data were initially filtered using proprietary DArT-sequencing pipelines (DArTsoft14). Filtering was performed on raw sequences using a minimum Phred score of 30 for the barcode region, and a minimum Phred score of 10 for the entire read.

5.2.3 Identification of Symbiodiniaceae *populations*

To identify community composition of Symbiodiniaceae within coral host samples, DNA was extracted using a modified version of Wayne's method (Wilson et al., 2002). DNA concentrations were quantified using a Qubit 3 Fluorometer and Qubit High Sensitivity Assay Kit (Invitrogen), and samples were then standardised to 10 ng μL^{-1} with an automated pipettor (QIAgility, QIAGEN). The internal transcribed spacer 2 (ITS2) region in Symbiodiniaceae was amplified using Polymerase Chain Reaction with forward and reverse primers from Pochon et al. (2001). The thermal cycler conditions included an initial incubation for 7 minutes at 95 °C, followed by 30 cycles at 95 °C, annealing at 59 °C, and extension at 72 °C for 30 seconds each. A final elongation completed the PCR at 72 °C followed by a 4 °C hold. Amplified PCR products underwent amplicon sequencing on the Illumina MiSeq platform at 2 x 300 bp paired-end V3 chemistry (Ramaciotti Centre for Genomics, UNSW). ITS2 type profiles and 'defining intragenomic variants' (DIVs) were analysed with SymPortal (Hume et al., 2019). A Generalised-UniFrac (G-UniFrac; $\alpha = 0.5$) score was calculated as a distance matrix to compare the relatedness between each symbiont community between individual coral samples and applies more even weighting to both rare and abundant sequences. A hierarchical clustering tree was then modelled using the G-UniFrac distance (Chen et al., 2012) to define symbiont clusters associated with each individual of *A.* cf *humilis* as per methods in Chapter 3.

5.2.4 QC filtering of host SNPS

All statistical analyses were conducted in R (R Core Team 2015) and analyses can be found at the Github link https://github.com/magenamarzonie/AcroporaDartseq. The initial host genetic filtering was conducted using the 'dartR' package (Gruber et al., 2022). First, secondaries were filtered out to lower the rate of linkage disequilibrium and retain a single SNP per locus. Loci were then filtered for reproducibility (< 0.98), call rate (< 0.80), and read depth (< 5x) to call by genotype. Multiple call rate scenarios were tested (0.80, 0.85, 0.90) and there were comparable outcomes for F_{ST} and PCAs using the three scenarios (SOM Figure S5.1). Therefore, the lowest call rate (0.80) was used in downstream analyses to maximise the number of loci used in gene-environment association analyses. Call rates were also filtered at the level of individuals (0.80) and four individuals with > 20% missing data were removed from the analysis. Minor allele frequencies below 0.05 were then filtered out to retain only common variants. Monomorphic loci were filtered out and missing data were imputed using the 'nearest neighbour' function.

5.2.5 Population structure analyses

Neutral loci must first be detected prior to assessing adaptive loci under selection. Therefore, I first assessed the neutral population structure of *A.* cf *humilis* across all 11 reefs where corals were genetically sampled. Both expected and observed heterozygosity were calculated (H_E and H_O), as well as inbreeding coefficient (F_{IS}) statistics with *hierfstat* (Goudet & Jombart, 2022). Global pairwise comparisons (F_{ST} values) were then computed using the 'WC84' method (*hierfstat*) following Weir & Cockerham (1984). A principal component analysis (PCA) was performed to visualise genetic variation among individuals and reefs without underlying assumptions on population structure (Figure S5.2). Isolation-by-distance models were run using the log of geographic distance vs. genetic distance (F_{ST} /1-F_{ST}) and significance was tested using a Mantel test in *vegan* (Oksanen et al., 2022) (Figure S5.3).

The number of genetic clusters (n = 3) detected from the PCA was validated using admixture analyses in LEA (Frichot & François, 2015). The *snmf* function (LEA) was used to run cross-entropy criterion models and estimate the optimal number of *K* ancestral populations (Figure S5.4). Ten repetitions were performed for each *K,* and the repetition with the lowest cross entropy was selected. A Q-value representing the proportion of each of the three lineages per individual sample was calculated to estimate admixture coefficients across individuals and averaged at the population (reef) level. Given three lineages of *A.* cf *humilis* were detected, all filtering statistics were run on the main lineage (AHCL1), as well as for all combined lineages (AHCL1, AHCL2, and AHCL3) (SOM Fig S5.5).

5.2.6 Genotype by environment association (GEA) analysis

RDA is a powerful approach to detect multi-locus signatures of adaptation, therefore the appropriate choice to use on a polygenic trait such as heat tolerance. Here, the drivers of genetic structure were tested using full and partial redundancy analysis (RDA) following Capblancq & Forester (2021) to identify the predictors correlated with individual SNPs. All genotype-by-environment association analyses were run in the package *vegan* (Oksanen et al., 2017). I first ran a full RDA with thermal, non-thermal, spatial, and host genetic variables (Table 5.1). Thermal variables were extracted from the NOAA Coral Reef Watch 5km resolution data set (Liu et al., 2014). Non-thermal variables were extracted from the RECIFS database (Selmoni et al., 2023). Geographic variables were calculated using distance-based Moran Eigenvector Models (db-MEMs) to account for spatial autocorrelation using the 'dbMEM' function in the *adespatial* package (Dray et al., 2023) (SOM Fig S5.6). Host PC1 and PC2 from the multidimension analyses were also incorporated to account for both neutral population structure and the three cryptic lineages identified (AHCL1, 2, and 3). When high correlation between predictor variables occurred, one of two variables were removed when collinearity was high ($r > |0.8|$) (*corrplot*) (Wei & Simko, 2021) (SOM Figure S5.7). Variance inflation

factor (VIF) scores were then checked to ensure all model predictors had a VIF score less than 5 (Oksanen et al., 2017). A forward stepwise selection model was then run on all variables using the 'ordistep' function to account for the simplest and best-fit model predictors using 999 permutations. Model variables with the highest adjusted R^2 value were selected for the partial RDA to use as conditional effects.

As heat tolerance is the trait of interest in this study, a partial RDA was then run to assess the thermal variables which most strongly predicted genetic structure in *Acropora* cf *humilis*. The Euclidean SNP-based, genetic distance of each individual was included as the response variable. The predictors included significant thermal variables from the RDA model, including recent maximum DHW (2016-2020), the number of DHW events > 4 (1986-2020), and the return time between DHW > 6 (1986-2020). In addition, conditional effects were included to account for non-thermal, spatial, and host genetic variation in the model including depth, mean sea current velocity, light attenuation, host cryptic species (neutral population structure), and spatial factors (Moran eigenvector models; MEM1, MEM2, and MEM3) (Table 5.1).

Table 5.1. Environmental, symbiont, and host genetic predictors and conditional effects incorporated into both gene-environment associations and the bleaching predictor model.

Type of predictor	Variable	Definition
Climatic	DHW4	The number of events where DHW > 4 between 1986-2020
	Return DHW6	The average return time between events where DHW > 6 between 1986-2020
	Recent max DHW	Maximum DHW experienced between 1986-2020
Environmental	Kd490	Light irradiance
	SCV	Mean sea current velocity
	Depth	Collection depth (m) of each coral genotype
Geographic	MEM1	Moran eigenvector map (1)
	MEM2	Moran eigenvector map (2)
	MEM3	Moran eigenvector map (3)
Symbiont community	Symbiont PC1	Symbiont principal component axis 1 of symbiont community structure
	Symbiont PC2	Symbiont principal component axis 2 of symbiont community structure
Host genetic	Host PC1	Principal component axis 1 of neutral population structure
	Host PC2	Principal component axis 2 of neutral population structure
	PGS	Polygenic score calculated as a cumulative rating from host adaptive loci per individual
	Max Cluster	The dominant host lineage representing cryptic speciation

5.2.7 Candidate adaptive loci from natural genetic samples

Candidate adaptive loci under selection were detected using partial redundancy analysis pRDA with the thermal predictors tested above (*vegan*). Stringent filtering parameters were used, where loci that occurred outside of 2.5 standard deviations of the mean were defined as outlier loci using methods from Capblancq & Forester (2021). Loci were then plotted to the strongest environmental co-variate per SNP. A polygenic score (PGS) was then calculated for each individual using the pRDA results, against the strongest environmental predictor (return time between DHW6 events; Table 5.1). The PGS for each individual was calculated between 0-1, where an average reading was scored using a nominal scoring per locus and whether the locus was adaptive for the specific individual.

5.2.8 Bleaching predictor model construction

To determine the relative contributions of host genetics, symbionts, and environment associated with phenotypic heat tolerance, a generalised mixed effects model was constructed using the package *glmmTMB* (Brooks et al., 2017). ED50 values were normally distributed across all samples, therefore a gaussian family distribution was used. Data were filtered to only include individuals that were subjected to heat stress experiments and therefore had a known bleaching phenotype, or ED50 (n = 168), at a subset of reef populations (n = 8). Phenotypic heat tolerance of each individual (ED50) was used as the response variable in the model. Models were progressively built up with ED50 as the response variable, where the effects of 'Reef', 'Host Cluster', 'Symbiont Cluster', thermal predictors, and adaptive polygenic score (PGS) were iteratively introduced into the model. The reef of coral collection was used as a random effect in each model. Model selection was informed with AICc scores (*MuMIn)* (Barton, 2022) and detailed parameters and AICc scores can be found in Table S5.3. Model residuals were assessed using *DHARMa* (Hartig, 2018) and residuals were confirmed to be normally distributed. *Post hoc* comparisons for predictor variables were then modelled using *emmeans* (Lenth, 2021).

5.3 Results

5.3.1 Cryptic speciation and neutral population structure of A. cf *humilis*

The total library prior to sequencing yielded 74,335 loci across 260 individuals of *Acropora* cf *humilis*. After filtering, 8,683 loci and 258 individuals were retained. Three distinct, genetic lineages of *Acropora* cf *humilis* were detected (hereafter: AHCL1, AHCL2, and AHCL3; Figure 1) with AHCL1 being the most sampled lineage across all reefs (n = 202) compared to either AHCL2 (n = 24) and AHCL3 (n = 30). Analysis of Molecular Variance (AMOVA)

revealed that for all three host lineages, genetic variation was significant within individuals (72.5%, $p < 0.001$) and between individuals (27.4%, $p < 0.001$), but not between populations (0.02%, $p = 0.34$) indicating low population structure. The genetic variance associated with the dominant lineage (AHCL1) was also strongly partitioned by within sample variation (67.4%, $p < 0.001$) and between sample variation (32.5%, $p < 0.001$). Population-level variation was significant when assessing AHCL1 alone, however made up a very small proportion of variance explained (0.07%, $p = 0.03$), reflecting low population structure within and among host lineages across the Coral Sea Marine Park.

Table 5.2. Library statistics for *Acropora* cf. *humilis*, including the number of samples (N), observed heterozygosity (H_o), expected heterozygosity (H_e), and population level F_{IS}.

	All clusters				***AHCL1 only***			
Reef	N	H_o	H_e	F_{is}	N	H_o	H_e	F_{is}
Osprey	13	0.11	0.17	0.29	12	0.11	0.18	0.33
Bougainville	20	0.08	0.18	0.44	6	0.1	0.19	0.36
Moore	20	0.11	0.17	0.29	20	0.11	0.18	0.32
Holmes	30	0.11	0.18	0.34	24	0.12	0.18	0.31
Chilcott	18	0.12	0.17	0.26	18	0.12	0.18	0.3
Herald	19	0.11	0.17	0.29	17	0.11	0.18	0.32
Lihou	31	0.11	0.17	0.30	30	0.11	0.18	0.33
Flinders	30	0.11	0.17	0.29	28	0.11	0.18	0.33
Marion	36	0.11	0.18	0.32	26	0.12	0.18	0.3
Frederick	15	0.10	0.18	0.36	8	0.11	0.18	0.32
Wreck	24	0.11	0.19	0.37	14	0.11	0.19	0.33

Global estimates of genetic relatedness (F_{ST}) revealed the three cryptic lineages, evidenced by high F_{ST} values for AHCL3 and AHCL2 (Global $F_{ST} = 0.17$), and AHCL3 and AHCL1 (Global $F_{ST} = 0.16$). The lineages AHCL1 and AHCL2 were the most genetically similar (Global $F_{ST} = 0.09$) and had greater similarities in morphology compared to AHCL3 (Figure 1d). The three

lineages occurred in sympatry and were detected at each of the 11 sampled reefs and the number of sampled genotypes per reef did not follow a latitudinal or longitudinal gradient (Fig 5.1a-b). The lineage AHCL3 was sampled in the highest proportion at one of the lowest latitude reefs (Bougainville) and the two highest latitude reefs (Frederick and Wreck) with very few individuals sampled from any central reefs (Fig 5.1a-b).

The pairwise comparisons among reefs for the main genetic cluster, AHCL1, were minimal (Global F_{ST} range: 0.001 – 0.01), indicating weak population structure compared to pairwise comparisons accounting for all three cryptic lineages (Fig S5.2, S5.4, S5.5). Isolation-by-distance patterns were significant for the main genetic cluster AHCL1 (R^2 = 0.244, p = 0.013), indicating a strong link between genetic and geographic distances for the dominant lineage of *Acropora* (Fig S5.3). When all host genetic clusters were included, there was no significant isolation-by-distance pattern (R^2 = 0.015, p-value = 0.279), indicating a stronger influence of cryptic speciation in driving population structure compared to geographic distance (Fig S5.3).

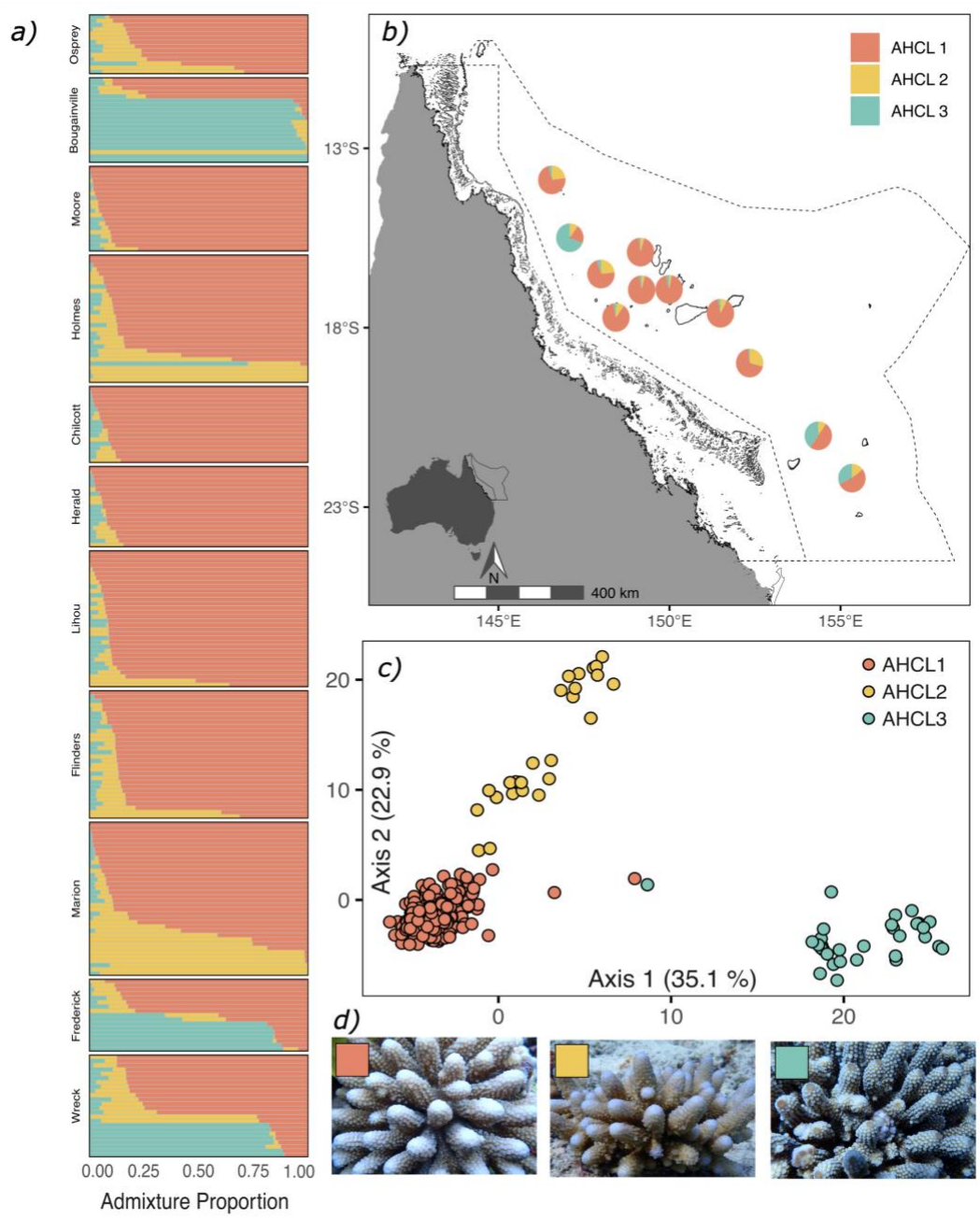

Figure 5.1. Neutral population structure and cryptic speciation of *Acropora* cf *humilis*. (A) Three morphotypes of *Acropora* cf *humilis*, which correspond to the three genetic clusters detected in the SNP genetic dataset. (B) Map of the Coral Sea Marine Park indicates admixture proportion per reef as pie charts, with colours representing the three genetic lineages of *A.* cf *humilis.* (C) PCoA of allele frequencies indicates three distinct clusters reflecting cryptic speciation. (D) Admixture proportions using the optimal number of *K* ancestral lineages (*K*=3) are coloured according to the three genetic clusters (AHCL1, AHCL2, and AHCL3).

5.3.2 Individual phenotypic bleaching scores and the influence of reefs, host cryptic species, and Symbiodiniaceae composition

Many individuals in this dataset were also exposed to heat stress experiments (n_{ind} = 181, n_{pop} = 8) and heat tolerance thresholds of each individual have been quantified as a 50% threshold to bleaching. Individual ED50 values varied significantly across the eight experimental reefs. Individual ED50s varied between 4.91°C – 8.87°C above the Maximum Monthly Mean of each reef (Figure 5.2a). Variation occurred within and among populations, however Wreck Reef maintained consistently higher ED50 value ranges (ED50 range = 7.47 - 8.89) among individuals compared to individuals from Lihou Reef (ED50 range = 5.64 - 7.38).

There was not a significant relationship between heat tolerance and the three genetic lineages when accounting for the random effect of the reef where individuals were sampled (Figure 2b), including between AHCL1 and AHCL2 (p = 0.58) and between AHCL1 and AHCL3 (p = 0.08). Similarly, Symbiodiniaceae community structure and ED50 bleaching phenotype were not correlated when accounting for the random effect of reef, including both PC1 (p = 0.43) and PC2 (p = 0.37) of the Symbiodiniaceae Principal Coordinates Analysis.

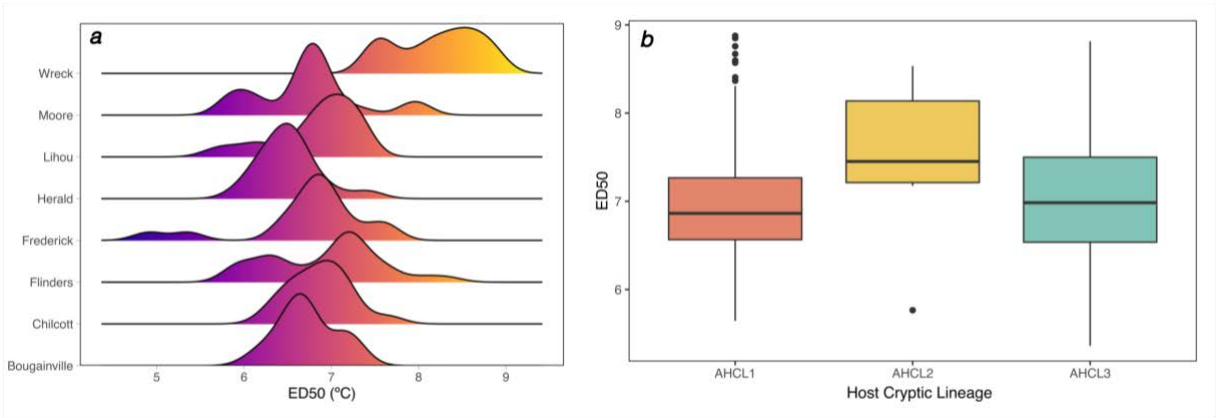

Figure 5.2. ED50 density plots structured by individuals within reefs, host cluster, and symbiont community composition. (a). Density distribution of phenotypic performance in *Acropora* cf *humilis* across the eight populations where experiments were conducted. ED50 represents the temperature above Maximum Monthly Mean where a 50% bleaching threshold was reached per individual. (b). Density distribution of phenotypic heat tolerance (ED50) relative to the three host genetic lineages (AHCL1, AHCL2, and AHCL3).

5.3.3 Thermal predictors of adaptive genetic variation

The redundancy analysis revealed 230 putatively adaptive loci in *A.* cf *humilis* which were correlated to two thermal metrics measured at the population level. The significant thermal predictors included the number of DHW > 4 between 1986-2020 ($p < 0.01$, Df = 1, F = 1.17) and the return time between DHW > 6 between 1986-2020 ($p < 0.01$, Df = 1, F = 1.15) (Figure 5.3). Both the return time between DHW6 and the number of DHW4 comprised 7.5% of all genetic variance explained in the RDA model, with 3.94 and 3.52% variance explained by RDA Axes 1 and 2, respectively (Figure 5.3). The recent maximum DHW was not significant in the model ($p = 0.07$, Df = 1, F = 1.08), indicating that thermal disturbances in the past five years (2016-2020) were not influential in structuring the adaptive capacity of thermal tolerance in corals compared to long-term thermal history metrics over the past 35 years (Figure 5.3).

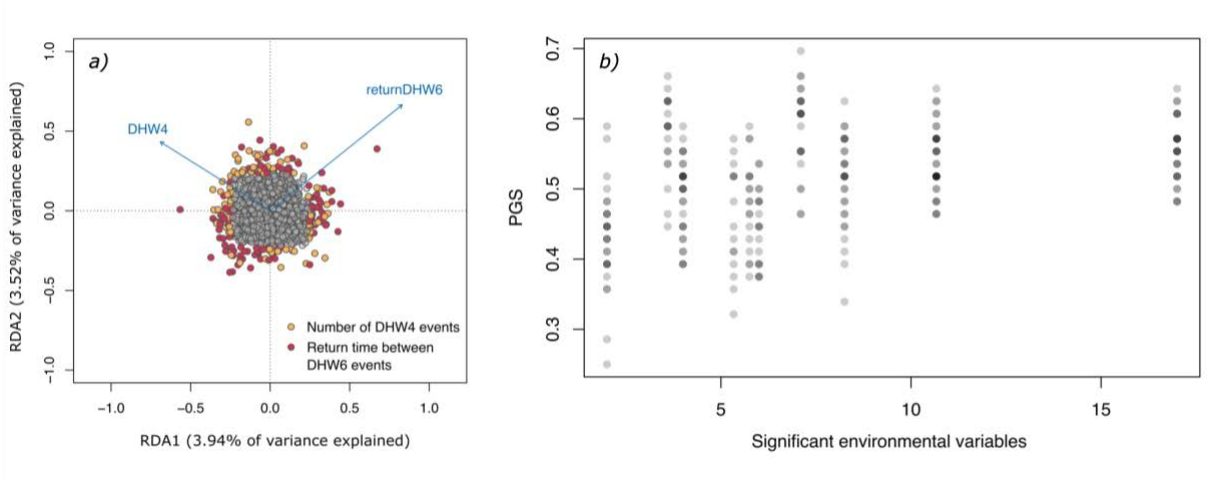

Figure 5.3. Candidate adaptive loci associated with *Acropora* cf *humilis*. (a) Each point represents a SNP (locus) which are coloured by the strongest thermal predictor of the relative locus, including the number of DHW > 4 experienced between 1985-2020 (DHW4) and the return time between DHW > 6 events (return DHW6). **(b)** Polygenic scores (PGS) were then calculated based on the strongest environmental drivers (number of DHW4 and return DHW6) using all candidate adaptive SNPs.

3.5 A polygenic score for heat tolerance

The effective dose to exhibit a 50% bleaching threshold in each coral individual (ED50) was used as the response variable to understand the strongest predictors of heat tolerance in relation to symbiont, host genetic, and environmental trends. The strongest heat tolerance predictors included the interaction between the number of mild heatwaves between 1985-2020 ($p < 0.001$) and the number of recent, severe heatwaves between 2016-2020 ($p < 0.035$). The additive fixed effects of symbiont community structure significantly influenced heat tolerance (Symbiont PC2; $p = 0.014$). Interestingly, there was no significant effect of host cryptic speciation (Host PC1; $p = 0.442$) or host polygenic score (PGS; $p = 0.928$) in driving heat tolerance of *A.* cf *humilis*.

ED50 values were modelled in a redundancy analysis against (1) the two host adaptive genetic axes, as well as the main thermal predictor, and (2) the number of long-term, mild heatwaves experienced between 1986-2020. Individuals of lower phenotypic heat tolerance tended to occur on reefs where mild heatwaves were not as frequent (Figure 5.4a). In contrast, individuals with high phenotypic heat tolerance (ED50 > 8) only occurred on reefs where more frequent, mild heatwaves had been experienced (Figure 5.4b). Genetic clustering also occurred strongly for individuals with high ED50s on reefs experiencing more frequent, mild heatwaves (Figure 5.4b).

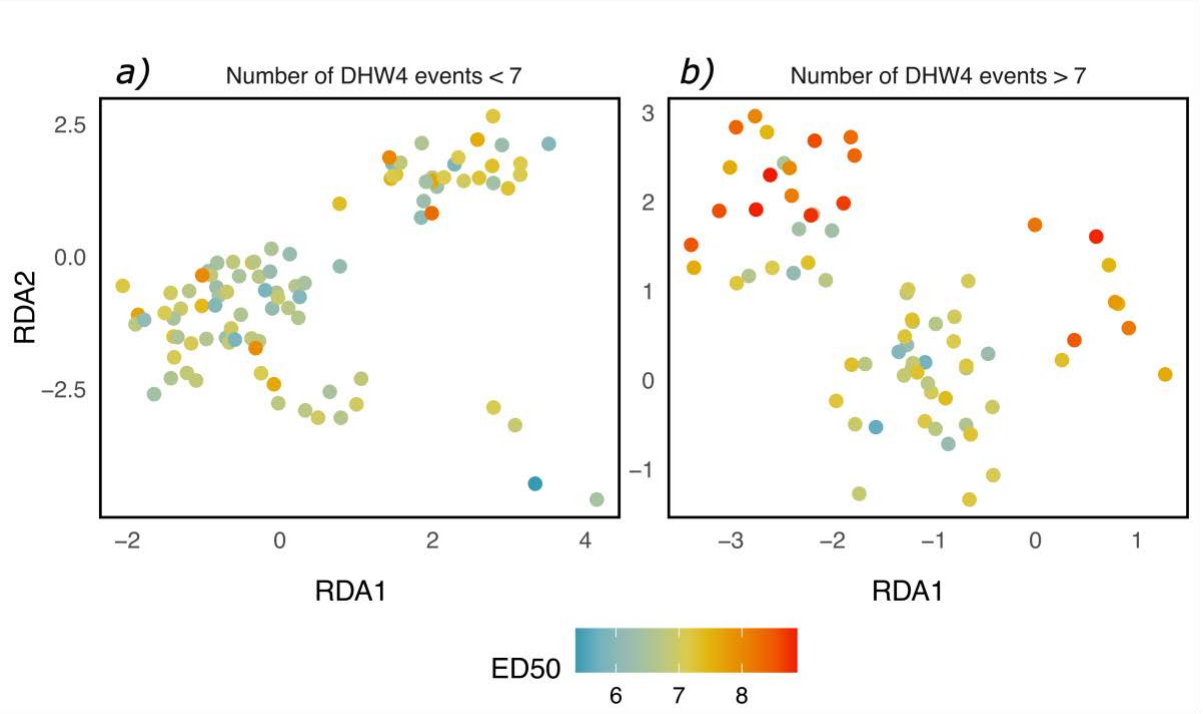

Figure 5.4. A bleaching predictor model for phenotypic heat tolerance. ED50 estimates against host adaptive genetic axes and the number of mild heatwaves (DHW4) for individuals experienced less than 7 events where DHW >4 between 1986-2020 (a), and those experiencing more than 7 events where DHW >4 between 1986-2020 (b).

5.4. Discussion

A bleaching predictor to understand phenotypic heat tolerance

Few studies have simultaneously examined both experimental and natural gene-environmental associations to detect the drivers of heat tolerance in corals. Here, I used a complementary approach, incorporating empirical heat tolerance phenotypes, as well as gene-environment associations to determine the relative influence of host genetics, symbionts, and thermal drivers in a common coral species. The number of mild heatwaves in the past 35 years explained both phenotypic heat tolerance thresholds and adaptive loci of the host, indicating the importance of mild heatwaves on coral heat tolerance. The return time between severe heatwaves over the past 35 years was a stronger predictor of adaptive loci, whereas severe, recent heatwaves and symbiont community structure were stronger determinants of phenotypic bleaching responses. Fuller et al. (2020) also found that symbiont type and local environment were the strongest predictors of phenotypic bleaching tolerance in *Acropora millepora,* with a negligible effect of host adaptation.

Adaptive loci correlate with thermal history metrics

The gene-environment association analysis revealed that putative adaptive loci in *Acropora* cf *humilis* correlated with the frequency of mild heatwaves (1985-2020) and the return time between strong heatwaves (return DHW6). In contrast, phenotypic population-level heat tolerance thresholds of these same corals correlated strongly to the frequency, severity, and return time between DHW, at both long-term (past 35 years) and short-term (2016-2020). The lack of recent severe heatwaves in structuring host adaptive loci indicates that more long-term predictors take several generations to select for more heat tolerant alleles, as adaptation occurs over generations and not within generations (Drury, 2020; Torda et al., 2017). Therefore, any

adaptive succession among populations will likely take multiple generations before adaptive signals can be detected (e.g., 10-15 years).

Short-term heat tolerance variation is likely correlated more to plasticity and acclimatisation among individuals and populations. Yet these strong marine heatwaves will potentially manifest as ecological and evolutionary predictors of heat tolerance in the next decades as climate change repeatedly affects reefs with higher frequency and severity (Selmoni et al., 2024). By comparing the commonalities and disparities among phenotypic heat tolerance and gene-by-environment interactions, it is possible to distinguish which predictors are associated with plasticity within a generation (e.g., recent maximum DHW) compared to genetic adaptation over generations (e.g., mild heatwaves over 35 years).

Minimal effects of cryptic host speciation or host symbionts on phenotypic heat tolerance

Three cryptic lineages within the *Acropora* cf *humilis* species complex were detected from Australia's Coral Sea Marine Park, with collected samples predominantly belonged to the AHCL1 lineage. When accounting for only the main lineage (AHCL1), minimal population structure was detected, potentially attributed to the broadcast spawning mode of reproduction and high gene flow in *Acropora* spp. (Thomas et al., 2020). Similar patterns of gene flow and population structure have been observed among broadcast spawning Acroporid species in other regions, *Acropora millepora* in the Great Barrier Reef (Fuller et al., 2020) and New Caledonia (Selmoni et al., 2021), and *Acropora* spp. across isolated atolls in Western Australia (Thomas et al., 2024). While greater spatial distance occurs between reefs in the Coral Sea Marine Park, high gene flow occurs in broadcast spawning corals despite the isolated nature of these reefs.

Heat tolerance among individuals was not significantly affected by cryptic host species. The effects of cryptic host speciation have previously shown an effect on heat tolerance and environmental interactions for *Stylophora pistillata* across the Great Barrier Reef (Meziere et

al., 2024), and *Acropora hyacinthus* in American Samoa (Rose et al., 2021). *Stylophora pistillata* and *A. hyacinthus* have lower heat tolerance thresholds than the digitate species examined in this study, *Acropora* cf. *humilis* (Loya et al., 2001), which may explain the lesser interaction of cryptic speciation and heat tolerance in this study compared to more heat susceptible coral taxa.

Considerations for bleaching as a heat tolerance metric

Bleaching responses are often a function of the health of the Symbiodiniaceae within the coral host, corroborating the strong influence of symbiont community composition as a bleaching predictor. The effect of the environment also potentially attributes to the horizontal mode of symbiont transmission, where both the host and symbionts have been exposed to various thermal disturbances prior to acquisition within the host, demonstrated in Chapter 3. While evidence exists that heat tolerance has a genetic effect and is heritable (Dixon et al., 2015; Elder et al., 2022; Howells et al., 2021), survival and mortality of coral individuals are important response variables are likely needed to capture this effect. Therefore, symbiont centric response variables including F_v/F_m and ED50, while rapid and non-obtrusive, are likely not capable to detect adaptive signals in association with the genetic architecture of the coral host.

Conclusion

Our findings indicate the importance of incorporating host adaptation, symbiont community structure, and thermal history to understand heat tolerance thresholds among individuals and populations. The lack of host adaptation influence for empirical heat tolerance thresholds (ED50) indicates that heat stress assays are valid for symbiont-centric questions but may not be representative as a reflection of host adaptation. Longer-term survival and mortality

experiments will likely encompass and reflect the predictive nature of both host genetic architecture and adaptation. However, the frequency of mild heatwaves was a strong predictor for both experimental and gene-environment methods which highlights the importance of repetitive, mild heatwaves as an indicator of population and individual level heat tolerance and should be considered as a predictor across other species, populations, and regions.

6. General Discussion

6.1 The multifaceted nature of heat tolerance

Understanding variation in the heat tolerance of corals is essential to predict the future of reefs against a backdrop of climate change. My thesis explored several biological levels of organisation (i.e., species, individuals, and populations) in relation to multiple drivers (i.e., environment, symbionts, and host genetics) to determine the primary factors that influence coral heat tolerance. The overarching findings indicate that heat tolerance is influenced by multiple biological and environmental factors, from molecules (host and symbiont genetics) to seascapes (thermal and environmental history). The type of species emerged as a key trait where heat tolerance variation occurred (Chapter 2), between genera (*Pocillopora* and *Acropora*), which corroborates previous evidence of hierarchical thermal tolerance among host taxa (Loya et al., 2001; Van Woesik et al., 2011). However, different levels of thermal tolerance emerged between closely related species (*Pocillopora meandrina* and *P. verrucosa*), despite both species maintaining mixed-mode reproduction and vertical transmission of symbionts. These patterns indicated that the 'winners' and 'losers' of recurrent coral bleaching events are not as clear as once thought. While species-level variation is important to predicting community-level shifts in response to climate change, understanding the genetic and environmental interactions leading to adaptation can provide further context to understand heat tolerance among populations over the next century (Lachs et al., 2023; Quigley, 2023).

Consistent patterns in heat tolerance thresholds occurred across populations for all three species, warranting a deeper investigation into their symbiotic and genetic structure. While recent and long-term climate history explained partial variation in heat tolerance (Chapter 2), host and symbiont genetic diversity and adaptive mechanisms were also responsible for variable patterns in individual and population-level heat tolerance (Chapters 3-5). Heat

tolerance was significantly attributed to symbiont community composition, particularly for *Acropora* cf. *humilis* which has horizontal transmission of symbionts, therefore allowing for symbiont interface with the environment and subsequent adaptation to these fluctuating climatic and environmental conditions (Chapter 3). The variability in *Pocillopora* heat tolerance was better explained by differences in symbiont community structure between the two coral host species (Chapter 3), as well as strong contrasts in population structure of the host across a large and heterogenous environmental gradient (Chapter 4). Ultimately, this indicates the importance of assessing species-specific trends in symbiont, host, and environmental interactions to gain a holistic understanding of heat tolerance at community and population levels (Figure 6.1).

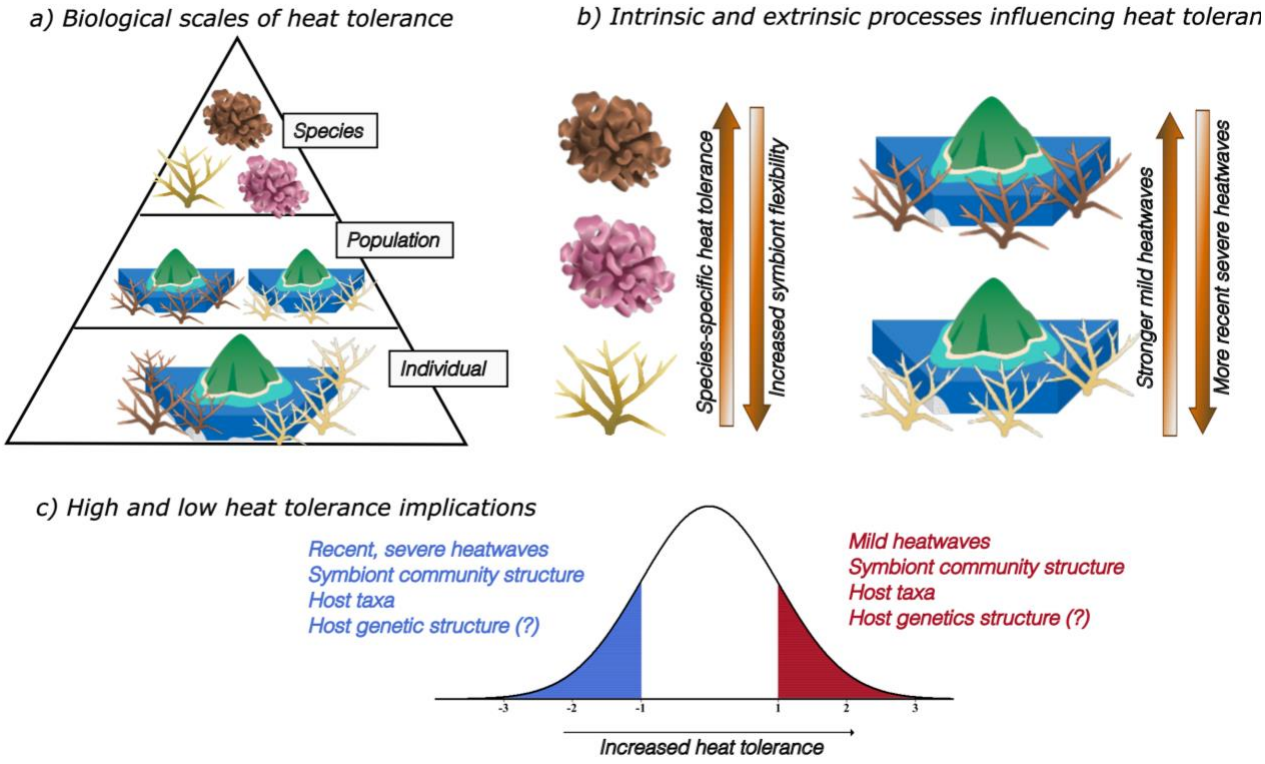

Figure 6.1. The multifaceted nature of heat tolerance. (a) Heat tolerance variation occurs across several biological scales including host species, populations, and individual levels. (b) The thesis findings indicate increased heat tolerance in *Pocillopora* compared to *Acropora,* but greater symbiont flexibility in Acroporids. Extrinsic processes including thermal history also mediate heat tolerance, where long-term, mild heatwaves provide increased heat tolerance, and more recent, severe heatwaves result in less heat tolerant populations and individuals. (c) Heat tolerance thresholds and the underlying factors influencing variation. Quantifying heat tolerance thresholds among populations and understanding the associated predictors can allow for the management and protection of both tolerant (red) and vulnerable reefs (blue).

6.2 Detecting ecological bright spots

The isolated and remote nature of the Coral Sea atolls allowed for the opportunity to use coral reefs as 'natural laboratories'. Specifically, the extensive spatial distances between reefs provided an opportunity to pinpoint reefs with high and low heat tolerance, as well as the factors underpinning increased heat tolerance. Ecological bright spots refer to populations that harbour greater resilience than what would be expected. The concept, first applied to reef fish diversity and biomass (Cinner et al., 2016) and more recently to reef coral cover and function (Sully et al., 2022), speaks to the ability (or inability) for populations to adapt to a rapidly changing climate. In this thesis, several reefs of higher thermal tolerance were detected, indicating potential sources of ecological 'bright spots' where reefs are adapting at a greater rate, therefore enabling population stability. High latitude and geographically isolated reefs in the Coral Sea (e.g., Wreck Reef) showed significantly higher heat tolerance ubiquitously across the three species relative to local thermal conditions. This enhanced heat tolerance was partially attributed to extrinsic factors such as the frequency and magnitude of historical bleaching events at this reef (Figure 6.2a-b).

In parallel with high heat tolerance, Wreck Reef demonstrated high divergence in symbiont community composition and host population structure among all coral taxa (*Pocillopora meandrina, P. verrucosa,* and *A.* cf. *humilis*) (Figure 6.2c-d). Environmental history and population genetic patterns indicate signs of both host and symbiont adaptive mechanisms. Local adaptation occurring at the distributional limits of coral reef communities in high latitude reefs are potential attributors to higher heat tolerance or adaptability to differential environmental fluctuations (Thomas et al., 2017; Underwood et al., 2009). Based on the findings in this thesis, high latitude reefs in the Coral Sea should be managed and monitored closely as potential thermal refugia, demonstrated by higher thermal tolerance in this period of rapid climate change.

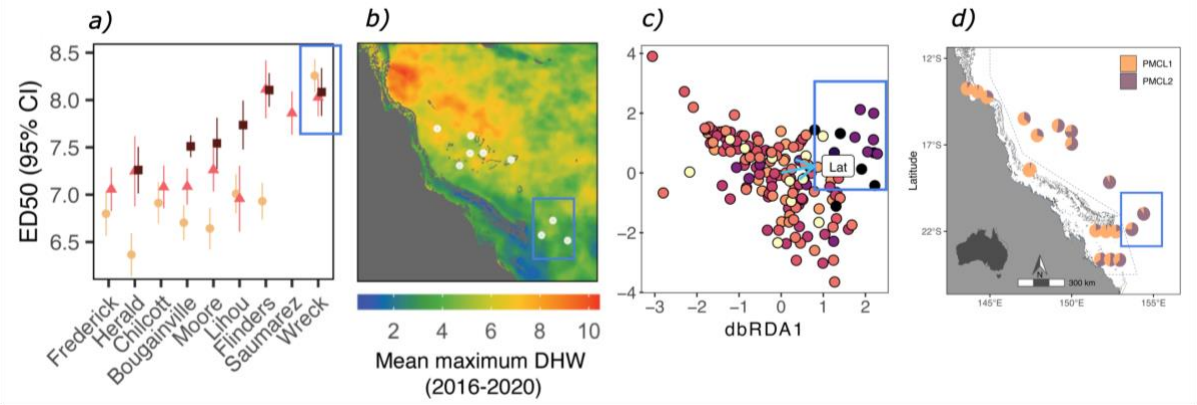

Figure 6.2. Ecological bright spots show higher thermal tolerance in high latitude reefs (a) was associated with thermal history (b), distinct symbiont communities (c), and strongly separated host population structure (d).

6.3 Can coral species and populations adapt at the rate of a changing climate?

The experimental, genetic, and environmental data from this thesis indicate that corals can adapt to marine heatwaves, but not at the rate of current and recent climate change (e.g., the recent past with 5 bleaching events in 8 years). These data corroborate previous model-based approaches to identify the rate of heat tolerance in parallel with empirically derived heat

tolerance thresholds (Lachs et al., 2023; Quigley, 2023). Higher phenotypic heat tolerance at the population level (Chapter 2), in tandem with shifting symbiont community composition (Chapter 3) and host adaptive loci (Chapter 5) all correlated to the number of mild marine heatwaves. This evidence indicates the capacity for coral species and populations to adapt over generations (both host and symbiont generations). The genetic basis of heat tolerance was reflected in genotype-environment analyses of *Acropora* cf. *humilis* (Chapter 5), where adaptive loci were most strongly linked to a longer return time in between strong heatwaves, as well as mild heatwaves (DHW4).

The comparisons between experimental and gene-environment analyses revealed that longer-term, mild heatwaves were a predictor of phenotypic heat tolerance (measured as ED50), as well as adaptive loci in the species *Acropora* cf *humilis* (Chapter 5). More recent, severe heatwaves (maximum DHW between 2016-2020) did not influence the adaptive genetic structure of *A.* cf *humilis*, indicating that while phenotypic heat tolerance is influenced by severe, recent heatwaves, a 5-year period is not substantial to invoke adaptive and evolutionary changes. However, the adaptive structure of corals will likely shift in response to the recurrent frequency and severity of marine heatwaves in the GBR and Coral Sea. This emphasises the need to continually monitor the phenotypic responses, in parallel with host genetic and symbiotic structure, to detect shifts in adaptive responses relative to environmental change.

6.4 Broader implications and future directions

There is growing interest among the coral community to combine genotype, phenotype, and environmental data to predict the vulnerability of reefs in response to the unfolding climate crisis. One key area of investigation moving forward is to understand genomic offsets in corals (i.e., genomic vulnerability or maladaptation). Specifically, genomic offsets quantify how much genetic change will be required for an individual or population to adapt at the rate of

various climate change trajectories (Capblancq & Forester, 2021; Fitzpatrick & Keller, 2015). Genomic offsets to 2050 and 2100 climate scenarios have been successfully modelled in the lodgepole pine across North America to determine spatial areas of high and low genomic vulnerability (Capblancq & Forester, 2021). This approach can be applied to marine organisms including corals, with changing model assumptions based on quantitative rates of connectivity and demographic rates in organisms with larval dispersal.

In tandem with genomic offset predictions for future climate change, proof-of-concept phenotype-environment studies can validate model simulated predictions using common garden or reciprocal transplant experiments (Quigley, 2023). This is an essential step to ground truth accurate predictions of tolerant and vulnerable populations, which can be cross validated using the same genotypes and populations under both contexts. Importantly, bleaching projections into 2050 and 2100 will be highly variable based on a) carbon emission scenarios and b) the rate of adaptation in coral populations. Whether adaptation and acclimation occur will depend on if heat tolerance is genetically fixed (i.e., adaptation) or is more so driven by phenotypic plasticity (i.e., acclimatisation) (Lachs et al., 2023; Matz et al., 2018) and the severity and frequency of marine heatwaves. The information provided in this thesis begins to uncover these patterns by providing a more comprehensive understanding of heat tolerance adaptation using both empirical and theoretical knowledge for guiding future directions in assessing heat tolerance across coral seascapes.

6.5 Concluding remarks

Coral reefs are increasingly threatened by climate impacts in the Anthropocene (Hughes et al., 2018; Oliver et al., 2018; Smale et al., 2019). As coral reefs continue to face pressures that threaten their persistence into the future, the factors that determine their survival are complex but underpinned by interactions with the environment, host, and algal symbionts. My thesis

builds on the investigation and interpretation of the biological and environmental mechanisms of adaptation in corals, as measured by acute heat stress experiments and complementary molecular approaches. Here, the incorporation of both molecules and seascapes clearly demonstrates that these adaptive mechanisms work at both host and symbiont levels and provides some hope for increasing thermal tolerance into the future. However, repetitive and extreme heatwaves question whether the adaptive responses for both the coral host and symbionts are enough to sustain coral populations and the reefs they build into the future. Overall, this body of work provides a timely contribution to understanding spatial heterogeneity in heat tolerance across reefs and species, and the underlying adaptive potential of corals and their Symbiodiniaceae to historical and contemporary disturbances. Moving forward, this knowledge can be incorporated in policy, conservation, and restoration to ensure the best protection of coral reef diversity and function into the future.

References

Abrego, D., Ulstrup, K. E., Willis, B. L., & Van Oppen, M. J. H. (2008). Species-specific interactions between algal endosymbionts and coral hosts define their bleaching response to heat and light stress. *Proceedings of the Royal Society B: Biological Sciences*, *275*(1648), 2273–2282. https://doi.org/10.1098/rspb.2008.0180

Ainsworth, T. D., Heron, S. F., Ortiz, J. C., Mumby, P. J., Grech, A., Ogawa, D., Eakin, C. M., & Leggat, W. (2016). Climate change disables coral bleaching protection on the Great Barrier Reef. *Science*, *352*(6283), 338–342. https://doi.org/10.1126/science.aac7125

Al-Sofyani, A. A., & Floos, Y. A. M. (2013). Effect of temperature on two reef-building corals Pocillopora damicornis and P. verrucosa in the Red Sea. *Oceanologia*. https://doi.org/10.5697/oc.55-4.917

Álvarez-Noriega, M., Marrable, I., Noonan, S. H. C., Barneche, D. R., & Ortiz, J. C. (2023). Highly conserved thermal performance strategies may limit adaptive potential in corals. *Proceedings of the Royal Society B: Biological Sciences*, *290*(1990). https://doi.org/10.1098/rspb.2022.1703

Ayre, D. J., & Hughes, T. P. (2000). Genotypic diversity and gene flow in brooding and spawning corals along the great barrier reef, Australia. *Evolution*, *54*(5), 1590–1605. https://doi.org/10.1111/j.0014-3820.2000.tb00704.x

Baird, A. H., Cumbo, V. R., Leggat, W., & Rodriguez-Lanetty, M. (2007). Fidelity and flexibility in coral symbioses. *Marine Ecology Progress Series*, *347*, 307–309. https://doi.org/10.3354/meps07220

Baker, A. C. (2003). Flexibility and specificity in coral-algal symbiosis: Diversity, ecology, and biogeography of Symbiodinium. In *Annual Review of Ecology, Evolution, and Systematics*. https://doi.org/10.1146/annurev.ecolsys.34.011802.132417

Baker, A. C., Glynn, P. W., & Riegl, B. (2008). Climate change and coral reef bleaching: An ecological assessment of long-term impacts, recovery trends and future outlook. *Estuarine, Coastal and Shelf Science*, *80*(4), 435–471. https://doi.org/10.1016/j.ecss.2008.09.003

Barshis, D. J., Ladner, J. T., Oliver, T. A., Seneca, F. O., Traylor-Knowles, N., & Palumbi, S. R. (2013). Genomic basis for coral resilience to climate change. *Proceedings of the National Academy of Sciences of the United States of America*, *110*(4), 1387–1392. https://doi.org/10.1073/pnas.1210224110

Barton, K. (2022). *MuMIn: Multi-Model Inference*. R Package Version 1.46.0.

Bay, R. A., & Palumbi, S. R. (2014). Multilocus adaptation associated with heat resistance in reef-building corals. *Current Biology*, *24*(24), 2952–2956. https://doi.org/10.1016/j.cub.2014.10.044

Berkelmans, R., & Van Oppen, M. J. H. (2006). The role of zooxanthellae in the thermal tolerance of corals: A “nugget of hope” for coral reefs in an era of climate change. *Proceedings of the Royal Society B: Biological Sciences*. https://doi.org/10.1098/rspb.2006.3567

Berkelmans, R., & Willis, B. L. (1999). Seasonal and local spatial patterns in the upper thermal limits of corals on the inshore Central Great Barrier Reef. *Coral Reefs*. https://doi.org/10.1007/s003380050186

Bernhardt, J. R., & Leslie, H. M. (2013). Resilience to climate change in coastal marine ecosystems. *Annual Review of Marine Science*, *5*, 371–392. https://doi.org/10.1146/annurev-marine-121211-172411

Borregaard, M. K., Amorim, I. R., Borges, P. A. V., Cabral, J. S., Fernández-Palacios, J. M., Field, R., Heaney, L. R., Kreft, H., Matthews, T. J., Olesen, J. M., Price, J., Rigal, F., Steinbauer, M. J., Triantis, K. A., Valente, L., Weigelt, P., & Whittaker, R. J. (2017). Oceanic island biogeography through the lens of the general dynamic model: Assessment and prospect. *Biological Reviews*, *92*(2), 830–853. https://doi.org/10.1111/brv.12256

Bridge, T. C. L., Beaman, R. J., Bongaerts, P., Muir, P. R., Ekins, M., & Sih, T. (2019). *The Great Barrier Reef and Coral Sea* (pp. 351–367). https://doi.org/10.1007/978-3-319-92735-0_20

Brooks, M. E., Kristensen, K., van Benthem, K. J., Magnusson, A., Berg, C. W., Nielsen, A., Skaug, H. J., Maechler, M., & Bolker, B. M. (2017). glmmTMB Balances Speed and Flexibility Among Packages for Zero-inflated Generalized Linear Mixed Modeling. *The R Journal*, *9*(2), 378–400. https://doi.org/10.32614/RJ-2017-066

Buitrago-López, C., Cárdenas, A., Hume, B. C. C., Gosselin, T., Staubach, F., Aranda, M., Barshis, D. J., Sawall, Y., & Voolstra, C. R. (2023). Disparate population and holobiont structure of pocilloporid corals across the Red Sea gradient demonstrate species-specific evolutionary trajectories. *Molecular Ecology*. https://doi.org/10.1111/mec.16871

Buitrago-López, C., Mariappan, K. G., Cárdenas, A., Gegner, H. M., & Voolstra, C. R. (2020). The Genome of the cauliflower coral *Pocillopora verrucosa*. *Genome Biology and Evolution*. https://doi.org/10.1093/gbe/evaa184

Burn, D., Hoey, A. S., Matthews, S., Harrison, H. B., & Pratchett, M. S. (2023). Differential bleaching susceptibility among coral taxa and colony sizes, relative to bleaching severity across Australia's Great Barrier Reef and Coral Sea Marine Parks. *Marine Pollution Bulletin*, *191*. https://doi.org/10.1016/j.marpolbul.2023.114907

Butler, C. C., Turnham, K. E., Lewis, A. M., Nitschke, M. R., Warner, M. E., Kemp, D. W., Hoegh-Guldberg, O., Fitt, W. K., van Oppen, M. J. H., & LaJeunesse, T. C. (2023). Formal recognition of host-generalist species of dinoflagellate (*Cladocopium*, Symbiodiniaceae) mutualistic with Indo-Pacific reef corals. *Journal of Phycology*. https://doi.org/10.1111/jpy.13340

Capblancq, T., & Forester, B. R. (2021). Redundancy analysis: A swiss army knife for landscape genomics. In *Methods in Ecology and Evolution* (Vol. 12, Issue 12, pp. 2298–2309). British Ecological Society. https://doi.org/10.1111/2041-210X.13722

Ceccarelli, D. M., McKinnon, A. D., Andréfouët, S., Allain, V., Young, J., Gledhill, D. C., Flynn, A., Bax, N. J., Beaman, R., Borsa, P., Brinkman, R., Bustamante, R. H., Campbell, R., Cappo, M., Cravatte, S., D'Agata, S., Dichmont, C. M., Dunstan, P. K., Dupouy, C., … Richardson, A. J. (2013). The Coral Sea. Physical environment, ecosystem status and biodiversity assets. In *Advances in Marine Biology*. https://doi.org/10.1016/B978-0-12-408096-6.00004-3

Chen, J., Bittinger, K., Charlson, E. S., Hoffmann, C., Lewis, J., Wu, G. D., Collman, R. G., Bushman, F. D., Li, H., & Bateman, A. (2012). Associating microbiome composition with environmental covariates using generalized UniFrac distances. *28*(16), 2106–2113. https://doi.org/10.1093/bioinformatics/bts342

Cinner, J. E., Huchery, C., MacNeil, M. A., Graham, N. A. J., McClanahan, T. R., Maina, J., Maire, E., Kittinger, J. N., Hicks, C. C., Mora, C., Allison, E. H., D'Agata, S., Hoey, A., Feary, D. A., Crowder, L., Williams, I. D., Kulbicki, M., Vigliola, L., Wantiez, L., … Mouillot, D. (2016). Bright spots among the world's coral reefs. *Nature*, *535*(7612), 416–419. https://doi.org/10.1038/nature18607

Coles, S., Jokiel, P., & Lewis, C. (1976). Thermal tolerance in tropical versus subtropical Pacific reef corals. *Pac. Sci.; (United States)*, *30:2*(2).

Cooke, I., Ying, H., Forêt, S., Bongaerts, P., Strugnell, J. M., Simakov, O., Zhang, J., Field, M. A., Rodriguez-Lanetty, M., Bell, S. C., Bourne, D. G., Jh Van Oppen, M., Ragan, M. A., & Miller, D. J. (2020). Genomic signatures in the coral holobiont reveal host adaptations driven by Holocene climate change and reef specific symbionts. *Sci. Adv* (Vol. 6). https://www.science.org

Cornwell, B., Armstrong, K., Walker, N., Lippert, M., Nestor, V., Golbuu, Y., & Palumbi, S. R. (2021). Widespread variation in heat tolerance and symbiont load are associated with growth tradeoffs in the coral *Acropora hyacinthus* in Palau. *ELife*, *10*, 1–15. https://doi.org/10.7554/eLife.64790

Cowman, P. F., Quattrini, A. M., Bridge, T. C. L., Watkins-Colwell, G. J., Fadli, N., Grinblat, M., Roberts, T. E., McFadden, C. S., Miller, D. J., & Baird, A. H. (2020). An enhanced target-enrichment bait set for Hexacorallia provides phylogenomic resolution of the staghorn corals (Acroporidae) and close relatives. *Molecular Phylogenetics and Evolution*. https://doi.org/10.1016/j.ympev.2020.106944

Cumbo, V. R., Baird, A. H., & van Oppen, M. J. H. (2013). The promiscuous larvae: Flexibility in the establishment of symbiosis in corals. *Coral Reefs*, *32*(1), 111–120. https://doi.org/10.1007/s00338-012-0951-7

Cunning, R., Parker, K. E., Johnson-Sapp, K., Karp, R. F., Wen, A. D., Williamson, O. M., Bartels, E., D'Alessandro, M., Gilliam, D. S., Hanson, G., Levy, J., Lirman, D., Maxwell, K., Million, W. C., Moulding, A. L., Moura, A., Muller, E. M., Nedimyer, K., Reckenbeil, B., … Baker, A. C. (2021). Census of heat tolerance among Florida's threatened staghorn corals finds resilient individuals throughout existing nursery populations. *Proceedings of the Royal Society B: Biological Sciences*, *288*(1961). https://doi.org/10.1098/rspb.2021.1613

Davies, S. W., Gamache, M. H., Howe-Kerr, L. I., Kriefall, N. G., Baker, A. C., Banaszak, A. T., Bay, L. K., Bellantuono, A. J., Bhattacharya, D., Chan, C. X., Claar, D. C., Coffroth, M. A., Cunning, R., Davy, S. K., del Campo, J., Díaz-Almeyda, E. M., Frommlet, J. C., Fuess, L. E., González-Pech, R. A., … Parkinson, J. E. (2023). Building consensus around the assessment and interpretation of Symbiodiniaceae diversity. *PeerJ*, *11*, e15023. https://doi.org/10.7717/peerj.15023

DeCarlo, T. M., Harrison, H. B., Gajdzik, L., Alaguarda, D., Rodolfo-Metalpa, R., D'Olivo, J., Liu, G., Patalwala, D., & McCulloch, M. T. (2019). Acclimatization of massive reef-building corals to consecutive heatwaves. *Proceedings of the Royal Society B: Biological Sciences*, *286*(1898). https://doi.org/10.1098/rspb.2019.0235

Dietzel, A., Connolly, S. R., Hughes, T. P., & Bode, M. (2021). The spatial footprint and patchiness of large-scale disturbances on coral reefs. *Global Change Biology*, *27*(19), 4825–4838. https://doi.org/10.1111/gcb.15805

Dixon, G. B., Davies, S. W., Aglyamova, G. A., Meyer, E., Bay, L. K., & Matz, M. V. (2015). Genomic determinants of coral heat tolerance across latitudes. *Science*. https://doi.org/10.1126/science.1261224

Dray, S., Bauman, D., Blanchet, G., Borcard, D., Clappe, S., Guenard, G., Jombart, T., Larocque, G., Legendre, P., Madi, N., & Wagner, H. H. (2023). *adespatial: Multivariate Multiscale Spatial Analysis*. https://github.com/sdray/adespatial

Dray, S., Chessel, D., & Thioulouse, J. (2003). Procrustean co-inertia analysis for the linking of multivariate datasets. *Ecoscience*, *10*(1), 110–119. https://doi.org/10.1080/11956860.2003.11682757

Drury, C. (2020a). Resilience in reef-building corals: The ecological and evolutionary importance of the host response to thermal stress. *Molecular Ecology*. https://doi.org/10.1111/mec.15337

Drury, C., & Lirman, D. (2021). Genotype by environment interactions in coral bleaching. *Proceedings of the Royal Society B*, *288*(1946). https://doi.org/10.1098/rspb.2021.0177

Drury, C., Manzello, D., & Lirman, D. (2017). Genotype and local environment dynamically influence growth, disturbance response and survivorship in the threatened coral, *Acropora cervicornis*. *PLoS ONE*. https://doi.org/10.1371/journal.pone.0174000

Elder, H., Million, W. C., Bartels, E., Krediet, C. J., Muller, E. M., & Kenkel, C. D. (2023). Long-term maintenance of a heterologous symbiont association in *Acropora palmata* on natural reefs. *The ISME Journal*, *17*(3), 486–489. https://doi.org/10.1038/s41396-022-01349-x

Elder, H., Weis, V. M., Montalvo-Proano, J., Mocellin, V. J. L., Baird, A. H., Meyer, E., & Bay, L. K. (2022). Genetic variation in heat tolerance of the coral *Platygyra daedalea* indicates potential for adaptation to ocean warming. *Frontiers in Marine Science*, *9*. https://doi.org/10.3389/fmars.2022.925845

Evensen, N. R., Fine, M., Perna, G., Voolstra, C. R., & Barshis, D. J. (2021). Remarkably high and consistent tolerance of a Red Sea coral to acute and chronic thermal stress exposures. *Limnology and Oceanography*, *66*(5), 1718–1729. https://doi.org/10.1002/lno.11715

Evensen, N. R., Parker, K. E., Oliver, T. A., Palumbi, S. R., Logan, C. A., Ryan, J. S., Klepac, C. N., Perna, G., Warner, M. E., Voolstra, C. R., & Barshis, D. J. (2023). The Coral Bleaching Automated Stress System (CBASS): A low-cost, portable system for standardized empirical assessments of coral thermal limits. *Limnology and Oceanography: Methods*, *21*(7), 421–434. https://doi.org/10.1002/lom3.10555

Evensen, N., Voolstra, C., Fine, M., Perna, G., Carol, B.-L., Cárdenas, A., Banc-Prandi, G., Rowe, K., & Barshis, D. (2022). Empirically derived thermal thresholds of four coral species along the Red Sea using a portable and standardized experimental approach. *Coral Reefs*. https://doi.org/10.1007/s00338-022-02233-y

Fitzpatrick, M. C., & Keller, S. R. (2015). Ecological genomics meets community-level modelling of biodiversity: Mapping the genomic landscape of current and future environmental adaptation. *Ecology Letters*, *18*(1), 1–16. https://doi.org/10.1111/ele.12376

Forsman, Z. H., Johnston, E. C., Brooks, A. J., Adam, T. C., & Toonen, R. J. (2013). Genetic evidence for regional isolation of Pocillopora corals from Moorea. *Oceanography*, *26*(3), 153–155. https://doi.org/10.5670/oceanog.2013.58

Frichot, E., & François, O. (2015). LEA: An R package for landscape and ecological association studies. *Methods in Ecology and Evolution*, *6*(8), 925–929. https://doi.org/10.1111/2041-210X.12382

Fujise, L., Suggett, D. J., Stat, M., Kahlke, T., Bunce, M., Gardner, S. G., Goyen, S., Woodcock, S., Ralph, P. J., Seymour, J. R., Siboni, N., & Nitschke, M. R. (2021). Unlocking the phylogenetic diversity, primary habitats, and abundances of free-living Symbiodiniaceae on a coral reef. *Molecular Ecology*, *30*(1), 343–360. https://doi.org/10.1111/mec.15719

Fuller, Z. L., Mocellin, V. J. L., Morris, L. A., Cantin, N., Shepherd, J., Sarre, L., Peng, J., Liao, Y., Pickrell, J., Andolfatto, P., Matz, M., Bay, L. K., & Przeworski, M. (2020). Population genetics of the coral *Acropora millepora*: Toward genomic prediction of bleaching. *Science*. https://doi.org/10.1126/science.aba4674

Galili, T. (2015). dendextend: an R package for visualizing, adjusting, and comparing trees of hierarchical clustering. *Bioinformatics*. https://doi.org/10.1093/bioinformatics/btv428

Gélin, P., Postaire, B., Fauvelot, C., & Magalon, H. (2017). Reevaluating species number, distribution and endemism of the coral genus *Pocillopora* Lamarck, 1816 using species

delimitation methods and microsatellites. *Molecular Phylogenetics and Evolution*, *109*, 430–446. https://doi.org/10.1016/j.ympev.2017.01.018
Glynn, P. W. (1984). Widespread coral mortality and the 1982–83 El Niño warming event. *Environmental Conservation*. https://doi.org/10.1017/S0376892900013825
Goudet, J., & Jombart, T. (2022). *hierfstat: Estimation and tests of hierarchical F-statistics*. https://CRAN.R-project.org/package=hierfstat
Graham, E. M., Baird, A. H., & Connolly, S. R. (2008). Survival dynamics of scleractinian coral larvae and implications for dispersal. *Coral Reefs*, *27*(3), 529–539. https://doi.org/10.1007/s00338-008-0361-z
Graham, N. A. J., Wilson, S. K., Jennings, S., Polunin, N. V. C., Robinson, J., Bijoux, J. P., & Daw, T. M. (2007). Lag effects in the impacts of mass coral bleaching on coral reef fish, fisheries, and ecosystems. *Conservation Biology*, *21*(5), 1291–1300. https://doi.org/10.1111/j.1523-1739.2007.00754.x
Grottoli, A. G., Toonen, R. J., van Woesik, R., Vega Thurber, R., Warner, M. E., McLachlan, R. H., Price, J. T., Bahr, K. D., Baums, I. B., Castillo, K. D., Coffroth, M. A., Cunning, R., Dobson, K. L., Donahue, M. J., Hench, J. L., Iglesias-Prieto, R., Kemp, D. W., Kenkel, C. D., Kline, D. I., … Wu, H. C. (2021). Increasing comparability among coral bleaching experiments. *Ecological Applications*, *31*(4). https://doi.org/10.1002/eap.2262
Grottoli, A. G., Warner, M. E., Levas, S. J., Aschaffenburg, M. D., Schoepf, V., Mcginley, M., Baumann, J., & Matsui, Y. (2014). The cumulative impact of annual coral bleaching can turn some coral species winners into losers. *Global Change Biology*. https://doi.org/10.1111/gcb.12658
Gruber, B., Unmack, P. J., Berry, O. F., & Georges, A. (2018). dartr: An r package to facilitate analysis of SNP data generated from reduced representation genome sequencing. *Molecular Ecology Resources*, *18*, 691–699. https://doi.org/10.1111/1755-0998.12745
Grummer, J.A., Beheregaray, L.B., Bernatchez, L., Hand, B.K., Luikart, G., Narum, S.R., & Taylor E.B. (2019). Aquatic landscape genomics and environmental effects on genetic variation. *Trends in ecology & evolution. 34*(7), 641-654.
Guest, J. R., Baird, A. H., Maynard, J. A., Muttaqin, E., Edwards, A. J., Campbell, S. J., Yewdall, K., Affendi, Y. A., & Chou, L. M. (2012). Contrasting patterns of coral bleaching susceptibility in 2010 suggest an adaptive response to thermal stress. *PLoS ONE*, *7*(3). https://doi.org/10.1371/journal.pone.0033353
Harrison, H. B., Álvarez-Noriega, M., Baird, A. H., Heron, S. F., MacDonald, C., & Hughes, T. P. (2019). Back-to-back coral bleaching events on isolated atolls in the Coral Sea. *Coral Reefs*. https://doi.org/10.1007/s00338-018-01749-6
Hartig, F. (2018). DHARMa: Residual Diagnostics for Hierarchical (Multi-Level / Mixed) Regression Models. In *R Packag version 020*. https://cir.nii.ac.jp/crid/1370580229833186830.bib?lang=en
Heron, S. F., Maynard, J. A., Van Hooidonk, R., & Eakin, C. M. (2016). Warming trends and bleaching stress of the world's coral reefs 1985-2012. *Scientific Reports*. https://doi.org/10.1038/srep38402
Hirose, M., Kinzie, R. A., & Hidaka, M. (2000). Early development of zooxanthella-containing eggs of the corals *Pocillopora verrucosa* and *P. eydouxi* with special reference to the distribution of zooxanthellae. *Biological Bulletin*, *199*(1), 68–75. https://doi.org/10.2307/1542708
Hoadley, K. D., Lewis, A. M., Wham, D. C., Pettay, D. T., Grasso, C., Smith, R., Kemp, D. W., LaJeunesse, T. C., & Warner, M. E. (2019). Host–symbiont combinations dictate the photo-physiological response of reef-building corals to thermal stress. *Scientific Reports*, *9*(1). https://doi.org/10.1038/s41598-019-46412-4

Hoey, A., McClure, E., Burn, D., Chandler, J., Huertas, V., Cresswell, B., Galbraith, G., & Morgan Pratchett. (2022). Coral Sea Marine Park coral reef health survey 2022. *Parks Australia*.

Hoffmann, A. A., & Sgró, C. M. (2011). Climate change and evolutionary adaptation. *Nature* (Vol. 470, Issue 7335, pp. 479–485). https://doi.org/10.1038/nature09670

Holderegger, R., Kamm, U., & Gugerli, F. (2006). Adaptive vs. neutral genetic diversity: Implications for landscape genetics. *Landscape Ecology* (Vol. 21, Issue 6, pp. 797–807). https://doi.org/10.1007/s10980-005-5245-9

Hoogenboom, M. O., Frank, G. E., Chase, T. J., Jurriaans, S., Álvarez-Noriega, M., Peterson, K., Critchell, K., Berry, K. L. E., Nicolet, K. J., Ramsby, B., & Paley, A. S. (2017). Environmental drivers of variation in bleaching severity of *Acropora* species during an extreme thermal anomaly. *Frontiers in Marine Science*. https://doi.org/10.3389/fmars.2017.00376

Howells, E. J., Abrego, D., Liew, Y. J., Burt, J. A., Meyer, E., & Aranda, M. (2021). Enhancing the heat tolerance of reef-building corals to future warming. *Sci. Adv* (Vol. 7).

Howells, E. J., Abrego, D., Meyer, E., Kirk, N. L., & Burt, J. A. (2016). Host adaptation and unexpected symbiont partners enable reef-building corals to tolerate extreme temperatures. *Global Change Biology*. https://doi.org/10.1111/gcb.13250

Howells, E. J., Bauman, A. G., Vaughan, G. O., Hume, B. C. C., Voolstra, C. R., & Burt, J. A. (2020). Corals in the hottest reefs in the world exhibit symbiont fidelity not flexibility. *Molecular Ecology*. https://doi.org/10.1111/mec.15372

Howells, E. J., Berkelmans, R., Van Oppen, M. J. H., Willis, B. L., & Bay, L. K. (2013). Historical thermal regimes define limits to coral acclimatization. *Ecology*. https://doi.org/10.1890/12-1257.1

Hughes, T. P., Anderson, K. D., Connolly, S. R., Heron, S. F., Kerry, J. T., Lough, J. M., Baird, A. H., Baum, J. K., Berumen, M. L., Bridge, T. C., Claar, D. C., Eakin, C. M., Gilmour, J. P., Graham, N. A. J., Harrison, H., Hobbs, J. P. A., Hoey, A. S., Hoogenboom, M., Lowe, R. J., … Wilson, S. K. (2018). Spatial and temporal patterns of mass bleaching of corals in the Anthropocene. *Science*. https://doi.org/10.1126/science.aan8048

Hughes, T. P., Kerry, J. T., Álvarez-Noriega, M., Álvarez-Romero, J. G., Anderson, K. D., Baird, A. H., Babcock, R. C., Beger, M., Bellwood, D. R., Berkelmans, R., Bridge, T. C., Butler, I. R., Byrne, M., Cantin, N. E., Comeau, S., Connolly, S. R., Cumming, G. S., Dalton, S. J., Diaz-Pulido, G., … Wilson, S. K. (2017). Global warming and recurrent mass bleaching of corals. *Nature*. https://doi.org/10.1038/nature21707

Hughes, T. P., Kerry, J. T., Baird, A. H., Connolly, S. R., Dietzel, A., Eakin, C. M., Heron, S. F., Hoey, A. S., Hoogenboom, M. O., Liu, G., McWilliam, M. J., Pears, R. J., Pratchett, M. S., Skirving, W. J., Stella, J. S., & Torda, G. (2018). Global warming transforms coral reef assemblages. *Nature*, *556*(7702), 492–496. https://doi.org/10.1038/s41586-018-0041-2

Hughes, T. P., Kerry, J. T., Connolly, S. R., Baird, A. H., Eakin, C. M., Heron, S. F., Hoey, A. S., Hoogenboom, M. O., Jacobson, M., Liu, G., Pratchett, M. S., Skirving, W., & Torda, G. (2019). Ecological memory modifies the cumulative impact of recurrent climate extremes. *Nature Climate Change*, *9*(1), 40–43. https://doi.org/10.1038/s41558-018-0351-2

Humanes, A., Lachs, L., Beauchamp, E. A., Bythell, J. C., Edwards, A. J., Golbuu, Y., Martinez, H. M., Palmowski, P., Treumann, A., van der Steeg, E., van Hooidonk, R., & Guest, J. R. (2022). Within-population variability in coral heat tolerance indicates

climate adaptation potential. *Proceedings of the Royal Society B: Biological Sciences*, *289*(1981). https://doi.org/10.1098/RSPB.2022.0872

Hume, B. C. C., Mejia-Restrepo, A., Voolstra, C. R., & Berumen, M. L. (2020). Fine-scale delineation of Symbiodiniaceae genotypes on a previously bleached central Red Sea reef system demonstrates a prevalence of coral host-specific associations. *Coral Reefs*, *39*(3), 583–601. https://doi.org/10.1007/s00338-020-01917-7

Hume, B. C. C., Smith, E. G., Ziegler, M., Warrington, H. J. M., Burt, J. A., LaJeunesse, T. C., Wiedenmann, J., & Voolstra, C. R. (2019). SymPortal: A novel analytical framework and platform for coral algal symbiont next-generation sequencing ITS2 profiling. *Molecular Ecology Resources*, *19*(4), 1063–1080. https://doi.org/10.1111/1755-0998.13004

Hutchinson, M. C., Cagua, E. F., Balbuena, J. A., Stouffer, D. B., & Poisot, T. (2017). paco: implementing Procrustean approach to cophylogeny in R. *Methods in Ecology and Evolution*, *8*(8), 932–940. https://doi.org/10.1111/2041-210X.12736

Jin, Y. K., Lundgren, P., Lutz, A., Raina, J. B., Howells, E. J., Paley, A. S., Willis, B. L., & Van Oppen, M. J. H. (2016). Genetic markers for antioxidant capacity in a reef-building coral. *Science Advances*. https://doi.org/10.1126/sciadv.1500842

Johnston, E. C., Cunning, R., & Burgess, S. C. (2022). Cophylogeny and specificity between cryptic coral species (*Pocillopora* spp.) at Mo′orea and their symbionts (Symbiodiniaceae). *Molecular Ecology*, *31*(20), 5368–5385. https://doi.org/10.1111/mec.16654

Johnston, E. C., Forsman, Z. H., Flot, J. F., Schmidt-Roach, S., Pinzón, J. H., Knapp, I. S. S., & Toonen, R. J. (2017). A genomic glance through the fog of plasticity and diversification in *Pocillopora*. *Scientific Reports*, *7*(1), 1–11. https://doi.org/10.1038/s41598-017-06085-3

Johnston, E. C., Forsman, Z. H., & Toonen, R. J. (2018). A simple molecular technique for distinguishing species reveals frequent misidentification of Hawaiian corals in the genus *Pocillopora*. *PeerJ*, *2018*(2), 1–14. https://doi.org/10.7717/peerj.4355

Jokiel, P. L., & Coles, S. L. (1990). Response of Hawaiian and other Indo-Pacific reef corals to elevated temperature. *Coral Reefs*, *8*(4), 155–162. https://doi.org/10.1007/BF00265006

Jones, A., & Berkelmans, R. (2010). Potential costs of acclimatization to a warmer climate: Growth of a reef coral with heat tolerant vs. sensitive symbiont types. *PLoS ONE*, *5*(5). https://doi.org/10.1371/journal.pone.0010437

Jurriaans, S., & Hoogenboom, M. O. (2020). Seasonal acclimation of thermal performance in two species of reef-building corals. *Marine Ecology Progress Series*. https://doi.org/10.3354/MEPS13203

Kamvar, Z. N., Brooks, J. C., & Grünwald, N. J. (2015). Novel R tools for analysis of genome-wide population genetic data with emphasis on clonality. *Front. Genet.*, *6*, 208. https://doi.org/10.3389/fgene.2015.00208

Kawecki, T. J., & Ebert, D. (2004). Conceptual issues in local adaptation. *Ecology Letters*, *7*(12), 1225–1241. https://doi.org/10.1111/j.1461-0248.2004.00684.x

Keith, S. A., Baird, A. H., Hughes, T. P., Madin, J. S., & Connolly, S. R. (2013). Faunal breaks and species composition of Indo-Pacific corals: The role of plate tectonics, environment and habitat distribution. *Proceedings of the Royal Society B: Biological Sciences*, *280*(1763). https://doi.org/10.1098/rspb.2013.0818

Kenkel, C. D., Goodbody-Gringley, G., Caillaud, D., Davies, S. W., Bartels, E., & Matz, M. V. (2013). Evidence for a host role in thermotolerance divergence between populations of the mustard hill coral (*Porites astreoides*) from different reef environments. *Molecular Ecology*, *22*(16), 4335–4348. https://doi.org/10.1111/mec.12391

Kenkel, C. D., & Matz, M. V. (2017). Gene expression plasticity as a mechanism of coral adaptation to a variable environment. *Nature Ecology & Evolution*, *1*(1), 1–6. https://doi.org/10.1038/s41559-016-0014

Kennedy, E. V., Tonk, L., Foster, N. L., Chollett, I., Ortiz, J. C., Dove, S., Hoegh-Guldberg, O., Mumby, P. J., & Stevens, J. R. (2016). *Symbiodinium* biogeography tracks environmental patterns rather than host genetics in a key caribbean reef-builder, *Orbicella annularis*. *Proceedings of the Royal Society B: Biological Sciences*, *283*(1842). https://doi.org/10.1098/rspb.2016.1938

Kilian, A., Wenzl, P., Huttner, E., Carling, J., Xia, L., Blois, H., Caig, V., Heller-Uszynska, K., Jaccoud, D., Hopper, C., Aschenbrenner-Kilian, M., Evers, M., Peng, K., Cayla, C., Hok, P., & Uszynski, G. (2012). Diversity arrays technology: A generic genome profiling technology on open platforms. *Methods in Molecular Biology*, *888*, 67–89. https://doi.org/10.1007/978-1-61779-870-2_5/COVER

Kirk, N. L., Howells, E. J., Abrego, D., Burt, J. A., & Meyer, E. (2018). Genomic and transcriptomic signals of thermal tolerance in heat-tolerant corals (*Platygyra daedalea*) of the Arabian/Persian Gulf. *Molecular Ecology*. https://doi.org/10.1111/mec.14934

Lachs, L., Donner, S. D., Mumby, P. J., Bythell, J. C., Humanes, A., East, H. K., & Guest, J. R. (2023). Emergent increase in coral thermal tolerance reduces mass bleaching under climate change. *Nature Communications*, *14*(1). https://doi.org/10.1038/s41467-023-40601-6

LaJeunesse, T. C., Parkinson, J. E., Gabrielson, P. W., Jeong, H. J., Reimer, J. D., Voolstra, C. R., & Santos, S. R. (2018). Systematic revision of Symbiodiniaceae highlights the antiquity and diversity of coral endosymbionts. *Current Biology*. https://doi.org/10.1016/j.cub.2018.07.008

LaJeunesse, T. C., Pettay, D. T., Sampayo, E. M., Phongsuwan, N., Brown, B., Obura, D. O., Hoegh-Guldberg, O., & Fitt, W. K. (2010). Long-standing environmental conditions, geographic isolation and host-symbiont specificity influence the relative ecological dominance and genetic diversification of coral endosymbionts in the genus *Symbiodinium*. *Journal of Biogeography*, *37*(5), 785–800. https://doi.org/10.1111/j.1365-2699.2010.02273.x

LaJeunesse, T. C., Smith, R. T., Finney, J., & Oxenford, H. (2009). Outbreak and persistence of opportunistic symbiotic dinoflagellates during the 2005 Caribbean mass coral "bleaching" event. *Proceedings of the Royal Society B: Biological Sciences*. https://doi.org/10.1098/rspb.2009.1405

LaJeunesse, T. C., & Thornhill, D. J. (2011). Improved resolution of reef-coral endosymbiont (*Symbiodinium*) species diversity, ecology, and evolution through psbA non-coding region genotyping. *PLoS ONE*, *6*(12). https://doi.org/10.1371/journal.pone.0029013

LaJeunesse, T. C., Wham, D. C., Pettay, D. T., Parkinson, J. E., Keshavmurthy, S., & Chen, C. A. (2014). Ecologically differentiated stress-tolerant endosymbionts in the dinoflagellate genus *Symbiodinium* (Dinophyceae) Clade D are different species. *Phycologia*, *53*(4), 305–319. https://doi.org/10.2216/13-186.1

Lenth, R. (2021). *emmeans: Estimated Marginal Means, aka Least-Squares Means* (R package version 1.6.3.).

Liew, Y. J., Aranda, M., & Voolstra, C. R. (2016). Reefgenomics.Org - A repository for marine genomics data. *Database*. https://doi.org/10.1093/database/baw152

Liu, G., Heron, S. F., Mark Eakin, C., Muller-Karger, F. E., Vega-Rodriguez, M., Guild, L. S., de la Cour, J. L., Geiger, E. F., Skirving, W. J., Burgess, T. F. R., Strong, A. E., Harris, A., Maturi, E., Ignatov, A., Sapper, J., Li, J., & Lynds, S. (2014). Reef-scale thermal stress monitoring of coral ecosystems: New 5-km global products from NOAA coral reef watch. *Remote Sensing*. https://doi.org/10.3390/rs61111579

Lough, J. M., Anderson, K. D., & Hughes, T. P. (2018). Increasing thermal stress for tropical coral reefs: 1871-2017. *Scientific Reports*, *8*(1), 1–8. https://doi.org/10.1038/s41598-018-24530-9

Lowe, W. H., & Allendorf, F. W. (2010). What can genetics tell us about population connectivity? *Molecular Ecology*, *19*(15), 3038–3051. https://doi.org/10.1111/j.1365-294X.2010.04688.x

Loya, Y., Sakai, K., Yamazato, K., Nakano, Y., Sambali, H., & Van Woesik, R. (2001). Coral bleaching: The winners and the losers. *Ecology Letters*. https://doi.org/10.1046/j.1461-0248.2001.00203.x

Lundgren, P., Vera, J. C., Peplow, L., Manel, S., & van Oppen, M. J. H. (2013). Genotype - environment correlations in corals from the Great Barrier Reef. *BMC Genetics*, *14*. https://doi.org/10.1186/1471-2156-14-9

MacArthur, R. H., & Wilson, E. O. (1967). *The theory of island biogeography*.

Manel, S., Schwartz, M.K., Luikart, G., & Taberlet, P. (2003). Landscape genetics: combining landscape ecology and population genetics. *Trends in ecology & evolution. 18*(4), 189-197.

Manzello, D. P., Matz, M. V., Enochs, I. C., Valentino, L., Carlton, R. D., Kolodziej, G., Serrano, X., Towle, E. K., & Jankulak, M. (2019). Role of host genetics and heat-tolerant algal symbionts in sustaining populations of the endangered coral *Orbicella faveolata* in the Florida Keys with ocean warming. *Global Change Biology*. https://doi.org/10.1111/gcb.14545

Marhoefer, S. R., Zenger, K. R., Strugnell, J. M., Logan, M., van Oppen, M. J. H., Kenkel, C. D., & Bay, L. K. (2021). Signatures of adaptation and acclimatization to reef flat and slope habitats in the coral *Pocillopora damicornis*. *Frontiers in Marine Science*, *8*(September). https://doi.org/10.3389/fmars.2021.704709

Matias, A. M. A., Popovic, I., Thia, J. A., Cooke, I. R., Torda, G., Lukoschek, V., Bay, L. K., Kim, S. W., & Riginos, C. (2023). Cryptic diversity and spatial genetic variation in the coral *Acropora tenuis* and its endosymbionts across the Great Barrier Reef. *Evolutionary Applications*, *16*(2), 293–310. https://doi.org/10.1111/eva.13435

Matz, M. V., Treml, E. A., Aglyamova, G. V., & Bay, L. K. (2018). Potential and limits for rapid genetic adaptation to warming in a Great Barrier Reef coral. *PLoS Genetics*. https://doi.org/10.1371/journal.pgen.1007220

McLachlan, R. H., Price, J. T., Solomon, S. L., & Grottoli, A. G. (2020). Thirty years of coral heat-stress experiments: a review of methods. *Coral Reefs*. https://doi.org/10.1007/s00338-020-01931-9

McManus, L. C., Forrest, D. L., Tekwa, E. W., Schindler, D. E., Colton, M. A., Webster, M. M., Essington, T. E., Palumbi, S. R., Mumby, P. J., & Pinsky, M. L. (2021). Evolution and connectivity influence the persistence and recovery of coral reefs under climate change in the Caribbean, Southwest Pacific, and Coral Triangle. *Global Change Biology*, *27*(18), 4307–4321. https://doi.org/10.1111/gcb.15725

McManus, L. C., Vasconcelos, V. V., Levin, S. A., Thompson, D. M., Kleypas, J. A., Castruccio, F. S., Curchitser, E. N., & Watson, J. R. (2020). Extreme temperature events will drive coral decline in the Coral Triangle. *Global Change Biology*, *26*(4), 2120–2133. https://doi.org/10.1111/gcb.14972

McRae, C. J., Huang, W. Bin, Fan, T. Y., & Côté, I. M. (2021). Effects of thermal conditioning on the performance of *Pocillopora acuta* adult coral colonies and their offspring. *Coral Reefs*, *40*(5), 1491–1503. https://doi.org/10.1007/s00338-021-02123-9

McWhorter, J. K., Halloran, P. R., Roff, G., Skirving, W. J., Perry, C. T., & Mumby, P. J. (2022). The importance of 1.5°C warming for the Great Barrier Reef. *Global Change Biology*, *28*(4), 1332–1341. https://doi.org/10.1111/gcb.15994

Meziere, Z., Popovic, I., Prata, K., Ryan, I., Pandolfi, J., & Riginos, C. (2024). Exploring coral speciation: Multiple sympatric *Stylophora pistillata* taxa along a divergence continuum on the Great Barrier Reef. *Evolutionary Applications*, *17*(1). https://doi.org/10.1111/eva.13644

Middlebrook, R., Hoegh-Guldberg, O., & Leggat, W. (2008). The effect of thermal history on the susceptibility of reef-building corals to thermal stress. *Journal of Experimental Biology*, *211*(7), 1050–1056. https://doi.org/10.1242/jeb.013284

Miller, K., & Mundy, C. (2003). Rapid settlement in broadcast spawning corals: Implications for larval dispersal. *Coral Reefs*, *22*(2), 99–106. https://doi.org/10.1007/s00338-003-0290-9

Moore, R. B., Ferguson, K. M., Loh, W. K. W., Hoegh-Guldberg, O., & Carter, D. A. (2003). Highly organized structure in the non-coding region of the psbA minicircle from clade C *Symbiodinium*. *International Journal of Systematic and Evolutionary Microbiology*, *53*(6), 1725–1734. https://doi.org/10.1099/ijs.0.02594-0

Morikawa, M. K., & Palumbi, S. R. (2019). Using naturally occurring climate resilient corals to construct bleaching-resistant nurseries. *Proceedings of the National Academy of Sciences of the United States of America*, *116*(21), 10586–10591. https://doi.org/10.1073/pnas.1721415116

Morris, L. A., Voolstra, C. R., Quigley, K. M., Bourne, D. G., & Bay, L. K. (2019). Nutrient availability and metabolism affect the stability of Coral–Symbiodiniaceae symbioses. *Trends in Microbiology*. https://doi.org/10.1016/j.tim.2019.03.004

Muscatine, L. (1990). The role of symbiotic algae in carbon and energy flux in reef corals. *Coral Reefs*, *25*(1.29).

Nitschke, M. R., Gardner, S. G., Goyen, S., Fujise, L., Camp, E. F., Ralph, P. J., & Suggett, D. J. (2018). Utility of photochemical traits as diagnostics of thermal tolerance amongst great barrier reef corals. *Frontiers in Marine Science*, *5*(FEB), 1–18. https://doi.org/10.3389/fmars.2018.00045

Oksanen, J., Simpson, G. L., Blanchet, F. G., Kindt, R., Legendre, P., Minchin, P. R., O'Hara, R. B., Solymos, P., Stevens, M. H. H., Szoecs, E., Wagner, H., Barbour, M., Bedward, M., Bolker, B., Borcard, D., Carvalho, G., Chirico, M., De Caceres, M., Durand, S., … Weedon, J. (2022). *vegan: Community Ecology Package*. https://CRAN.R-project.org/package=vegan

Oliver, E. C. J., Donat, M. G., Burrows, M. T., Moore, P. J., Smale, D. A., Alexander, L. V., Benthuysen, J. A., Feng, M., Sen Gupta, A., Hobday, A. J., Holbrook, N. J., Perkins-Kirkpatrick, S. E., Scannell, H. A., Straub, S. C., & Wernberg, T. (2018). Longer and more frequent marine heatwaves over the past century. *Nature Communications*. https://doi.org/10.1038/s41467-018-03732-9

Oliver, T. A., & Palumbi, S. R. (2011). Do fluctuating temperature environments elevate coral thermal tolerance? *Coral Reefs*, *30*(2), 429–440. https://doi.org/10.1007/s00338-011-0721-y

Osman, E. O., Smith, D. J., Ziegler, M., Kürten, B., Conrad, C., El-Haddad, K. M., Voolstra, C. R., & Suggett, D. J. (2018). Thermal refugia against coral bleaching throughout the northern Red Sea. *Global Change Biology*, *24*(2), e474–e484. https://doi.org/10.1111/gcb.13895

Oury, N., Gélin, P., & Magalon, H. (2021). High connectivity within restricted distribution range in *Pocillopora* corals. *Journal of Biogeography*, *48*(7), 1679–1692. https://doi.org/10.1111/JBI.14104

Palumbi, S. R., Barshis, D. J., Traylor-Knowles, N., & Bay, R. A. (2014). Mechanisms of reef coral resistance to future climate change. *Science*, *344*(6186), 895–898. https://doi.org/10.1126/science.1251336

Paradis, E., & Schliep, K. (2019). ape 5.0: an environment for modern phylogenetics and evolutionary analyses in R. *Bioinformatics*, *35*, 526–528. https://doi.org/10.1093/bioinformatics/bty633

Parkinson, J. E., Baker, A. C., Baums, I. B., Davies, S. W., Grottoli, A. G., Kitchen, S. A., Matz, M. V., Miller, M. W., Shantz, A. A., & Kenkel, C. D. (2019). Molecular tools for coral reef restoration: Beyond biomarker discovery. *Conservation Letters*. https://doi.org/10.1111/conl.12687

Payet, S. D., Pratchett, M. S., Saenz-Agudelo, P., Berumen, M. L., DiBattista, J. D., & Harrison, H. B. (2022). Demographic histories shape population genomics of the common coral grouper (*Plectropomus leopardus*). *Evolutionary Applications*, *15*(8), 1221–1235. https://doi.org/10.1111/eva.13450

Pinheiro, J., Bates, D., DebRoy, S., Sarkar, D., & Team, R. D. C. (2021). *nlme: Linear and Nonlinear Mixed Effects Models* (R package version 3.1-152).

Pinzón, J. H., Sampayo, E., Cox, E., Chauka, L. J., Chen, C. A., Voolstra, C. R., & Lajeunesse, T. C. (2013). Blind to morphology: Genetics identifies several widespread ecologically common species and few endemics among Indo-Pacific cauliflower corals (*Pocillopora*, Scleractinia). *Journal of Biogeography*, *40*(8), 1595–1608. https://doi.org/10.1111/jbi.12110

Pochon, X., Pawlowski, J., Zaninetti, L., & Rowan, R. (2001). High genetic diversity and relative specificity among Symbiodinium-like endosymbiotic dinoflagellates in soritid foraminiferans. *Marine Biology*. https://doi.org/10.1007/s002270100674

Pratchett Morgan S. and Heron, S. F. and M. C. and C. G. S. (2021). Recurrent mass-bleaching and the potential for ecosystem collapse on Australia's Great Barrier Reef. *Ecosystem Collapse and Climate Change* (pp. 265–289). Springer International Publishing. https://doi.org/10.1007/978-3-030-71330-0_10

Quigley, K. M. (2023). Breeding and selecting corals resilient to global warming. *Annual Review of Animal Biosciences.* https://doi.org/10.1146/annurev-animal-021122

Quigley, K. M., Bay, L. K., & Oppen, M. J. H. (2020). Genome-wide SNP analysis reveals an increase in adaptive genetic variation through selective breeding of coral. *Molecular Ecology*. https://doi.org/10.1111/mec.15482

Quigley, K. M., Ramsby, B., Laffy, P., Harris, J., Mocellin, V. J. L., & Bay, L. K. (2022). Symbioses are restructured by repeated mass coral bleaching. *Science Advances.* https://www.science.org

Quigley, K. M., Randall, C. J., van Oppen, M. J. H., & Bay, L. K. (2020). Assessing the role of historical temperature regime and algal symbionts on the heat tolerance of coral juveniles. *Biology Open*. https://doi.org/10.1242/bio.047316

Quigley, K. M., Warner, P. A., Bay, L. K., & Willis, B. L. (2018). Unexpected mixed-mode transmission and moderate genetic regulation of *Symbiodinium* communities in a brooding coral. *Heredity*, *121*(6), 524–536. https://doi.org/10.1038/s41437-018-0059-0

Quigley, K. M., Willis, B. L., & Bay, L. K. (2017). Heritability of the *Symbiodinium* community in vertically-and horizontally-transmitting broadcast spawning corals. *Scientific Reports*. https://doi.org/10.1038/s41598-017-08179-4

R Core Team. (2023). *R: A Language and Environment for Statistical Computing*. https://www.R-project.org/

Rellstab, C., Gugerli, F., Eckert, A. J., Hancock, A. M., & Holderegger, R. (2015). A practical guide to environmental association analysis in landscape genomics. *Molecular Ecology* (Vol. 24, Issue 17, pp. 4348–4370). https://doi.org/10.1111/mec.13322

Ries, L., Fletcher, R. J., Battin, J., & Sisk, T. D. (2004). Ecological responses to habitat edges: Mechanisms, models, and variability explained. *Annual Review of Ecology, Evolution, and Systematics* (Vol. 35). https://www.jstor.org/stable/30034125

Riginos, C., Crandall, E. D., Liggins, L., Bongaerts, P., & Treml, E. A. (2016). Navigating the currents of seascape genomics: How spatial analyses can augment population genomic studies. *Current Zoology*. https://doi.org/10.1093/cz/zow067

Riginos, C., & Liggins, L. (2013). Seascape genetics: Populations, individuals, and genes marooned and adrift. *Geography Compass* (Vol. 7, Issue 3, pp. 197–216). https://doi.org/10.1111/gec3.12032

Ritz, C., Baty, F., Streibig, J. C., & Gerhard, D. (2015). Dose-response analysis using R. *PLoS ONE*, *10*(12). https://doi.org/10.1371/JOURNAL.PONE.0146021

Roberts, K. E., Cook, C. N., Beher, J., & Treml, E. A. (2021). Assessing the current state of ecological connectivity in a large marine protected area system. *Conservation Biology*, *35*(2), 699–710. https://doi.org/10.1111/cobi.13580

Rose, N. H., Bay, R. A., Morikawa, M. K., & Palumbi, S. R. (2018). Polygenic evolution drives species divergence and climate adaptation in corals. *Evolution*. https://doi.org/10.1111/evo.13385

Rose, N. H., Bay, R. A., Morikawa, M. K., Thomas, L., Sheets, E. A., & Palumbi, S. R. (2021). Genomic analysis of distinct bleaching tolerances among cryptic coral species. *Proceedings of the Royal Society B: Biological Sciences*, *288*(1960). https://doi.org/10.1098/rspb.2021.0678

Safaie, A., Silbiger, N. J., McClanahan, T. R., Pawlak, G., Barshis, D. J., Hench, J. L., Rogers, J. S., Williams, G. J., & Davis, K. A. (2018). High frequency temperature variability reduces the risk of coral bleaching. *Nature Communications*. https://doi.org/10.1038/s41467-018-04074-2

Sansaloni, C., Petroli, C., Jaccoud, D., Carling, J., Detering, F., Grattapaglia, D., & Kilian, A. (2011). Diversity Arrays Technology (DArT) and next-generation sequencing combined: genome-wide, high throughput, highly informative genotyping for molecular breeding of Eucalyptus. *BMC Proceedings*, *5*(S7). https://doi.org/10.1186/1753-6561-5-s7-p54

Santos, A. M. C., Field, R., & Ricklefs, R. E. (2016). New directions in island biogeography. *Global Ecology and Biogeography*, *25*(7), 751–768. https://doi.org/10.1111/geb.12477

Sardi, M., & Gasch, A. P. (2017). Incorporating comparative genomics into the design-test-learn cycle of microbial strain engineering. *FEMS Yeast Research*, *17*(5). https://doi.org/10.1093/femsyr/fox042

Savolainen, O., Lascoux, M., & Merilä, J. (2013). Ecological genomics of local adaptation. *Nature Reviews Genetics*, *14*(11), 807–820. https://doi.org/10.1038/nrg3522

Schliep, K. P. (2011). phangorn: phylogenetic analysis in R. *Bioinformatics*, *27*(4), 592–593. https://doi.org/10.1093/bioinformatics/btq706

Schmidt-Roach, S., Miller, K. J., Woolsey, E., Gerlach, G., & Baird, A. H. (2012). Broadcast spawning by *Pocillopora* species on the Great Barrier Reef. *PLoS ONE*, *7*(12). https://doi.org/10.1371/journal.pone.0050847

Schoepf, V., Stat, M., Falter, J. L., & McCulloch, M. T. (2015). Limits to the thermal tolerance of corals adapted to a highly fluctuating, naturally extreme temperature environment. *Scientific Reports*. https://doi.org/10.1038/srep17639

Schreiber, U. (2004). Pulse-Amplitude-Modulation (PAM) fluorometry and saturation pulse method: An overview. *Chlorophyll a Fluorescence*, *1367*, 279–319. http://link.springer.com/10.1007/978-1-4020-3218-9_11

Seah, B. K. B., Schwaha, T., Volland, J. M., Huettel, B., Dubilier, N., & Gruber-Vodicka, H. R. (2017). Specificity in diversity: Single origin of a widespread ciliate-bacteria symbiosis. *Proceedings of the Royal Society B: Biological Sciences*, *284*(1858). https://doi.org/10.1098/rspb.2017.0764

Selmoni, O., Bay, L. K., Exposito-Alonso, M., & Cleves, P. A. (2024). Finding genes and pathways that underlie coral adaptation. *Trends in Genetics*. Elsevier Ltd. https://doi.org/10.1016/j.tig.2024.01.003

Selmoni, O., Cleves, P. A., & Exposito-Alonso, M. (2024). Global coral genomic vulnerability explains recent reef losses. *BioRxiv*.

Selmoni, O., Lecellier, G., Berteaux-Lecellier, V., & Joost, S. (2023). The Reef Environment Centralized InFormation System (RECIFS): An integrated geo-environmental database for coral reef research and conservation. *Global Ecology and Biogeography*, *32*(5), 622–632. https://doi.org/10.1111/geb.13657

Selmoni, O., Lecellier, G., Magalon, H., Vigliola, L., Oury, N., Benzoni, F., Peignon, C., Joost, S., & Berteaux-Lecellier, V. (2021). Seascape genomics reveals candidate molecular targets of heat stress adaptation in three coral species. *Molecular Ecology*, *30*(8), 1892–1906. https://doi.org/10.1111/mec.15857

Selmoni, O., Rochat, E., Lecellier, G., Berteaux-Lecellier, V., & Joost, S. (2020). Seascape genomics as a new tool to empower coral reef conservation strategies: An example on north-western Pacific *Acropora digitifera*. *Evolutionary Applications*. https://doi.org/10.1111/eva.12944

Sheets, E. A., Warner, P. A., & Palumbi, S. R. (2018). Accurate population genetic measurements require cryptic species identification in corals. *Coral Reefs*, *37*(2), 549–563. https://doi.org/10.1007/s00338-018-1679-9

Siebeck, U. E., Marshall, N. J., Klüter, A., & Hoegh-Guldberg, O. (2006). Monitoring coral bleaching using a colour reference card. *Coral Reefs*, *25*(3), 453–460. https://doi.org/10.1007/s00338-006-0123-8

Silverstein, R. N., Cunning, R., & Baker, A. C. (2015). Change in algal symbiont communities after bleaching, not prior heat exposure, increases heat tolerance of reef corals. *Global Change Biology*, *21*(1), 236–249. https://doi.org/10.1111/gcb.12706

Smale, D. A., Wernberg, T., Oliver, E. C. J., Thomsen, M., Harvey, B. P., Straub, S. C., Burrows, M. T., Alexander, L. V., Benthuysen, J. A., Donat, M. G., Feng, M., Hobday, A. J., Holbrook, N. J., Perkins-Kirkpatrick, S. E., Scannell, H. A., Sen Gupta, A., Payne, B. L., & Moore, P. J. (2019). Marine heatwaves threaten global biodiversity and the provision of ecosystem services. In *Nature Climate Change*. https://doi.org/10.1038/s41558-019-0412-1

Smith, E. G., Ketchum, R. N., & Burt, J. A. (2017). Host specificity of *Symbiodinium* variants revealed by an ITS2 metahaplotype approach. *ISME Journal*, *11*(6), 1500–1503. https://doi.org/10.1038/ismej.2016.206

Starko, S., Fifer, J. E., Claar, D. C., Davies, S. W., Cunning, R., Baker, A. C., & Baum, J. K. (2024). Marine heatwaves threaten cryptic coral diversity and erode associations among coevolving partners. *Science Advances*, *9*(32), eadf0954. https://doi.org/10.1126/sciadv.adf0954

Suggett, D. J., & Smith, D. J. (2011). Interpreting the sign of coral bleaching as friend vs. foe. *Global Change Biology*, *17*(1), 45–55. https://doi.org/10.1111/j.1365-2486.2009.02155.x

Sully, S., Burkepile, D. E., Donovan, M. K., Hodgson, G., & van Woesik, R. (2019). A global analysis of coral bleaching over the past two decades. *Nature Communications*. https://doi.org/10.1038/s41467-019-09238-2

Sully, S., Hodgson, G., & van Woesik, R. (2022). Present and future bright and dark spots for coral reefs through climate change. *Global Change Biology*, *28*(15), 4509–4522. https://doi.org/10.1111/gcb.16083

Thomas, L., Kennington, W. J., Evans, R. D., Kendrick, G. A., & Stat, M. (2017). Restricted gene flow and local adaptation highlight the vulnerability of high-latitude reefs to rapid

environmental change. *Global Change Biology*, *23*(6), 2197–2205. https://doi.org/10.1111/gcb.13639

Thomas, L., Şahin, D., Adam, A. S., Grimaldi, C. M., Ryan, N. M., Duffy, S. L., Underwood, J. N., Kennington, W. J., & Gilmour, J. P. (2024). Resilience to periodic disturbances and the long-term genetic stability in Acropora coral. *Communications Biology*, *7*(1). https://doi.org/10.1038/s42003-024-06100-0

Thomas, L., Underwood, J. N., Adam, A. A. S., Richards, Z. T., Dugal, L., Miller, K. J., & Gilmour, J. P. (2020). Contrasting patterns of genetic connectivity in brooding and spawning corals across a remote atoll system in northwest Australia. *Coral Reefs*, *39*(1), 55–60. https://doi.org/10.1007/s00338-019-01884-8

Thomas, L., Underwood, J. N., Rose, N. H., Fuller, Z. L., Richards, Z. T., Dugal, L., Grimaldi, C. M., Cooke, I. R., Palumbi, S. R., & Gilmour, J. P. (2022). Spatially varying selection between habitats drives physiological shifts and local adaptation in a broadcast spawning coral on a remote atoll in Western Australia. In *Sci. Adv* (Vol. 8). https://www.science.org

Torda, G., Donelson, J. M., Aranda, M., Barshis, D. J., Bay, L., Berumen, M. L., Bourne, D. G., Cantin, N., Foret, S., Matz, M., Miller, D. J., Moya, A., Putnam, H. M., Ravasi, T., Van Oppen, M. J. H., Thurber, R. V., Vidal-Dupiol, J., Voolstra, C. R., Watson, S. A., … Munday, P. L. (2017). Rapid adaptive responses to climate change in corals. *Nature Climate Change*, *7*(9), 627–636. https://doi.org/10.1038/nclimate3374

Turnham, K. E., Aschaffenburg, M. D., Pettay, D. T., Paz-García, D. A., Reyes-Bonilla, H., Pinzón, J., Timmins, E., Smith, R. T., McGinley, M. P., Warner, M. E., & Lajeunesse, T. C. (2023). High physiological function for corals with thermally tolerant, host-adapted symbionts. *Proceedings of the Royal Society B: Biological Sciences*, *290*(2003). https://doi.org/10.1098/rspb.2023.1021

Turnham, K. E., Wham, D. C., Sampayo, E., & LaJeunesse, T. C. (2021). Mutualistic microalgae co-diversify with reef corals that acquire symbionts during egg development. *ISME Journal*, *15*(11), 3271–3285. https://doi.org/10.1038/s41396-021-01007-8

Underwood, J. N., Richards, Z., Berry, O., Oades, D., Howard, A., & Gilmour, J. P. (2020). Extreme seascape drives local recruitment and genetic divergence in brooding and spawning corals in remote north-west Australia. *Evolutionary Applications*, *13*(9), 2404–2421. https://doi.org/10.1111/eva.13033

Underwood, J. N., Smith, L. D., Van Oppen, M. J. H., & Gilmour, J. P. (2009). Ecologically relevant dispersal of corals on isolated reefs: Implications for managing resilience. *Ecological Applications*, *19*(1), 18–29. https://doi.org/10.1890/07-1461.1

van der Ven, R. M., Heynderickx, H., & Kochzius, M. (2021). Differences in genetic diversity and divergence between brooding and broadcast spawning corals across two spatial scales in the Coral Triangle region. *Marine Biology*, *168*(2). https://doi.org/10.1007/s00227-020-03813-8

Van Hooidonk, R., Maynard, J., Tamelander, J., Gove, J., Ahmadia, G., Raymundo, L., Williams, G., Heron, S. F., & Planes, S. (2016). Local-scale projections of coral reef futures and implications of the Paris Agreement. *Scientific Reports*, *6*(December), 1–8. https://doi.org/10.1038/srep39666

van Oppen, M. J. H., Lutz, A., De'ath, G., Peplow, L., & Kininmonth, S. (2008). Genetic traces of recent long-distance dispersal in a predominantly self-recruiting coral. *PLoS ONE*, *3*(10), 1–12. https://doi.org/10.1371/journal.pone.0003401

van Oppen, M. J. H., & Medina, M. (2020). Coral evolutionary responses to microbial symbioses. *Philosophical Transactions of the Royal Society B: Biological Sciences*. https://doi.org/10.1098/rstb.2019.0591

Van Woesik, R., Sakai, K., Ganase, A., & Loya, Y. (2011). Revisiting the winners and the losers a decade after coral bleaching. *Marine Ecology Progress Series*. https://doi.org/10.3354/meps09203

van Woesik, R., Shlesinger, T., Grottoli, A. G., Toonen, R. J., Vega Thurber, R., Warner, M. E., Marie Hulver, A., Chapron, L., McLachlan, R. H., Albright, R., Crandall, E., DeCarlo, T. M., Donovan, M. K., Eirin-Lopez, J., Harrison, H. B., Heron, S. F., Huang, D., Humanes, A., Krueger, T., … Zaneveld, J. (2022). Coral-bleaching responses to climate change across biological scales. *Global Change Biology*, *28*(14), 4229–4250. https://doi.org/10.1111/gcb.16192

Vollmer, S. V, Selwyn, J. D., Despard, B. A., & Roesel, C. L. (2023). *Genomic signatures of disease resistance in endangered staghorn corals*. https://www.science.org

Voolstra, C. R., Buitrago-López, C., Perna, G., Cárdenas, A., Hume, B. C. C., Rädecker, N., & Barshis, D. J. (2020). Standardized short-term acute heat stress assays resolve historical differences in coral thermotolerance across microhabitat reef sites. *Global Change Biology*. https://doi.org/10.1111/gcb.15148

Voolstra, C. R., Valenzuela, J. J., Turkarslan, S., Cárdenas, A., Hume, B. C. C., Perna, G., Buitrago-López, C., Rowe, K., Orellana, M. V., Baliga, N. S., Paranjape, S., Banc-Prandi, G., Bellworthy, J., Fine, M., Frias-Torres, S., & Barshis, D. J. (2021). Contrasting heat stress response patterns of coral holobionts across the Red Sea suggest distinct mechanisms of thermal tolerance. *Molecular Ecology*, *30*(18), 4466–4480. https://doi.org/10.1111/mec.16064

Wei, T., & Simko, V. (2021). *R package "corrplot": Visualization of a Correlation Matrix*. https://github.com/taiyun/corrplot

Weir, B. S., & Cockerham, C. C. (1984). *Estimating F-Statistics for the Analysis of Population Structure* (Vol. 38, Issue 6).

Weis, V. M. (2008). Cellular mechanisms of Cnidarian bleaching: Stress causes the collapse of symbiosis. *Journal of Experimental Biology* (Vol. 211, Issue 19, pp. 3059–3066). https://doi.org/10.1242/jeb.009597

Weis, V. M., Davy, S. K., Hoegh-Guldberg, O., Rodriguez-Lanetty, M., & Pringle, J. R. (2008). Cell biology in model systems as the key to understanding corals. *Trends in Ecology and Evolution*, *23*(7), 369–376. https://doi.org/10.1016/j.tree.2008.03.004

Wickham, H. (2016). *ggplot2: Elegant Graphics for Data Analysis*. Springer-Verlag New York. https://ggplot2.tidyverse.org

Wilkinson, S. (2018). *kmer: an R package for fast alignment-free clustering of biological sequences*. https://doi.org/10.5281/zenodo.1227690

Wilson, K., Li, Y., Whan, V., Lehnert, S., Byrne, K., Moore, S., Ballment, E., Fayazi, Z., Swan, J., Kenway, M., & Benzie, J. (2002). Genetic mapping of the black tiger shrimp *Penaeus monodon* with amplified fragment length polymorphism. *Aquaculture*. https://doi.org/10.1016/S0044-8486(01)00842-0

Wood, S., Paris, C. B., Ridgwell, A., & Hendy, E. J. (2014). Modelling dispersal and connectivity of broadcast spawning corals at the global scale. *Global Ecology and Biogeography*, *23*(1), 1–11. https://doi.org/10.1111/geb.12101

Wright, E. S. (2016). Using DECIPHER v2.0 to analyze big biological sequence data in R. *The R Journal*, *8*(1), 352–359.

Yu, X., Yu, K., Huang, W., Liang, J., Qin, Z., Chen, B., Yao, Q., & Liao, Z. (2020). Thermal acclimation increases heat tolerance of the scleractinian coral *Acropora pruinosa*. *Science of The Total Environment*, *733*, 139319. https://doi.org/https://doi.org/10.1016/j.scitotenv.2020.139319

Appendices

Appendix A: Supplementary material to Chapter 2

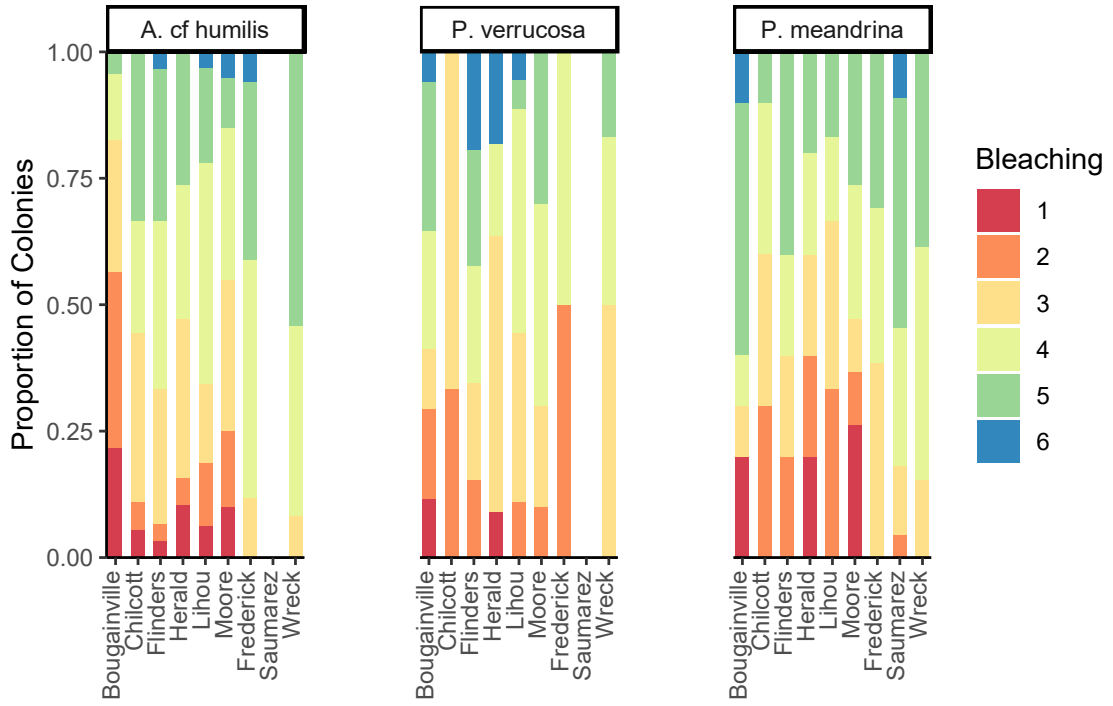

Figure S2.1. Coral colonies collected from the nine reefs of the Coral Sea Marine Park ranged in conditions from healthy (1) to severely bleached (6). Due to an ongoing bleaching event, I sampled colonies of all bleaching categories to avoid biasing collections towards bleached or unbleached coral colonies. During collection, each colony was assessed visually for bleaching and scored along a 6-point scale.

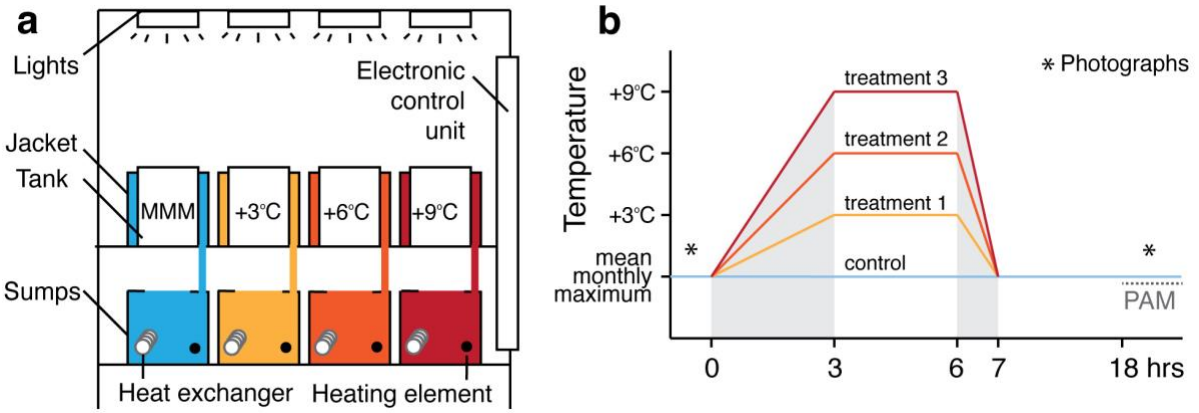

Figure S2.2. Design of the experimental aquaria system. The system features four heat and light independent treatments: the maximum monthly mean (MMM), and +3 ˚C, +6 ˚C and +9 ˚C from the

MMM for each reef (a). Standardised temperature ramping profile of the acute heat stress system includes a 3h ramp up to the treatment temperature, 3h hold at treatment temperature, 1h ramp down to ambient and 11h hold overnight (b).

Table S2.1. Pulse amplitude fluorometry settings for each reef and experiment. For each experiment, settings were specified for actinic light (AL, mmol photons m^{-2} s^{-1}), measuring light intensity (ML), saturation light intensity (SI, mmol photons m^{-2} s^{-1}), saturation pulse width (SP, seconds), actinic width (AW), gain and damp.

Reef	AL	ML	SI	SP	AW	Gain	Damp
Saumarez	1	11	8	0.8	0.3	3	2
Wreck	1	11	8	0.8	0.3	3	2
Frederick	1	11	8	0.8	0.3	3	2
Flinders	1	11	8	0.8	0.3	3	2
Herald	1	11	8	0.8	0.3	3	2
Chilcott	1	11	8	0.8	0.3	3	2
Lihou	1	11	8	0.8	0.3	3	2
Moore	1	12	8	0.8	0.3	4	2
Bougainville	1	12	8	0.8	0.3	4	2

Table S2.2. Experimental target temperatures and actual temperature profiles (± standard deviation) recorded for the 3-hour hold.

Reef	Experimental Target Temperature (3h hold, ˚C)				Actual Experimental Temperature (3h hold, ˚C) (± SD)			
	Ambient	T3	T6	T9	Ambient	T3	T6	T9
Saumarez	29.63	30.9	33.9	36.9	30.40 (± 0.10)	30.95 (± 0.04)	34.05 (± 0.33)	36.81 (±0.18)
Wreck	29.55	30.41	33.41	36.41	29.71 (± 0.13)	30.41 (± 0.06)	33.20 (± 0.16)	36.24 (± 0.33)
Frederick	29.98	30.77	33.77	36.77	30.02 (± 0.17)	30.64 (± 0.16)	33.47 (± 0.95)	35.73 (± 1.16)
Flinders	30.67	31.64	34.64	37.64	30.74 (± 0.08)	31.66 (± 0.08)	34.74 (± 0.45)	37.56 (± 0.51)
Herald/Chilcott	29.93	31.65	34.65	37.65	30.16 (± 0.13)	31.66 (± 0.19)	34.72 (± 0.48)	36.83 (± 0.94)
Lihou	30.48	31.44	34.44	37.44	30.52 (± 0.04)	31.43 (±0.16)	34.43 (± 0.38)	37.28 (± 0.39)
Moore	30.45	31.83	34.83	37.83	30.63 (± 0.06)	31.91 (± 0.12)	34.90 (± 0.51)	37.32 (± 0.60)
Bougainville	29.99	31.96	34.96	37.96	30.57 (± 0.05)	32.06 (± 0.24)	34.97 (± 0.36)	36.33 (± 0.90)

1. Species Models

Table S2.3. Model parameters and Akaike's Information Criteria (AIC) index for log-logistic 'Species' model selection.

Model name	Slope (b)	Upper asymptote (d)	ED50 (e)	Random Factors	DF	AICc
Species.1	1	1	Species	e ~ 1|Reef	7	-2131.489
Species.2	1	Species	Species	e ~ 1|Reef	9	-2179.997
Species.3	Species	1	Species	e ~ 1|Reef	9	-2171.099
Species.4	Species	Species	Species	e ~ 1|Reef	11	-2203.347
Species.5	1	Species	Species	e ~ Reef | Depth	10	-2177.997
Species.6	1	Species	Species	e ~ Reef | Tank	10	-2177.081
Species.7	1	Species	Species*catBleaching	e ~ 1|Reef	15	-2181.960
Species.8	1	Species*catBleaching	Species	e ~ 1|Reef	15	-2230.468
Species.9	1	Species*catBleaching	Species*catBleaching	e ~ 1|Reef	21	-2244.262
Species.9.1	1	Species*catBleaching	Species*catBleaching	d + e ~ 1|Reef	23	-2277.888
Species9.2	1	Species*catBleaching	Species*catBleaching	d + e ~ 1|Reef	23	-2982.373
Species9.3	Species*catBleaching	Species*catBleaching	Species*catBleaching	b + d + e ~ 1|Reef	**34**	**-3109.717**
Species9.5	catBleaching	Species*catBleaching	Species*catBleaching	b + d + e ~ 1|Reef	28	-3034.841

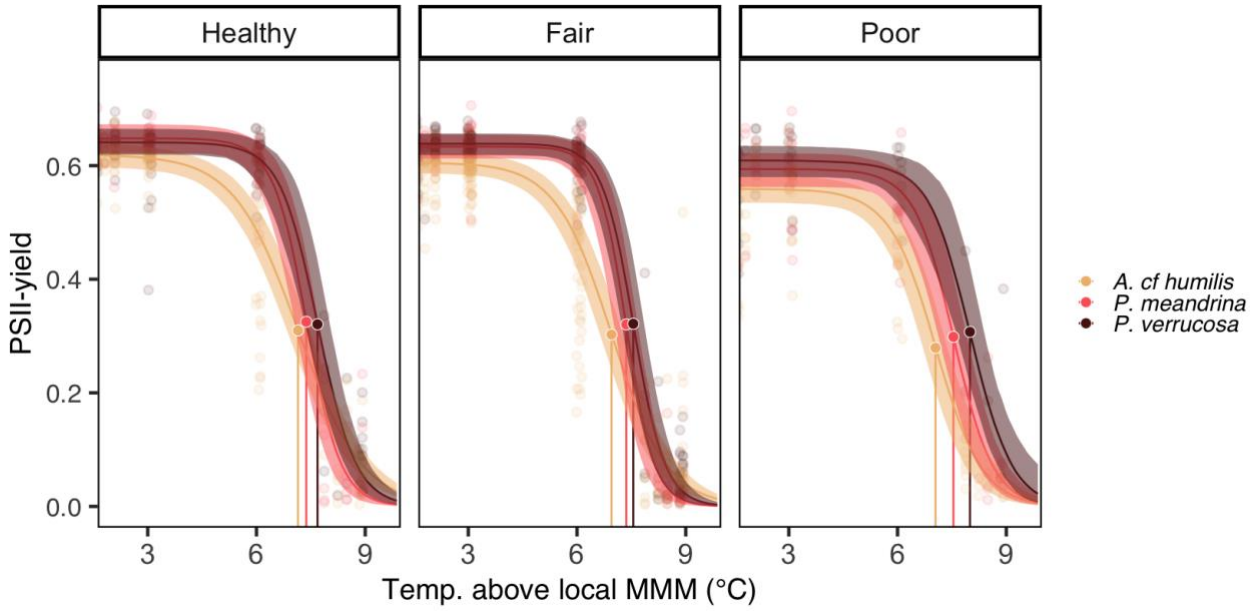

Fig S2.3. Model outputs of 'Species' ED50 models grouped by Bleaching Category at the time of coral collection. PSII-yield (F_v/F_m) is modelled against relative temperature above local MMM to obtain ED50 values. Corals were partitioned into three groups: Healthy (Bleaching Score 5-6), Fair (Bleaching Score 3-4) and Poor (Bleaching Score 1-2). Coloured lines represent each of the three species.

Table S2.4. Estimated marginal means for Species non-linear mixed effects model. See https://github.com/HugoBH/CoralSea-ED50-GCB for contrast plots. (SE: Standard Error, df: degrees of freedom, lower and upper CL: Confidence Limits)

Species	Estimate	SE	df	lower.CL	upper.CL
A. cf humilis	7.05	0.154	1148	6.75	7.35
P. meandrina	7.42	0.159	1148	7.11	7.74
P. verrucosa	7.74	0.16	1148	7.43	8.06

Table S2.5. Pairwise contrasts for Species non-linear mixed effects model. See https://github.com/HugoBH/CoralSea-ED50-GCB for contrast plots. (SE: Standard Error, df: degrees of freedom)

Contrast	Estimate	SE	df	t.ratio	p.value
A. cf humilis - P. meandrina	-0.376	0.0765	1148	-4.914	<.0001
A. cf humilis - P. verrucosa	-0.696	0.0767	1148	-9.067	<.0001
P. meandrina - P. verrucosa	-0.32	0.0857	1148	-3.733	0.0006

2. Reef Models

Table S2.6. Model parameters and Akaike's Information Criteria (AIC) index for log-logistic 'Reef' model selection. Models were developed using *A.* cf *humilis* data to test model selection criteria. Model outputs and descriptions of selection can be found at https://github.com/HugoBH/CoralSea-ED50-GCB.

Model name	Slope (b)	Upper asymp (d)	ED50 (e)	Random Factors	df	AICc
Reef.ahum.1	1	1	Reef	e ~ 1|Vial	10	-1177.798
Reef.ahum.2	1	Reef	Reef	e ~ 1|Vial	15	-1221.154
Reef.ahum.3	1	Reef*catBleaching	Reef*catBleaching	e ~ 1|Vial	39	-1220.852
Reef.ahum.4	1	Reef	Reef*catBleaching	e ~ 1|Vial	27	-1221.605
Reef.ahum.5	1	Reef*catBleaching	Reef	e ~ 1|Vial	27	-1225.515
Reef.ahum.6	**1**	**Reef**	**Reef**	**d ~ 1|catBleaching + e ~ 1|Vial**	**15**	**-1221.154**
Reef.ahum.7	1	Reef	Reef	e ~ 1|catBleaching	15	-1221.154
Reef.ahum.8	1	Reef	Reef	d ~ 1|catBleaching	15	-1221.154
Reef.ahum.9	1	Reef	Reef	d + e ~ 1|Vial	17	-1217.154
Reef.ahum.10	1	Reef	Reef	d + e ~ 1|catBleaching/Vial	20	-1211.154
Reef.ahum.11	1	Reef	Reef	d + e ~ 1|catBleaching	17	-1217.154

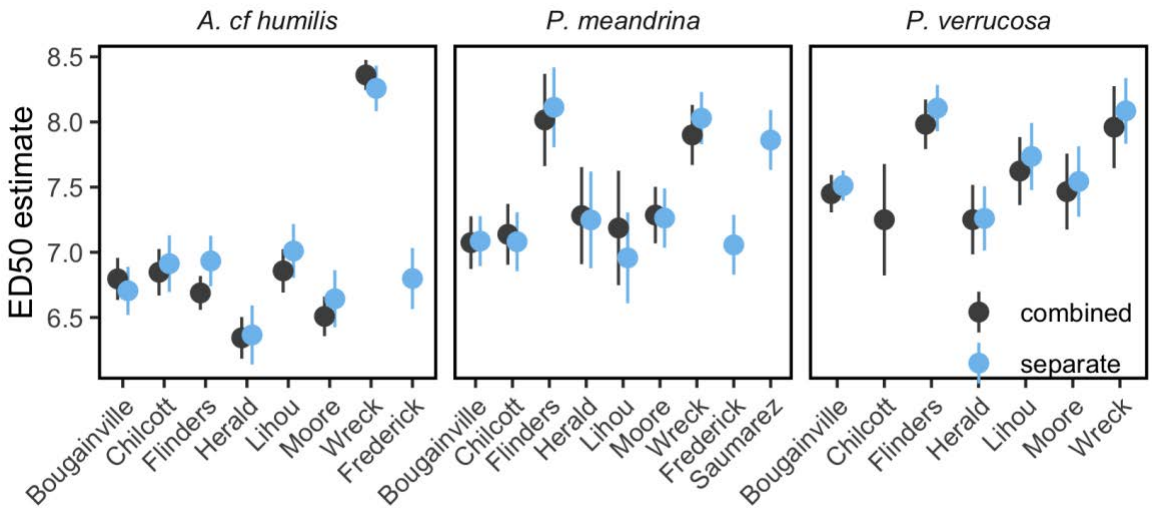

Figure S2.4. Comparisons of model outputs for 'combined' and 'separate' model outputs for reef ED50s. Relative ED50 estimates (temperature above local MMM) are modelled for each species (panels) and reef. Combined (grey) points show the combined model, which includes all reefs into a single model, but only includes reefs that are present for all three species. Separate (blue) points show the separate model ED50 estimates that are estimated separately for each species, in order to include all reefs from the datasets.

Table S2.7. Tukey's pairwise comparisons derived from emmeans for *Acropora* cf. *humilis* from the 'Reef' non-linear mixed effects model.

Contrast	Estimate	SE	df	t.ratio	p.value
Bougainville - Chilcott	-0.2083	0.144	468	-1.447	0.8346
Bougainville - Flinders	-0.2288	0.135	468	-1.69	0.6938
Bougainville - Frederick	-0.0943	0.151	468	-0.626	0.9985
Bougainville - Herald	0.3385	0.148	468	2.287	0.3028
Bougainville - Lihou	-0.3057	0.14	468	-2.187	0.3614
Bougainville - Moore	0.0612	0.145	468	0.423	0.9999
Bougainville - Wreck	**-1.5534**	**0.127**	**468**	**-12.208**	**<.0001**
Chilcott - Flinders	-0.0205	0.147	468	-0.139	1
Chilcott - Frederick	0.114	0.161	468	0.707	0.9968
Chilcott - Herald	**0.5468**	**0.159**	**468**	**3.44**	**0.0146**
Chilcott - Lihou	-0.0974	0.151	468	-0.645	0.9982
Chilcott - Moore	0.2695	0.156	468	1.731	0.6672
Chilcott - Wreck	**-1.3451**	**0.14**	**468**	**-9.592**	**<.0001**
Flinders - Frederick	0.1345	0.153	468	0.88	0.9877
Flinders - Herald	**0.5673**	**0.151**	**468**	**3.756**	**0.0048**
Flinders - Lihou	-0.0769	0.139	468	-0.553	0.9993
Flinders - Moore	0.29	0.146	468	1.992	0.4881
Flinders - Wreck	**-1.3246**	**0.135**	**468**	**-9.834**	**<.0001**
Frederick - Herald	0.4328	0.165	468	2.624	0.1499
Frederick - Lihou	-0.2114	0.157	468	-1.349	0.8792
Frederick - Moore	0.1555	0.162	468	0.963	0.9793
Frederick - Wreck	**-1.4591**	**0.147**	**468**	**-9.897**	**<.0001**
Herald - Lihou	**-0.6442**	**0.155**	**468**	**-4.156**	**0.001**
Herald - Moore	-0.2773	0.16	468	-1.737	0.6629
Herald - Wreck	**-1.8919**	**0.144**	**468**	**-13.113**	**<.0001**
Lihou - Moore	0.3669	0.15	468	2.449	0.2203
Lihou - Wreck	**-1.2477**	**0.139**	**468**	**-8.98**	**<.0001**
Moore - Wreck	**-1.6146**	**0.143**	**468**	**-11.293**	**<.0001**

Table S2.8. Tukey's pairwise comparisons derived from emmeans for *Pocillopora meandrina* from the 'Reef' non-linear mixed effects model.

Contrast	Estimate	SE	df	t.ratio	p.value
Bougainville - Chilcott	0.00496	0.15	271	0.033	1
Bougainville - Flinders	**-1.02701**	**0.18**	**271**	**-5.717**	**<.0001**
Bougainville - Frederick	0.02894	0.148	271	0.195	1
Bougainville - Herald	-0.16248	0.211	271	-0.771	0.9975
Bougainville - Lihou	0.12858	0.203	271	0.633	0.9994
Bougainville - Moore	-0.17636	0.149	271	-1.184	0.9593
Bougainville - Saumarez	**-0.7757**	**0.146**	**271**	**-5.298**	**<.0001**
Bougainville - Wreck	**-0.94347**	**0.136**	**271**	**-6.951**	**<.0001**
Chilcott - Flinders	**-1.03197**	**0.194**	**271**	**-5.318**	**<.0001**
Chilcott - Frederick	0.02398	0.163	271	0.147	1
Chilcott - Herald	-0.16743	0.22	271	-0.762	0.9977
Chilcott - Lihou	0.12362	0.208	271	0.594	0.9996
Chilcott - Moore	-0.18131	0.161	271	-1.123	0.9704
Chilcott - Saumarez	-0.78065	0.164	271	-4.758	**0.0001**
Chilcott - Wreck	**-0.94842**	**0.154**	**271**	**-6.144**	**<.0001**
Flinders - Frederick	**1.05595**	**0.188**	**271**	**5.603**	**<.0001**
Flinders - Herald	**0.86454**	**0.243**	**271**	**3.562**	**0.0128**
Flinders - Lihou	**1.15559**	**0.241**	**271**	**4.792**	**0.0001**
Flinders - Moore	**0.85065**	**0.191**	**271**	**4.445**	**0.0004**
Flinders - Saumarez	0.25131	0.184	271	1.366	0.9095
Flinders - Wreck	0.08355	0.176	271	0.475	0.9999
Frederick - Herald	-0.19141	0.22	271	-0.871	0.9943
Frederick - Lihou	0.09964	0.214	271	0.465	0.9999
Frederick - Moore	-0.20529	0.161	271	-1.273	0.9382
Frederick - Saumarez	**-0.80463**	**0.157**	**271**	**-5.132**	**<.0001**
Frederick - Wreck	**-0.9724**	**0.147**	**271**	**-6.605**	**<.0001**
Herald - Lihou	0.29105	0.258	271	1.128	0.9695
Herald - Moore	-0.01388	0.219	271	-0.063	1
Herald - Saumarez	-0.61322	0.219	271	-2.797	0.1212
Herald - Wreck	**-0.78099**	**0.212**	**271**	**-3.678**	**0.0085**
Lihou - Moore	-0.30493	0.211	271	-1.446	0.8788
Lihou - Saumarez	**-0.90427**	**0.218**	**271**	**-4.147**	**0.0015**
Lihou - Wreck	**-1.07204**	**0.211**	**271**	**-5.09**	**<.0001**
Moore - Saumarez	**-0.59934**	**0.16**	**271**	**-3.737**	**0.0069**
Moore - Wreck	**-0.76711**	**0.151**	**271**	**-5.082**	**<.0001**
Saumarez - Wreck	-0.16777	0.141	271	-1.187	0.9587

Table S2.9. Tukey's pairwise comparisons derived from emmeans for *Pocillopora verrucosa* from the 'Reef' non-linear mixed effects model.

Contrast	Estimate	SE	df	t.ratio	p.value
Bougainville - Flinders	**-0.5949**	**0.0938**	**229**	**-6.339**	**<.0001**
Bougainville - Herald	0.2514	0.1373	229	1.83	0.4483
Bougainville - Lihou	-0.224	0.1311	229	-1.709	0.5275
Bougainville - Moore	-0.0317	0.1418	229	-0.224	0.9999
Bougainville - Wreck	**-0.5736**	**0.1311**	**229**	**-4.375**	**0.0003**
Flinders - Herald	**0.8463**	**0.1536**	**229**	**5.511**	**<.0001**
Flinders - Lihou	0.3708	0.1314	229	2.822	0.0576
Flinders - Moore	**0.5631**	**0.1481**	**229**	**3.801**	**0.0025**
Flinders - Wreck	0.0212	0.1348	229	0.157	1
Herald - Lihou	-0.4754	0.1798	229	-2.644	0.091
Herald - Moore	-0.2832	0.1844	229	-1.535	0.6418
Herald - Wreck	**-0.825**	**0.1785**	**229**	**-4.623**	**0.0001**
Lihou - Moore	0.1923	0.1728	229	1.112	0.8759
Lihou - Wreck	-0.3496	0.1611	229	-2.17	0.2559
Moore - Wreck	**-0.5419**	**0.1746**	**229**	**-3.104**	**0.0259**

Table S2.10. Summary tables derived from emmeans for relative temperature ED50 values related to each reef and species combination (95% confidence intervals).

Reef	*A.* cf *humilis*	*P. meandrina*	*P. verrucosa*
Frederick	6.8 (6.56-7.03)	7.06 (6.83-7.29)	-
Herald	6.37 (6.14-6.59)	7.25 (6.88-7.62)	7.26 (7.01-7.51)
Chilcott	6.91 (6.7-7.13)	7.08 (6.85-7.31)	-
Bougainville	6.7 (6.52-6.89)	7.09 (6.89-7.28)	7.51 (7.4-7.63)
Moore	6.64 (6.42-6.86)	7.26 (7.03-7.49)	7.54 (7.27-7.81)
Lihou	7.01 (6.8-7.22)	6.96 (6.61-7.31)	7.74 (7.48-7.99)
Flinders	6.93 (6.74-7.13)	8.11 (7.81-8.42)	8.11 (7.93-8.28)
Saumarez	-	7.86 (7.63-8.09)	-
Wreck	8.26 (8.08-8.43)	8.03 (7.83-8.23)	8.09 (7.83-8.34)

Table S2.11. Summary tables derived from emmeans for absolute temperature ED50 values related to each reef and species combination (95% confidence intervals).

Reef	*A.* cf *humilis*	*P. meandrina*	*P. verrucosa*
Frederick	34.57 (34.33-34.80)	34.83 (34.60-35.06)	-
Herald	34.96 (34.73-35.18)	35.84 (35.47-36.21)	35.85 (35.60-36.10)
Chilcott	35.50 (35.29-35.72)	35.67 (35.45-35.90)	-
Bougainville	35.67 (35.48-35.85)	36.05 (35.85-36.24)	36.47 (36.36-36.59)
Moore	35.47 (35.26-35.69)	36.09 (35.86-36.32)	36.37 (36.10-36.64)
Lihou	35.45 (35.24-35.66)	35.40 (35.05-35.75)	36.18 (35.92-36.43)
Flinders	35.57 (35.38-35.77)	36.75 (36.45-37.06)	36.75 (36.57-36.92)
Saumarez	-	35.76 (35.53-35.99)	-
Wreck	35.67 (35.49-35.84)	35.44 (35.24-35.64)	35.50 (35.24-35.75)

3. Relative ED50 Environmental and Climatic Predictors Model

Table S2.12. Definitions for 24 environmental and thermal history (climatic) variables considered for model parameters. Climatic and thermal history metrics were calculated from NOAA Coral Reef Watch Operational Daily Near-Real-Time Global 5-km Satellite Coral Bleaching Monitoring Product Version 3.1 for each site within reef from 1986– 2020.

Parameter	Definition (based on NOAA)
Complexity	Averaged across 4 transects on a scale of 1-5
DHW2020	Number of Degree Heating Weeks (DHW)experienced during the time of experiments conducted in 2020
DHW2	Number of DHW events greater than 2 ºC-weeks between 1986 - 2020
DHW3	Number of DHW events greater than 3ºC-weeks between 1986 - 2020
DHW4	Number of DHW events greater than 4ºC-weeks between 1986 - 2020
DHW6	Number of DHW events greater than 6C-weeks between 1986 - 2020
DHW8	Number of DHW events greater than 8ºC-weeks between 1986 - 2020
DHW9	Number of DHW events greater than 9ºC-weeks between 1986 - 2020
Lat	Latitude
Long	Longitude
maxDHW	Maximum DHW experienced between 1986 - 2020
maxSST	Maximum Sea Surface Temperature (SST) between 1986 - 2020
meanDHW	Average DHWs experienced between 1986 - 2020
meanSST	Average Sea Surface Temperature (SST) between 1986 - 2020
minSST	Max Sea Surface Temperature (SST) between 1986 - 2020
MMM	Maximum Monthly Mean SST between 1986 - 2010
rangeSST	Range between Max and Min SST values between 1986 - 2020
Recent.maxDHW	Maximum DHW exposure between 2016 - 2020
Recent.meanDHW	Average maximum DHW exposure between 2016 - 2020
ReefArea	Size of reef polygons in hectares (3dGBR)
ReturnDHW3	The return time in years between events where DHW exceeded 3ºC-weeks
ReturnDHW4	The return time in years between events where DHW exceeded 4ºC-weeks
ReturnDHW6	The return time in years between events where DHW exceeded 6ºC-weeks
varSST	Variability in SST between 1986 - 2020

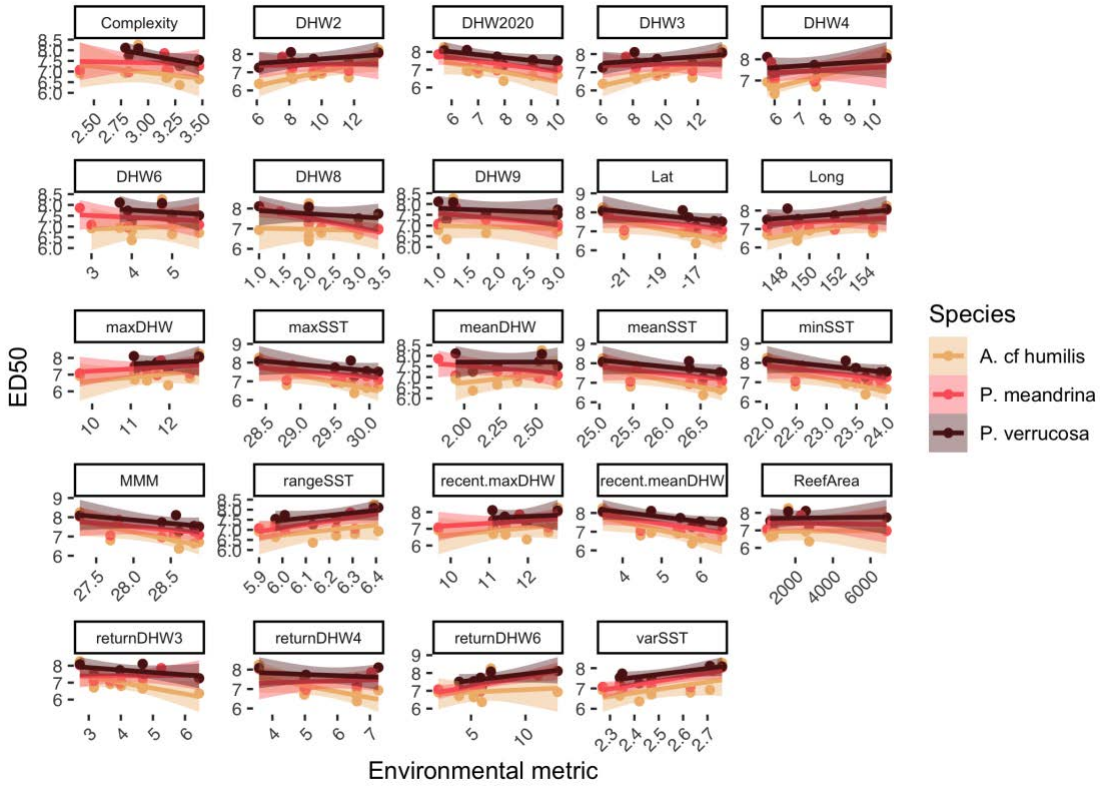

Figure S2.5. Plots of 24 environmental and climatic variables measured against relative ED50 values derived from 'Species' and 'Reef' models. Coloured lines represent the three species. See Table S12 for detailed descriptions of how each climatic or environmental variable was calculated.

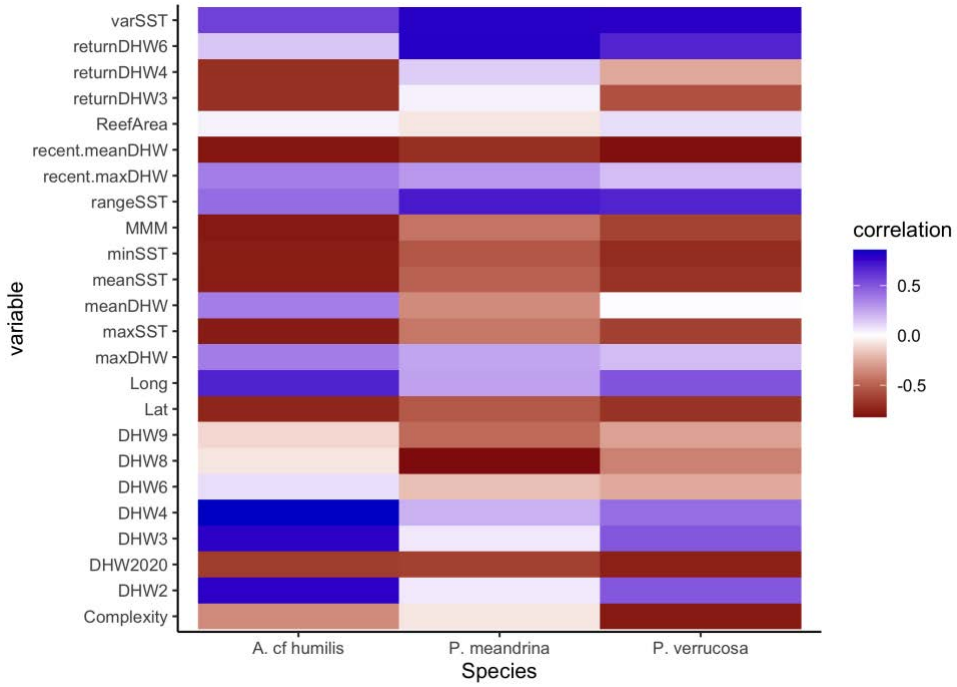

Figure S2.6. Correlation matrix of relative ED50s for coral species (*Acropora* cf *humilis, Pocillopora meandrina,* and *Pocillopora verrucosa*) against the 24 environmental and climatic variables.

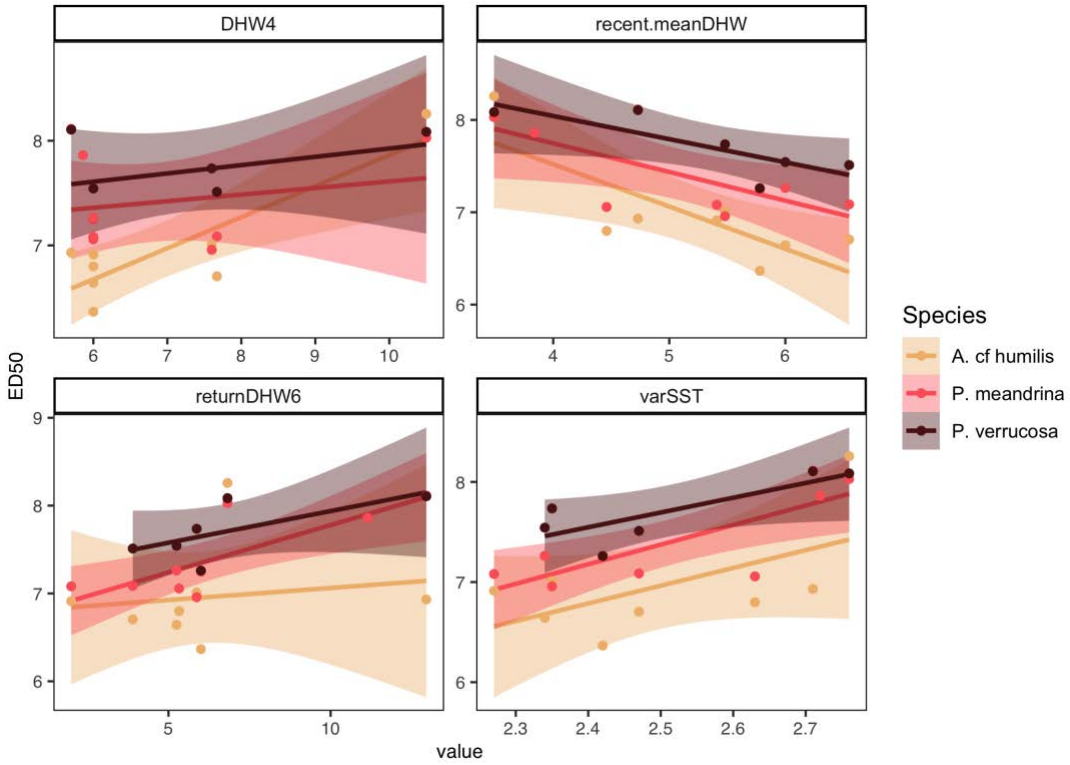

Figure S2.7. Climatic predictors that were included in the dredging model to obtain the model of best fit for relative ED50s among reefs and species. These predictors were chosen based on their low collinearity amongst other present variables, and high correlation to Species and Reef ED50 values.

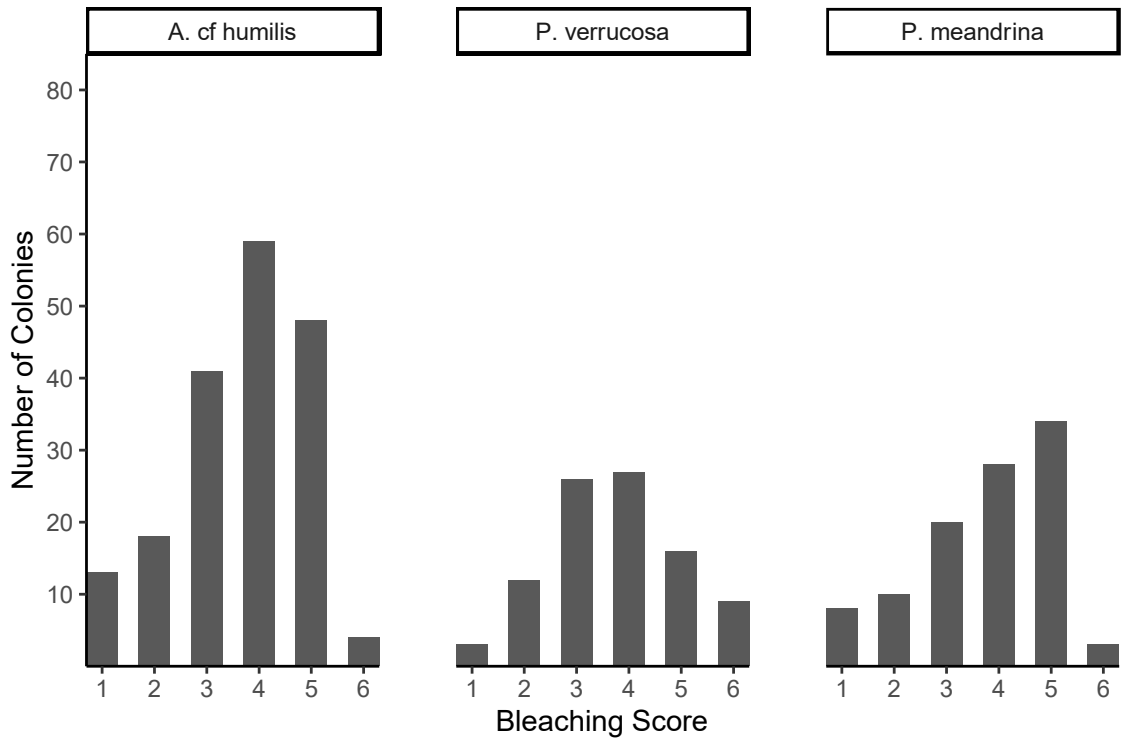

Figure S2.8. Number of individual colony fragments for each species and bleaching score. Bleaching score of '1' represents the most bleached, and score of '6' the least bleached. Corals were collected from *Acropora* cf. *humilis, Pocillopora verrucosa* and *Pocillopora meandrina*.

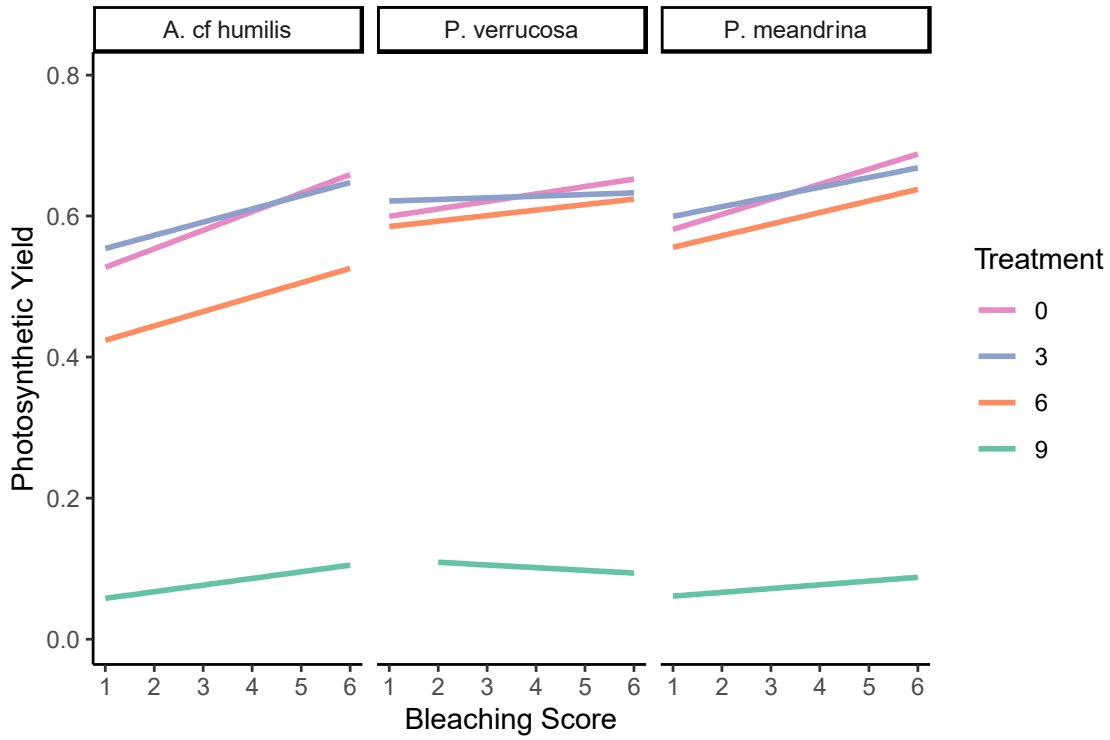

Figure S2.9. Raw, un-transformed photosynthetic yield (Fv/Fm) data in relation to bleaching scores. Each panel represents one of the three species: *Acropora* cf. *humilis, Pocillopora verrucosa* and *Pocillopora meandrina.* Coloured lines represent each of the four experimental treatments at 0 ˚C, 3 ˚C, +6 ˚C and +9 ˚C above local MMM. Bleaching scores range from most bleached (‘1’) to least bleached (‘6) as scored using a Coral Watch Health Chart ‘D’ Colour Chart.

Table S2.13. Estimates for environmental predictors of relative heat tolerance derived from a linear model with three environmental predictors: the number of events where DHW >4, the recent mean maximum DHW and the return time between events where DHW > 6. An interaction term between each coral species x DHW4 is also included in the model.

Fixed effect	Estimate	SE	t	Pr (> |*t*|)
Species (*A. cf humilis*)	5.78952	0.76071	7.611	< 0.001
Species (*P. meandrina*)	1.84012	0.55064	3.342	0.005
Species (*P. verrucosa*)	2.19242	0.60783	3.607	0.003
returnDHW6	0.05255	0.02162	2.431	0.028
Species (*A. cf humilis*) x DHW4	0.25490	0.06028	4.229	< 0.001
Species (*P. meandrina*) x DHW4	-0.20679	0.07812	-2.647	0.018
Species (*P. meandrina*) x DHW4	-0.21270	0.08280	-2.569	0.021

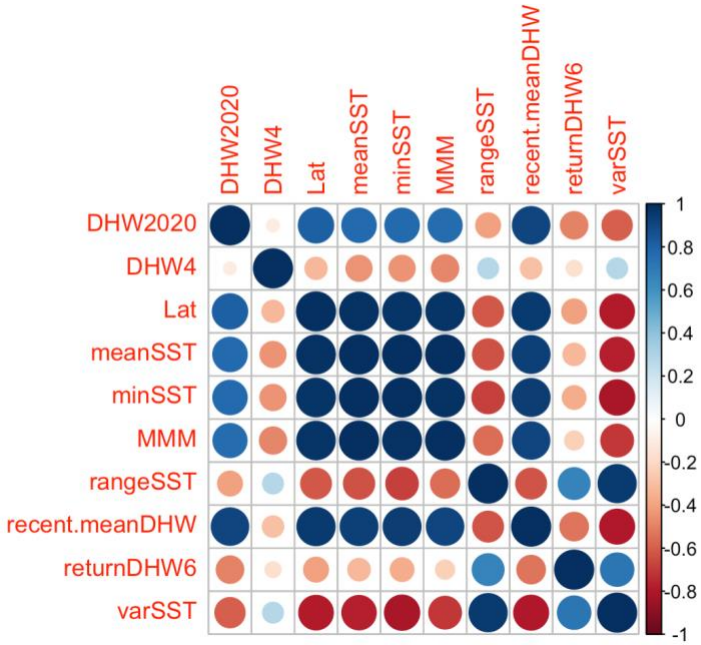

Figure S2.10. Ten environmental variables that exhibited moderate to high collinearity with relative ED50 values (R > 0.40). Six of these variables were removed from the model selection criteria due to high collinearity (> 0.80) with other variables in the model (DHW2020, Lat, meanSST, minSST, MMM, rangeSST).

4. Absolute ED50 Environmental and Climatic Predictors Model

A case can be made to use absolute ED50 values instead of relative ED50 values to consider the effects of MMM on ED50 and its interaction with other environmental drivers. However, I caution this experimental design is not necessarily fit to measure absolute ED50s since they were conducted relative to MMM. To do so, I would suggest having consistent temperature treatments across all sampled populations rather standardised to MMM. Nevertheless, I explored the relationship between absolute ED50 values and this suite of environmental and climatic variables to investigate whether it changes the drivers of heat tolerance in corals.

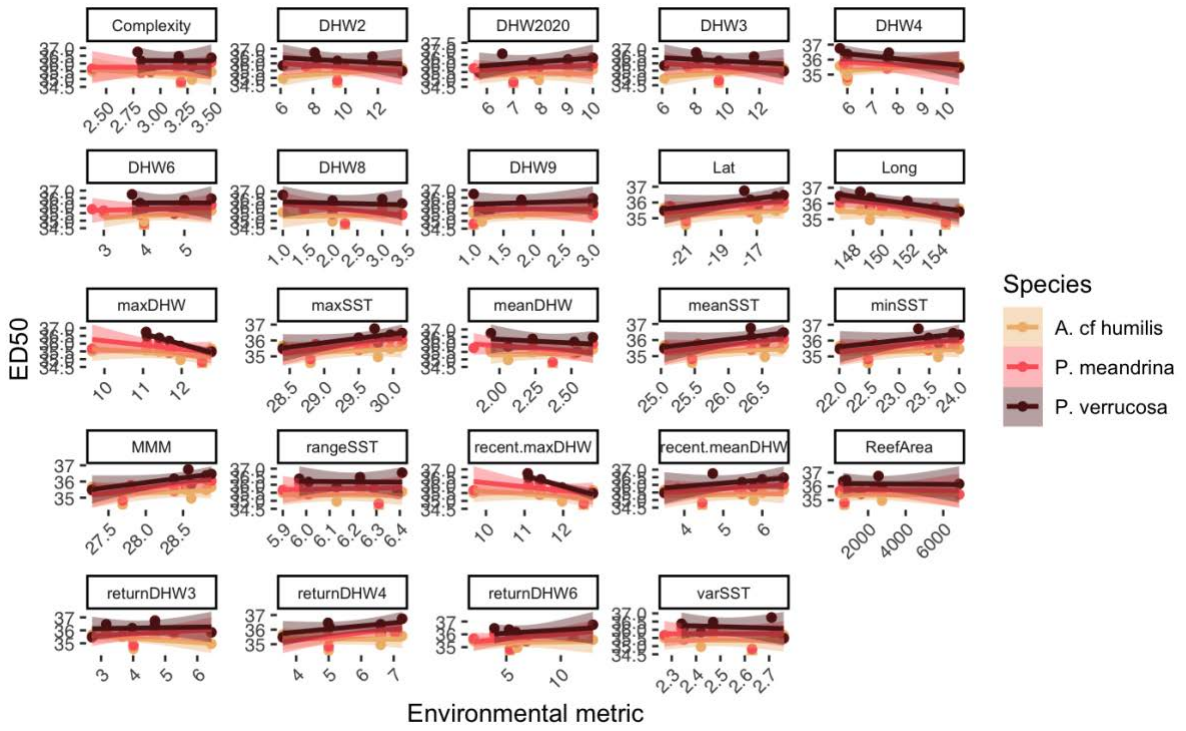

Figure S2.11. Plots of 24 environmental and climatic variables measured against absolute ED50 values derived from 'Species' and 'Reef' models. Coloured lines represent the three species. See Table S12 for detailed descriptions of how each climatic or environmental variable was calculated.

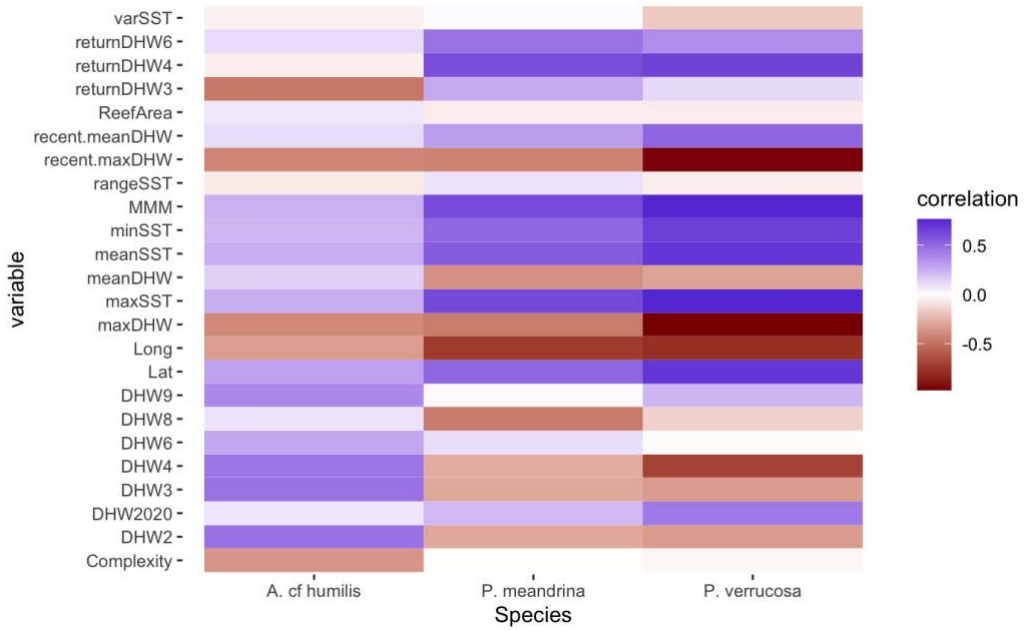

Figure S2.12. Correlation matrix of absolute ED50s for coral species (*Acropora* cf *humilis, Pocillopora meandrina,* and *Pocillopora verrucosa*) against the 24 environmental and climatic variables.

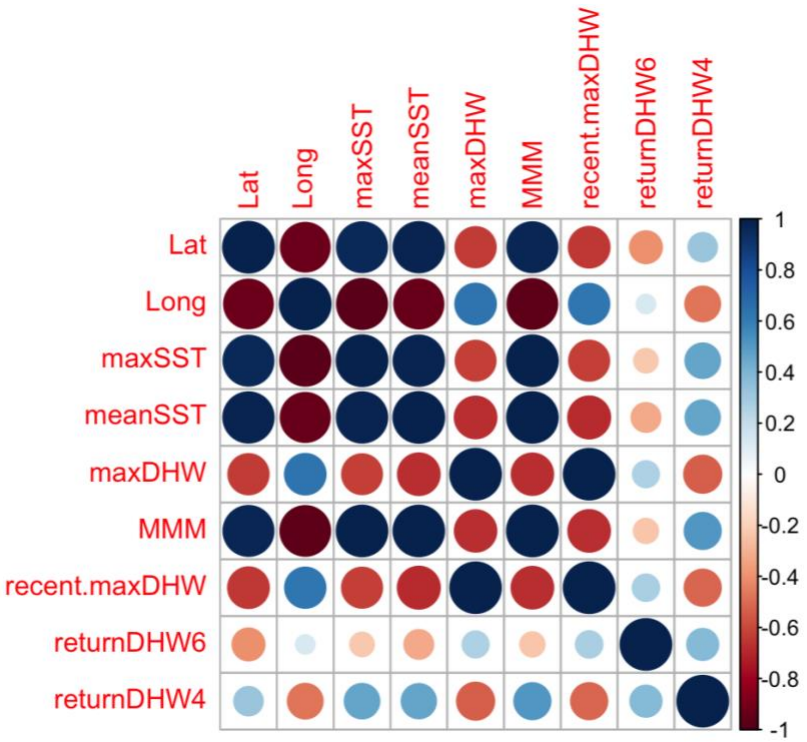

Figure S2.13. Nine environmental variables that exhibited moderate to high collinearity with absolute ED50 values (R > 0.30). Five of these variables were removed from the model selection criteria due to high collinearity (> 0.80) with other variables in the model (Lat, Long, maxSST, meanSST, maxDHW).

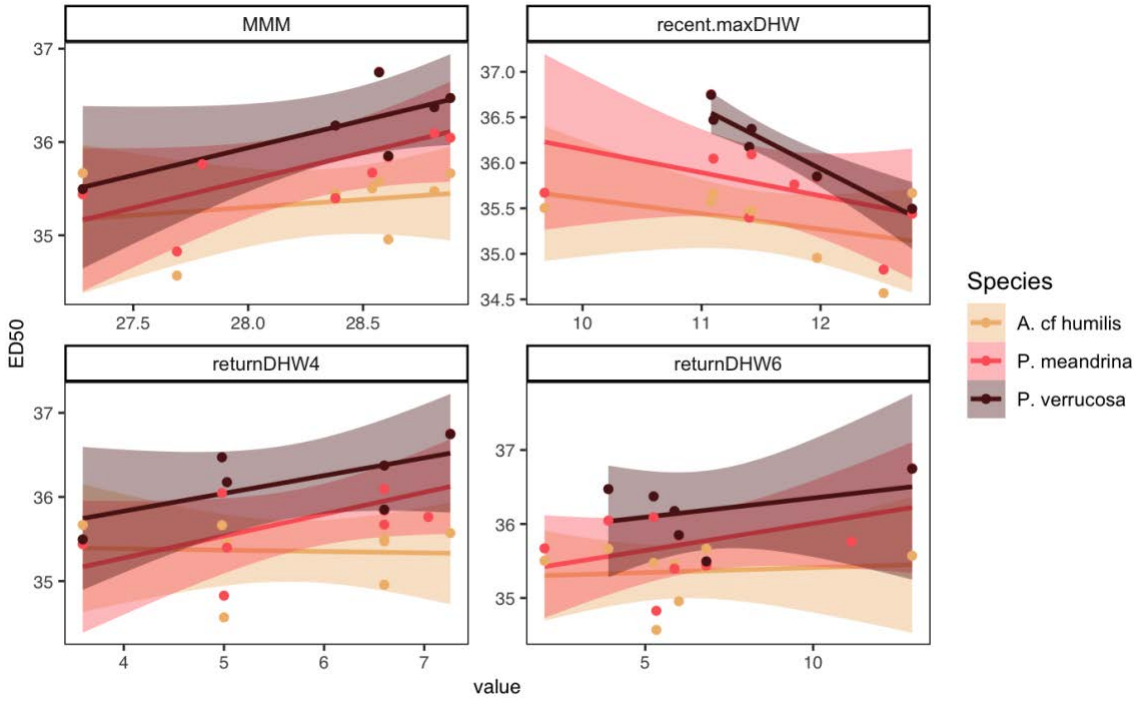

Figure S2.14. Climatic predictors that were included in the dredging model to obtain the model of best fit for absolute ED50s among reefs and species. These predictors were chosen based on their low collinearity amongst other present variables, and high correlation to Species and Reef absolute ED50 values.

Table S2.14. Estimates for environmental predictors of absolute heat tolerance derived from a linear model with the fixed effects of Species, Maximum Monthly Mean, the recent maximum DHW and the return time between events where DHW > 6. No species interactions were included in this model.

Fixed effect	Estimate	SE	t	Pr (> |*t*|)
Species (*A. cf humilis*)	28.26421	6.56317	4.306	< 0.001
Species (*P. meandrina*)	0.38856	0.16961	2.291	0.035
Species (*P. verrucosa*)	0.77659	0.19066	4.073	< 0.001
MMM	0.30933	0.19298	1.603	0.127
recent.maxDHW	-0.18039	0.12601	-1.432	0.170
returnDHW6	0.06616	0.02420	2.733	0.015

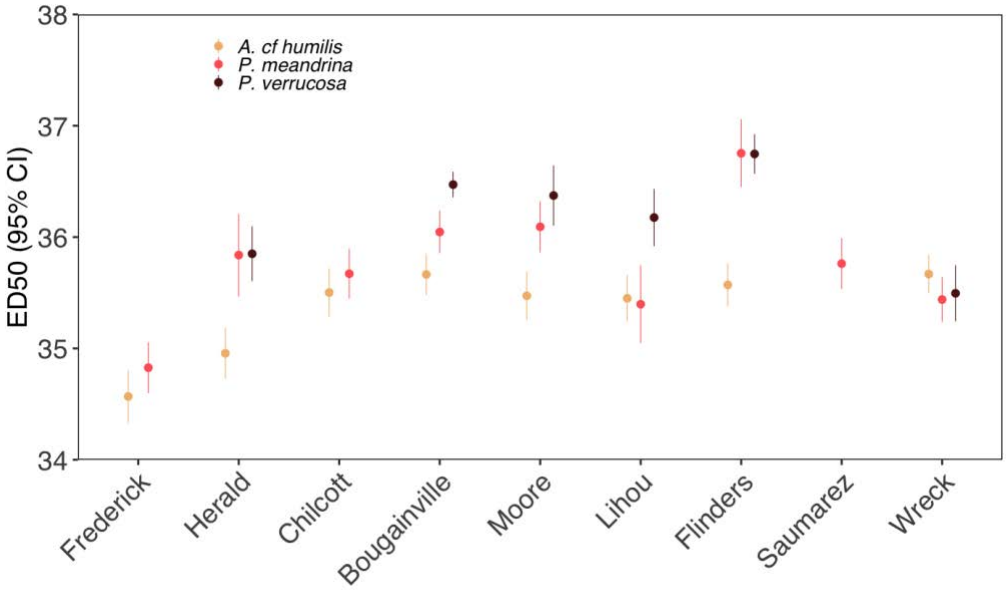

Figure S2.15. Absolute heat tolerance ED50s to induce a 50% loss in F_v/F_m relative to absolute temperatures for nine reefs and three coral species.

Appendix B: Supplementary material to Chapter 3

I. Library Statistics

Table S3.1. Reef sampling locations, GPS latitude (S) and longitude (E) coordinates and sample collection dates. The number of samples for *Pocillopora verrucosa, Pocillopora meandrina, Pocillopora* haplotype 8a and *Acropora* cf. *humilis* that were collected at each reef. Reefs are sorted from lowest to highest latitude.

Reef	GPS coordinates (S)	GPS coordinates (E)	Collection date	Number of samples collected			
				(*P. meandrina*)	(*P. verrucosa*)	(Haplotype 8a)	(*A.* cf *humilis*)
Osprey	13.88078	146.5588	11/3/2020	4	11	-	14
Bougainville	15.49273	147.08638	10/3/2020	10	18	10	22
Moore	15.89218	149.15359	7/3/2020	19	10	7	20
Willis	16.28728	149.9593	6/3/2020	9	14	1	-
Holmes	16.5045	147.99681	8/3/2020	7	20	3	30
Chilcott	16.9315	149.98988	1/3/2020	10	3	3	18
Herald	16.94348	149.18565	29/2/2020	5	11	3	19
Lihou	17.59707	151.48956	4/3/2020	6	18	4	32
Flinders	17.71357	148.43713	27/2/2020	5	26	3	30
Marion	18.98541	152.34488	23/2/2020	11	13	9	36
Frederick	21.0113	154.35043	22/2/2020	13	2	5	17
Saumarez	21.88607	153.64764	18/2/2020	22	-	6	-
Wreck	22.19267	155.33405	20/2/2020	13	6	7	24

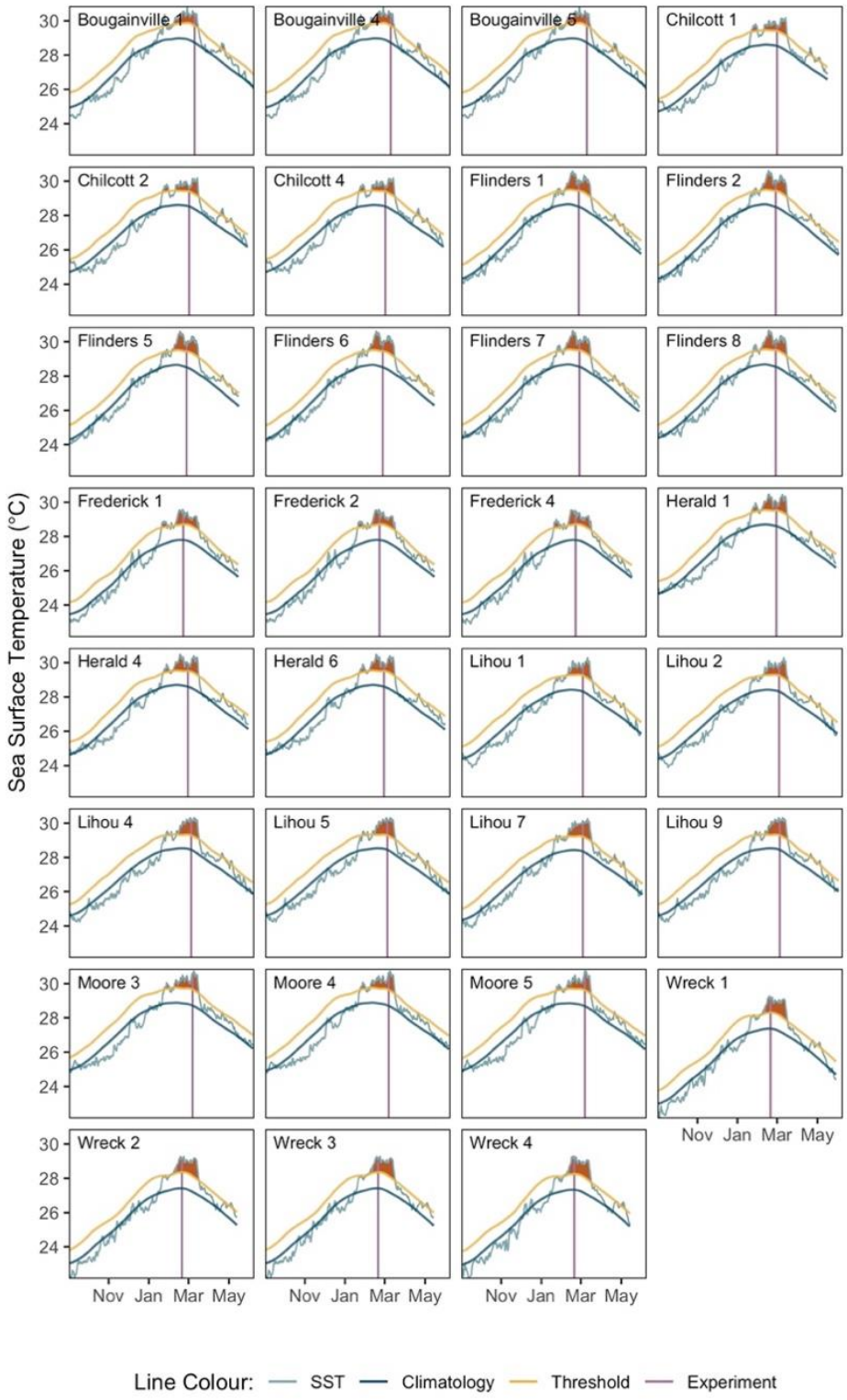

Figure S3.1. Coral sampling during the mass bleaching event of 2020. Panels depict the average SST, climatology (MMM), and thermal thresholds of each reef from November 2019 – May 2020. Red lines depict the bleaching event at each reef, and the purple vertical line depicts when the coral sampling was conducted at each reef. Note that sampling was conducted at the height of the 2020 bleaching event for all reefs in the Coral Sea in Feb-March 2020.

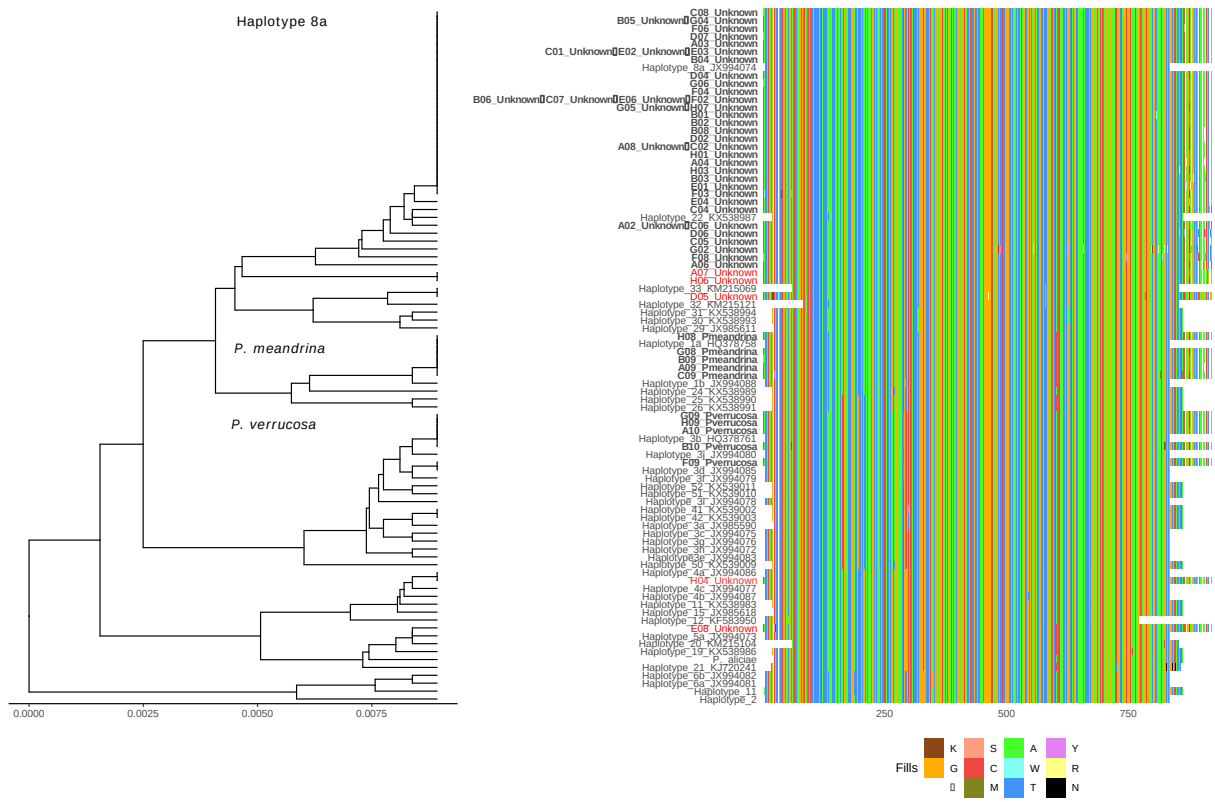

Figure S3.2. mtORF hamming distances for all *Pocillopora* spp. Samples of *Pocillopora* haplotype 8a (orange), *P. meandrina* (yellow), and *P. verrucosa* (green) are represented from this study. Samples were mapped to mtORF reference sequences collated from Pinzon et al. (2013), Forsman et al. (2013), and Gelin et al. (2017).

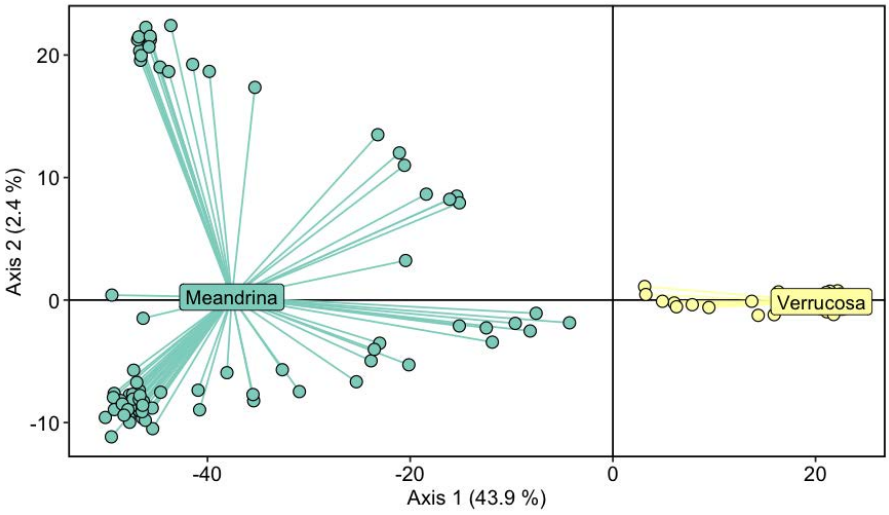

Figure S3.3. Principal Coordinates Analysis (PCoA) illustrating differences between *P. meandrina* and *P. verrucosa* host genetic clusters.

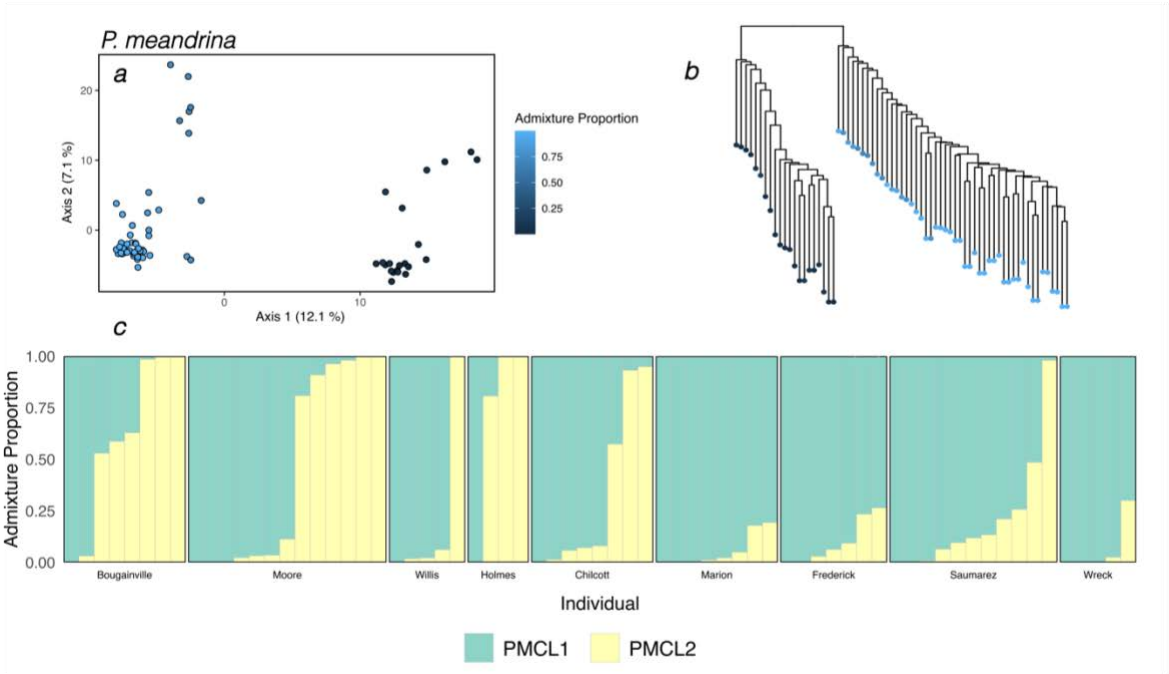

Figure S3.4. Statistical tests used to measure the genetic differentiation of the coral host among individuals in *P. meandrina*. Tests included (a) Principal coordinates analysis, (b) Neighbour-Joining Tree and (c) Admixture proportion assignments. (a) and (b) are coloured by admixture proportion of PMCL1.

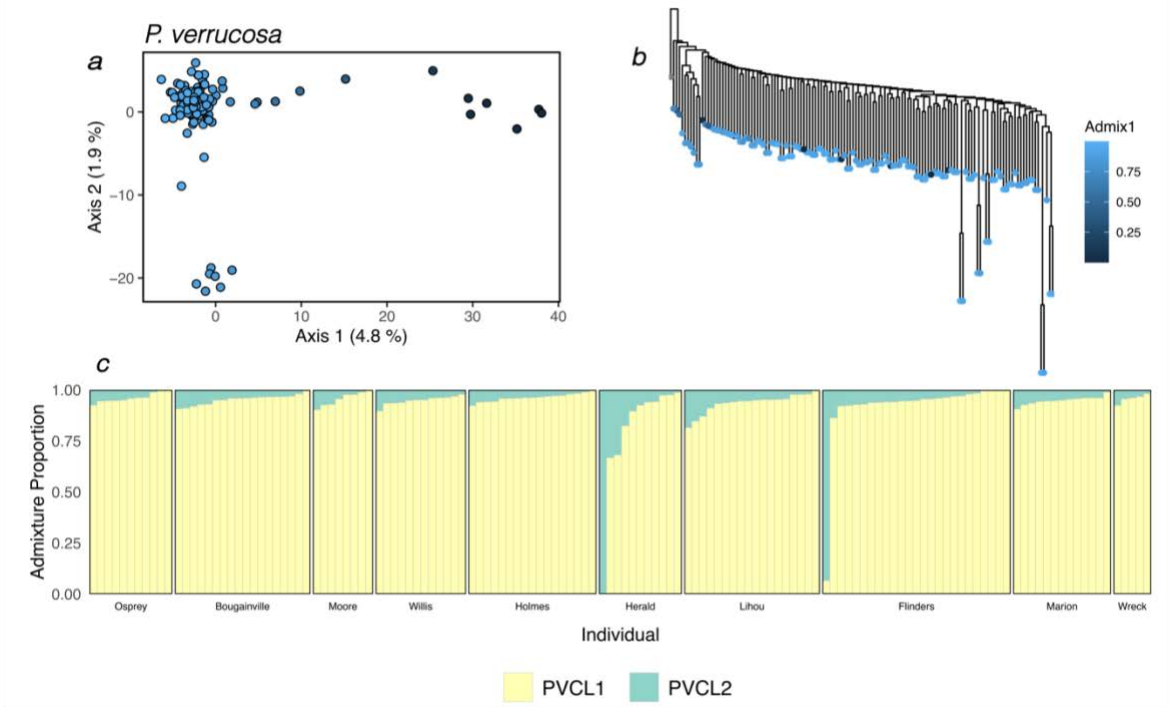

Figure S3.5. Statistical tests used to measure the genetic differentiation of the coral host among individuals in *P. verrucosa*. Tests included (a) Principal coordinates analysis, (b) Neighbour-Joining Tree and (c) Admixture proportion assignments. (a) and (b) are coloured by admixture proportion of PMCL1.

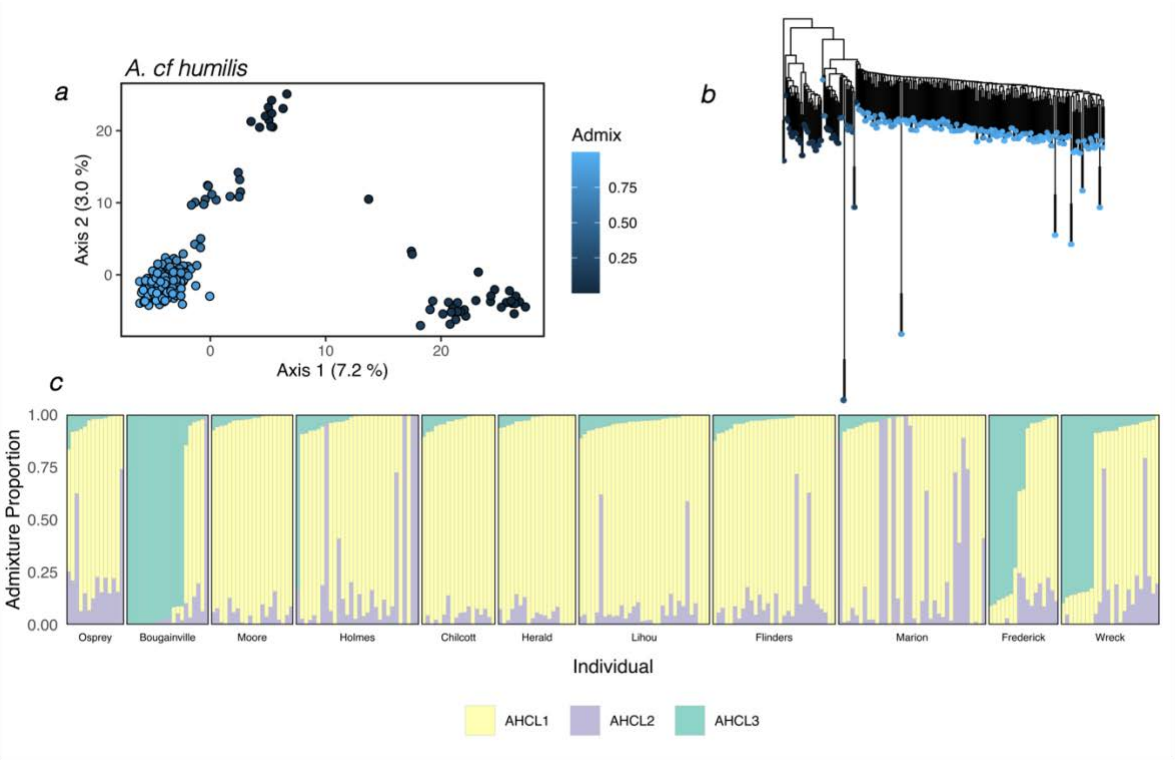

Figure S3.6. Statistical tests used to measure the genetic differentiation of the coral host among individuals in *Acropora* cf. *humilis*. Tests included (a) Principal coordinates analysis, (b) Neighbour-Joining Tree and (c) Admixture proportion assignments. (a) and (b) are coloured by admixture proportion of PMCL1.

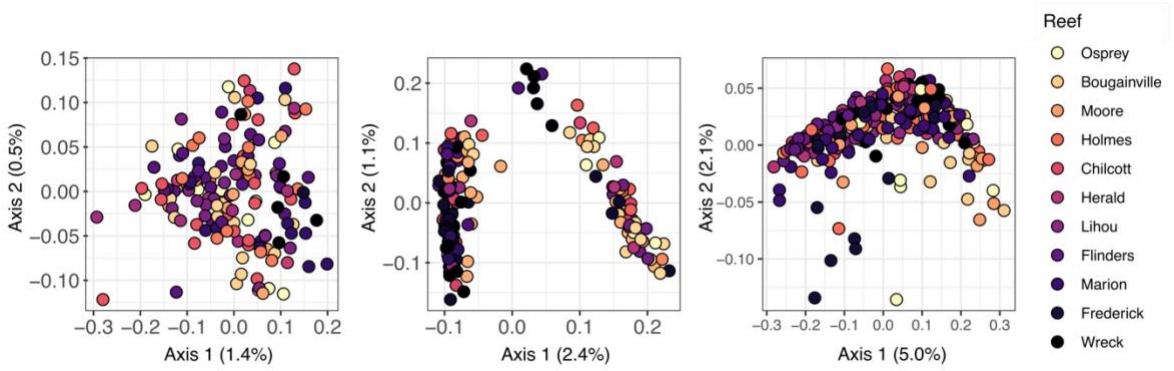

Figure S3.7. Principal Coordinates Analysis (PCoA) results of symbiont community composition, coloured by reef. Each panel is plotted per host species, including *P. verrucosa* (a), *P. meandrina* (b), and *A.* cf. *humilis* (c) coloured by reef.

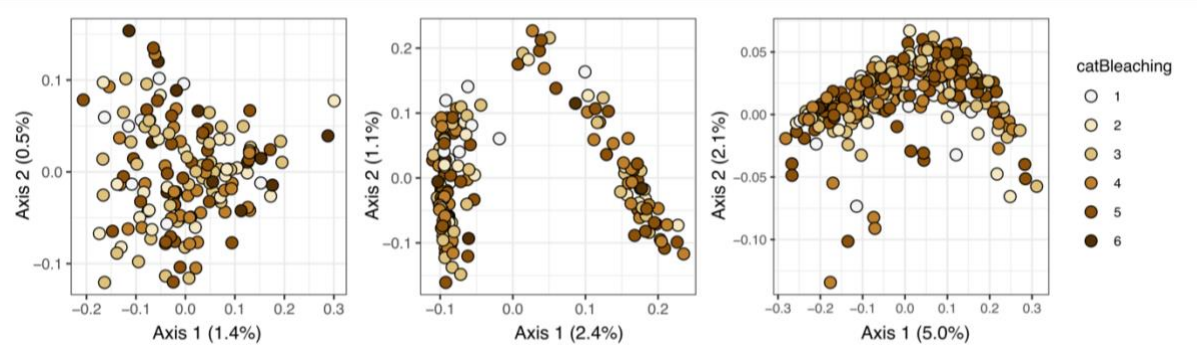

Figure S3.8. Principal Coordinates Analysis (PCoA) results of symbiont community composition by bleaching condition of the host. Each panel is plotted per host species, including *P. verrucosa* (a), *P. meandrina* (b), and *A.* cf. *humilis* (c) and coloured by bleaching category of the coral host.

Table S3.2. Environmental Metrics Table. Definitions for 7 climatic and environmental parameters which were included in the full distance-based redundancy analysis (dbRDA).

Environmental Parameter	Definition
catBleaching	Bleaching category/condition of coral at time of coral collection, ranging from '1' (most bleached) to '6' (least bleached) using Coral Watch Health Chart D-scale.
Depth	Collection depth of corals (m).
DHW2020	DHW experienced at each reef at the time of coral collection between Feb – March 2020.
Latitude	GPS South coordinates.
Longitude	GPS East coordinates.
maxDHW	Maximum DHW experienced between 1986 - 2020
MMM	Maximum Monthly Mean SST between 1986 - 2010
Kd490	Light attenuation at 490 nm between 2010 - 2019.
Secchi	Secchi depth at 488 nm between 2010 - 2019
Chla	Overall mean chlorophyll *a* content between 2010 - 2019.

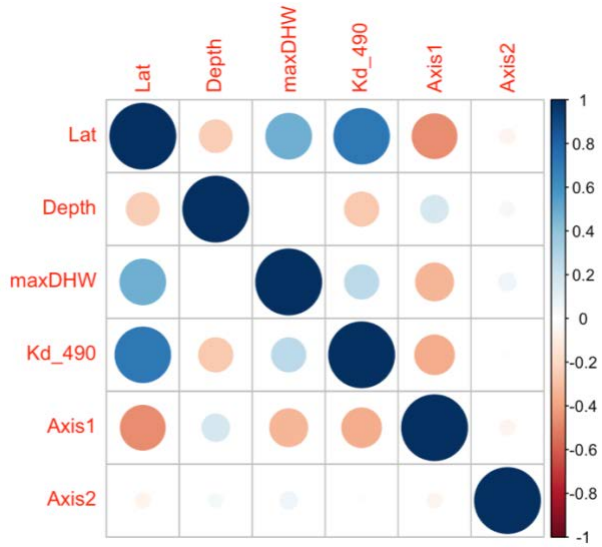

Figure S3.9. Correlation plots for environmental and biogeographic drivers of symbiont communities for *P. meandrina*. Only numeric factors are shown. Refer to SOM Table S2 for definitions of each environmental variable.

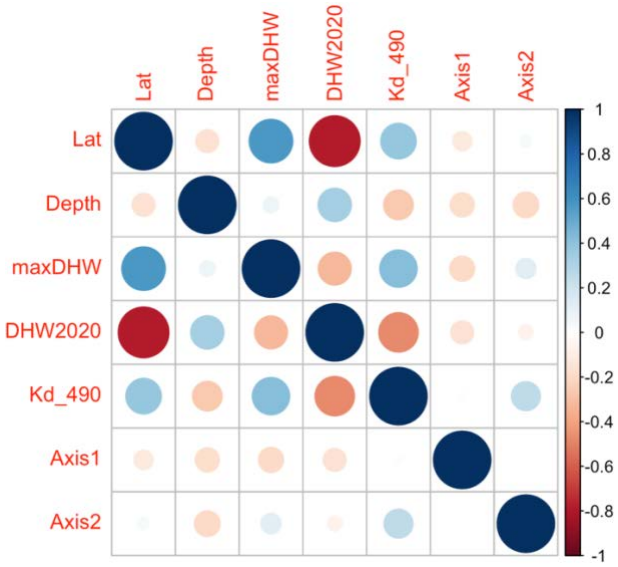

Figure S3.10. Correlation plots for environmental and biogeographic drivers of symbiont communities for *P. verrucosa*. Only numeric factors are shown. Refer to SOM Table S6 for definitions of each environmental variable.

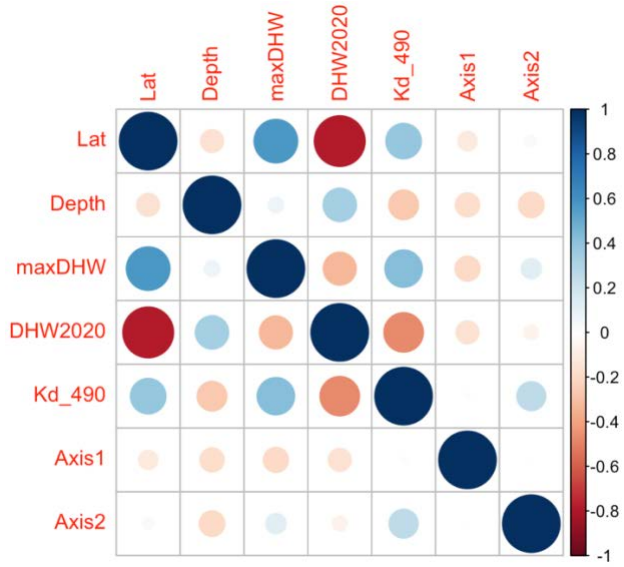

Figure S3.11. Correlation plots for environmental and biogeographic drivers of symbiont communities for *Acropora* cf *humilis.* Only numeric factors are shown. Refer to SOM Table S2 for definitions of each environmental variable.

Table S3.3. SymPortal ITS2 Type Profiles for *Pocillopora meandrina.*

ITS2 Type Profile	Number of samples	Proportion of samples	Cumulative proportion
p_C1/C42.2/C42g/C42a-C1b-C1au-C1az-C42h-C3	74	0.548	0.548
p_C1/C42.2/C42u-C1b-C42a-C1au-C115l-C1az-C115d	33	0.244	0.793
p_C42u/C42a/C1/C42.2/C42b-C1b-C1au	9	0.067	0.859
p_C42.2/C1/C42a/C1b-C1au-C1az-C3-C115d	5	0.037	0.896
p_C42.2/C1/C42a-C1b-C42g-C42b-C1au-C1az	5	0.037	0.933
p_C42g/C42a/C42.2/C1-C42h-C42b-C1b-C1au	3	0.022	0.956
p_C42g-C42.2-C1-C1b-C42h-C42a-C42ba-C42b	1	0.007	0.963
p_C42a/C1/C42.2/C1b/C1j-C1au-C3-C115l	1	0.007	0.970
p_A1/A1h	1	0.007	0.978
p_C15h	1	0.007	0.985
p_C42.2/C1dh/C1/C1d-C1b-C3cg	1	0.007	0.993
p_C1ag/C1/C42.2/C1bi-C3cg-C1b-C3cw-C45c	1	0.007	1.000

Table S3.4. SymPortal ITS2 Type Profiles for *Pocillopora* haplotype 8a.

ITS2 Type Profile	Number of samples	Proportion of samples	Cumulative proportion
p_C1/C42.2/C42g/C42a-C1b-C1au-C1az-C42h-C3	22	0.564	0.564
p_C1/C42.2/C42u-C1b-C42a-C1au-C115l-C1az-C115d	9	0.231	0.795
p_C42u/C42a/C1/C42.2/C42b-C1b-C1au	2	0.051	0.846
p_C42g/C42a/C42.2/C1-C42h-C42b-C1b-C1au	2	0.051	0.897
p_C42u-C1-C42.2-C42a-C1b-C1au-C115k-C115d	2	0.051	0.949
p_C42.2/C1/C42a/C1b-C1au-C1az-C3-C115d	1	0.026	0.974
p_C1/C42.2/C42g/C42a-C1b-C1az-C3-C1au	1	0.026	1.000

Table S3.5. SymPortal profiles for *Pocillopora verrucosa.*

ITS2 Type Profile	Number of samples	Proportion of samples	Cumulative proportion
p_C1d/C1/C42.2/C3-C1b-C3cg-C115k-C45c-C1au-C41p	71	0.461	0.461
p_C1d/C1/C42.2-C3cg-C1b-C45c-C115k-C1au	36	0.234	0.695
p_C1d/C1/C1ba-C42.2-C3cg-C1b-C115k	13	0.084	0.779
p_C42.2/C1dh/C1/C1d-C1b-C3cg	8	0.052	0.831
p_C1ag/C1/C1ah-C42.2-C3cg-C1b	6	0.039	0.870
p_C1d-C42.2-C1-C1k-C1b-C3cg	5	0.032	0.903
p_C1ag/C1/C42.2-C3cg-C1b-C1bi	4	0.026	0.929
p_C1ag-C1-C42.2-C1bi-C3cg-C1b-C1bk	2	0.013	0.942
p_C1d/C15h-C1-C42.2	2	0.013	0.955
p_C1/C42.2/C42g/C42a-C1b-C1au-C1az-C42h-C3	1	0.006	0.961
p_C1/C42.2/C42u-C1b-C42a-C1au-C115l-C1az-C115d	1	0.006	0.968
p_C3-C3k	1	0.006	0.974
p_C1ag/C1-C42.2-C3cg-C1b	1	0.006	0.981
p_C1d	1	0.006	0.987
p_C1ag/C1/C42.2/C1bi-C3cg-C1b-C3cw-C45c	1	0.006	0.994
p_C1ag/C1-C1m-C42.2-C1lr-C1bi-C3cg	1	0.006	1.000

Table S3.6. SymPortal ITS2 Type Profiles for *Acropora* cf *humilis*.

ITS2 Type Profile	Number of samples	Proportion of samples	Cumulative proportion
p_C3k/C3-C50a-C29-C21ab-C3b	160	0.593	0.593
p_C3k/C3-C50a-C21ab-C50f-C3ba-C3dq	52	0.193	0.785
p_C3k/C3-C50a-C3ba-C50f-C3dq-C21-C3a	14	0.052	0.837
p_C3k/C3-C50a-C3jv-C3vx-C3vy	12	0.044	0.881
p_C3bo/C3k-C3-C3bp-C50a-C29	6	0.022	0.904
p_C3k/C3/C1-C50a-C21ab	4	0.015	0.919
p_C3k-C3-C50a-C21ab-C3b	3	0.011	0.930
p_C3k-C3-C50a-C21ab-C50f-C3ba	2	0.007	0.937
p_C1/C42.2	2	0.007	0.944
p_C1/C1c	2	0.007	0.952
p_C1/C42.2/C42g/C42a-C1b-C1au-C1az-C42h-C3	1	0.004	0.956
p_A1	1	0.004	0.959
p_C3/C3k-C29-C21ab-C3b-C3gj-C21.12	1	0.004	0.963
p_C3-C21-C3k-C3at-C3b-C3av-C3dp	1	0.004	0.967
p_C40/C1-C3-C115	1	0.004	0.970
p_C42.2/C42a/C1-C1b	1	0.004	0.974
p_C1d/C1	1	0.004	0.978
p_C1/C3k-C1b-C3-C42.2-C1bh-C1br	1	0.004	0.981
p_C3/C21/C3av-C3at-C3b-C3dp	1	0.004	0.985
p_C3k-C50a-C3cz	1	0.004	0.989
p_C42a/C1-C42.2	1	0.004	0.993
p_C1/C3-C1c-C1b-C1w	1	0.004	0.996
p_C3k/C50a	1	0.004	1.000

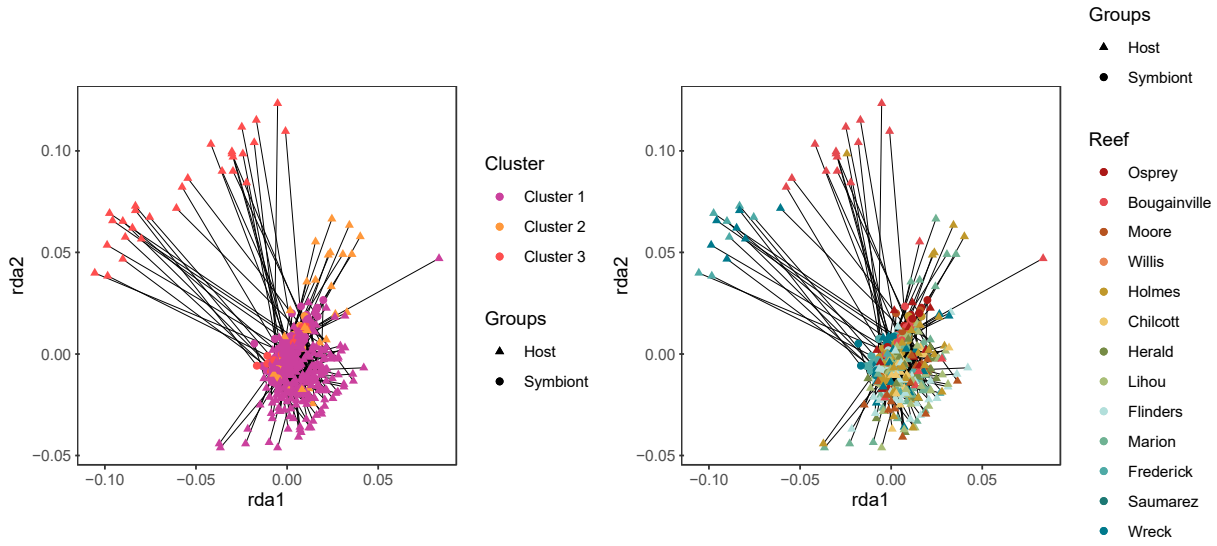

Figure S3.12. Procrustes rotation plots coloured by host cluster. Full Procrustes Rotation Analysis coloured by host genetic cluster for *A.* cf *humilis*.

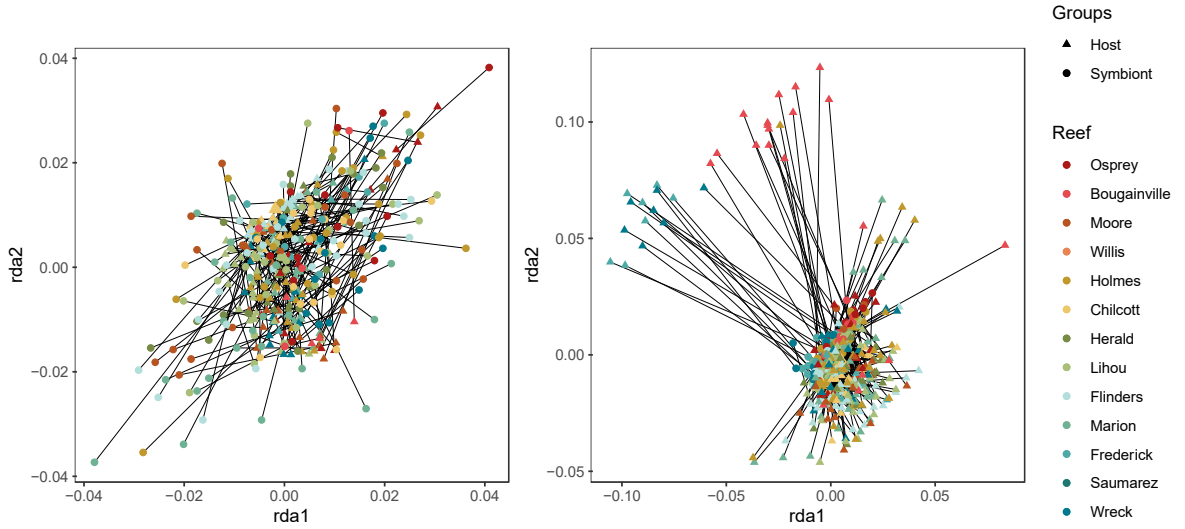

Figure S3.13. Procrustes rotation analyses comparisons. Reduced subset of only *A.* cf *humilis* cluster AHCL1 (left) and all three host genetic clusters (AHCL1, 2, and 3) are shown on the right. Points are coloured by reef. Each line connects the same individual sample from host (circle) and symbiont (triangle).

Appendix C: Supplementary material to Chapter 4

Table S4.1. List of sample collection reefs, their assigned sector groupings, latitude, longitude, and Maximum Monthly Mean for each reef.

Region	Sector	Reef	Lat	Lon	MMM
Coral Sea	CS1	Osprey	13.88078	146.5588	29.01
		Bougainville	15.49273	147.08638	28.96
	CS2	Holmes	16.5045	147.99681	28.75
		Flinders	17.71357	148.43713	28.64
	CS3	Moore	15.89218	149.15359	28.83
		Willis	16.28728	149.9593	28.69
	CS4	Chilcott	16.9315	149.98988	28.59
		Herald	16.94348	149.18565	28.59
	CS5	Lihou	17.59707	151.48956	28.44
		Marion	18.98541	152.34488	28.08
	CS6	Frederick	21.0113	154.35043	27.77
		Saumarez	21.88607	153.64764	27.9
		Wreck	22.19267	155.33405	27.41
Great Barrier Reef	Cape Grenville	Lagoon	12.3922	143.7394	28.54
		Mantis	12.33836	143.86078	28.44
	Princess Charlotte Bay	Corbett	13.92266	144.24052	28.58
		Davie	13.96772	144.44553	28.58
		13-124	13.85169	144.09059	28.66
		Sandbank	14.19803	144.9055	28.55
	Cairns	Mackay	16.0384	145.65137	28.63
	Townsville	Chicken	18.40233	147.42382	28.46
		Davies	18.4962	147.37608	28.45
		Kelso	18.254064	146.590664	28.63
	Capricorn Bunker	Lady Musgrave	23.90737	152.38654	27.07
		Hoskyns	23.80801	152.2836	27.06
		Fitzroy Reef	23.62972	152.13611	
	Swains	Chinaman	22.01369	152.65425	27.42
		22-084	22.00282	152.45695	27.52
		21-550	21.96184	152.31235	27.56

Table S4.2. Number of loci retained after each filtering parameter.

Filtering Step	*P. meandrina*	*P. verrucosa*
All SNPs	43980	44310
Secondaries	27253	25796
Reproducibility (0.98)	22029	21945
Call Rate (0.80)	3696	7283
Read Depth (5x)	3608	6672
MAF (0.05)	2075	3722

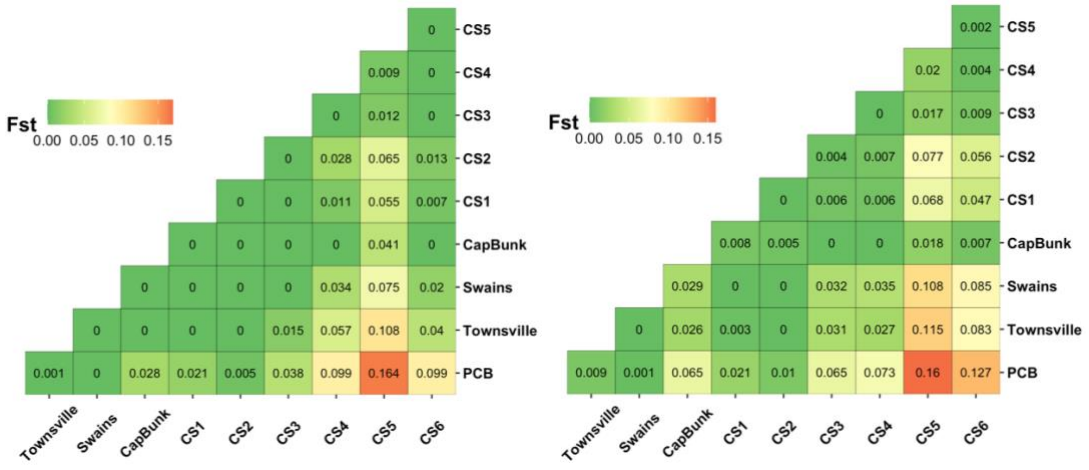

Figure S4.1. *P. meandrina* genetic pairwise comparisons (F_{ST}) for a subset reduced to n = 5 randomly subsampled from each sector (left) compared to the full model with all samples present (right).

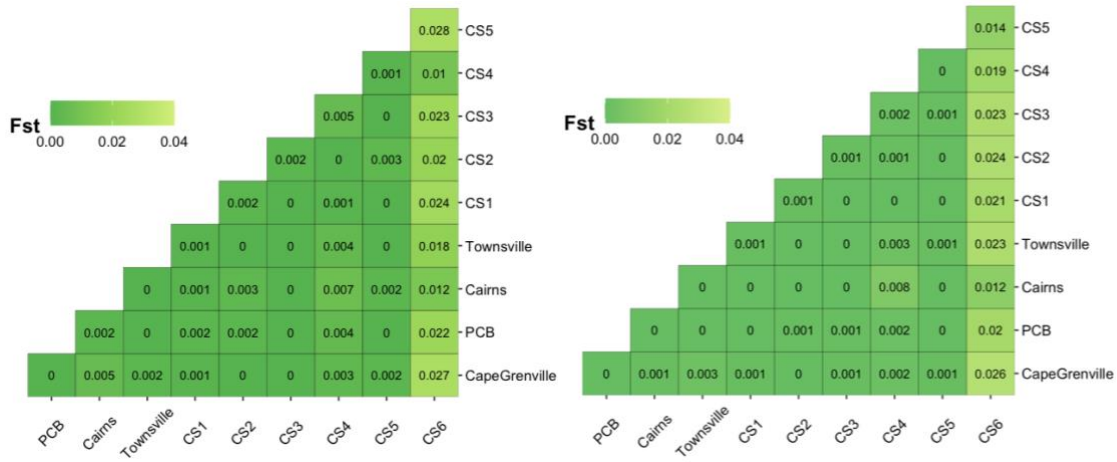

Figure S4.2. *P. verrucosa* genetic pairwise comparisons (F_{ST}) for a subset reduced to n = 5 randomly subsampled from each sector (left) compared to the full model with all samples present (right).

Table S4.3. Analysis of Molecular Variance (AMOVA) summary statistics for *P. meandrina* to assess the proportion of genetic variance explained within samples, between samples, and among sectors.

Obs	Std.Obs	Alter	p-value	Sigma	%
Variations within samples	118.38	-38.63	0.001	118.38	62.32
Variations between samples	70.13	27.54	0.001	70.13	36.92
Variations between Sector	1.44	2.01	0.035	1.44	0.76
Total variations				189.95	100

Table S4.4. Analysis of Molecular Variance (AMOVA) summary statistics for *P. verrucosa* to assess the proportion of genetic variance explained within samples, between samples, and among sectors.

Obs	Std.Obs	Alter	p-value	Sigma	%
Variations within samples	376.12	-44.03	0.001	376.12	74.07
Variations between samples	130.93	35.95	0.001	130.93	25.79
Variations between Sector	0.72	3.54	0.002	0.72	0.14
Total variations				507.77	100

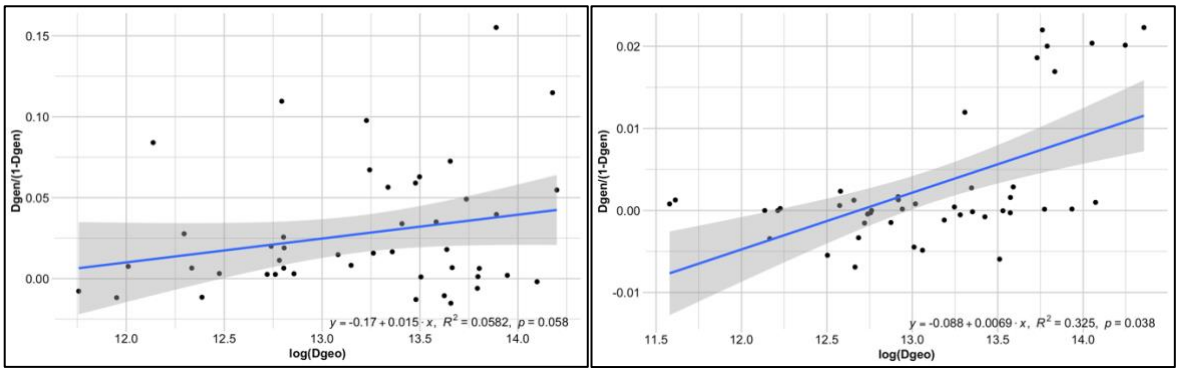

Figure S4.3. Isolation-by-distance models for *P. meandrina* (left) and *P. verrucosa* (right) using the log of geographic distance vs. genetic distance (F_{st} /1-F_{st}), including significance and correlation using a Mantel test.

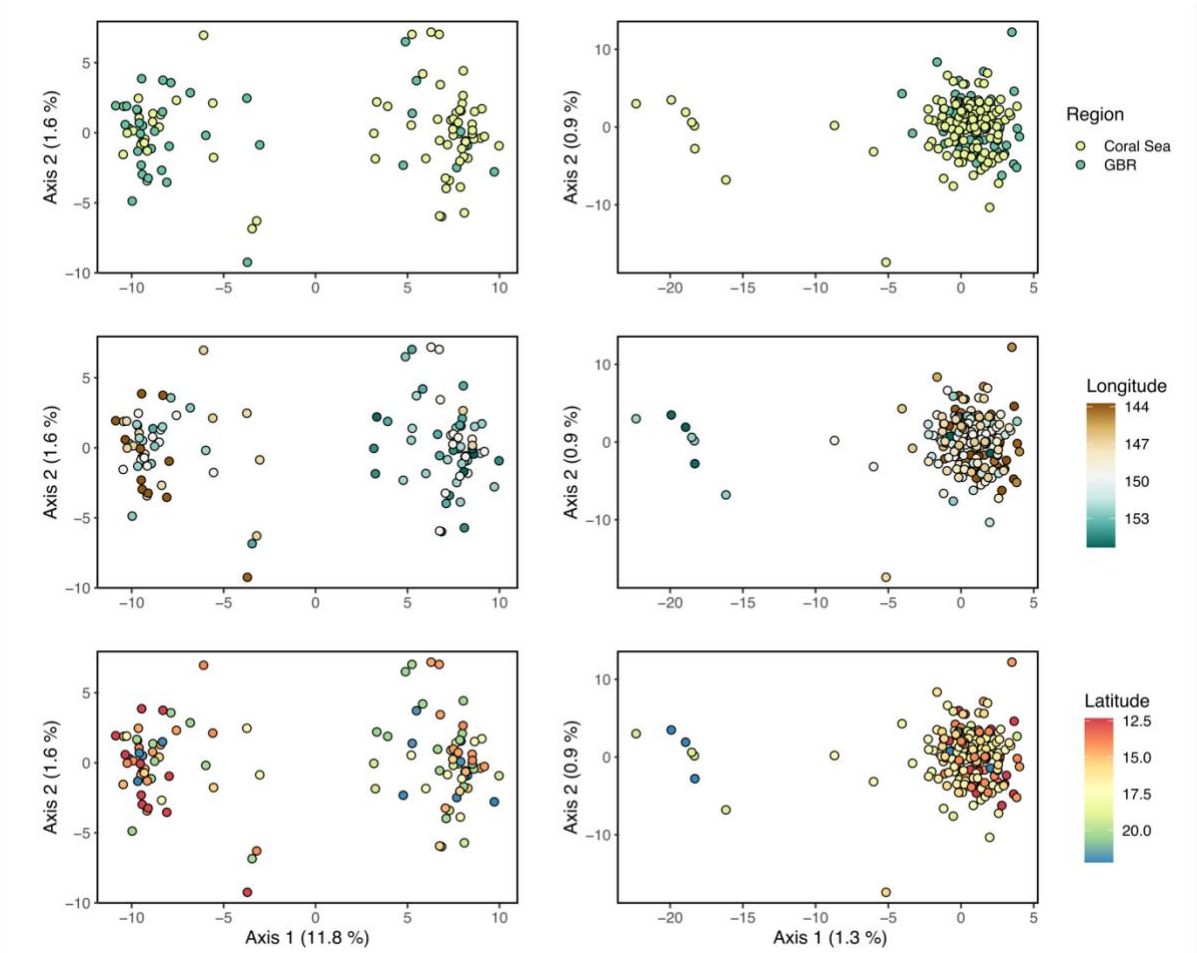

Figure S4.4. PCAs depicting neutral population structure of *P. meandrina* (left) and *P. verrucosa* (right). Individual genetic distances (points) are coloured by region (top), longitude (middle), and latitude (bottom).

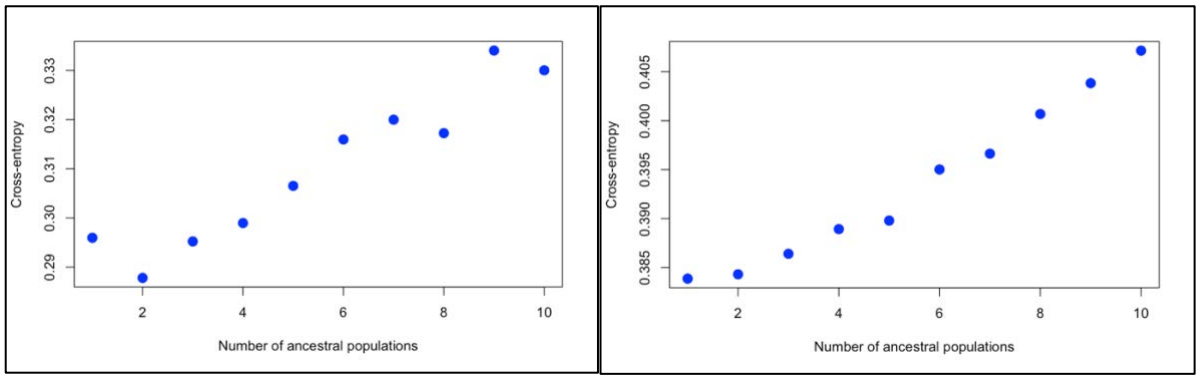

Figure S4.5. Cross-entropy criterion showing optimal K-cluster value for *P. meandrina* (left) and *P. verrucosa* (right).

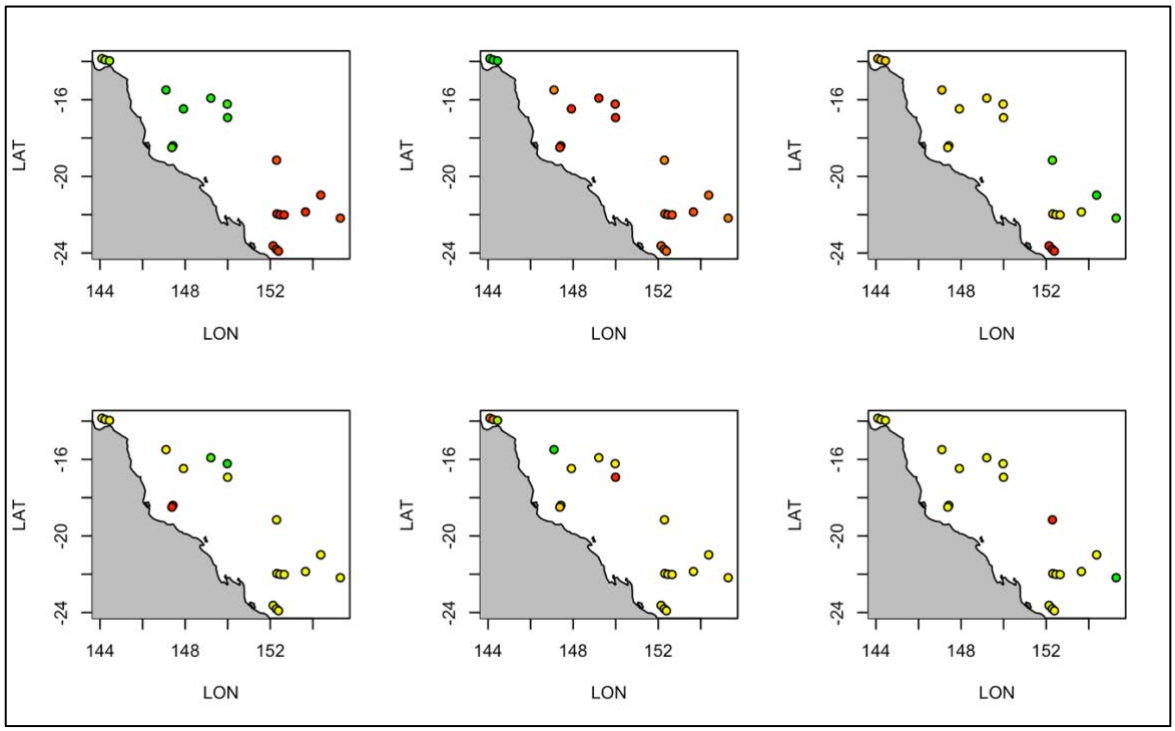

Figure S4.6. Distance-based Moran Eigenvector Models (db-MEMs) for *Pocillopora meandrina.*

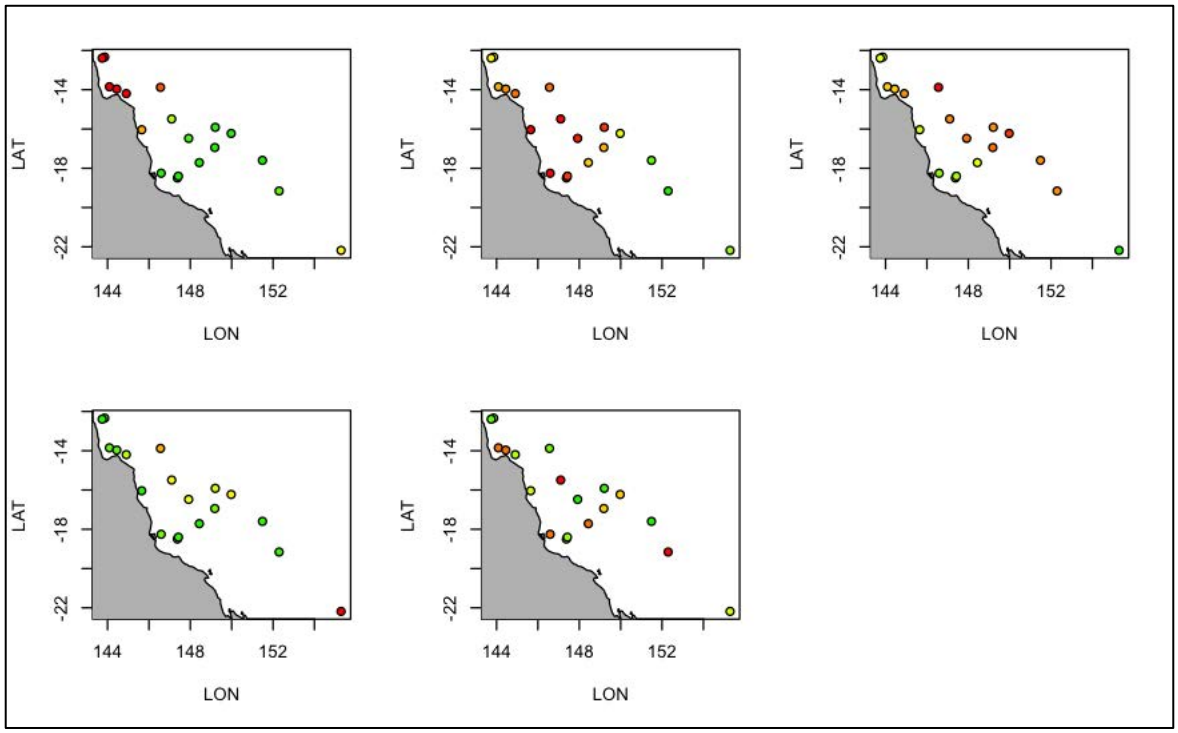

Figure S4.7. Distance-based Moran Eigenvector Models (db-MEMs) for *Pocillopora verrucosa.*

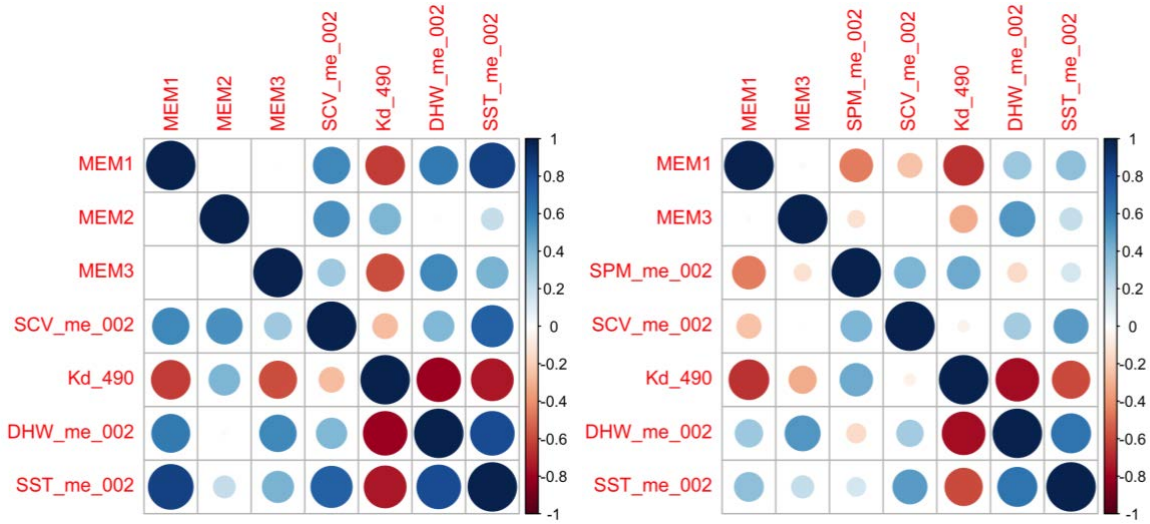

Figure S4.8. Correlation plots for climate, environmental, and geographic drivers of host population structure for *P. meandrina* (left) and *P. verrucosa* (right). Only numeric factors are shown. Refer to SOM Table S4 for definitions of each variable.

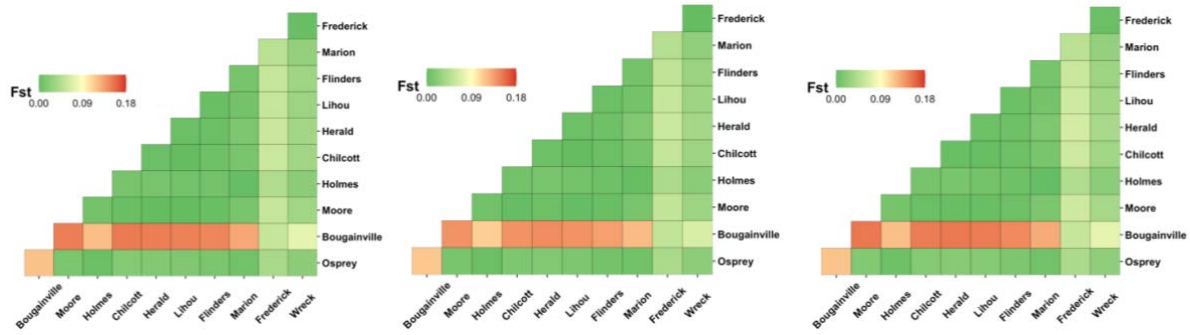

Figure S5.1. Variable call rate filtering scenarios indicate comparable outcomes for population-level global statistics (Fst) and PCAs. Fst call rate scenarios to filter loci with a call rate of 0.80 (a), 0.85 (b), and 0.90 (c).

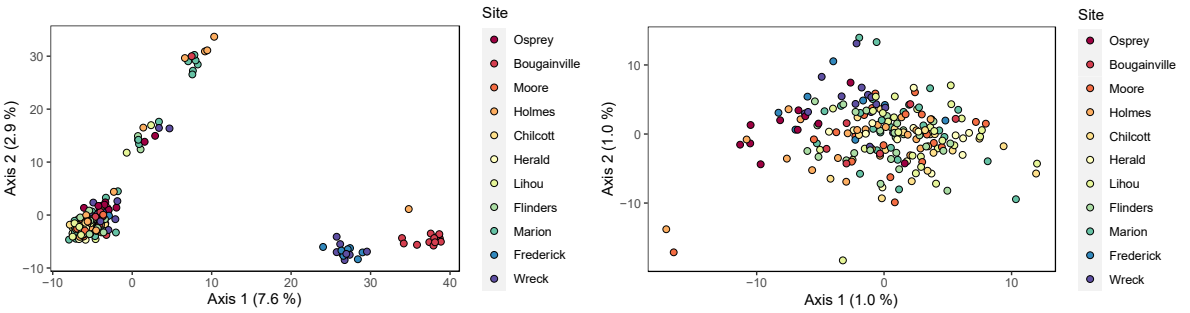

Figure S5.2. Comparisons of PCAs between all three host lineages (left) and only AHCL1 (right).

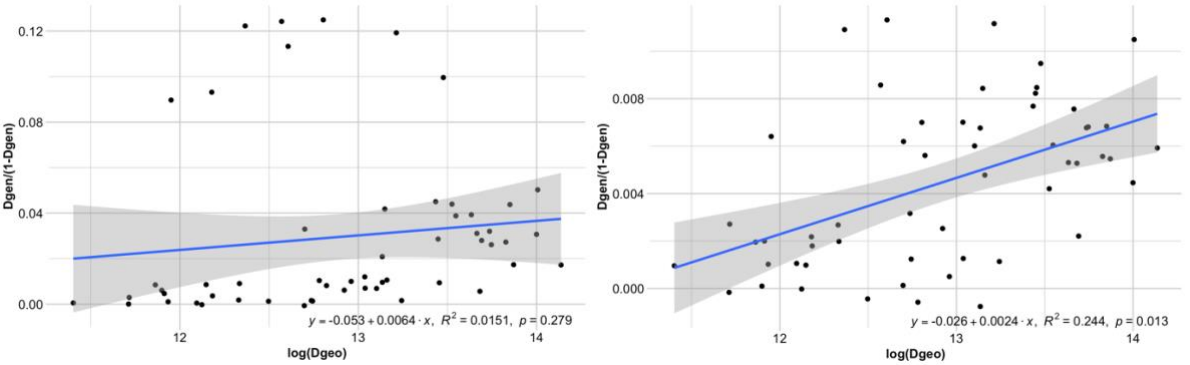

Figure S5.3. Isolation-by-distance models for *A.* cf. *humilis* depicting the relationship between genetic and geographic distance. All host genetic clusters grouped together (left), and the main genetic lineage (AHCL1, right) are shown.

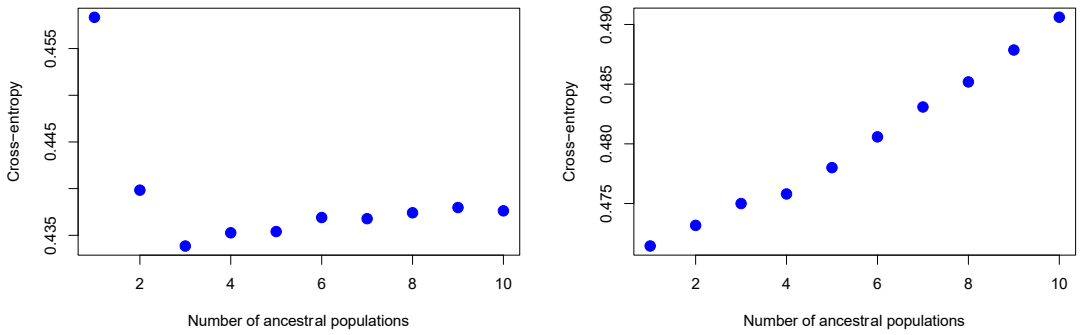

Figure S5.4. Cross-entropy criterion for *A.* cf *humilis.* Results indicate $K = 3$ as the optimal K-clustering value for all three host clusters (left) and $K = 1$ for AHCL1 only (right).

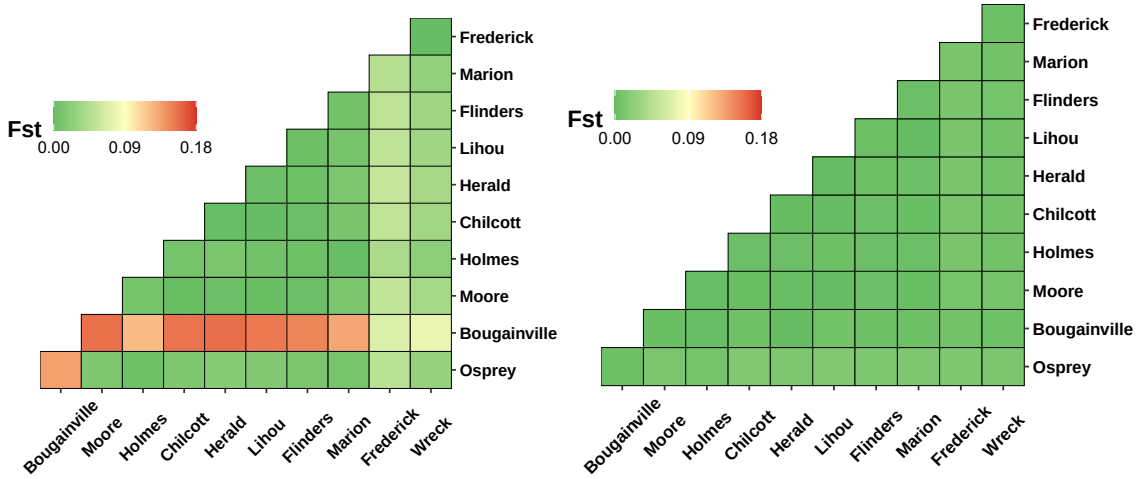

Figure S5.5. Global pairwise comparisons (F_{ST}) among Coral Sea reefs for all host clusters (a) and for the main cluster only, AHCL1 (b).

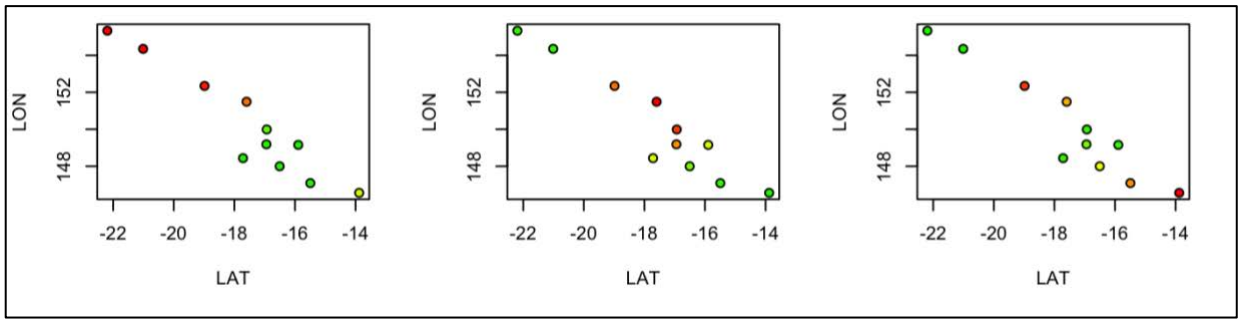

Figure S5.6. Distance-based Moran Eigenvector Models (db-MEMs) for *Acropora* cf. *humilis.* Models were incorporated as a spatial indicator of geographic distance in gene-environment associations.

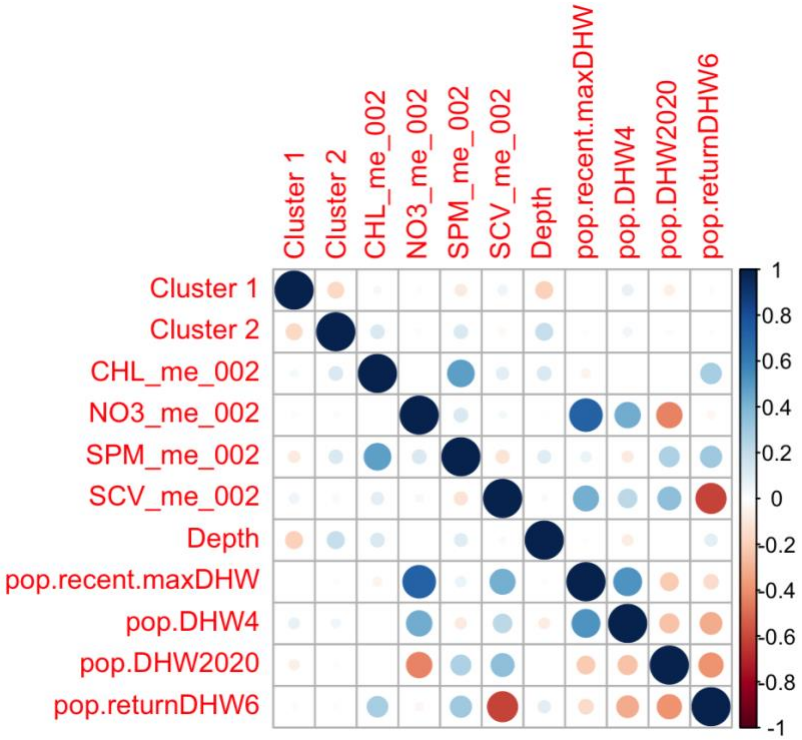

Figure S5.7. Correlation matrix for environmental and host genetic variables in gene-environment associations.

Table S5.1. Akaike information criterion (AICc) scores for different model parameters using ED50 as a response variable against environmental, host genetic, and symbiont community structure.

Model name	Model Parameters	Random Factors	AICc
glm.1	ED50 ~ Host PC1 + PC2	None	355.59
glm.2	ED50 ~ Host PC1	Reef	266.53
glm.3	ED50 ~ Host PC2	Reef	267.01
glm.4	ED50 ~ Host PC1 + PC2	Reef	267.71
glm.5	ED50 ~ Host PC1 + Symbiont PC1	Reef	268.46
glm.6	ED50 ~ Host PC1 + Symbiont PC2	Reef	268.43
glm.7	ED50 ~ Host PC1 + Symbiont PC1 + Symbiont PC2	Reef	270.25
glm.8	ED50 ~ Symbiont PC1 + Symbiont PC2	Reef	269.99
glm.9	ED50 ~ Symbiont PC2	Reef	268.48
glm.10	ED50 ~ Host PC1 + Symbiont PC2 + recent max DHW	Reef	268.99
glm.11	ED50 ~ Host PC1 + Symbiont PC2 + DHW4	Reef	261.36
glm.12	ED50 ~ Host PC1 + Symbiont PC2 + return DHW6	Reef	270.49
glm.13	ED50 ~ Host PC1 + Symbiont PC2 + recent max DHW + DHW4	Reef	263.49
glm.14	ED50 ~ Host PC1 + Symbiont PC2 + recent max DHW * DHW4	Reef	245.84
glm.15	ED50 ~ PGS + Symbiont PC2 + recent max DHW * DHW4	Reef	247.75
glm.16	ED50 ~ Host PC1 + PGS + Symbiont PC2 + recent max DHW * DHW4	Reef	247.88

glm.17	ED50 ~ PGS(centred) + Symbiont PC2 (centred) + Host PC1 (centred) + DHW4 (centred) + recent max DHW (centred)	Reef	50.26
glm.18	ED50 ~ PGS(centred) + Symbiont PC2 (centred) + Host PC1 (centred) + DHW4 (centred) * recent max DHW (centred)	Reef	44.14

Appendix E: Publications arising from thesis chapters

Marzonie, M. R., Bay, L. K., Bourne, D. G., Hoey, A. S., Matthews, S., Nielsen, J. J. V., Harrison, H. B. (2023). The effects of marine heatwaves on acute heat tolerance in corals. *Global Change Biology*, *00*, 1–13. https://doi.org/10.1111/gcb.16473

Marzonie, M. R., Nitschke, M. R., Bay, L. K., Bourne, D. G., Harrison, H. B. (2024). Symbiodiniaceae diversity varies by host and environment across thermally distinct reefs. *Molecular Ecology*, *Molecular Ecology,* https://doi.org/10.1111/mec.17342

Appendix F: Other peer-reviewed manuscripts and book chapters published during candidature

Burn, D., Marzonie, M.R., and Pratchett, M.S. (2024). Chapter 29: Quantifying coral bleaching and other injuries. *Routledge Handbook of Coral Reefs.* Taylor and Francis *in press.*

Marzonie, M.R, Flores, F., Sadoun, N., Thomas, M. C., Valada-Mennuni, A., Kaserzon, S., Mueller, J. F., & Negri, A. P. (2021). Toxicity thresholds of nine herbicides to coral symbionts (Symbiodiniaceae). *Scientific Reports*, *11*(1). https://doi.org/10.1038/s41598-021-00921-3

Nielsen, J. J. V., Matthews, G., Frith, K. R., Harrison, H. B., Marzonie, M. R., Slaughter, K. L., Suggett, D. J., & Bay, L. K. (2022). Experimental considerations of acute heat stress assays to quantify coral thermal tolerance. *Scientific Reports 2022 12:1*, *12*(1), 1–13. https://doi.org/10.1038/s41598-022-20138-2

Quigley, K. M., Marzonie, M.R., Ramsby, B., Abrego, D., Milton, G., van Oppen, M. J. H., & Bay, L. K. (2021). Variability in Fitness Trade-Offs Amongst Coral Juveniles With Mixed Genetic Backgrounds Held in the Wild. *Frontiers in Marine Science*, *8*, 161. https://doi.org/10.3389/fmars.2021.636177